

Development of nanocarriers for siRNA based on cationic polymers

A Ph.D Thesis presented by

Haliza Katas

Supervised by
Professor H. Oya Alpar



School of Pharmacy
University of London

This research project is submitted in partial fulfilment of the requirements for the degree of Doctor of Philosophy of the University of London.

February 2007



ProQuest Number: 10104732

All rights reserved

INFORMATION TO ALL USERS

The quality of this reproduction is dependent upon the quality of the copy submitted.

In the unlikely event that the author did not send a complete manuscript and there are missing pages, these will be noted. Also, if material had to be removed, a note will indicate the deletion.



ProQuest 10104732

Published by ProQuest LLC(2016). Copyright of the Dissertation is held by the Author.

All rights reserved.

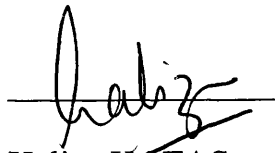
This work is protected against unauthorized copying under Title 17, United States Code.
Microform Edition © ProQuest LLC.

ProQuest LLC
789 East Eisenhower Parkway
P.O. Box 1346
Ann Arbor, MI 48106-1346

Plagiarism Statement

The report contained herein this project, is to the best of my knowledge my own work and does not in any way violate the school's policy on plagiarism. All work contained therein from relevant source have been referenced.

Yours faithfully,



Haliza KATAS

Acknowledgements

I would like to express my sincere gratitude to my supervisor, Professor H. Oya Alpar for not only giving me the opportunity to undertake Ph.D but also giving me an excellent guidance, support and encouragement throughout the project.

Special thanks to my fellow CDDR vaccine group and all my friends at the School of Pharmacy especially to Dr. Xiong Wei Li and Dr, S. Somavarapu for their technical assistances and useful advices.

I also would like to express my acknowledgement to Dr. Sterghios Moschos and Dr. Mark Lindsay of Biopharmaceutics Research Department, National Heart and Lung Institute, Imperial College London for giving me the chance to carry out further research with siRNA MAPK14.

To my beloved husband, Mr. Ahmad Muhazza Mustapha for his understanding and always being a true moral supporter in my life. Not to forget, to all my families in Malaysia especially to my dear father and mother for always supporting me.

Finally, I would like to acknowledge my sponsor, Ministry of Science, Technology and Innovative as well as Universiti Kebangsaan Malaysia for giving me an opportunity to improve myself to the highest level and funding my 3 years of study.

Abstract

A diverse range of viral and non-viral strategies has been developed more than a decade for a gene delivery such as plasmid DNA (pDNA) and oligodeoxynucleotides (ODN). Recently, the development has been extended to a newly discovered class of molecule, small interfering RNA (siRNA). The use of cationic and biodegradable polymeric particles has been widely utilised for delivery of these moieties. This study therefore, aimed to develop and investigate cationic polymers mainly chitosan and polyethylenimine (PEI) as well as their derivative particles; PLGA-PEI and -chitosan nanoparticles as siRNA carriers. Additionally, TAT-peptide has also been investigated as one of the delivery systems for siRNA.

Certain process and formulation parameters have been extensively studied with regards of physical and biological properties of the above systems to obtain an optimal delivery system. Physical properties particularly particle size, surface charge as well as particle morphology have been found to be influenced by certain parameters such as homogenisation or stirring rate, molecular weight and concentration of polymers as well as other processes involved in obtaining final products (e.g. centrifugation, freeze-drying).

In-vitro evaluations in cultured cells have revealed that the derivative PLGA-PEI nanoparticles are capable of transfecting mammalian cells with siRNA better than the parent compound, PEI. In addition to that, chitosan nanoparticles simply prepared by ionic gelation have been shown to be more competent as siRNA carriers compared to other types of chitosan-based nanoparticles investigated in this study, either chitosan-siRNA complexes or PLGA-chitosan nanoparticles. Although type and molecular weight of chitosan are important in delineating characteristics of particle size and surface charge (the two factors normally important in determining capability of particulate systems to transfect cells), it appears that the type and molecular weight of chitosan have not shown any obvious correlation with the level of the targeted gene knockdown by siRNA. TAT-peptide siRNA complexes were shown to be capable of successfully delivering siRNA into cells without the need of chemical conjugation and the effect could be enhanced by the addition of calcium into the particle suspensions before transfection.

Further investigations using chitosan nanoparticles prepared by ionic gelation, have been used to deliver MAPK-14 siRNA in the macrophage cell line, J774A.1 have shown that the system has the ability to transfect cells and subsequently allow the delivered siRNA to knockdown the targeted endogenous gene, MAPK p38 α with a sustained effect and a relatively low cytotoxicity.

In conclusion, the ability of these polymers as a carrier for siRNA is highly dependent on the method of preparation and their physicochemical characteristics of each of these polymeric particles.

CONTENT

Acknowledgement	i
Abstract	ii
Figure	vii
Table	xiv
1 INTRODUCTION	1
1.1 RNA interfering (RNAi)	1
1.1.1 Mechanism of RNAi actions	3
1.1.2 Comparison of siRNA to RNase-H dependent antisense	5
1.2 siRNA	6
1.2.1 Therapeutics of siRNAs	6
1.2.1.1 Cancer treatment	6
1.2.1.2 Treatment of viral infection	7
1.2.2 Stable induction of siRNA	8
1.2.2.1 siRNA expressing plasmid	9
1.2.2.2 Viral vectors	10
1.3 <i>In-vitro</i> delivery of siRNA	10
1.4 <i>In-vivo</i> delivery of siRNA in the animal	12
1.5 Delivery strategies	16
1.5.1 Liposomes	16
1.5.2 Cationic polymers	17
1.5.2.1 Polyethyleneimine	18
1.5.2.2 Chitosan	22
1.5.2.3 Cell penetrating Peptides (CPPs)	24
1.5.3 Biodegradable polymers	28
1.5.3.1 Micro- or nanoparticles preparation	33
1.5.3.1.1 Emulsification-solvent evaporation method	33
1.5.3.1.2 Emulsification diffusion method	34
1.6 Objectives of the study:	38
2 MATERIALS AND METHODS	39
2.1 Materials	39
2.1.1 Polymer	39
2.1.2 siRNA	39
2.1.3 pDNA	39
2.1.4 Others	39
2.2 Preparation of polyplexes	40
2.2.1 Polyethyleneimine	40
2.2.2 Chitosan	40
2.2.3 TAT-peptides	41
2.3 Preparation of cationic nanospheres	41
2.3.1 Emulsification diffusion method	41
2.3.1.1 PLGA-PEI nanoparticles	41
2.3.1.2 PLGA-chitosan nanoparticles	42
2.3.2 Ionic gelation of chitosan-TPP nanoparticles	43
2.4 Determination of particle size	43

2.5	Zeta potential determination	45
2.6	Determination of particle morphology	45
2.6.1	Transmission Electron Microscopy	45
2.6.2	Scan Electron microscopy	46
2.7	Quantification of chitosan incorporated into PLGA particles	46
2.8	Preparation of phosphate buffer	46
2.9	Adsorption of siRNA or pDNA onto the particles	47
2.9.1	PLGA-PEI nanoparticles	47
2.9.2	PLGA-chitosan nanoparticles	47
2.9.3	Chitosan-TPP nanoparticles	47
2.10	Quantification of siRNA	48
2.11	Quantification of pDNA	48
2.11.1	Depletion Method	48
2.11.2	Extraction method	48
2.11.3	PicoGreen® assays	49
2.12	Agarose gel electrophoresis	49
2.12.1	siRNA	49
2.12.2	pDNA	49
2.13	DNase protection assays for pDNA	50
2.14	Serum protection assay for siRNA	50
2.15	Determination of biological activity of pDNA and siRNA	51
2.15.1	Transfection studies for pDNA	51
2.15.2	Gene knockdown studies for siRNA	52
2.15.3	RNA preparation and reverse-transcriptase PCR (rt-pcr)	52
2.16	Cytotoxicity studies	53
 3 STUDIES OF PHYSICAL AND BIOLOGICAL CHARACTERISTICS OF PEI AS DELIVERY SYSTEMS FOR SIRNA		 54
3.1	siRNA-PEI polyplexes	54
3.1.1	Effect of nitrogen to phosphate ratio of PEI to siRNA on the physical characteristics of siRNA-PEI complexes	55
3.1.2	Comparison of physical characteristics of siRNA- to plasmid DNA-PEI complexes	57
3.2	PLGA-PEI nanoparticles	60
3.2.1	Effect of formulation parameters on PLGA-PEI nanoparticles	61
3.2.1.1	PLGA to PEI weight ratio	61
3.2.1.2	Type and concentration of surfactant	63
3.2.1.2.1	Poloxamer	63
3.2.1.2.2	Polyvinyl alcohol	67
3.2.1.3	PLGA polymer	68
3.2.1.4	Lyoprotectant agent	70
3.2.2	siRNA adsorption onto the surface of PLGA-PEI nanoparticles	74
3.2.2.1	Adsorption medium	77
3.2.3	Effect of ionic strength on the colloidal stability of PLGA-PEI nanoparticles	79
3.2.4	Serum protection of PLGA-PEI nanoparticles with adsorbed siRNA	80
3.3	<i>In-vitro</i> studies	83

3.3.1	Biological studies of siRNA-PEI complexes and PLGA-PEI with adsorbed siRNA	83
3.3.1.1	Effect of N/P ratio and stabiliser on siRNA silencing	83
3.3.1.2	Effect of cell line on siRNA silencing	86
3.3.2	Transfection efficiency of PLGA-PEI nanoparticles with adsorbed pDNA	88
3.3.2.1	Effect of PLGA to PEI weight ratio	88
3.3.2.2	Effect of stabilisers	89
3.4	Cytotoxicity effect	93
3.5	Conclusions	94
4	MANIPULATION OF CHITOSAN AS SAFER CARRIERS FOR SIRNA	96
4.1	Chitosan-siRNA complexes by simple complexation	96
4.1.1	Particle size	96
4.1.1.1	Effect of chitosan to siRNA concentration ratio	97
4.1.1.2	Effect of type and molecular weight of chitosan	98
4.1.1.3	Effect of solution pH	99
4.1.2	Particle surface charge	99
4.1.3	Comparing siRNA- to pDNA- chitosan complexes	101
4.1.3.1	Particle size	101
4.1.3.2	Surface charge	103
4.1.3.3	Binding efficiency	105
4.2	Chitosan-TPP nanoparticles using ionic gelation	106
4.2.1	Optimisation of the gelation process	106
4.2.1.1	Conditions of mixing	107
4.2.1.2	Molecular weight and concentration of chitosan	109
4.2.1.3	Chitosan to TPP weight ratio	110
4.2.2	Effect of pH on particle size and surface charge	111
4.2.3	Effect of ionic strength	112
4.2.4	Stability of chitosan-TPP nanoparticles	114
4.2.5	Association of siRNA to chitosan-TPP nanoparticles	115
4.2.5.1	siRNA adsorption onto the chitosan-TPP nanoparticles	115
4.2.5.1.1	Effect of chitosan-TPP nanoparticles to siRNA weight ratio	115
4.2.5.1.2	Effect of pH and ionic strength of adsorption medium	116
4.2.5.2	siRNA entrapment into chitosan-TPP nanoparticles	118
4.2.5.2.1	Particle size and surface charge	118
4.2.5.2.2	Effect of pH on chitosan-TPP nanoparticles with entrapped siRNA	118
4.2.6	siRNA binding and loading efficiency	119
4.2.7	siRNA stability in serum	120
4.3	Cationic PLGA-chitosan nanoparticles prepared by the emulsification diffusion method	122
4.3.1	Particle size	123
4.3.1.1	Homogenization speed	123
4.3.1.2	Effect of PVA concentration	123
4.3.1.3	Type and molecular weight of chitosan	125
4.3.2	Surface charge	126
4.3.3	Effect of centrifugation on particle size	127
4.3.4	Effect of PLGA polymer	129
4.3.5	Morphology	131
4.3.6	siRNA adsorption onto the surface of PLGA-chitosan nanoparticles	133
4.3.7	siRNA protection by PLGA-chitosan nanoparticles in serum	135
4.3.8	Comparison of PLGA-chitosan nanoparticles with adsorbed either siRNA or pDNA	136
4.4	Biological activity of siRNA	138
4.4.1	Chitosan-siRNA complex and chitosan-TPP nanoparticles associated with siRNA	138
4.4.2	PLGA-chitosan nanoparticles with adsorbed siRNA	143

4.5	Cytotoxicity assay	144
4.5.1	Chitosan-siRNA complex and chitosan-TPP nanoparticles associated with siRNA	144
4.5.2	PLGA-chitosan nanoparticles with adsorbed siRNA	146
4.6	Conclusions	147
5	THE USE OF TAT-PEPTIDE TO DELIVER SIRNA	149
5.1	siRNA-TAT-peptide complexes	149
5.1.1	Particle size	149
5.1.2	Particle surface charge	150
5.1.3	siRNA binding efficiency	151
5.1.4	siRNA protection by TAT-peptide in the serum	152
5.1.5	Biological activities of siRNA-TAT-peptide complexes	153
5.1.5.1	Effect of TAT-peptide to siRNA ratio	154
5.1.5.2	Effect of cell lines	155
5.1.5.3	Effect of calcium	155
5.1.6	Cytotoxicity assays of siRNA-TAT-peptide complexesA-TAT-peptide complexes	158
5.2	Conclusions	160
6	<i>IN-VITRO</i> INVESTIGATION TARGETING P38 MAPK	162
6.1	Chitosan-TPP nanoparticles as a vector	166
6.1.1	Particle size and surface charge	166
6.1.2	Serum stability	167
6.1.3	<i>In-vitro</i> study	169
6.2	Conclusion	175
7	GENERAL DISCUSSION AND FUTURE WORKS	176
7.1	Future works	184

FIGURE

Chapter 1: Introduction

- Figure 1.1: Petunia flower exhibiting sense cosuppression (RNAi) pattern of chalcone synthase silencing (courtesy of Beal 2005). 2**
- Figure 1.2: RNAi pathway (courtesy of Van Rij and Andino 2006, Van Rij and Andino 2005). 4**
- Figure 1.3: Hurdles of siRNA delivery *in-vivo* (courtesy of Xie *et al.* 2006). 13**
- Figure 1.4: Chemical structure of phosphodiester and chemically modified siRNA (adapted from Paroo and Corey 2004). 15**
- Figure 1.5: Schematic representation of the proton sponge theory. First, the complex of the DNA and the nanoparticles enters into the cell by endocytosis. The protonated amine groups of the nanoparticles capture H^+ in acidic environment of endosome that allows the endosome to pump in more H^+ and Cl^- ions. The pH value of the endosome is then increased and subsequently H_2O molecules are imported into the endosome by osmosis; lastly, DNA is released from the endosome due to endosomal swelling and rupturing (courtesy of Pang *et al.* 2002). 18**
- Figure 1.6: Structures of branched (a) and linear polyethyleneimine (b) (courtesy of Kakui *et al.* 2005). 19**
- Figure 1.7: Schematic representation of PEI mediated DNA uptake by mammalian cells. DNA is condensed into a small complex in the presence of PEI. This polyplex interacts with the negatively charged cell membrane and is internalized within endosomes. The polyplex is then released *via* a proton sponge effect resulting in an opening of the endosome. The polyplex can then progress to the nucleus (courtesy of Zhang *et al.* 2004). 20**
- Figure 1.8: Chemical structure of chitin and chitosan. 23**
- Figure 1.9: Different steps in CPP-mediated intracellular delivery. (1) Interaction of the CPP (represented as a green bar) with the cell-surface proteoglycans (in red), (2) The endocytic pathway, (3a) the degradative route to lysosomes in clathrin-mediated endocytosis, (3b) CPP ultimately reach the Golgi apparatus (in purple) or endoplasmic reticulum (ER, in grey) in caveolin-mediated endocytosis, (3c) Endosomal release (courtesy of Pujal *et al.* 2006). 26**
- Figure 1.10: Type of nanoparticles: Nanosphere (Top) and nanocapsule (bottom) (adapted from Brigger *et al.* 2002). 29**
- Figure 1.11: Structures of glycolic acid (PGA), lactic acid (PLA) and their PLGA copolymer. 31**
- Figure 1.12: Schematic description of proposed formation mechanism of PLA/PLGA nanoparticles by the emulsification diffusion method (courtesy of Kwon *et al.* 2001). 35**
- Figure 1.13: The diffusion process of partially water- miscible solvent into the aqueous phase (adapted form Choi *et al.* 2002). 36**

Chapter 2: Materials and methods

- Figure 2.1: Sonicator (Sanyo MSE Soniprep 150, Sanyo Gallempk PLC, Leicester, UK) used to prepare PLGA-PEI nanoparticles. 42**
- Figure 2.2: IKA[®]-WERKE T25 Basic S2 homogenizer (A) and Amicon Stirred Cell Model 8400, Millipore (B) used to create emulsion in particle preparation and to wash as well as collect particles by filtration, respectively. 43**
- Figure 2.3: Malvern Zetasizer[®] S (A) and Mastersizer S (B), Malvern, U.K for particle size measurement. 45**

Chapter 3: Studies of physical and biological characteristics of PEI as delivery systems for siRNA

- Figure 3.1: Effect of N/P ratio of PEI to siRNA on particle morphology of siRNA-PEI complexes. The complexes with a N/P ratio 5:1 were solid small rounded condensates but aggregation was seen for the complexes at a N/P ratio 2:1 which thought to be due to a relatively less pronounce of its particle surface charge. 56**
- Figure 3.2: Binding efficiency of pDNA (A) and siRNA (B) to the PEI at various N/P ratios. Electrophoresis was carried out using 4 % agarose (LMP) gel in TAE buffer (0.04 M Tris-Acetate, 0.002 M EDTA) and TBE buffer (4.45 mM tris-base, 1 mM sodium EDTA, 4.45 mM boric acid, pH 8.3) containing 0.5 µg/ml ethidium bromide at pH 8 for pDNA and siRNA, respectively. 20 µl of sample was loaded to each well with 1:6 dilution of loading dye (Blue/orange, Promega) and electrophoresis was carried out at a constant voltage of 80 and 55 V for pDNA and siRNA, respectively. Complete binding of pDNA and siRNA to the PEI were at a N/P ratio 1:1 and 5:1, respectively. 59**
- Figure 3.3: Comparison of particle morphology of pDNA-PEI complexes (A) and siRNA-PEI complex (B) at N/P ratio of 10:1. 60**
- Figure 3.4: Effect of PLGA to PEI weight ratio on particle size (n=3) and morphology of PLGA-PEI nanoparticles by Malvern Zetasizer[®] and SEM, respectively. Particles were prepared using 0.5% m/v poloxamer-188 as stabiliser. 62**
- Figure 3.5: Effect of PLGA to PEI weight ratio on the particle surface charge of PLGA-PEI nanoparticles stabilised by poloxamer-188 at 0.5% m/v (n=3). Standard deviation was ±1.1, ±1.3, ±0.5 and ±0.2 for the PLGA to PEI weight ratio of 5:1, 11:1, 29:1 and 59:1, respectively. 63**
- Figure 3.6: Poly(ethylene glycol) and poly(polypropylene glycol) molecular structures of poloxamer and their copolymer. 64**
- Figure 3.7: Effect of surfactant concentrations on the morphology of PLGA-PEI nanoparticles of 59:1 weight ratio after freeze-drying. A: 0.5% m/v poloxamer-188, B: 2% m/v poloxamer-188. 66**
- Figure 3.8: Schematic representation of molecular orientation of PVA bound to PLGA molecules at the surface of PLGA nanoparticles. A hydrophobic bonding between the hydroxyl groups of PVA molecules to the acetyl groups of PLGA results in strong adsorption of PVA on the surface of PLGA nanoparticles (courtesy of Murakami *et al.* 1999) 68**

- Figure 3.9: SEM images of PLGA-PEI nanoparticles made of PLGA 50:50 3A and 4A.** 70
- Figure 3.10: Effect of glycerol on particle size of PLGA-PEI nanoparticles (PLGA to PEI weight ratio of 29:1) after freeze-drying (n=3) as determined by Malvern Zetasizer[®]. Particle size of PLGA-PEI nanoparticles which higher than 1 μm was further analysed using Malvern Mastersizer[®] where the size was 4 ± 0.35 , 2.3 ± 0.15 and 1.7 ± 0.3 μm , for lyophilised particles made using poloxamer-188 (0.5% m/v), poloxamer-188 (5% m/v) and poloxamer-407 (5% m/v + 10% glycerol), respectively.** 73
- Figure 3.11: Effect of N/P ratio PLGA-PEI to siRNA on efficiency of siRNA adsorption onto the PLGA-PEI nanoparticles made using PVA (MW: 30-70 kDa). Electrophoresis was carried out using 4% agarose (LMP) gel in TBE buffer (4.45 mM tris-base, 1 mM sodium EDTA, 4.45 mM boric acid) containing 0.5 $\mu\text{g/ml}$ ethidium bromide at pH 8. A complete binding of siRNA to the PLGA-PEI nanoparticles was achieved at a N/P ratio 20:1.** 75
- Figure 3.12: Binding efficiency of pDNA adsorbed onto the PLGA-PEI nanoparticles made using PVA (MW: 30-70 kDa) at various N/P ratios. Electrophoresis was carried out using 1% agarose (LE) gel in TAE buffer (0.04 M Tris-Acetate, 0.002 M EDTA) containing 0.5 $\mu\text{g/ml}$ ethidium bromide at pH 8. A complete binding of pDNA to the PLGA-PEI nanoparticles was achieved at a N/P ratio 10:1.** 76
- Figure 3.13: Influence of adsorption medium on the siRNA loading efficiency adsorbed onto the PLGA-PEI nanoparticles (n=3). Distilled water used in this study was RNase free.** 78
- Figure 3.14: Effect of ionic strength on colloidal stability of PLGA-PEI nanoparticles at pH 7.4 and 5.8 (n=3).** 80
- Figure 3.15: Effect of serum (10% FBS in DMEM) on the stability of siRNA adsorbed onto the PLGA-PEI nanoparticles at 37°C. The integrity of siRNA was analysed by 15% polyacrylamide gel containing 7 M urea and TBE (0.089 M Tris base, 0.089 M boric acid, and 2 mM sodium EDTA, pH 8.3) buffer. siRNA bands were visualised under a UV transilluminator after staining for 40 min with a 1:1000 dilution of SYBR-Green II RNA gel stain (Molecular Probes) prepared in DEPC treated water.** 82
- Figure 3.16: Relative Response Ratio of PLGA-PEI nanoparticles with adsorbed siRNA in comparison to siRNA-Lipofectamine 2000 complexes in HEK 294 cells (n=9). Experiments were performed on growing cells at 5×10^3 cell/ well. PLGA-PEI nanoparticles appeared to be more efficient than PEI in transfecting cells with siRNA and showed a comparable effect with Lipofectamine 2000 (Invitrogen). Keynotes: Lipo-siRNA= Lipofectamine 2000-siRNA complexes, Lipo-siRNA M= Lipofectamine 2000-siRNA mismatch complexes and pGL3= control cells without siRNA treatment.** 85
- Figure 3.17: RT-PCR of total RNA extracted from HEK 293 cells treated with different formulations at 24 h post-transfection. RT-PCR analysis shows a reduction of mRNA level for firefly luciferase after treatment with the siRNA delivered by PLGA-PEI nanoparticles or Lipofectamine 2000 (Invitrogen) meanwhile PEI-siRNA complexes and siRNA alone show a minimal mRNA reduction. B-actin was used as an internal experimental control. Keynotes: pGL3= cells transfected with pDNA encoded firefly luciferase without siRNA treatment (negative control), non-treatment control = non-treated cells either with pDNA or siRNA (negative control), Lipo-siRNA= Lipofectamine 2000-**

- siRNA complexes (positive control), PLGA-PEI-siRNA= PLGA-PEI nanoparticles (PVA 13-23 kDa was used as stabiliser) with adsorbed siRNA (N/P ratio 35:1) and PEI-siRNA= PEI-siRNA complexes (N/P ratio 10:1). 86
- Figure 3.18:** Gene silencing effect of PLGA-PEI nanoparticles with adsorbed siRNA and siRNA-PEI complexes in CHO K1 cells (n=9). Experiments were performed on growing cells at 5×10^3 / well. Keynote: pGL3= control cells without siRNA treatment. 87
- Figure 3.19:** Relative Response Ratio of PLGA-PEI nanoparticles with adsorbed siRNA in comparison to siRNA-Lipofectamine 2000 complexes (n=9) in CHO K1 cells. Experiments were performed on growing cells at 5×10^3 / well. Keynotes: Lipo-siRNA= Lipofectamine 2000-siRNA complexes, Lipo-siRNA M= Lipofectamine 2000-siRNA mismatch and pGL3= control cells without siRNA treatment. 88
- Figure 3.20:** Effect of PLGA to PEI weight ratio of PLGA-PEI nanoparticles (poloxamer-188, 5% m/v) on pDNA transfection in HEK 293 cells at 24 h post-transfection (n=3). Experiments were performed on growing cells at 2×10^4 / ml/ well. Luciferase protein expression was measured using Luciferase assay Reagent (Promega). RLUs were normalised to total protein concentration in the cell extracts. Non-treatment cells were used as a negative control. 89
- Figure 3.21:** Effect of stabiliser types on pDNA transfection of PLGA-PEI nanoparticles with adsorbed pDNA (N/P ratio of 10:1) and stabiliser concentration used was 5.0% m/v (n=3). Experiments were performed on HEK 293 growing cells at 2×10^4 / ml/ well. Luciferase protein expression was measured using Luciferase assay Reagent (Promega). RLUs were normalised to total protein concentration in the cell extracts. Non-treatment cells were used as a negative control. 90
- Figure 3.22:** pDNA transfection efficiency of PLGA-PEI nanoparticles with adsorbed pDNA at different N/P ratio at 24, 48 and 72 h post-transfection (n=3). Experiments were performed in HEK 293 growing cells at 2×10^4 / ml/ well. Luciferase protein expression was measured using Luciferase assay Reagent (Promega). RLUs were normalised to total protein concentration in the cell extracts. Non-treatment cells were used as a negative control. Luciferase protein expression was measured using Luciferase assay Reagent (Promega). Non-treatment cells were used as a negative control. 92
- Figure 3.23:** Toxicity effect of PLGA-PEI nanoparticles with adsorbed siRNA in HEK 293 cells at 5×10^3 / well, n=3. Keynotes: M siRNA: Mismatch siRNA. 93
- Figure 3.24:** Toxicity effect of PLGA-PEI nanoparticles with adsorbed siRNA in CHO K1 cells at 5×10^3 / well (n=3). Keynotes: Lipo-siRNA= Lipofectamine 2000-siRNA complexes and Lipo-siRNA M= Lipofectamine 2000-siRNA mismatch. 94

Chapter 4: Manipulation of chitosan as safer carriers for siRNA

- Figure 4.1:** The effect of chitosan concentration or chitosan to siRNA weight ratio (in bracket) on mean particle size of siRNA-chitosan complexes using different type and molecular weight of chitosan as determined by Malvern System 4700c Submicron particle analyser (n=3). 98
- Figure 4.2:** Effect of chitosan concentration on particle surface charge of chitosan-siRNA complexes (n=3). 100

Figure 4.3: Comparison of particle surface charge in RNase free water and acetate buffer (pH 4.5, 0.1 M) for chitosan-siRNA complexes using chitosan hydrochloride, CI113.	101
Figure 4.4: Comparison of particle size of chitosan-siRNA and -DNA complexes with increasing concentration of chitosan or chitosan to polyanion weight ratio (in bracket) as determined by Malvern System 4700c Submicron particle analyser, (n=3).	102
Figure 4.5: Morphology of pDNA-chitosan (A) and siRNA-chitosan (B) complexes at weight ratio of 2.5: 1 of chitosan to pDNA or siRNA.	103
Figure 4.6: Comparison of particle surface charge between siRNA- and pDNA-chitosan complexes. A: CI213, 270 kDa and B: CI113, 110 kDa (n=3).	104
Figure 4.7: Binding efficiency of pDNA-chitosan complexes (A) and siRNA-chitosan complexes (B) at different chitosan concentrations.	106
Figure 4.8: Effect of chitosan concentrations on particle size of chitosan-TPP nanoparticles made from four different molecular weights of chitosan as determined by Malvern Zetasizer® (n=3). Chitosan-TPP nanoparticles were prepared by ionic gelation under a low rate of magnetic stirring (1100 rpm). The TPP concentration was fixed at 0.84 mg/ml and the chitosan concentration was ranging from 2 to 5 mg/ml	110
Figure 4.9: Effect of chitosan solution pH on particle size of chitosan-TPP nanoparticles (n=3) as determined by Malvern Zetasizer®.	112
Figure 4.10: Effects of ionic strength on ionic-gelation of chitosan-TPP nanoparticles at pH 5 as determined by Malvern Zetasizer® (n=3).	113
Figure 4.11: Binding capacity of siRNA onto the chitosan-TPP nanoparticles as determined by 4% agarose (LMP) gel electrophoresis in TBE buffer, pH 8 containing 0.5 µg/ml ethidium bromide.	116
Figure 4.12: Effect of pH on Z-ave diameter and particle surface charge of chitosan-TPP-siRNA as determined by Malvern Zetasizer® (n=3). Keynote: Bar represents Z-ave diameter (nm) and line represents surface charge (mV)	119
Figure 4.13: Binding efficiency of siRNA entrapped into chitosan-TPP nanoparticles as determined by 4% agarose (LMP) gel electrophoresis in TBE buffer, pH 8 containing 0.5 µg/ml ethidium bromide.	120
Figure 4.14: Electrophoretic mobility of chitosan-TPP-siRNA nanoparticles following incubation with FBS. The integrity of the siRNA was analysed by 15% polyacrylamide gel containing 7 M urea and TBE (0.089 M Tris base, 0.089 M boric acid, and 2 mM sodium EDTA, pH 8.3) buffer. siRNA bands were visualised under a UV transilluminator after staining for 40 min with a 1:1000 dilution of SYBR-Green II RNA gel stain (Molecular Probes) prepared in DEPC treated water. Image A: 5% FBS and image B: 50% FBS.	122
Figure 4.15: Effect of type and molecular weight of chitosan on particle size of PLGA-chitosan nanoparticles as determined by Malvern Zetasizer® (n=3).	125
Figure 4.16: Surface charge of PLGA-chitosan nanoparticles at different concentrations of chitosan (n=3).	126
Figure 4.17: Effect of centrifugation on particle size of PLGA-chitosan nanoparticles after two cycles of centrifugation as determined by Malvern Zetasizer®, U.K (n=3). A drop in particle size was observed for the PLGA-chitosan nanoparticles after centrifugation. PLGA-chitosan nanoparticles were prepared by emulsification diffusion method made from different types and molecular weights of chitosan.	128

- Figure 4.18: Effect of filtration and freeze-drying on particle size of PLGA-chitosan nanoparticles made from different types and molecular weights of chitosan, (n=3). Particle size was measured using Malvern Zetasizer® (Malvern, UK). 129**
- Figure 4.19: Effect of chitosan concentration on particle morphology of PLGA-chitosan nanoparticles (2% m/v PVA). 132**
- Figure 4.20: Effect of washing technique on particle morphology of PLGA-chitosan nanoparticles (2% m/v PVA). A and C: PLGA-G113 and -G213 washed and collected by centrifugation, B and D: PLGA-G113 and -G213 washed and collected by filtration. 133**
- Figure 4.21: siRNA binding efficiency of various PLGA 3A-chitosan nanoparticles. Lane 1: Free siRNA, Lane 2: PLGA nanoparticles (without chitosan), Lane 3-5 respectively are: 1, 3 and 5 mg/ml of PLGA-C1113 nanoparticles, Lane 6-8 respectively are: 1, 3 and 5 mg/ml of PLGA-C1213 nanoparticles, Lane 9-11 respectively are 1, 3 and 5 mg/ml of PLGA-C1113 nanoparticles with heparin, Lane 12-14 respectively are: 1, 3 and 5 mg/ml of PLGA-C1213 nanoparticles with heparin and Lane 15: PLGA nanoparticles with heparin. 134**
- Figure 4.22: siRNA binding efficiency of various PLGA 2A-chitosan nanoparticles. Lane 1: Free siRNA, Lane 2-4 respectively are: 1, 3 and 5 mg/ml of PLGA-C1113 nanoparticles with heparin and Lane 5-7 respectively are 1, 3 and 5 mg/ml of PLGA-C1213 nanoparticles with heparin, Lane 8-10 respectively are: 1, 3 and 5 mg/ml of PLGA-C1113 nanoparticles and Lane 11-13 respectively are: 1, 3 and 5 mg/ml of PLGA-C1213 nanoparticles. 135**
- Figure 4.23: Serum protection assay (DMEM containing 50% FBS) of naked siRNA (A) and PLGA-chitosan with adsorbed siRNA (B) at different time points. The integrity of the siRNA was analysed by 15% polyacrylamide gel containing 7 M urea and TBE (0.089 M Tris base, 0.089 M boric acid, and 2 mM sodium EDTA, pH 8.3) buffer. siRNA bands were visualised under a UV transilluminator after staining for 40 min with a 1:1000 dilution of SYBR-Green II RNA gel stain (Molecular Probes) prepared in DEPC treated water. 136**
- Figure 4.24: Effect of chitosan molecular weight and method of siRNA association to the chitosan nanoparticles on percentage of gene knockdown of pGL3 luciferase in CHO K1 cells (5×10^3 cell/ well) at 24 and 48 h post transfection (n=6). Keynotes: Lipo= Lipofectamine 2000 and siRNA M= siRNA mismatch. 139**
- Figure 4.25: Relative Response Ratio (RRR) of chitosan nanoparticles prepared from chitosan glutamate, G213 in CHO K1 and HEK 293 cells (5×10^3 cell/ well) at 24 h post-transfection. Keynotes: Lipo-siRNA M= Lipofectamine 2000-siRNA mismatch complexes, pGL3= pDNA encoded luciferase gene delivered by lipofectamine 2000. 142**
- Figure 4.26: RT-PCR analysis of firefly luciferase downregulation by chitosan-TPP nanoparticles with entrapped siRNA in CHO K1 cells which transiently integrated with pGL3 luciferase control (at 24 h post-transfection). Lane A: untreated cells, Lane B: Lipofectamine 2000-mismatch siRNA, Lane C: chitosan-TPP nanoparticles with entrapped siRNA and Lane D: Lipofectamine 2000-siRNA. B-actin was used as a control. 142**
- Figure 4.27: Effect of nanoparticles to siRNA weight ratio on percentage of gene knockdown by PLGA-chitosan nanoparticles with adsorbed siRNA targeting against firefly luciferase at 24 h post-transfection in HEK 293 cells (n=3). Gel**

image shows downregulation of firefly luciferase mRNA by PLGA-chitosan nanoparticles with adsorbed siRNA in HEK 293 cells transiently integrated pGL3 luciferase gene at 24 h post-transfection. Lane 1: Lipofectamine 2000, Lane 2: PLGA-chitosan (CI113) nanoparticles, PLGA-chitosan (CI213) nanoparticles and Lane 4: untreated cells. 144

Figure 4.28: Effect of chitosan molecular weight and method of preparation on percentage of cells viability of CHO K1 with cells density of 5×10^3 cell/ well (n=3). Keynotes: non-treatment cells were used as control, lipo-siRNA= lipofectamine 2000-siRNA complexes and Lipo-siRNA M= Lipofectamine 2000-siRNA mismatch complexes. 146

Figure 4.29: Effect of PLGA-chitosan nanoparticles with adsorbed siRNA on percentage of HEK 293 (5×10^3 cell/ well) cell viability (n=3). Keynotes: 100:1, 300:1, 500:1 PLGA-CI113 and PLGA-CI213 respectively represent the varying weight ratio of PLGA-chitosan nanoparticles of CI113 and CI213 to siRNA. Lipo-siRNA= Lipofectamine 2000-siRNA complexes. 147

Chapter 5: The use of TAT-peptide to deliver siRNA

Figure 5.1: Particle surface charge of siRNA-TAT-peptide complexes at different TAT-peptide to siRNA weight ratio (n=3). 151

Figure 5.2: Binding efficiency of siRNA to TAT-peptide at different TAT-peptide to siRNA weight ratio as determined by 4% agarose (LMP) gel electrophoresis in TBE buffer, pH 8 containing 0.5 μ g/ml ethidium bromide. 152

Figure 5.3: Effect of serum (10% FBS) on stability of siRNA alone (A) and siRNA-TAT-peptide complexes (B) with time. The integrity of the siRNA was analysed by 15% polyacrylamide gel containing 7 M urea and TBE (0.089 M Tris base, 0.089 M boric acid, and 2 mM sodium EDTA, pH 8.3) buffer. siRNA bands were visualised under a UV transilluminator after staining for 40 min with a 1:1000 dilution of SYBR-Green II RNA gel stain (Molecular Probes) prepared in DEPC treated water. 153

Figure 5.4: Effect of calcium on biological activities of siRNA-TAT-peptide complexes in HEK 293 cell with cells density of 5×10^3 cell/ well at 24 h post-transfection (n=3). Keynotes: pGL3 alone= without siRNA treatment (negative control). * The difference between the addition of calcium at 5 or 6 mM to the suspension of TAT-peptide-siRNA complexes and TAT-peptide-siRNA complexes (without calcium) was significant ($p < 0.05$). 156

Figure 5.5: Comparison of gene silencing efficiency of siRNA-TAT-peptide complexes with increasing molar ratios of calcium compared to the negative control of siRNA-Lipofectamine 2000 complexes (Lipo-siRNA) and positive control of without siRNA treatment (pGL3) (n=3). Keynote: Lipo-siRNA M= Lipofectamine 2000-siRNA mismatch complexes, TAT-peptide-siRNA=siRNA-TAT-peptide-complexes at a TAT-peptide to siRNA ratio 20:1. 158

Figure 5.6: Effect of siRNA-TAT-peptide complexes at different TAT-peptide to siRNA ratio on percentage of CHO K1 cells viability 5×10^3 cell/ well after 24 and 48 h of post-incubation (n=6). Keynote: Lipo-siRNA= Lipofectamine 2000 siRNA complexes. 159

Figure 5.7: Effect of calcium at various molar concentrations on percentage of HEK 293 cell viability (5×10^3 cell/ well) (n=3). Keynotes: Lipo-siRNA=

Chapter 6: *In-vitro* investigation targeting p38 MAPK

Figure 6.1: The p38 mitogen activated protein (MAP) kinase (MAPK) activation cascade. This schematic diagram shows activation pathways which leads to the activation of p38 MAPK isoforms. Various stimuli or stresses that act on cells may cause activation of p38 MAPK isoforms through the sequential activation of the MAP kinase kinase kinases (MAP3K), which phosphorylate and activate the MAP kinase kinases (MAP2K). These in turn phosphorylate the p38 MAPKs, which on activation, are able to phosphorylate several targets including downstream kinases as well as other effectors (courtesy of Newton and Holden 2006). Keynotes: ARE, AU response element; ASK1, apoptosis signal-regulating kinase 1; ATF, activating transcription factor; CHOP, CCAAT/enhancer-binding protein (C/EBP) homologous protein; cPLA₂, cytosolic phospholipase A₂; CREB, cyclic AMP response element binding protein; eIF4E, eukaryotic initiation factor 4E; HMG-14, high mobility group 14; hsp27, heat shock protein 27; MAPK, mitogen-activated protein kinase; MAP2K, mitogen-activated protein kinase kinase; MAP3K, mitogen-activated protein kinase kinase kinase; MAPKAP-K (or MK), MAPK-activated protein kinase; MEF2C, myocyte-specific enhancer binding factor 2C; MEKK, mitogen-activated protein kinase/extracellular protein kinase kinase kinase; MKK, MAP kinase kinase; MNK, MAPK-interacting kinase; MSK, mitogen- and stress-activated protein kinase; PRAK, p38-related/activated protein kinase; STAT, signal transducer and activator of transcription; TAK, TGFβ activated kinase; TAOs, thousand and one kinases; TBP, TATA-binding protein; TTP, Tristetraprolin, TCF, ternary complex factor; 5LO, 5-lipoxygenase; hnRNP, heterogenous nuclear ribonuclear protein. 164

Figure 6.2: siRNA binding efficiency to the chitosan-TPP nanoparticles by gel retardation assay using 20% polyacrylamide gel in TBE buffer (pH 8), followed by 40 min staining with Sybr Gold (Invitrogen). 167

Figure 6.3: siRNA stability in 50% v/v mouse serum. A: naked siRNA, B: siRNA entrapped in chitosan-TPP nanoparticles (C1113) and C: siRNA entrapped in chitosan-TPP nanoparticles (G213). 168

Figure 6.4: Percentage of gene expression for naked siRNA, chitosan-TPP-siRNA (chi-siRNA) nanoparticles and Lipofectamine-2000-siRNA complexes (lipo-siRNA) in J774A.1 cells at different time-points post-transfection, (n=9). Gene expression of the total RNA from the lysis cells was analysed by quantitative real-time PCR using primers and taqman probe. In addition, 18S rRNA was used as an internal standard (housekeeping gene). Transfections were performed in J774A.1 cells at density of 1 x 10⁴ cells/ well. * The difference between chitosan-TPP-siRNA nanoparticles and Lipofectamine 2000-siRNA complexes was significant (p<0.05). 171

- Figure 6.5: Effect of dose and duration of incubation with naked siRNA, trasfecting agents or combination of both on percentage of J774A.1 cell viability, n=9. 173**
- Figure 6.6: Cell viability of formulations in L929s cells at 24 h post-incubation, n=9. Keynotes: Lipo-siRNA = Lipofectamine 2000-siRNA and chitosan=chitosan-TPP nanoparticles. 174**
- Figure 6.7: Cell viability of formulations in L929s cells at different time-points, n=9. Keynotes: Lipo-siRNA=Lipofectamine 2000-siRNA MAPK14 complexes and Lipo-siRNA M= Lipofectamine 2000-siRNA mismatch. 175**

TABLE

Chapter 1: Introduction

Table 1.1: Examples of biodegradable polymers used in drug delivery (adapted from Dunn and Ottenbrite 1991).	30
Table 1.2: Biodegradation kinetics. Information from Alkermers® - Medisorb *For medisorb polymers the standard end group is lauryl ester (capped) unless the polymer is marked either A, M or C. 'A' polymers contain a free carboxyl end group (uncapped), 'M' polymers contain a methyl ester end group (capped) and 'C' polymer are custom polymer (www.alkermers.com/polymer/products.html).	32
Table 1.3: Solubility of organic solvent in water or PLGA in organic solvent (Adapted from Song <i>et. al.</i> 2006).	37

Chapter 3: Studies of physical and biological characteristics of PEI as delivery systems for siRNA

Table 3.1: Effect of N/P ratio on polyplexes particle size and size distribution (n=3) as determined by Malvern System 4700c Submicron particle analyser (Malvern, U.K). Keynotes: * particle size was inaccurate due to a high polydispersity index.	55
Table 3.2: Influence of PEI to pDNA N/P ratio on particle size as well as size distribution and surface charge of pDNA-PEI complexes determined by Malvern System 4700c Submicron particle analyser and Malvern ZetaMaster®, respectively (n=3).	57
Table 3.3: The difference properties of poloxamer-188 and -407 used in the study.	65
Table 3.4: Effect of type and concentration of poloxamer on particle size of PLGA-PEI nanoparticles as determined by Malvern Zetasizer® (n=3).	65
Table 3.5: Effect of PVA molecular weight and concentration on particle size of PLGA-PEI nanoparticles at a PLGA to PEI weight ratio 29:1 as determined by Malvern Zetasizer® before washing (n=3). A smaller particle size and PI were observed with the increase of PVA concentration from 0.5 to 5 % m/v.	67
Table 3.6: Effect of polymer type on particle size and surface charge of PLGA-PEI nanoparticles determined by Malvern Zetasizer® (n=3).	69
Table 3.7: Advantages and disadvantages of several lyoprotectant agents based on polysaccharides.	72
Table 3.8: Effect of glycerol on particle surface charge and pDNA loading efficiency of PLGA-PEI nanoparticles (n=6).	74
Table 3.9: Effect of PVA concentrations on pDNA loading efficiency of PLGA-PEI nanoparticles with adsorbed siRNA at N/P ratio of 3:1 (n=3).	77

Chapter 4: Manipulation of chitosan as safer carriers for siRNA

- Table 4.1: Effect of mixing conditions on particle size and size distribution (PI) of chitosan-TPP nanoparticles as determined by Malvern Zetasizer[®]. Chitosan to TPP weight ratio of 6:1 (n=3). 108**
- Table 4.2: The effects of NaCl molar concentration on siRNA loading efficiency of chitosan-TPP nanoparticles at weight ratio of 100:1 (n=3). 117**
- Table 4.3: Effect of PVA concentration on particle size of PLGA nanoparticles prepared at homogenization speed of 17 500 rpm before and after centrifuging as determined by Malvern Zetasizer[®] (n=3). 124**
- Table 4.4: Effect of trehalose on particle size and polydispersity index of PLGA-chitosan nanoparticles as determined by Malvern Zetasizer[®] (n=3). Keynotes: BC= before centrifugation and AC= after centrifugation. *Particle size was further measured using Malvern Mastersizer and the particle size was 4 ± 0.8 , 5 ± 1.1 and 3.5 ± 0.6 μm for C1113 AF, C1213 AF and 10% trehalose C1213, respectively. 131**
- Table 4.5: Relationship between particle surface charges with pDNA loading efficiency of PLGA-chitosan nanoparticles with adsorbed pDNA. pDNA adsorption was carried out at nanoparticle to pDNA ratio of 100:1 (n=3). 137**

Chapter 5: The use of TAT-peptide to deliver siRNA

- Table 5.1: Effect of TAT-peptide to siRNA weight ratio on the particle size of siRNA-TAT-peptide complexes as determined by Malvern System 4700c Submicron particle analyser (n=3). *The particle size was inaccurate due to high polydispersity index. 150**

Chapter 6: *In-vitro* investigation targeting p38 MAPK

- Table 6.1: Particle size and surface charge of chitosan-TPP nanoparticles with entrapped siRNA, n=9. 166**

Chapter 1

Introduction

1 Introduction

Antisense technology is a tool with significant potential for controlling cellular processes and has been pursued for target validation as well as for a potential therapeutic agent. The term antisense therapeutic encompasses several types of nucleic acids that have the ability to modulate gene expression such as antisense oligonucleotides (ODNs), ribozymes (RNA enzymes) and DNAzymes (DNA enzymes). This type of approach could selectively silence any gene product before it is translated where the targeted mRNA transcript hybridizes in a sequence manner to homologous DNA, RNA or chemically altered nucleic acids, thereby inhibits their expression post-transcriptionally (Shuey *et al.* 2002, Dean 2001).

The design and development of antisense oligodeoxynucleotides (ODNs) for the treatment of genetically based diseases has been extensively investigated for over a decade. Several types of ODNs have also been undergoing clinical trial evaluations in the treatment of malignant and infectious diseases such as chronic and acute myelogenous leukemias as well as AIDS (Hudson *et al.* 1996, Agrawal and Akhtar 1995). However, its success as a therapeutic so far has been disappointing and has failed to fulfil its initial promise. To date, there is only one approved product on the market, a phosphorothioate ODN (VitraveneTM) that has been approved by the FDA for the treatment of cytomegalovirus retinitis (Lebedeva *et al.* 2000, Anderson *et al.* 1996).

1.1 RNA interfering (RNAi)

Recently, gene silencing by RNA interference (RNAi) technology has proven to be an efficient and convenient tool for controlling gene expression in cultured mammalian cells. RNAi works by blocking expression of specific proteins within the cell at the mRNA level using short nucleic acid fragments (Beal 2005). Therefore, the use of RNAi for inhibiting gene expression in animals could provide the basis for new therapeutic strategies. RNAi was first reported in plants (Napoli *et al.* 1990) and initially considered as a bizarre phenomenon confined to some species as reviewed by Cogoni and Macino (2000) which has been termed as Post-Transcriptional Gene Silencing (PTGS). It was discovered serendipitously by Richard Jorgensen and researchers at the University of Arizona in the late 1980s, during a search for transgenic petunia flowers that were expected to be more purple in colour. However, the

introduction of a gene encoding a pigment producing enzyme, *chalcone synthase*, resulted in the flowers losing their colour or becoming white (Napoli *et al.* 1990).



Figure 1.1: Petunia flower exhibiting sense cosuppression (RNAi) pattern of chalcone synthase silencing (courtesy of Beal 2005).

Over the past few years, the investigation of this phenomenon has then been extended to bacterial and differentiated cultured mammalian cells and the term interfering RNA (RNAi) was used to describe this phenomenon in animals. RNAi was originally described in the nematode worm *Caenorhabditis elegans*. It is a naturally occurring process that induces gene silencing, triggered by long double stranded RNA (dsRNA) molecules complementary to mRNA sequences, that are introduced into cells either experimentally or are derived from endogenous sources such as replicating viruses and mobilisation of transposable genetic elements (transposon) (Leung and Whittaker 2005, Tijsterman *et al.* 2002).

1.1.1 Mechanism of RNAi actions

These long dsRNAs (replicating viruses, transposons) are processed by an RNase III enzyme called Dicer into discrete short interfering RNA (siRNA), with two-nucleotide 3' overhang and 5'-phosphate termini (Bernstein *et al.* 2001). Subsequently, this siRNA is presented to RNA-induced silencing complex (RISC) which contains a helicase responsible for unwinding the duplex strands of siRNA and is capable of recognising the target RNA complementary to the guide strand of the siRNA. Each strand which is incorporated with RISC is then associated to the target specific mRNA, resulting in mRNA cleavage.

Recent reports however, have revealed the involvement of small RNA in the RNAi pathway which is known as microRNA (miRNA) and it has been identified as part of the RNAi machinery. miRNA is a class of small and non-coding RNAs encoded in the genome (Van Rij and Andino 2006, Bartel 2004), composed of ~22 nucleotides which was coincidentally discovered during genomic screening in *C. elegans* (Chalfie *et al.* 1981). These naturally occurring miRNAs are synthesized in the nucleus as long precursor forms, ranging from several hundreds to thousands of base pairs known as primary precursor miRNA (pri-pre-miRNA). Subsequently, these primary miRNAs are transcribed into pre-miRNAs (~70 nucleotides of stem-loop structures) by Drosha (RNase III) which are then exported to the cytoplasm by the Exportin-5-Ran-GTP complex. In the cytoplasm, miRNAs are processed by the Dicer to form mature miRNAs. The mature miRNAs are loaded into a RISC complex which guides inhibition of translation (Van Rij and Andino 2006). Therefore, it is clear that a crucial difference between siRNA and miRNA is their mechanism of action. siRNA forms a perfect duplex with the target mRNA, leading to the specific mRNA cleavage with the cleaved mRNA degraded by cellular RNase. Contrary to siRNA, miRNA induces translational arrest without destroying the target mRNA as its sequence usually contains one or several mismatch nucleotides or insertions, leading to the formation of small bulges following hybridisation with their complementary mRNA (Pekarik 2005).

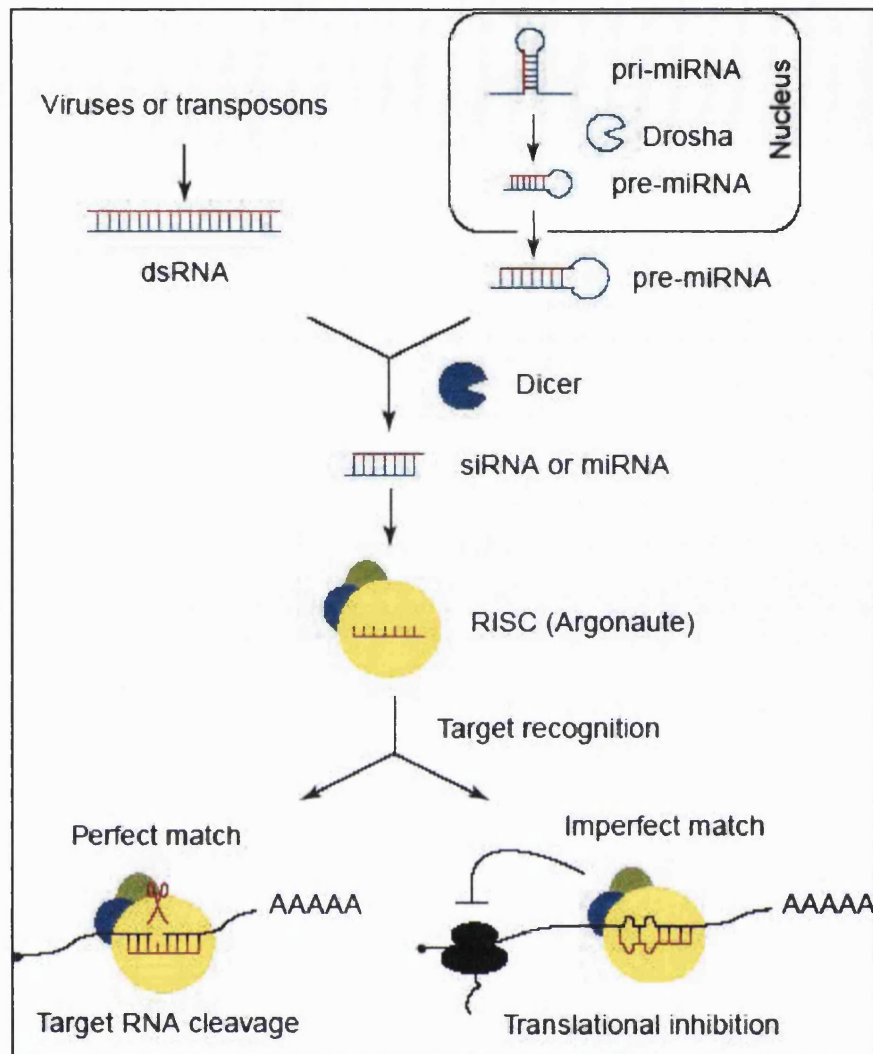


Figure 1.2: RNAi pathway (courtesy of Van Rij and Andino 2006, Van Rij and Andino 2005).

In *C. elegans* and *D. melanogaster*, specific regulation of genes can be achieved by introducing long dsRNA through direct injection (Fire *et al.* 1998), feeding them with bacteria expressing dsRNA (Timmons *et al.* 2001) or soaking in a solution of dsRNA (Tabara *et al.* 1998). In mammalian cells however, a sequence-specific RNAi-mediated gene silencing was difficult to demonstrate due to a non-specific shutdown of protein production as reviewed by Schiffelers *et al.* 2004. The introduction of long dsRNA (>30 nucleotides) in mammalian cells may activate dsRNA-dependent protein kinase (PKR) and 2', 5' oligoadenylate synthetase. This leads to the production of type 1 interferon which subsequently results in the generalized inhibition of translation and the induction of apoptosis (reviewed in Schiffelers *et al.* 2004, Sioud and Sørensen

2003, Sen 2001). Therefore, the use of RNAi in mammalian cells was initially hampered by these non specific responses until researchers discovered that these could be circumvented by using short dsRNA or siRNA as it has been shown to induce sequence specific mRNA degradation which could bypasses the activation of non-specific responses (Elbashir *et al.* 2001).

1.1.2 Comparison of siRNA to RNase-H dependent antisense

siRNA shares more features with antisense oligodeoxynucleotides (ODN) compared to plasmid DNA (pDNA) as they are short nucleic acids of only approximately 20 bases. They both also induce post-transcriptional gene silencing by targeting target mRNAs, leading to the cleavage of the target mRNA. Both of them are capable of inducing the degradation of targeted mRNA, but this effect is mediated by different cellular mechanisms; activation of RISC for siRNA and on the other hand, activation of RNase-H or steric inhibition for ODNs. Duplex siRNA is also shown to be more stable than single stranded antisense ODNs and a previous study by Bertrand *et al.* (2002) has reported that siRNA is more stable in both cell extracts and inside cells than the ODNs. Therefore, the effect triggered by siRNA delivered by Cytfectin GSV in Hela-GFP cells is higher and last longer than ODN (Bertrand *et al.* 2002). siRNA also requires less chemical modification to achieve a satisfactory half-life in cell medium (Braasch *et al.* 2003) and only a lower concentration of siRNA is required compared to ODN to achieve an equivalent level of knockdown (Bertrand *et al.* 2002, Fire *et al.* 1998). Therefore, siRNA has often shown a better potency than ODN. Nevertheless, a potential advantage of ODN is its ability to target pre-mRNA in the nucleus (Vickers *et al.* 2003).

Due to the advantages of siRNA, it appears that this approach is more robust and efficient in comparison to the antisense and ribozymes technologies. Moreover, siRNA has gained such tremendous attentions as a promising new class of therapeutics due to its ease of synthesis and cost-effective approach (Lee and Sinko 2006). In contrast, ODNs have failed to be used as effective gene knockdown tools because of the requirement of an extensive experimental testing just to find effective target sites within the gene of interest (Behlke 2006). Finally, the RNAi strategy which is also based on nucleic acid technology but activates a normal cellular process is believed to be more acceptable by the public (Beal 2005) to be used as a therapeutic agent. Nevertheless,

antisense ODN technology should be considered as an alternative, particularly in the case of genes that are refractory to siRNA mediated degradation or when further controls are required to definitively establish the role of a target (Cocks and Theriault 2004).

1.2 siRNA

The siRNA is a double stranded RNA (dsRNA) (Hutvagner and Zamore 2002) of 21-25 nucleotides in length. The ability of siRNA to silence gene expression in somatic mammals has provided many researchers a new strategy in the treatment of genetic-based diseases (Sioud 2004) and it has also been widely used as an experimental tool for the target validation of functional genes. Briefly, the administered siRNAs are incorporated into a RNA-induced silencing complex (RISC) through the natural RNAi pathway and consequently silence gene expression as described in the earlier section.

1.2.1 Therapeutics of siRNAs

Since researchers have discovered that chemically synthesized siRNA which is exogenously introduced into mammalian cells could mediate the degradation of targeted RNA with high specificity and efficiency, siRNA has been pursued as a potential therapeutic agent in the treatment of a wide range of diseases where aberrant gene expression is involved such as cancers and infectious diseases.

1.2.1.1 Cancer treatment

In the case of cancer, the potential targets for siRNA technology are oncogenic and mutant tumour suppressing genes (Sioud 2004) as well as growth factors (Xie *et al.* 2006). For example, by targeting antiapoptotic BCL-2 genes and its related proteins that regulate apoptosis and mediate the resistance of cancer to a wide spectrum of chemotherapeutic drugs (Hannon, 2002), this results in the destruction of targeted mutated p53 but not the wild type products. The ability of siRNA to discriminate between mutant and wild type alleles would therefore provide a more attractive treatment option than conventional chemotherapy which lacks the selectivity to distinguish tumour cells from the normal cells (Uprichard 2005).

Furthermore, overexpression of wide ranges of gene in cancers is an attractive target for siRNA silencing like BCL-2 (chronic lymphocytic leukaemia/lymphoma) and

ABCB1 genes. The use of siRNA has been shown to enhance intracellular accumulation of various chemotherapeutic agents and selectively restore chemosensitivity by inhibiting ABCB1 or BCL-2 gene expression. Overexpression of ABCB1 gene products in many human tumors has also been reported to cause one form of multi-drug resistance which leads to the reduction of the intracellular concentration of drugs (Sioud 2004, Tsuruo *et al.* 2003). Therefore, the combination of siRNA with other existing chemotherapeutic drugs may become a promising therapy for cancer. In fact, siRNA has been used as a complementary chemotherapy for the treatment in patients that develop multi-drugs resistant due to an overexpression of the multi-drug transporter gene, MDR1 and MDR1 gene suppression by siRNA has been reported to re-sensitize cells to the effect of chemotherapy (Uprichard 2005, Cioca *et al.* 2003, Zangemeister-Wittke 2003, Futami *et al.* 2002). Besides these, there are many more types of genes that have been investigated as potential target genes in the treatment of cancers such as survivin (regulator in mitosis), Stat3 (signal transduction protein), telomeric DNA (essential for maintaining immortalized state of cells) and others.

1.2.1.2 Treatment of viral infection

In plants and insects, RNAi is well established as one of the host organism's defence mechanism against viruses; however the involvement of RNAi in mammalian cells for the similar function is still under investigation. It has been argued that mammals have evolved highly sophisticated and effective systems of innate and adaptive immune responses to infections based on protein recognition and therefore, they might not need the more ancient nucleic acid- based response (Van Rij and Andino 2006).

Nevertheless, several researchers have exploited RNAi technology for the development of antiviral agents as the genome sequences of a range of pathogenic viruses is now available (<http://www.ncbi.nlm.nih.gov/genomes/VIRUSES/viruses.htm>) which make it possible to target a conserved region and limit the ability of virus to create escape mutants (Ren *et al.* 2006). In addition, siRNA appears to be ideal to combat infection by viruses as most of them are RNA viruses and unlike vaccines, its efficacy is not related to the status of the host immune system (Lee and Sinko 2006).

Recently, synthetic siRNA or plasmid-driven expression of short hairpin RNA (shRNA) has been found can inhibit viral infection of human cells by targeting viral

genes that are vital for virus replication or production, as well as host genes that are responsible for the virus entry as reviewed by Leung and Whittaker (2005). These antiviral effects could be achieved by targeting the viral genome, for example, targeting the HIV-1 major regulating genes such as *rev*, *tat*, *nef* and *vif* which could reduce HIV-1 replication and virus production. Furthermore, inhibiting cellular genes that are required for HIV-1 infection or entry into the cells such as the CD4 surface receptor and chemokine receptors CCR5 and CXCR4, results in the decrease of expression of these receptors and reduced HIV-1 infection. The RNAi approach has also been used in the treatment of Hepatitis B infection (HBV), or as an adjuvant therapy to lamivudine (antiviral agent based on nucleoside analogs) as it can reduce the levels of HBV viral transcript and protein even in the absence of active viral replication (Ren *et al.* 2006).

It has been described that viruses could effectively develop resistance to antiviral drugs. This could also happen to RNAi based approaches as a single mismatch within the targeted region can result in the escape of viruses from the RNAi pathway, for example by poliovirus (Van Rij and Andino 2006, Gitlin *et al.* 2005, Gitlin *et al.* 2002), HIV-1 (Van Rij and Andino 2006, Das *et al.* 2004, Boden *et al.* 2003) and Hepatitis C virus (Van Rij and Andino 2006, Wilson *et al.* 2005). However, several approaches can be applied to circumvent this problem; either by using siRNA pool (combination of different siRNAs) or by targeting the untranslated regions (UTRs) of RNA viruses which are essential for virus replication and sensitive to mutation as a point mutation in this region might lead to loss of function (Van Rij and Andino 2006).

In contrast to viruses, the use of siRNA is not effective to directly inhibit bacterial infection as they mainly replicate outside of host cells and in the absence of cellular machinery (Leung and Whittaker 2005, Lieberman *et al.* 2003). However, it was reported that siRNA could be used as a potential agent to reduce an adverse effect induced by host immune responses and host genes involved in bacterial invasion, for instance by reducing the expression of proinflammatory cytokines (Leung and Whittaker 2005).

1.2.2 Stable induction of siRNA

In *C. elegans*, RNAi effects are stable, long lasting and even passed onto the offspring (Leung and Whittaker 2005, Grishok and Mello 2002). In contrast, these effects in mammalian cells are transient due to the lack of a particular enzyme, known

as RNA-dependent RNA polymerase that is responsible for amplifying siRNA in *C. elegans* (Leung and Whittaker 2005) which is also known as transitive RNA process.

In this process, fragments of the target mRNA can itself be processed to become siRNAs and take part in the RNAi pathway (Cocks and Theriault 2004). Moreover, the silencing activity of siRNA is transient due to the fact that the dilution of siRNA throughout several cell divisions results in the reduction of its concentration below the threshold of the active concentration (Leung and Whittaker 2005, Pekarik 2005). Therefore, an approach to circumvent these problems is to deliver DNA or RNA templates encoding siRNA sequences to cells that can be transcribed to express siRNA (Chiu et al. 2004, Shi 2003). Such approaches however are highly relying on plasmid or viral vectors (Sioud 2004) for delivery.

1.2.2.1 siRNA expressing plasmid

One of the strategies to synthesize short RNAs *in-vitro* is by introducing a plasmid with the ability to make *de-novo* siRNAs inside the cell (Agrawal *et al.* 2003). Several research groups have used a plasmid that encodes a promoter; either RNA polymerase III (pol III), such as a small nuclear RNA U6, human RNase H1 (Agrawal *et al.* 2003, Shuey 2002, Brummelkamp *et al.* 2002, Lee *et al.* 2002, Miyagishi and Kazunari 2002) or polymerase II (pol II) (Sioud 2004, Xie *et al.* 2003, Brummelkamp *et al.* 2002, Miyagishi and Kazunari 2002, Lee *et al.* 2002) to produce annealed siRNA of separate sense and antisense strands from different promoters (Sioud 2004) or short hairpin RNAs (shRNA) that are cleaved by Dicer through a RNAi pathway to produce siRNA (Leung and Whittaker 2005). shRNA is a newly discovered compound, composed of 19-29 base pair stems and 4-9 nucleotide loops thus mimicking the structure of siRNA which induces similarly efficient RNAi (Lee and Roth 2003, Paddison *et al.* 2002, McCaffrey *et al.* 2002). Generally, shRNA is produced in the nucleus and exported into the cytoplasm through nuclear pores as a part of a complex with exportin 5-Ran-GTP (Pekarik 2005, Lund *et al.* 2004, Yi *et al.* 2003). These strategies allow for a longer period and stable expression as compared to exogenously administered siRNAs because of their continual siRNA synthesis and due to the fact that these strategies consist of an intracellular amplification step in which a large amount of siRNA can be produced from each individual template (Uprichard 2005).

Thus, the use of these constructs could obviate the need of repeated delivery of synthetic siRNA when long term biological effects are desired (Sioud 2004).

Recently, Wooddell *et al.* (2005) reported that regardless of the promoter, plasmid siRNA expression constructs were more effective than PCR constructs (linear DNA fragments encoded siRNA expression cassettes) and the constructs that were containing the H1 promoter were significantly less effective than those utilising the U6 promoter to transfect mice with siRNA. Examples of these plasmid-based vectors are pSilencer 1.0 (Ambion) and pSuper (DNA engine) that are commercially available. Although plasmid-based vectors are superior to chemically synthetic siRNA in providing a longer silencing effect, but their usefulness has been limited by numerous disadvantages such as low and variable transfection efficiency (Agrawal *et al.* 2003).

1.2.2.2 Viral vectors

In addition to plasmid vectors, adenoviral and lentiviral-based vectors have also been used to deliver si/shRNA successfully. Viral vectors show very high transfection efficiency and stable expression of the constructs in a wide range of mammalian cells including primary cells. Unlike retroviral vectors which infect actively dividing cells during mitosis (Lewis *et al.* 1994, Mille *et al.* 1994), lentiviral and adenoviral vectors can infect both dividing and non-dividing cells (Quantine *et al.* 1992, Li *et al.* 1993). Adeno associated virus (AAV) vectors however have a lower toxicity than other viral vectors because they are specifically integrated into the AAVS1 region of chromosome 19 (chromosome 19 of the human genome has been reported and has no important encoded gene) which is unlikely to cause insertional mutagenesis. However, each type of viral vector brings with it a unique set of risks and safety concerns (Uprichard 2005, Tomanin and Scarpa 2004) as they are detected by the immune system and induce an immune response directed against them (Bivas-Benita *et al.* 2005).

1.3 *In-vitro* delivery of siRNA

Introduction of unmodified and unassisted siRNA in cell culture normally results in unsuccessful knockdown of the target gene, because mammalian cells appear to lack the effective dsRNA-uptake machinery that is found in other species such as *Caenorhabditis elegans* (Rozema and Lewis 2003). Furthermore, siRNA is a polyanion and hydrophilic molecule which cannot freely cross the lipid bilayers of the cell

membrane (Muratovska and Eccles 2004). Similar to other nucleic acids such as pDNA and antisense ODN, siRNA appears to be transported onto the cells by some form of endocytosis and is subsequently sequestered within endosomal/ lysosomal vesicles where it may undergo degradation by nucleases (Gilmore *et al.* 2004, Hollins *et al.* 2004, Beale *et al.* 2003, Rozema and Lewis 2003). Both compartments of endosome and lysosome have acidic interiors (pH 5-6.5) (reviewed in Murthy *et al.* 2003, Mellman 1996) and lysosomes contain hydrolases including ribonuclease, deoxyribonuclease, acid phosphatases, phosphodiesterase and pyrophosphatase (Hudson *et al.* 1996) which together can result in the degradation of siRNA entering the lysosomes. Consequently, the uptake of siRNA through endocytosis does not result in the release of siRNA into the cytoplasm, and thus does not induce RNAi (Rozema and Lewis 2003).

In addition, synthetic siRNA has been reported to localise to perinuclear regions and not in the nucleus after transfection by liposomes, even after an extended period of time (Keller 2005, Spagnaou *et al.* 2004, Chiu *et al.* 2004). In contrast, ODNs which are introduced directly into the cytosol (bypassing the endocytic pathway) can migrate rapidly into the nucleus (Hughes *et al.* 2001, Leonetti *et al.* 1991) which can be seen as another site of 'antisense' activity besides cytoplasm (Hughes *et al.* 2001).

As discussed in the earlier section, siRNA can be introduced into mammalian cells either as synthetic siRNA, or intracellularly expressed siRNA following introduction of encoding genetic information by pDNA or viral siRNA (Gilmore *et al.* 2004). The difference is only that the pDNA or shRNA needs nuclear rather than cytosolic delivery, as transcription of the encoded DNA construct occurs in the nucleus. Although, a successful *in-vivo* delivery of siRNA is more difficult to achieve compared to *in-vitro* delivery, due to the problems related to target selectivity and homeostasis (Schiffelers *et al.* 2004) but, cellular membrane is still a major barrier for the siRNA to be efficiently transported into the target site even for *in-vitro* delivery.

A number of strategies have been demonstrated to deliver siRNA into cells: by incorporating siRNA into cations such as cationic liposomes or cationic polymers, delivery by virus and distortion of cell membrane integrity by physical stimuli either forcing the siRNA into the cells (gene gun, magnetofection) or lowering the cell membrane barrier (electroporation, ultrasound) (Schiffelers *et al.* 2004, Niidome and Huang 2002). However, the use of physical stimuli such as electroporation has been

shown to potentially reduce cells viability to less than 60% although high cellular uptake and activity could be achieved (McManus *et al.* 2002). In addition, transfection of mammalian cells with siRNA has been shown to be dependent on cellular characteristics like cell type, confluency and passage number. Moreover, in the case of cationic vectors as a delivery system, their compatibility in the growth medium, toxic effect to the cells and physical characteristics of the cationic particle (e.g. particle size and the strength of electrostatic interaction between siRNA and cationic entity) also have important effect on transfection efficiency of siRNA (Schiffelers *et al.* 2004). For example, although the cationic particles are small enough and ready to be taken up by cells through endocytosis; they should be able to escape from endolysosomal vesicles to allow RNAi to occur.

1.4 *In-vivo* delivery of siRNA in the animal

The delivery of siRNA in mammalian cells *in-vitro* has shown to be successful in most of cell lines and therefore, siRNA is also being used to knockdown targeted genes in animal models *in-vivo*. However, to deliver siRNA *in-vivo* is challenging and complicated because there are several hurdles. The first obstacle is due to relatively small size of siRNA that makes it is more likely to be degraded by RNase activity in serum and rapidly excreted through urine (Schiffelers *et al.* 2005, Braasch *et al.* 2004) even though chemically modified siRNA molecules are stable enough to escape from RNase degradation. In fact, a study reported that pronounced accumulation of fluorescence was detected in cortical region in the kidney as siRNA was subjected to the glomerular filtration, and following this by accumulation in the liver after intravenous injection of fluorescently labelled siRNA in mice (Schiffelers *et al.* 2005). Secondly, the distribution of siRNA throughout the body by systemic administration will significantly decrease the local concentration of siRNA at the target cells and is responsible for loss of the majority of the injected dose. Finally, although siRNA reaches the target cells, it still requires efficient endocytosis followed by endolysosomal release of an intact double stranded structure to induce RNAi in the cells (Xie *et al.* 2006).

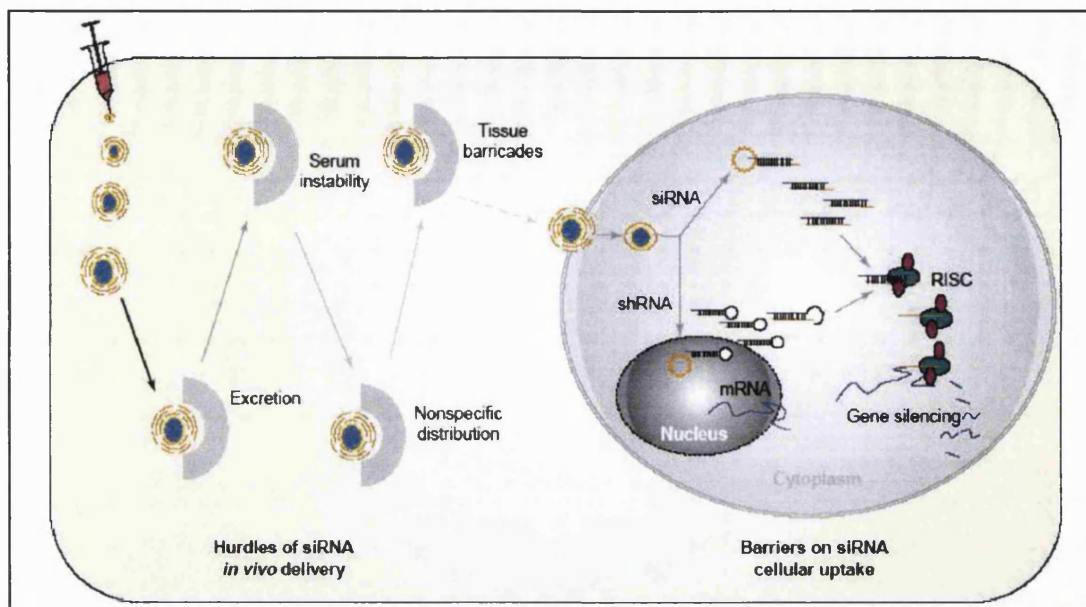


Figure 1.3: Hurdles of siRNA delivery *in-vivo* (courtesy of Xie *et al.* 2006).

In order to increase stability of siRNA *in-vivo*, one approach that has been described is through chemical modification. As ODN has been studied for its structure and activity relationship, it provides a starting point to design and develop chemically modified siRNA. For example, a phosphothioate linkage has been introduced into siRNA to improve its thermal stability and resistance to nuclease activity. A study reported that a heteroduplex of phosphodiester and phosphothioate RNA is more stable against nuclease degradation up to 72 h than a homoduplex of phosphodiester RNA when they were incubated in 50% of mouse serum at 37°C (Braasch *et al.* 2003).

Other modifications include locked nucleic acids (LNA) and modification of the 2' position of the ribose by substituting with 2' fluoro or o-methyl bases (figure 1.4). This has been described as increasing the thermal stability of siRNA without compromising the efficiency of RNAi (Paroo and Corey 2004, Braasch *et al.* 2003). LNA is however, a different class of 2' modification as a methylene bridge connects the 2'-O with the 4'-C of the ribose. This modification, therefore “locks” the ribose which improves both duplex stability and nuclease resistance (Behlke 2006). In addition, introduction of LNA in siRNA sense-strand could also be used to reduce off-target effects by either lowering incorporation of the siRNA sense-strand and/ or by reducing inappropriately cleavage of the non-target mRNA which was guided by the sense strand (Elmen *et al.* 2005). This strategy has been investigated due to the facts that the cells

can incorporate both strands of siRNA into the RISC complex (Elmen *et al.* 2005, Elbashir *et al.* 2001, Nykanen *et al.* 2001) but the strand that displays the weakest binding energy at its 5' base pair is incorporated preferentially (Elmen *et al.* 2005, Khvorova *et al.* 2003, Schwarz *et al.* 2003) and the incorporation of unwanted, non-target sense strand may cause off-target effects by limiting incorporation of intended antisense strand (Elmen *et al.* 2005, Jackson *et al.* 2003).

The elimination of the 2' hydroxyl also simplifies synthesis, deprotection and purification protocols which may assist in the production of cost-effective siRNA for therapeutic application (Braasch *et al.* 2003). Recently, an alternative approach has been investigated by synthesizing lipophilic derivatives of siRNA which significantly improves *in-vitro* and *in-vivo* delivery. Some authors have also reported that conjugating cholesterol to siRNA can improve serum protein binding, pharmacokinetics and increase delivery to hepatocytes (Behlke 2006, Lorenz *et al.* 2004, Soutschek *et al.* 2004) as well as improve permeability of siRNA (Lee and Sinko 2006, Lorenz *et al.* 2004).

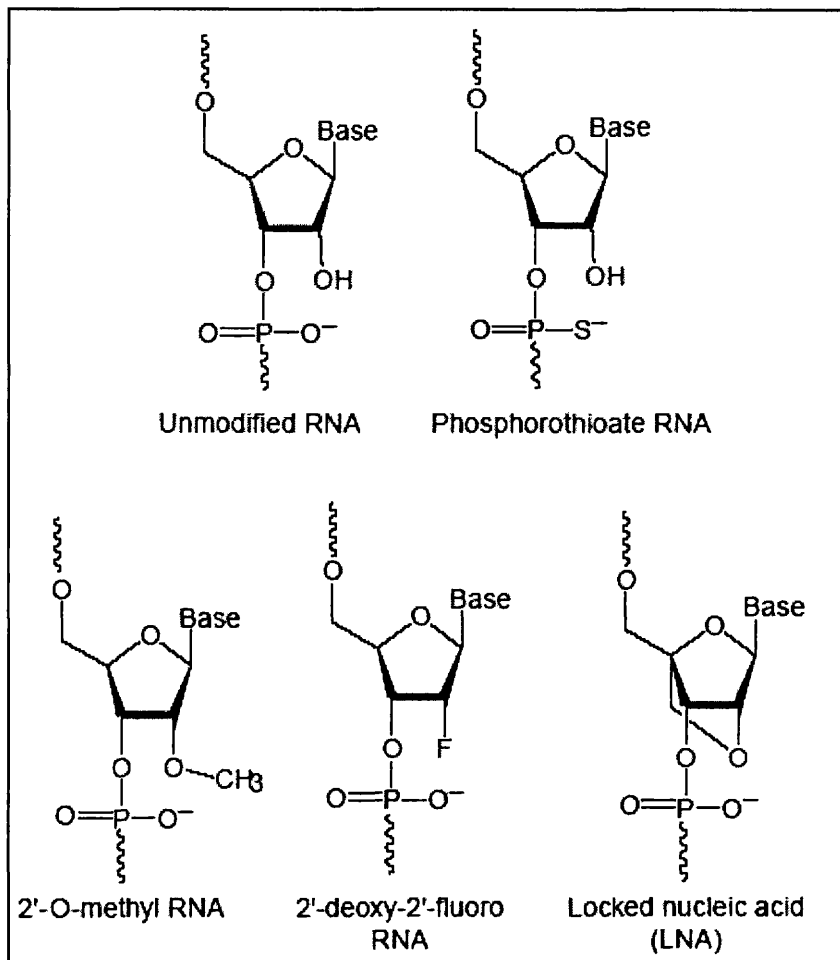


Figure 1.4: Chemical structure of phosphodiester and chemically modified siRNA (adapted from Paroo and Corey 2004).

Another approach that has been described to efficiently protect and deliver siRNA *in vivo* is the use of viral (adenovirus, lentivirus) and non-viral vectors (cationic lipids or polymers) which will be discussed in following chapters. Furthermore, the route of administration is also an important factor to be considered for siRNA delivery in animals. A number of strategies have been described to deliver siRNA *in vivo* and from among these strategies, rapid infusion by hydrodynamic injection of siRNA is shown to efficiently deliver siRNA and subsequently, results in silencing of the target gene. In this technique, a large volume of siRNA solution is rapidly injected into the tail vein of a mouse which transiently disrupts vascular and tissue integrity, consequently achieving successful delivery (Behlker 2006, Lewis and Wolff 2005). This method is however, restricted to highly vascularised tissues such as liver, spleen and kidney and

therefore, it is not suitable for systemic delivery. Additionally, success depends on the technique and skill of the operator although morbidity of the animals can be significant (Behlker 2006). Nevertheless, the hydrodynamic injection is currently not a viable technique in human clinical studies although it is very efficient for target validation in animals (Xie *et al.* 2006).

Other approaches that have also been used are electroporation and local injection or administration of siRNA directly into targeted tissues or organs such as eyes, kidneys, skin, and even brains of rodents. However, all vector systems or techniques that have been discussed above show several drawbacks such as the need for a very high amount of siRNA, being restricted to certain tissues or organs (Aigner 2006, Hassani *et al.* 2005) and therefore allowing local rather than systemic delivery of siRNA and are restricted to a site-specific injection (Aigner 2006).

Although, currently the delivery of siRNA *in-vivo* is challenging, the development and optimisation of siRNA delivery in animals is a worthy effort to accelerate the emerging potential for therapeutic applications of siRNA.

1.5 Delivery strategies

Even though, siRNA strategies have emerged as exciting novel therapeutic agents, several biopharmaceutical problems such as limited blood stability, insufficient cellular uptake and poor accessibility to the target sites have limited their usefulness (Zhang *et al.* 2006). Thus, to improve cellular uptake of siRNA, a number of strategies have been investigated and utilised. In general, these problems could be overcome by incorporating siRNA with cationic lipids or polymers to form complexes which could protect and deliver siRNA to the target cells.

1.5.1 Liposomes

Liposomes have been extensively studied as delivery systems for genetic materials such as pDNA, ODNs and recently, they have been investigated as a carrier for siRNA. siRNA has been incorporated into different types of liposomes including cationic liposomes (Sioud and Sørensen 2003, Spagnou *et al.* 2004, Yamauchi *et al.* 2006) and fusogenic liposomes (Hassani *et al.* 2005). Generally, liposomes are microscopic spheres composed of one or more closed, concentric phospholipid bilayer membranes surrounding an internal aqueous compartment (Lebedeva *et al.* 2000, Sessa

and Weissmann 1968). They can either encapsulate nucleic acids within an aqueous centre or form lipid nucleic acid complexes through electrostatic interaction between the negatively charged sugar phosphate backbone and cationic surface of the liposomes (Hughes *et al.* 2001, Islam *et al.* 2000, Maurer *et al.* 1999). The forming complex is a polyelectrolyte nanoparticle that can be readily taken up intracellularly by endocytosis (Jeong *et al.* 2003). DOTAP (1,2-Dioleoyl-3-trimethylammonium propane) is one of the lipids that has been widely employed to deliver nucleic acid which can be mixed with helper lipids such as dioleoyl phosphatidylethanolamine (DOPE) that promote fusion of the particles with the endosomal membrane, leading to endosomal escape (Schiffelers *et al.* 2005). From among the cationic liposomes, Lipofectamine 2000 is a commonly used transfection reagent to deliver siRNA *in-vitro*; however, complexation of these liposomes with siRNA allow little control over the preparation process which therefore results in an excessive size and low stability of lipoplexes with incomplete encapsulation of siRNA molecules which thereby exposes siRNA to degradation (Zhang *et al.* 2006). In addition, its application has been reported to be specific to only certain types of cells and toxic to cells as well as animals (Zhang *et al.* 2006, Chiu *et al.* 2004, Ohki *et al.* 2001) which limits its usefulness.

Liposomes are typically made from natural, biodegradable, non-toxic, non-immunogenic lipid molecules which resemble cell membranes in their structure and composition (Lasic 1998, Lasic 1993); however there are some limitations on their use. For instance, low stability of liposomes in the presence of serum or in the blood (Kakizawa *et al.* 2006, Yamauchi *et al.* 2006, Zhang *et al.* 2006, Ahktar 1998) and their tendency to accumulate in the reticuloendothelial system, have led to a short life and reduced access to other tissues (Chirila *et al.* 2002, Litzinger 1997). Moreover, liposomes also display poor encapsulation efficiencies (Yamauchi *et al.* 2006) and cationic liposomes may display significant cytotoxicity (Zhang *et al.* 2006, Zimmer *et al.* 1999, Lappalainen *et al.* 1994) especially its immunotoxicity effects which could exacerbate the disease like arthritis (Madberry *et al.* 20004).

1.5.2 Cationic polymers

After internalisation, active biological agents such as ODN and siRNA are normally accumulated in endosomal vesicles within the cells, severely limiting their ability to interact with the targeted mRNA and exert their biological effects. Thus, great

efforts have been undertaken to enhance endolysosomal escape. One strategy that has been examined is the use of a polycation with intrinsic endosomolytic activity such as polyethyleneimine (PEI) and starburst polyamidoamine dendrimers (Okuda *et al.* 2004). They show endosomal disruption activity due to the proton sponge effect. This effect occurs due to the lower pKa of the amine groups to endosomal pH, producing a buffering effect of the gene carrier itself that leads to its escape from the endosome (figure 1.5) (Okuda *et al.* 2004).

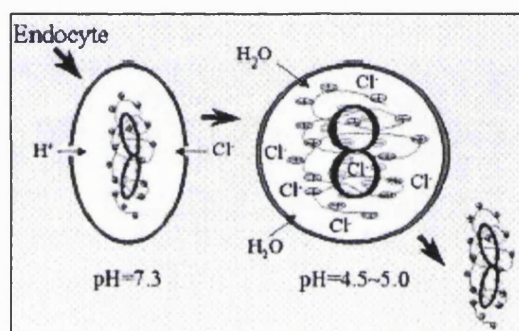


Figure 1.5: Schematic representation of the proton sponge theory. First, the complex of the DNA and the nanoparticles enters into the cell by endocytosis. The protonated amine groups of the nanoparticles capture H^+ in acidic environment of endosome that allows the endosome to pump in more H^+ and Cl^- ions. The pH value of the endosome is then increased and subsequently H_2O molecules are imported into the endosome by osmosis; lastly, DNA is released from the endosome due to endosomal swelling and rupturing (courtesy of Pang *et al.* 2002).

1.5.2.1 Polyethyleneimine

PEI is one of the most successful and the longest-standing polymers for non-viral nucleic acid delivery systems (Schiffelers *et al.* 2005, Godbey and Mikos 2001). PEI is a highly polycationic synthetic polymer that is very soluble in water and has a high capacity for positive charge as every third atom in the main molecular backbone is ionisable nitrogen (Chirila *et al.* 2002, Kircheis *et al.* 2001). It is available in both linear and branched forms as shown in figure 1.6 (Godbey and Mikos 2001). The branched form is produced by cationic polymerization from aziridine monomers via a chain-

growth mechanism, with branch sites arising from specific interactions between two growing polymer molecules. Polymer growth is terminated by “back biting,” or intramolecular macrocyclic ring formation. On the other hand, the linear form of PEI also arises from cationic polymerization, but from a 2-substituted 2-oxazoline monomer. The product (for example linear poly(N-formalethylenimine) is then hydrolyzed to yield linear PEI and it is attainable from the same process as that used to attain branched PEI, but the reaction must take place at relatively low temperature (Godbey *et al.* 1999 and reviewed in Tomalia and Killat 1985). The branched form contains 1°, 2° and 3° amines whereby each of them are likely to be protonated in physiological pHs and this has been used as a standard PEI for gene delivery due to its greater success in cell transfection compared to the linear form (Godbey *et al.* 1999). The explanation of PEI protonation will be explained further on page 54.

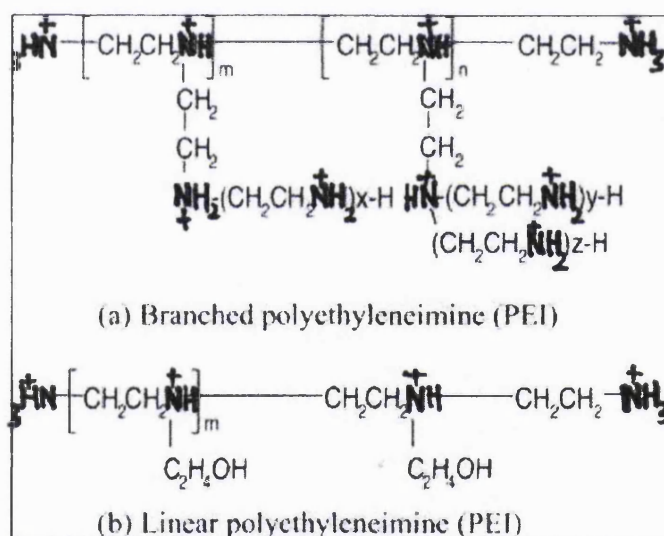


Figure 1.6: Structures of branched (a) and linear polyethylenimine (b) (courtesy of Kakui *et al.* 2005).

Due to its high positive charge density, PEI provides a strong electrostatic interaction with negatively charged polyanions such as pDNA, ODNs and siRNA to form a small and reproducible complex (polyplex) which confers protection for the pDNA, ODNs or siRNA from degradation by nuclease activity. Apart from this, it has

been shown that PEI is an excellent transfection reagent which could facilitate endosomal escape after entering the cells as it acts as a 'proton sponge' during acidification of the endosome (figure 1.7) (Dailey *et al.* 2004, Godbey and Mikos 1999, Boussif *et al.* 1995). Although PEI offers vastly greater protection and transfection for genetic molecules, it is not the ideal transfection reagent. An overall positive charge of these polyplexes exhibit numerous problems such as interaction with blood components (Rudolph *et al.* 2002, Zou *et al.* 2000, Kircheis and Wagner 2000, Kircheis *et al.* 1999) and activation of the complement system (Godbey and Mikos 1999) which result in rapid clearance of complexes from the bloodstream as well as attributing to the toxic effects at cellular level (Merdan *et al.* 2000).

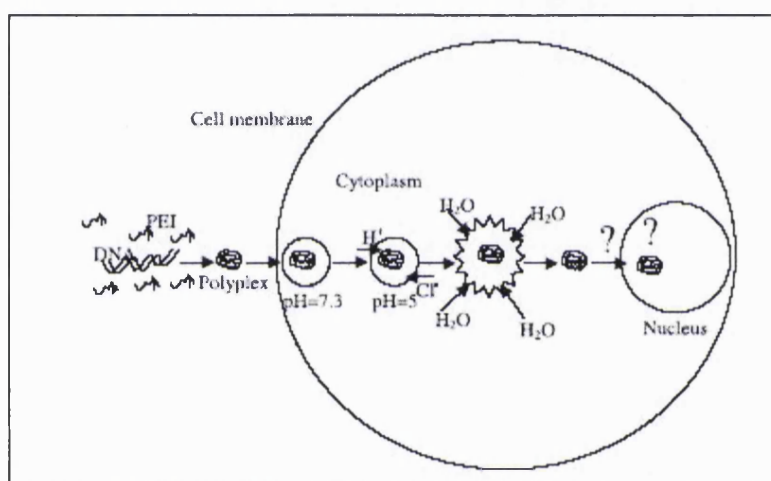


Figure 1.7: Schematic representation of PEI mediated DNA uptake by mammalian cells. DNA is condensed into a small complex in the presence of PEI. This polyplex interacts with the negatively charged cell membrane and is internalized within endosomes. The polyplex is then released *via* a proton sponge effect resulting in an opening of the endosome. The polyplex can then progress to the nucleus (courtesy of Zhang *et al.* 2004).

Several strategies have been applied to circumvent these problems, for example by masking the polyplex with a protective copolymer such as polystyrene and polyethylene glycol (PEG) (Kleeman *et al.* 2005, Rudolph *et al.* 2002, Davis 2002, Finsinger *et al.* 2000) which not only yields polyplexes with a lower surface charge, but

is also responsible for decreased polyplex aggregation, decreased interactions with protein plasma as well as decreased cell toxicity (Godbey and Mikos 2001, Ogris *et al.* 1999). Woodle *et al.* (2001) reported that conjugation of PEG with PEI containing ODNs could not only enhance stability of the complexes but also allow them to circulate for a longer period in the blood and reduce non-specific interactions due to stabilization by PEG. In addition, other strategies have been employed such as manipulation of the PEI amine to DNA phosphate ratio (Godbey *et al.* 1999) as well as the attachment of sugar moieties to the PEI for targeting purposes, for example, the use of mannosylated PEI/DNA complexes to target Antigen Presenting Cells (APC) (Godbey and Mikos 2001, Diebold *et al.* 1999) and galactose- conjugated PEI for hepatocyte targeting (Godbey and Mikos 2001, Zanta *et al.* 1997) by specific binding to the receptor that presence on the surface of the cell membrane.

Recently, attempts have also been made by several groups to enhance the biocompatibility as well as transfection efficiency of PEI by employing low molecular weight PEI, linear PEI (Dailey *et al.* 2004, Kleeman *et al.* 2004), biodegradable PEI (Dailey *et al.* 2004) and a combination of cationic lipid- or polymer with the PEI to form a hybrid gene delivery system with improved biocompatibility (Brownlie *et al.* 2004). The optimal structural and molecular weight of PEI for efficient gene delivery however is still uncertain as some authors have reported that low molecular weight PEIs were more effective than branched PEI (25 kDa) (Kunath *et al.* 2003) and some others revealed that transfection efficiency increased with the increase of PEI molecular weight (Ahn *et al.* 2002; Godbey *et al.* 1999). These contradictions are possibly due to the differences between commercially available sources of PEI in molecular weight dispersion as well as its purity leading to differences in both transfection and toxicity (Zhang *et al.* 2004).

On the other hand, PEI has been widely used to modify the overall particle surface charge of other polymers to produce a net positively charged particle. In this case, PEI is incorporated into the polymeric particles either by encapsulating (blending) it within the polymer (De Rosa *et al.* 2003; Bivas-Benita *et al.* 2004) or by coating/ adsorbing the surface of the polymer-based carriers with PEI (Messai *et al.* 2003, Kasturi *et al.* 2005). Such carriers have the potential advantages including increased bioavailability, improved loading efficiency (Kasturi *et al.* 2005) as well as controlled release of encapsulated genetic materials from the particles which in turn could reduce

the need for repeated dosing (García del Barrio *et al.* 2003). In addition to that, adsorption of nucleic acid onto the preformed cationic particles could preserve the structural integrity of nucleic acid from the harsh environment during particles preparation.

PEI adsorption onto polymer particles such as poly(lactic acid) (PLA) or poly(lactide-co-glycolide) (PLGA) occurs through electrostatic interaction between the negatively charged PLA/ PLGA particles and the polycation. A study done by Messai *et al.* (2003) reported that the adsorption of PEI to the PLA particles took place at optimum pH of 5.8 as both of the carboxyl groups of PLA and amine groups of PEI had to be ionized to permit electrostatic interactions. The same study also reported that PEI was adsorbed onto the PLA particles as a monolayer at low ionic strength media whereas adsorption was multilayer at high ionic strength (Messai *et al.* 2003). This approach of either blending or adsorbing PEI with PLGA/PLA however, has been reported to suffer from premature release of PEI during formulation or prior to reaching the target cells leading to unwanted cytotoxicity (Kasturi *et al.* 2005). PEI has therefore been covalently conjugated to PLGA to allow efficient surface loading of nucleic acids as well as enhancing transfection with relatively low toxicity (Kasturi *et al.* 2005, Manuel *et al.* 2001).

1.5.2.2 Chitosan

Chitosan is also considered to be a good candidate for gene delivery systems (Kim *et al.* 2005). Chitosan is a natural cationic polysaccharide (Lee *et al.* 2005, Lòpez-Leòn *et al.* 2005) consisting of β -1, 4 linked monomers of glucosamine and N-acetylglucosamine as shown in figure 1.8 (Li *et al.* 2003). Chitosan is obtained from partial deacetylation of chitin, the major component of crustacean shells (Lòpez-Leòn *et al.* 2005, Jane *et al.* 2001) and the second most abundant natural polymer after cellulose (Kost and Goldbart 1997). The natural chitin or chitosan often exists as a copolymer of glucosamine and acetylated glucosamines. Chitin is insoluble in water and most solvents which has restricted its usefulness. In contrast, chitosan can form salts with a variety of inorganic and organic salts due to the presence of free amines in its structure. Therefore, chitosan can be dissolved in an aqueous solution of almost all the organic and inorganic acids. Therefore, the percentage of glucosamine units in the polymer is very important and known as degree of deacetylation or DDA (Cho *et al.* 2006) which

can be determined by UV spectroscopy, chromatography, X-ray diffraction and other methods (Kost and Goldbart 1997).

Chitosan is an attractive vector for gene delivery due to advantages such as low toxicity, excellent biodegradability and biocompatibility (Shu and Zhu 2002). The polymer undergoes a slow break down process to harmless products (amino sugars) and is completely absorbed by the human body (Agnihotri *et al.* 2004, Nicol 1991). In addition, chitosan is a useful polymer for mucosal drug delivery (Janes *et al.* 2001) as it has ability to transiently open tight junctions between epithelia cells, thus facilitating the transport of macromolecules through well organised epithelial (Janes *et al.* 2001, Schipper *et al.* 1999, Schipper *et al.* 1997, Schipper *et al.* 1996, Borchard *et al.* 1996, Artursson *et al.* 1994).

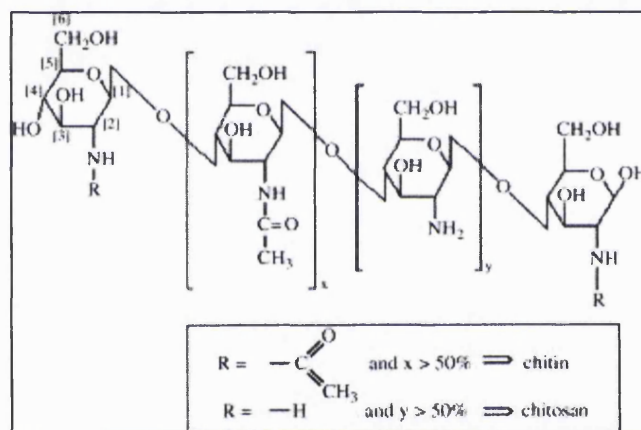


Figure 1.8: Chemical structure of chitin and chitosan.

Chitosan contains free amino groups which undergo protonation in acidic pH thus, enabling it to interact with negatively charged of anions such as pDNA or multivalent polyanions to form a complex or nanoparticles. A complex can be easily formed by electrostatic interaction between cationic chitosan and negatively charged polyanions such as pDNA, ODNs or even siRNA therefore protecting these nucleic acids from nuclease degradation (Richardson *et al.* 1999). Aside from chitosan complexation, it has the ability to gel spontaneously upon contact with multivalent polyanions such as tripolyphosphate (TPP) ions through inter- and intramolecular cross linkage between TPP phosphates and chitosan amino groups (Gan *et al.* 2005, Janes *et al.* 2001).

In fact, several techniques have been used to obtain chitosan nanoparticles including ionic complexation (Borchard 2001, Liu *et al.* 2005), ionic gelation (Shu and Zhu 2002, Vila *et al.* 2004, Gan *et al.* 2005), desolvation (Mao *et al.* 2001, Akbuğa *et al.* 2004) and covalent cross-linking (López-Leòn *et al.* 2005, Gupta and Jabrail 2006). From among above methods, ionic-complexation and ionic-gelation are the most useful methods to obtain chitosan nanoparticles due to their simplicity and the provision of mild conditions to produce nanoparticles without any need for toxic chemical such as glutaraldehyde, a cross-linking molecule used in the covalent cross-linking method (López-Leòn *et al.* 2005). Glutaraldehyde has been shown to have negative effects on cell viability as well as the integrity of macromolecules as reviewed by Janes *et al.* (2001) and therefore it is not favourable for use in the development of pharmaceutical products.

However, the ionic gelation method is preferable to simple complexation because manipulation of resulting particle size and surface charge can be easily controlled by adjusting preparation parameters (Gan *et al.* 2005, Janes *et al.* 2001) such as different concentrations of chitosan and TPP ratio (Janes *et al.* 2001) as well as stirring rate. Nevertheless, physical characteristics of chitosan nanoparticles by ionic gelation may vary significantly depending on purity, the type of acid salt and molecular weight of chitosan employed (Janes *et al.* 2001).

Since chitosan has been discovered to have high affinity for the cell membrane, it has been utilised as a coating agent or surface modifier by incorporating or adsorbing chitosan onto the nanoparticles (Janes *et al.* 2001). Besides this, nucleic acids may be adsorbed onto the surface of chitosan-coated PLA nanoparticles to avoid nucleic acid degradation during formulation processes such as high shearing and the use of organic solvent (Messai *et al.* 2005, Munier *et al.* 2005). Another study by Ravi Kumar *et al.* (2004), has also successfully incorporated chitosan into PLGA polymer by the emulsification diffusion method to obtain positively charged PLGA nanoparticles.

1.5.2.3 Cell penetrating Peptides (CPPs)

An alternative approach to deliver siRNA is the use of peptides which have the ability to translocate to the cell membrane. CPPs initially were defined as short cationic peptides (less than 30 amino acids) with a net positive charge that have the ability to translocate through the plasma membrane of eukaryotic cells *via* a receptor- and

endocytosis-independent mechanisms namely passive diffusion or inverted micelle formation (reviewed in Järver and Langel 2004, Pujal *et al.* 2006). However, it was then discovered that these findings were an artefact from membrane disruption of the cell fixation protocols as the harsh cell fixation process resulted in the release of CPPs into the cytosol and nucleus (Richard *et al.* 2003, reviewed in Pujal *et al.* 2006, Järver and Langel 2004). Therefore, fixation procedures need to be avoided when studying cellular localisation of CPP.

Recent studies with unfixed cells revealed that CPP internalisation into the cells might involve endocytosis as the uptake of CPP was inhibited at 4°C and the depletion of intracellular ATP was observed using sodium azide and 2-deoxy-D-glucose (Richard *et al.* 2003, reviewed in Pujal *et al.* 2006). In addition, other studies discovered that the uptake of CPPs was reduced by known endocytosis inhibitors (reviewed in Järver and Langel 2004). For example, the presence of the metabolic inhibitor iodoacetamide or endocytosis inhibitor cytochalasin D was shown to inhibit the uptake of TAT-liposomes at 37°C by OVCAR-3 cells (Fretz *et al.* 2004). Meanwhile, in a different study, the uptake of octa-arginine (R8) peptide by HeLa cells was significantly suppressed by the macropinocytosis inhibitor ethylisopropylamiloride (EIPA) and the F-actin polymerization inhibitor cytochalasin D but the uptake of penetratin was found to be less sensitive to EIPA (Nakase *et al.* 2004). Recent review also reported that internalisation of CPP begins with interactions between CPP and the extracellular matrix, requiring the capture of the CPP by cell-surface proteoglycans (PGs) such as cell-surface heparan sulphate (HSPGs), leading to peptide uptake at multiple sites of the cell surface (Pujal *et al.* 2006). This interaction has been shown through electrostatic interaction between the sulphated polysaccharides and the Arg-rich peptides which play a crucial role in cell membrane penetration. The binding between CPPs and HSPGs then induces aggregation and CPPs are concentrated at the cell surface for subsequent internalisation through direct membrane penetration, classical endocytosis or caveolar endocytosis (Pujal *et al.* 2006).

CPPs are trapped in the compartments such as endosomes or golgi apparatus after internalisation through endocytosis. If the CPPs are taken up by the cells *via* Clathrin-mediated endocytosis (degradative pathway), these normally end up in the endolysosomal compartment while in golgi apparatus or endoplasmic reticulum (ER) for internalisation *via* the caveolin-mediated route (non-digestive route) as shown on

figure 1.9. It has been reported that the changes of pH in the endosome, results in changes in the CPP conformation, which allows them to cross the endosomal membrane and release into the cytoplasm (Potocky *et al.* 2003, reviewed in Pujal *et al.* 2006).

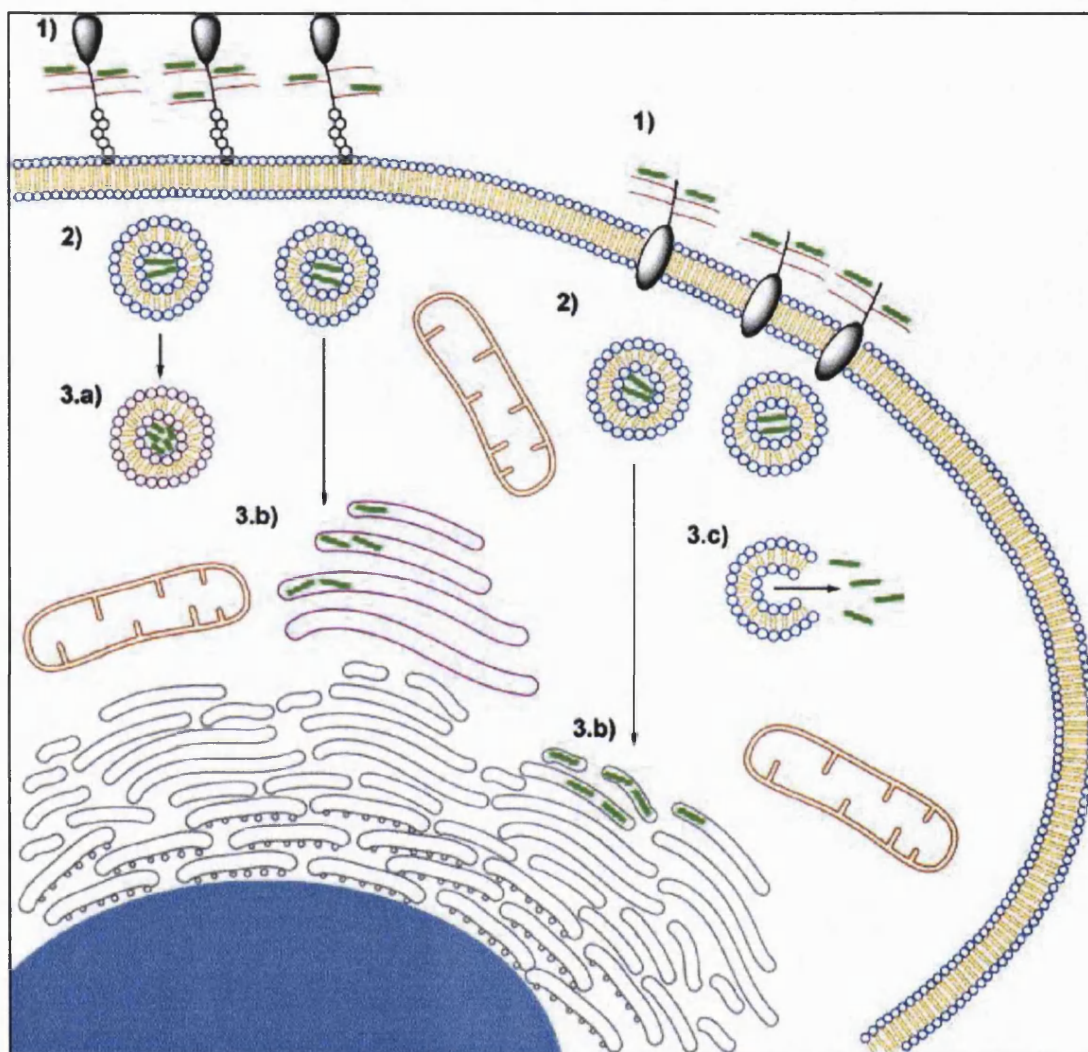


Figure 1.9: Different steps in CPP-mediated intracellular delivery. (1) Interaction of the CPP (represented as a green bar) with the cell-surface proteoglycans (in red), (2) The endocytic pathway, (3a) the degradative route to lysosomes in clathrin-mediated endocytosis, (3b) CPP ultimately reach the Golgi apparatus (in purple) or endoplasmic reticulum (ER, in grey) in caveolin-mediated endocytosis, (3c) Endosomal release (courtesy of Pujal *et al.* 2006).

TAT-peptide is one of the CPP that has been widely used to deliver nucleic acids. TAT-peptide is a fragment of natural protein and an essential viral regulatory

protein derived from HIV-1. TAT is encoded by two exons of 86 to 102 amino acids in length depending on the strain of virus (Patel *et al.* 2006, Wadia and Dowdy 2005); the first exon has been shown to mediate transactivation of HIV-1 gene expression whereas the second exon encodes the C-terminal domain of TAT which contains an arginine-glycine-aspartic acid (RGD) sequence, mediating the binding of extracellular TAT to integrin receptors, leading to TAT internalisation (Patel *et al.* 2006, Chang *et al.* 1997). The length and amino acid sequence of TAT-peptide however, could vary with different studies but in this study, TAT-peptide with the length of 11 amino acids (YGRKKRRQRRR, MW: 1739 Da) has been investigated.

The TAT-peptide has been reported to be taken up predominantly *via* an endocytotic pathway following electrostatic interaction of positively charge of TAT with negatively charged cell surface components (Shiraishi *et al.* 2005, Thoren *et al.* 2003) particularly HSPGs. Some HSPGs have a high number of sulphate and carboxylic groups (Vives 2005) which have been shown to be important in TAT uptake through electrostatic interaction or hydrogen binding with the guanidium group of arginine (Pujals *et al.* 2006, Fernandez-Carneado *et al.* 2005, Haack *et al.* 2003, Sanchez-Quesada *et al.* 1996, Salvatella *et al.* 1996). TAT-peptide on the other hand has a high content of arginine which has been shown to be responsible for mediating cellular uptake. In fact, the guanidium group of the arginine side chain is more potent in facilitating cellular uptake of TAT than other cationic groups such as lysine, histidine or ornithine (Brooks *et al.* 2005, Mitchell *et al.* 2000). Deletion or substitution of one arginine residue therefore could reduce or even abolish the uptake of TAT into the cells (Silhol *et al.* 2002, Wender *et al.* 2000, Vivès *et al.* 1997).

The TAT-peptide has been used to internalise a wide range of cargoes from small to large molecules for example, liposomes (Frezt *et al.* 2004), PEG-PEI polyplexes (Kleeman *et al.* 2005), *N*-(2-hydroxypropyl)methacrylamide (HPMA) copolymer (Nori *et al.* 2003); anionic nanoparticles (Patel *et al.* 2006) even pDNA (Kleeman *et al.* 2005) and ODNs (Turner *et al.* 2005, Astriab-Fisher *et al.* 2000). TAT-peptide normally attaches to these cargoes by covalent linkage and a disulfide bridge between these two entities is the most convenient bond formation as the reduction of the disulfide bridge is expected to release its cargo once they reach the cytoplasmic compartment (Brooks *et al.* 2005). However, the internalisation of TAT-peptide and its

cargo is also highly dependent on the size of cargoes, the exposure level of arginine and chemical linkage between TAT and cargo (reviewed in Brooks *et al.* 2005).

Other peptide based delivery systems that have been studied are the family of polycationic sequences such as poly-arginine and poly-lysine (reviewed in Vivès 2005) and recently the branched histidine-lysine polymers which are known as HK-polymer (Schiffelers *et al.* 2005). The advantages of these peptide based carriers besides their biodegradability are that the manipulation of the amino acid building blocks, branching and sequence could easily be done for specific applications (Schiffelers *et al.* 2005). For example, in the case of HK polymers, specific delivery either for siRNA or pDNA could be manipulated by changing the ratio and sequence of histidine and lysine (Schiffelers *et al.* 2005).

1.5.3 Biodegradable polymers

Another major limitation of siRNA as a therapeutic agent is that they are likely to be short-lived due to their rapid degradation in the biological environment which therefore, might require repeated administrations to obtain the desired biological effects. The use of a biodegradable polymeric delivery system has been reported to obviate the need for repeated dosing through their ability in providing sustained release of the active compound. Furthermore, the use of biodegradable polymers as a delivery system could improve drug stability and reduce toxicity or non-specific activity associated with the drug (Hughes *et al.* 2001). In fact, in this type of delivery system, the drug is not normally chemically attached to the polymer; therefore they remain in a biologically active form which can exert their effects as soon as they are released from the polymeric matrix (Dunn and Ottenbrite 1991).

From among the drug carriers, biodegradable polymeric nanoparticles have shown interesting potential to deliver small molecules like ODNs efficiently into cells (Lambert *et al.* 2001). Nanoparticles are defined as submicron (<1 μm) colloidal systems, generally made of polymers that can be in the form of nanocapsules or nanospheres (figure 1.10) (Lambert *et al.* 2001). Nanocapsules are vesicular systems in which the drug is confined to a cavity surrounded by a unique polymeric membrane whereas nanospheres are matrix systems in which the drug is dispersed throughout the particles (Lambert *et al.* 2001). A number of different polymers have been employed in

formulating biodegradable nanoparticles, and these are either synthetic (poly(lactic acid), polyacrylates, polycaprolactones) or natural (collagen and chitosan) (Jain 2000).

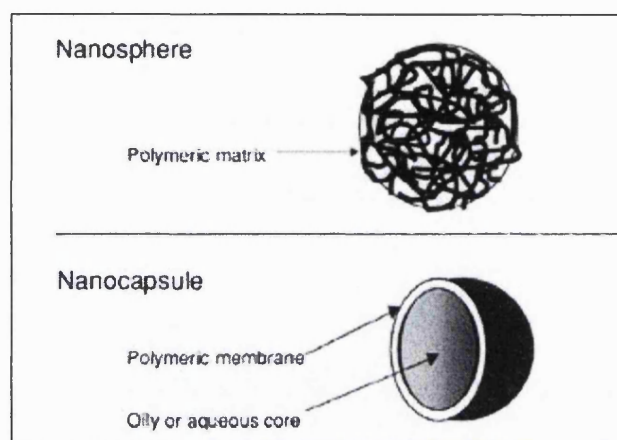


Figure 1.10: Type of nanoparticles: Nanosphere (Top) and nanocapsule (bottom) (adapted from Brigger *et al.* 2002).

Non-protein biodegradable polymers are those that require some chemical reactions such as hydrolysis before they become water soluble substances. These reactions usually occur over an extended period of time in the presence of water and therefore they can be used for longer-term drug delivery (Dunn and Ottenbrite 1991). There are several approaches used for achieving such changes in the body and examples of each category are shown in table 1.1: (1) the polymer can have a side chain substituent which undergoes hydrolysis in the body to produce hydroxyl, carboxyl or other dehydrating group (category I), (2) to crosslink a water-soluble polymer with a hydrolyzable crosslinking agent that makes the polymer water-insoluble. But, when it is introduced into the body, the crosslinking group is hydrolysed or degraded to give a water-soluble polymer (Category II), (3) to use a water insoluble polymer that contains hydrolyzable function groups directly in the polymer chain and as these group are hydrolysed in the body, the polymer chain is slowly reduced eventually becoming water soluble (Category III) (Dunn and Ottenbrite 1991).

Category I

Poly(maleic anhydride) copolymer

Category II

Gelatin-formaldehyde

Acrylamide-N,N'-methylenebisacrylamide

N-vinyl pyrrolidone-N,N'-methylenebisacrylamide

Fumaric acid/polyethylene glycol-N-vinyl pyrrolidone

Fumaric acid/diglycolic acid-N-vinyl pyrrolidone

Fumaric acid/ketomalonic acid-N-vinyl pyrrolidone

Category III

Poly(lactic acid)

Polyanhydrides

Polyglycolic acid

Polyorthoester

Polycaprolactone

Poly(amino acids)

Polyhydroxybutyrate

Pseudopolyamino acids

Table 1.1: Examples of biodegradable polymers used in drug delivery (adapted from Dunn and Ottenbrite 1991).

The use of natural polymers however is limited due to their higher costs and questionable purity (Jain 2000, Jalil and Nixon 1990). Therefore, synthetic biodegradable polymers have been widely used for drug delivery. The most extensively studied biodegradable polymers are poly(lactic acid) (PLA) and copolymer of lactic acid and glycolic acid (PLGA) (Panyam and Labhasetwar 2003, Hughes *et al.* 2001, Jain 2000, Langer 1997). These polymers are currently used in humans due to their excellent biocompatibility and biodegradability and relatively low toxicity.

Although lactic acid and glycolic acid have similar chemical structure, they are quite different in chemical, physical and mechanical properties due to the presence of a methyl group on the alpha carbon of lactic acid (figure 1.11) (Perrin and English 1997). Lactic acid exhibits a stereoirregularity of the C atom in β -position and therefore it can form D and DL and L polymers. The L form is found to be semicrystalline in nature whereas the DL-form is an amorphous polymer (Jain 2000, Wu 1995, Tice and Cowsar 1984). Therefore, the DL polymer form is more suitable for particle production because it is less crystalline than L form (Müller 1991) which enables a more homogenous

dispersion of drug in the polymer matrix (Jain 2000, Cohen *et al.* 1994, Tice and Cowsar 1984). On the other hand, glycolic acid is highly crystalline due to the lack of methyl side groups of the lactic acid (Jain 2000, Wu 1995, Tice and Cowsar 1984) and more hydrophilic which results in faster degradation than lactic acid as it absorbs more water (Jain 2000, Wu 1995, Cohen *et al.* 1994). Furthermore, the absence of the methyl group in glycolic acid causes the carbonyl of the ester linkage to be more accessible to hydrolytic attack which also causes it to degrade faster than lactic acid (Perrin and English 1997).

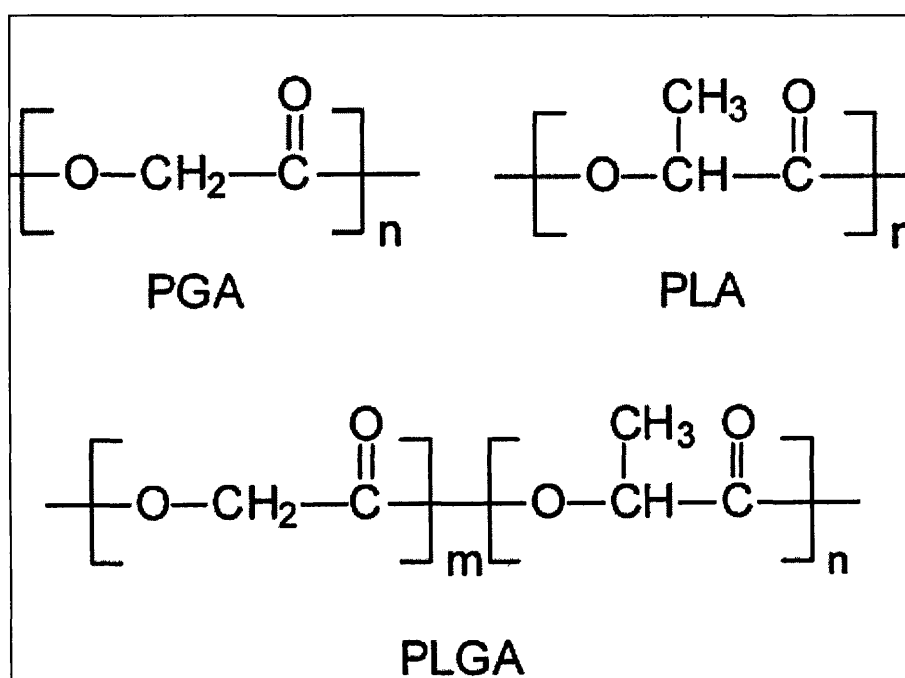


Figure 1.11: Structures of glycolic acid (PGA), lactic acid (PLA) and their PLGA copolymer.

These polymers are polyesters. Therefore, they undergo hydrolysis upon introduction into the body forming the biologically compatible and degradable moieties of lactic acid and glycolic acid. These moieties are then removed from the body by citric acid cycle (Kreb's cycle) (Panyam and Labhasetwar 2003). The homopolymers degrade more slowly than their co-polymers. In fact, the complete degradation of copolymer containing a high percentage of glycolide is faster than a low percentage of glycolide

(table 1.2). The physical properties of these polymers such as molecular weight could not only control polymer biodegradation rate but also the mechanical strength of the polymer as well as its ability to be formulated as drug delivery devices or systems (Jain 2000, Lewis 1990, Kitchell and Wise 1985).

Medisorb polymers	Inherent Viscosity, IV (DL/G)	DL lactide/glicolide Molar ratio	Degradation information
100 DL high IV	0.66-0.80	100/0	12-16 months
100 DL low IV	0.50-0.65	100/0	12-16 months
8515 DL high IV	0.66-0.80	85/15	5-6 months
8515 DL low IV	0.50-0.65	85/15	5-6 months
7525 DL high IV	0.66-0.80	75/25	4-5 months
7525 DL low IV	0.50-0.65	75/25	4-5 months
6535 DL high IV	0.66-0.80	65/35	3-4 months
6535 DL low IV	0.50-0.65	65/35	3-4 months
5050 DL high IV	0.66-0.80	50/50	1-2 months
5050 DL low IV	0.50-0.65	50/50	1-2 months
5050 DL 1A	0.08-0.12	50/50	1-2 weeks
5050 DL 2A	0.13-0.20	50/50	2-3 weeks
5050 DL 2.5A	0.21-0.31	50/50	2-4 weeks
5050 DL 3A	0.25-0.43	50/50	3-4 weeks
5050 DL 4A	0.38-0.48	50/50	3-4 weeks

Table 1.2: Biodegradation kinetics. Information from Alkermers[®] - Medisorb *For medisorb polymers the standard end group is lauryl ester (capped) unless the polymer is marked either A, M or C. 'A' polymers contain a free carboxyl end group (uncapped), 'M' polymers contain a methyl ester end group (capped) and 'C' polymer are custom polymer (www.alkermers.com/polymer/products.html).

The factors that influence the degradation rates of polymer microspheres have been extensively studied. Jeffery et al. (2003) reported that the degradation rate of PLA is controlled by polymer molecular weight, polymer crystallinity and lactide:glycolide ratio. Meanwhile, Tracy and co-workers have found that *in-vivo* degradation of PLGA microspheres was faster than *in-vitro* and the degradation rate was dependent on the

chemistry of the polymer end group (uncapped PLGA degrading faster than capped PLGA) and molecular weight (faster degradation with the lower molecular weight PLGA). They also have reported that zinc carbonate can retard the degradation of capped PLGAs (Tracy *et al.* 1999). Another thing that we should bear in mind is that DNA degradation may also be initiated by the hydration of microspheres *in vivo* and *in vitro*. This is due to an acidic microenvironment created by PLGA degradation that may chemically modify the DNA over time and ultimately can result in DNA degradation (Hao *et al.* 2000). Therefore, as mentioned earlier, PLGA or PLA polymers were incorporated with other cationic polymers to produce improved properties of PLGA or PLA particles.

1.5.3.1 Micro- or nanoparticles preparation

A number of micro- or nanoparticles particles preparations have been reported to date. However, the preparation that is commonly used is based on the formation of an emulsion with an inner phase made of an organic solvent in which the polymer is dissolved and an external phase consisting of a non-miscible solvent, normally water with or without a surfactant (Delie *et al.* 2001). These strategies however have been modified or improved to suit the nature of the polymer, the active molecule and intended use. The methods that have been reported and used for micro-or nanoparticles preparation are described below:

1.5.3.1.1 Emulsification-solvent evaporation method

This conventional technique consists of three major steps: (1) emulsification of a water-immiscible organic solution with an aqueous phase containing stabilizer, (2) removal of solvent by extraction or evaporation and (3) isolation of micro- or nanoparticles by filtration or centrifugation (Kwon *et al.* 2001, Cleland 1998, Sah *et al.* 1996). This process involves either oil in water (o/w) (single emulsion) or water in oil in water (w/o/w) (double emulsion) emulsification. One disadvantage of single emulsion however is poor entrapment efficiency for moderately or highly hydrophilic molecules such as protein, pDNA, ODNs and siRNA. The hydrophilic drug would be diffused out or partition from the dispersed oil phase into the aqueous continuous phase and deposit on the particles or it could diffuse wholly into aqueous phase to be lost during washing

(Jain 2000, Wada *et al.* 1988, Cavalier *et al.* 1986). Therefore, the double emulsion method is better suited in order to encapsulate water soluble drugs.

However, there are several drawbacks related to the solvent evaporation technique including the use of chlorinated solvent such as chloroform or dichloromethane (DCM) and difficulties in preparing nanoparticles with diameters less than 100 nm (Kwon *et al.* 2001). In addition, this technique normally requires sonication to create the first emulsion since it generates a more homogenous dispersion with high encapsulation efficiency. Sonication has been demonstrated to be a major cause of exposing protein or macromolecules to a number of mechanical stresses which can denature them such as the introduction of high pressures, temperature gradients, shear forces (>15000 rpm) and free radicals during the process (Kang and Singh 2003, Krishnamurthy *et al.* 2000). Furthermore, sonication exposes the protein to the denaturing action of organic solvent across a very large interfacial area (Krishnamurthy *et al.* 2000) and all of these factors can result in loss of biological activity of protein or macromolecules. Due to all the above reasons, homogenization has been used to substitute sonication for creating the first emulsion even though the size of microspheres prepared using sonication is slightly smaller than that of particles prepared using homogenization (Hsu *et al.* 1999).

1.5.3.1.2 Emulsification diffusion method

In order to eliminate the drawbacks related to solvent evaporation, it also would be ideal to try the emulsification diffusion method. In this method, nanoparticles are prepared by emulsifying an organic solution of the polymer in an aqueous solution of stabilising agent followed by rapid displacement of the solvent from the internal to external phase which results in solid particle formation (Jelcic 2004, Quintanar-Guerrero *et al.* 1998). Theoretically, in the emulsification diffusion method, stirring causes the dispersion of polymer-solvent globules and the stabilising agent is then adsorbed on the large interface between solvent and the external phase created. The addition of water causes solvent diffusion from internal to the external phase and during the transport of solute, new globules are produced which are gradually poorer in solvent (figure 1.12) (Kwon *et al.* 2001).

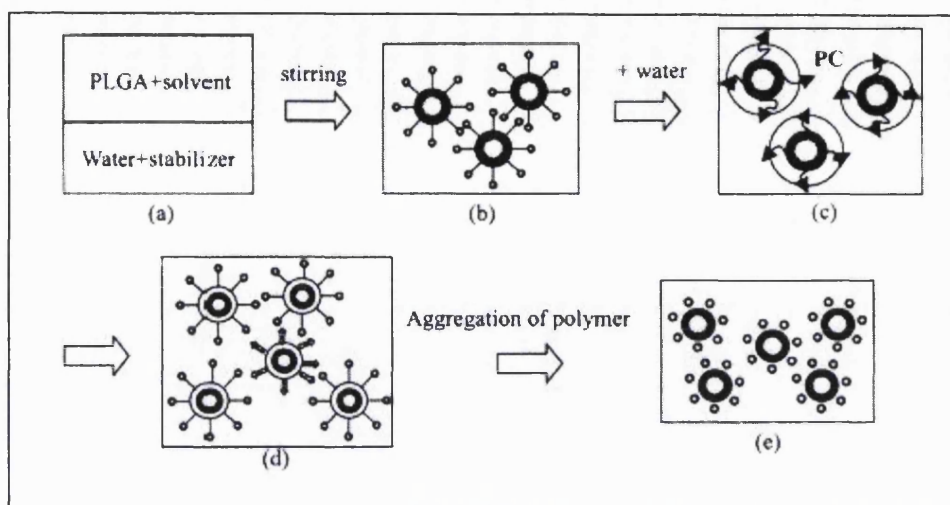


Figure 1.12: Schematic description of proposed formation mechanism of PLA/PLGA nanoparticles by the emulsification diffusion method (courtesy of Kwon *et al.* 2001).

In general, selections of solvent as well as preparation parameters are the most important factors that affect the physical characteristics of the yielded nanoparticles (Jelcic 2004). In this method, the solvents used are usually fully or partially water-miscible solvents such as acetone, benzyl alcohol, propylene carbonate or ethyl acetate. Therefore, the diffusion of these solvents from the globules carries polymer molecules into the aqueous phase, forming local regions of supersaturation from which, new globules or polymer aggregates are formed (figure 1.13). In contrast, organic solvent of low water solubility, for example chloroform produces bigger particle sizes due to its low precipitation and microparticles will be formed by the solvent loss from the surface of the droplet (Choi *et al.* 2002).

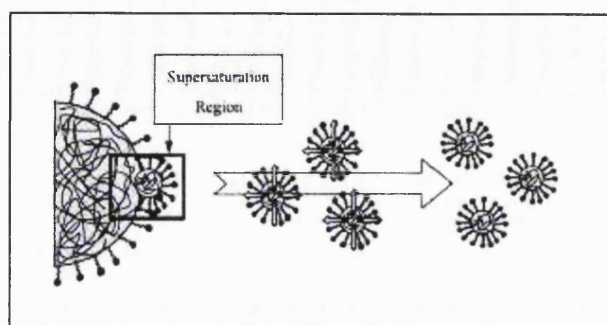


Figure 1.13: The diffusion process of partially water- miscible solvent into the aqueous phase (adapted form Choi *et al.* 2002).

This method has been suggested to be superior to the solvent-evaporation method as it requires the use of non-chlorinated solvents and low shear speeds (<1500 rpm) because rapid diffusion of solvents from the internal phase into the external phase causes creation of an interfacial turbulence between two phases, leading to the formation of smaller particles (Soppimath *et al.* 2001). It is very important to avoid the use of chlorinated solvents whenever possible because most of them have relatively high toxicity and have to be extensively purified to produce a practically solvent-free formulation (Leroux *et al.* 1995, Allemann *et al.* 1993). If not, these solvent impurities become toxic to the body and may degrade the drug within the polymer matrix (Soppimath *et al.* 2001).

In general, benzyl alcohol (BZA) is one of the most commonly used solvents in the emulsification diffusion method (Delie *et al.* 2001; Berton *et al.* 1999a; b; Leroux *et al.* 1995) because it has low toxicity compared to chlorinated solvents. The physical properties of BZA which is immiscible with water at a low water to solvent ratio but miscible at ratios above 1:25 in fact, makes it a suitable solvent to be used in the emulsification diffusion process (table 1.3). Additionally, BZA has been widely used in pharmaceutical formulations for humans due to its antimicrobial and solubilizing properties (Leroux *et al.* 1995). Various other partially-water miscible solvents also have been tested for particle formation such as propylene carbonate (PC), methyl ethyl ketone (MEK) and ethyl acetate (EC) (Choi *et al.* 2002). Besides being chemically stable and odourless, PC has been reported to be a good solvent for polymers and has relatively low oral as well as skin toxicity. Therefore, it was thought to be a suitable solvent for the emulsification diffusion method to produce emulsions of good physical

and chemical stability (Quintanar-Guerrero *et al.* 1996, Dahl and Burke 1990, Ong and Manaukian 1998, Stephens and Felkel 1975, Stephens and Suddeth 1967, Merodith and Tobias 1961).

	Solvent		
	Ethyl Acetate (EC)	Propylene carbonate (PC)	Acetone (ACE)
Water	Slightly soluble (10% v/v at 25°C)	Slightly soluble (17.5% v/v at 25°C)	Very soluble (infinitely at 25°C)
PLGA	Good solvent	Good solvent	Good solvent

Table 1.3: Solubility of organic solvent in water or PLGA in organic solvent (Adapted from Song *et al.* 2006).

Several researchers have studied the relations between preparation parameters (type of solvents, type and concentration of stabilisers) and particle size of nanoparticles produced by the emulsification diffusion method. Quintanar-Guerrero *et al.* (1996) reported that the particle size of nanoparticles could be reduced by increasing the concentration of stabiliser and stirring rate. A similar study also has been done by Kwon *et al.* (2001) which reported that preparative variables such as the type as well as concentrations of stabilizer and homogenizer speed are crucial factors for the formation of PLGA nanoparticles by the emulsification diffusion method. In fact, in this report, they also claimed that particle size of resultant nanoparticles increased with the increase of polymer concentration in the organic phase (Kwon *et al.* 2001). Several selections of partially water immiscible solvents (EC, MEK, PC, BZA) have also been studied for their effect on the particle size of nanoparticles prepared by the emulsification diffusion method (Choi *et al.* 2002). In this study, they found that the size of PLGA nanoparticles was decreased with the decrease of exchange ratio, R ($R = D_{sw}/D_{ws}$; diffusion coefficients = $D_{\text{solvent to water}}$, $D_{\text{water to solvent}}$) and the increased of the solvent-polymer interaction parameter (χ). Recently, Song *et al.* (2006) has studied the effect of various solvents on the particle size of nanoparticles produced by the emulsification diffusion method including partially water soluble solvents, fully water soluble (ACE) and water-immiscible solvent (DCM). From this study, they reported that ACE and DCM produced larger particle than partially water soluble solvent (PC and EC). DCM

produced larger particles as a result of significant aggregation due to its immiscible nature with water. On the other hand, acetone which is completely miscible with water is expected to form an unstable emulsion which immediately precipitates as sub-micron particles upon mixing the organic and aqueous phases (Song *et al.* 2006, Thioune *et al.* 1997)

1.6 Objectives of the study:

(a) Formulation and optimisation of cationic nanoparticles based on cationic polymers: PEI, chitosan and TAT-peptide for siRNA delivery using simple complexation. For chitosan nanoparticles, optimisation of another method of preparation namely ionic gelation using TPP ions will also be evaluated.

(b) Development and optimisation of biodegradable cationic polymeric nanoparticles for siRNA delivery based on incorporation of PLGA and cationic polymers such as PEI and chitosan by the emulsification diffusion method.

(c) Characterisation of subsequent physical properties of these nanoparticles in terms of particle size, surface charge, morphology and siRNA loading and binding capacity/efficiency.

(d) Evaluation of biological activities of siRNA delivered by these nanoparticles *in-vitro* as well as evaluating their potential toxicity.

(e) Comparison of physical as well as biological properties of the above nanoparticles when loading with siRNA and pDNA.

Chapter 2

Materials and Methods

2 Materials and methods

2.1 Materials

2.1.1 Polymer

Poly (D,L-lactide-co-glycolide) with a monomer ratio of 50:50 2A (14 kDa), 3A (46 kDa) and 4A (58.8 kDa) Medisorb[®] were purchased from Alkermers. Poly(vinyl alcohol) (PVA, molecular weight: 13-23 kDa and 30-70 kDa, 87-89% hydrolysed), poloxaner-188 and -407 were from Sigma Aldrich. Branched form of PEI (molecular weight: 25 kDa) was also purchased from Sigma. Four different types of chitosan were medical grade chitosan hydrochloride with molecular weight of 270 kDa and 110 kDa as well as chitosan glutamate with molecular weight of 470 kDa and 160 kDa (Degree of deacetylation of 86%, Protasan Ultra-pure, Pronova Biomedical, Norway). TAT-peptide (YGRKKRRQRRR, MW: 1739 Da) was a gift from Dr. Sylviane Muller, Immunologie et Chimie Thérapeutiques, Institut de Biologie Moléculaire et Cellulaire (IBMC).

2.1.2 siRNA

siRNA targeting against pGL3 luciferase gene (sense: 5'-CUUACGCU-GAGUACUUCGATT-3', antisense: 3'-TTGAAUGCGACUCAUGAAGCU-5') and control siRNA (non-silencing) (sense: 3'-UUCUCCGAACGUGUCACGUTT-3', antisense: 3'-TTAAGAGGCUUGCACAAGUGCA-5') were synthesized by Proligo (France).

2.1.3 pDNA

Reporter vectors, pGL3 control and pRL-TK were purchased from Promega (UK) and pDNA of gwiz[™] luciferase (10 mg/ml in water) was purchased from Aldevron, USA.

2.1.4 Others

Pentasodium tripolyphosphate or TPP (Merk, Germany) and sodium acetate was obtained from Sigma-Aldrich. Dual-Glo Luciferase Assay system, agarose gel (low melting point and general use), Tris-borate-EDTA (TBE) and Tris-acetate-EDTA (TAE)

buffers pH 8.3 were from Promega, UK. Lipofectamine 2000 and Opti-MEM I reduced serum medium were purchased from Invitrogen, UK. MTT (3-(4, 5-dimethyl-thiazol-2-yl)-2, 5-diphenyl-tetrazolium bromide, 10 mg), Dulbecco's Modified Eagles Medium (DMEM), fetal bovine serum, penicillin 10 000 unit/ml and streptomycin 10 mg/ml solution, L-glutamine 200 mM, MEM non essential amino acid 100X and dimethyl sulfoxide (DMSO) were from Sigma. Acetone, ethyl acetate and dichloromethane were analytical grade.

2.2 Preparation of polyplexes

In this study, various types of polyplexes were synthesized by simple mixing of siRNA solution with a solution of cationic polymer (complexation). Subsequently, these polyplexes were formed through electrostatic interaction between negatively charged siRNA and positively charged cationic polymer.

2.2.1 Polyethyleneimine

PEI-siRNA complexes were prepared at different N/P ratios, ranging from 1:1 to 25:1. siRNA and PEI were separately diluted to 500 μ l with RNase free water. The complex was then prepared by gently mixing siRNA (50 ng) to an equal volume of PEI (the exact amount of PEI depends on the N/P ratio) and left for 1 h incubation at room temperature before use. The same protocols were used to prepare PEI-pDNA complexes.

2.2.2 Chitosan

Chitosan was dissolved either in distilled water or acetate buffer (0.1 M sodium acetate/0.1 M acetic acid, pH 4.5) to form different concentrations of chitosan solution, ranging from 25-300 μ g/ml. Chitosan-siRNA complexes were prepared by adding chitosan solution drop-wise to an equal volume of siRNA solution (20 μ g/ml) and quickly mixed before incubating them at room temperature for 30 min. The final volume of the mixture in each preparation was limited to below 500 μ l in order to yield uniform size nanoparticles. The same protocols were used to prepare PEI-pDNA complexes.

2.2.3 TAT-peptides

TAT-peptide-siRNA complexes were prepared by a simple-complexation method. To prepare the complex, 20 µg/ml of siRNA in RNase free water was added to a series of different concentration of TAT-peptide solution, ranging from 40 to 200 µg/ml in RNase free water. The addition of siRNA to the TAT-peptide solution was performed drop-wise over a period of approximately 30 s before quickly mixing by shaking the tube up and down for another 30 s. The mixture was then incubated at room temperature for 30 min.

2.3 Preparation of cationic nanospheres

In this study, cationic nanospheres based on PLGA polymers were prepared using a single emulsion method by manipulating the emulsification diffusion process. However, the simple and mild method of ionic gelation was also used for the preparation of chitosan nanoparticles.

2.3.1 Emulsification diffusion method

2.3.1.1 PLGA-PEI nanoparticles

The preparation method of PLGA-PEI nanoparticles was a modification of the technique described by Bivas-Benita et al. (2004). Briefly, 1 ml of 10% (m/v) PLGA 50:50 2A in dichloromethane was stirred for 30 min. PEI solution in acetone was prepared to a final concentration of 0.1% (m/v). PEI was then added to the PLGA solution and their volumes were mixed according to the PLGA to PEI weight ratio of 29:1 and 59:1. Tween-80[®] was added to a final concentration of 1% (m/v) and acetone added up to 5 ml. This organic phase was mixed and poured into an aqueous phase of 10 ml of 5% (m/v) PVA in double distilled water (in 50 ml tall beaker), followed by sonication with 15% of the maximum amplitude in continuous mode using an exponential probe with a diameter of 6 mm (Sanyo MSE Soniprep 150 with a frequency of 23 kHz, Sanyo Gallemkamp PLC, Leicester, UK, figure 2.1) for 4 min. The dichloromethane was then evaporated for 4 h before centrifuging (Centrifuge Sorvall Combi Plus, Kendo, USA) at 20 000 rpm for 30 min twice. After centrifuging, the particle suspension was freeze-dried using an Edward Freeze Dryer (Micro Modulo, Edwards High Vacuum, England).



Figure 2.1: Sonicator (Sanyo MSE Soniprep 150, Sanyo Gallempkamp PLC, Leicester, UK) used to prepare PLGA-PEI nanoparticles.

2.3.1.2 PLGA-chitosan nanoparticles

PLGA 50:50 2A was dissolved in ethyl acetate to produce 2.5 ml solution of 2% m/v. The organic phase was then added to 5 ml of aqueous phase, the mixture of 2% m/v of PVA and 1.2% chitosan. Subsequently, the mixture was homogenised at 17 500 rpm for 5 min using IKA[®]-WERKE T25 Basic S2 homogenizer, Germany and (figure 2.2A, probe diameter: 6 mm). After 5 min, 30 ml of distilled water was added drop-wise over a period of approximately 2 min under magnetic stirring and kept stirring at room temperature for another 2 h. The nanoparticles were washed and harvested by centrifugation (Centrifuge Sorvall Combi Plus, Kendo, USA) at 20 000 rpm for 25 min at 10°C twice before freeze-drying using an Edward Freeze Dryer (Micro Modulo, Edwards High Vacuum, England). For the nanoparticles collected by filtration, the particles suspensions were filtrated using Amicon Stirred Cell (Model 8400, Millipore, figure 2.2B) through Polyvinylidene fluoride (PVDF) membrane with 0.1 μm pore size. Filtration was carried out until 10 times of particle suspension original volume by continuously adding distilled water.

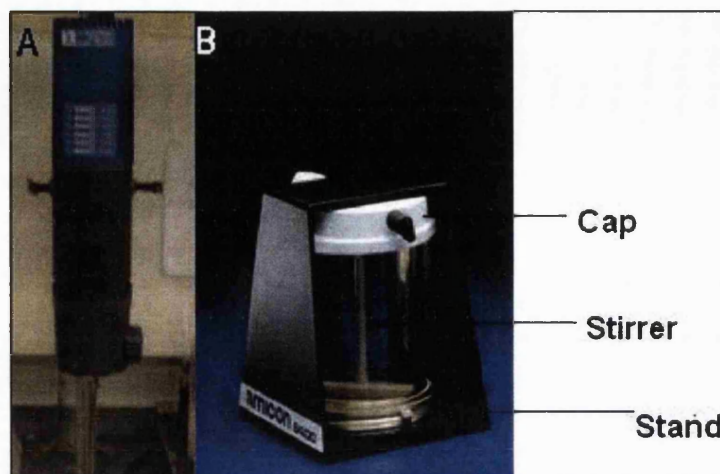


Figure 2.2: IKA®-WERKE T25 Basic S2 homogenizer (A) and Amicon Stirred Cell Model 8400, Millipore (B) used to create emulsion in particle preparation and to wash as well as collect particles by filtration, respectively.

2.3.2 Ionic gelation of chitosan-TPP nanoparticles

Nanoparticles were produced based on modified ionic gelation of tripolyphosphate (TPP) and chitosan as described elsewhere (Lopez-Leon *et al.* 2005). Nanoparticles were spontaneously obtained upon the addition of 1.2 ml (1 mg/ml) of a TPP aqueous solution to 3 ml of chitosan solution (2 mg/ml) under constant magnetic stirring at room temperature. For siRNA association with the chitosan nanoparticles (chitosan-TPP with entrapped siRNA), siRNA in RNase free water (10 µg/ml) was added to the TPP solution before adding the mixture drop-wise to the chitosan solution. The particles were then incubated at room temperature for 30 min before use or further analysis. Nanoparticles were collected by centrifugation at 13 000 X g for 10 min (IEC Micromax, USA). The supernatants were discarded and nanoparticles were resuspended in filtered (Millex® GP filter unit, Millipore, Ireland) RNase free water.

2.4 Determination of particle size

Particle size (Z-average diameter) and polydispersity (PI) of nanoparticles was measured by photon correlation spectroscopy (PCS) method using Malvern Zetasizer® S (Malvern, U.K.) (figure 2.3A). Applications of this method are based on the fact that light scattering occurs on polarised solid and liquid particles bathed in electromagnetic field of light beam because of the difference in the dielectric properties of the material

and the surrounding media, and the varying field induces oscillating dipoles in the particles radiating light in all directions. The intensity of scattered electromagnetic field depends on the ratio between the particle size and the incident light wavelength (λ), and at maximum ratio, the shorter the λ value the smaller the particle. The short term intensity fluctuation (dynamic) of the scattered light on the other hand arises from the fact that the scattering particles are in the motion (e.g. Brownian motion for particle of 5 μm and below) or the particle motion under external forces (e.g. particle sedimentation due to gravitation) where these motions cause short-term fluctuations in the measured intensity of the scattered light (Gun'ko *et al.* 2003).

The measurements of particle size were made at 25° C in triplicate. For analysis of particle size of PLGA-PEI, PLGA-chitosan before freeze-drying and chitosan-TPP nanoparticles, 1 ml of particle suspension were diluted to 4 ml of RNase free water. On the other hand, for lyophilized particles, a known amount of lyophilized particles (3–4 mg) was re-suspended in RNase free water (1.0 ml) and sonicated for 3 min prior to the measurement using bath sonicator (Clifton Ultrasonic Bath) to achieve full re-dispersion of the particles. Particle size was first measured using Malvern Mastersizer[®] to detect the presence of any particle populations with extreme sizes, either too big or too small. Particle size higher than 1 μm was analysed using Mastersizer S[®] (Malvern, U.K) (figure 2.3B) which suitable for the particle with the size range between 0.05-900 μm . Meanwhile, particle size below 1 μm was analysed using Malvern Zetasizer[®] (Malvern, U.K). On the other hand, no further dilution was performed for particles prepared by simple complexation and the size of the complexes was determined using Malvern System 4700c Submicron particle analyser (Malvern, U.K) which suitable for a lower concentration of sample (100 $\mu\text{g}/\text{ml}$ and below). To validate the techniques, standard polystyrene beads were analysed before measuring the samples for each experiment.

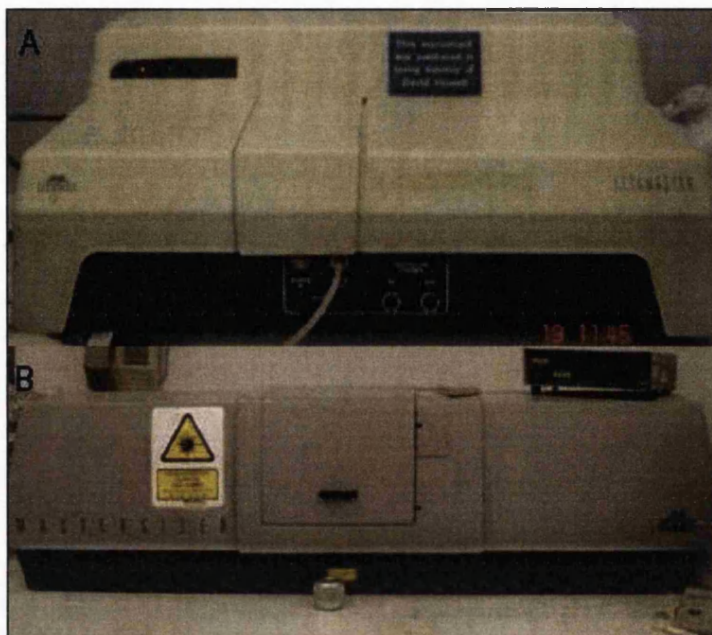


Figure 2.3: Malvern Zetasizer® S (A) and Mastersizer S (B), Malvern, U.K for particle size measurement.

2.5 Zeta potential determination

The zeta potential of the nanoparticle suspension was measured using Malvern Zetasizer® S (Malvern, U.K), after diluting the particles with RNase free water into the appropriate concentration to yield a count rate per second (KCps) in the range of 2500-3500. The instrument was calibrated routinely with a -50 mV of polystyrene standard solution (Malvern). Data were collected for 10 cycles and a minimum of three measurements was carried out on each sample. The measurements were made at 25° C.

2.6 Determination of particle morphology

Morphology of complexes or nanoparticles was investigated by two method of microscopy, Transmission Electron Microscopy (TEM) and Scanning Electron Microscopy (SEM).

2.6.1 Transmission Electron Microscopy

The morphology of the complexes was observed under a transmission electron microscope (TEM). For TEM, samples were stained with 2% m/v of phosphotungstic

acid and placed on copper grid with Formvar films for viewing under the TEM (Philips CM12, Philips Co., Eindhoven, Netherlands).

2.6.2 Scan Electron microscopy

The morphology of the nanospheres was investigated by scanning electron microscope (SEM) utilised a Philips XL30, Philips Co. (Eindhoven, Netherlands). Briefly, dried particles were dried with Samdri 780 critical point dryer (Maryland, USA) mounted onto an SEM stub with a double-sided carbon impregnated discs using a fine hair painbrush. Samples were then sputter-coated with gold using an Emscope Sputtering Coater (Ashford, UK) for 2 min at 30 mA before viewing under SEM.

2.7 Quantification of chitosan incorporated into PLGA particles

Incorporation of chitosan into PLGA particles was quantified using a modified chitosan titration assay as reported by Messai and Delair (2006) based on the use of Orange IIC, an anionic dye which strongly absorbs at 505 nm and can form complexes with ammonium groups of chitosan, hence reducing the absorbance. Free chitosan was assayed according to a depletion method where PLGA-chitosan nanoparticles supernatant of known volume after each washing was collected and 1 ml of the supernatant was then added to 4 ml of Orange IIC dye in distilled water at a concentration of 0.03 g/L. After that, the absorbance of the mixture was measured at 505 nm using a spectrophotometer (Varian, UK). The obtained absorbance values of the sample were subtracted from the absorbance of a control or reference (supernatant of PLGA nanoparticles without chitosan) to give the normalised absorbance of free chitosan in the supernatant. The normalised absorbance of the sample was then extrapolated to standard curves of absorbance to known concentrations of chitosan in distilled water (0.01 to 0.1 mg/ml) in order to calculate the free chitosan concentrations in the supernatant of which were then subtracted from the initial concentration of chitosan added during particle preparation.

2.8 Preparation of phosphate buffer

Phosphate buffer was prepared by adding monobasic and dibasic sodium phosphate stock solution. 0.2 M monobasic stock solution was prepared by dissolving 27.6 g of monobasic sodium phosphate (monohydrate) in water and after the salt was fully

dissolved, water was added up to 1 liter. Then, a dibasic 0.2 M stock solution was prepared by dissolving 35.61 g dibasic sodium phosphate in water and water was further added up to 1 liter. After that, 46 ml of monobasic and 4 ml dibasic sodium stock solutions were mixed and water was added up to 100 ml to obtain a 0.1 M phosphate buffer with the desired pH of 5.8.

2.9 Adsorption of siRNA or pDNA onto the particles

siRNA or pDNA was adsorbed onto the surface of various nanoparticles as described below:

2.9.1 PLGA-PEI nanoparticles

siRNA adsorption onto PLGA-PEI nanoparticles was carried out in TE buffer or phosphate buffer pH 7.4. A fixed amount of siRNA was added drop-wise to an equal volume of various concentrations of PLGA-PEI nanoparticles depending on nitrogen to phosphate ratio of PEI and siRNA (N/P ratio of 50:1 to 1:1). The suspension was then briefly mixed and incubated at room temperature for 1 h. The same protocols were used for pDNA adsorption.

2.9.2 PLGA-chitosan nanoparticles

siRNA adsorption onto the PLGA-chitosan nanoparticles was analysed as a function of nanoparticles to siRNA weight ratio, ranging from 10:1 to 100:1. A fixed amount of siRNA was added drop-wise to an equal volume of PLGA-chitosan nanoparticles in TE buffer, pH 7.4 and the suspension was then briefly mixed and incubated at room temperature for 1 h before use. The same protocols were used for pDNA adsorption.

2.9.3 Chitosan-TPP nanoparticles

Chitosan nanoparticles were dispersed in RNase free water to yield a chitosan concentration, ranging from 0.1-1 mg/ml. To adsorb siRNA onto the surface of chitosan nanoparticles, chitosan suspension was added drop-wise to the siRNA in RNase free water (10 µg/ml) and quickly mixed by inverting the interaction tube up and down. Then, the particles were incubated for 2 h at room temperature before further analysis.

2.10 Quantification of siRNA

Quantification of siRNA loading was determined by spectrophotometry. To measure the loading of siRNA, chitosan-siRNA nanoparticles (entrapped or adsorbed siRNA) were spun down at 13 000 X g for 10 min whereas PLGA-PEI and PLGA-chitosan with adsorbed siRNA was spun at 10 000 X g for 5 min (IEC micromax, USA). The supernatants were collected and siRNA content in the supernatants was measured using a spectrophotometer (Varian, UK). Absorbance at 260 nm was measured and supernatants collected from unloaded nanoparticles were used as a reference. siRNA loading efficiency (%) was the amount of condensed siRNA, (difference between the total amount of siRNA added for the nanoparticles preparation and the amount of non-entrapped siRNA remaining in the supernatant) calculated as a percent of the total amount of siRNA added.

2.11 Quantification of pDNA

2.11.1 Depletion Method

After adsorbing pDNA overnight, the particle suspension; either PLGA-PEI or PLGA-chitosan with adsorbed pDNA, was centrifuged at 10 000 X g for 5 min (IEC micromax, USA). The supernatant was taken off and put into a fresh 1.5 ml centrifuge tube. This was then analysed by PicoGreen[®] assay (Molecular Probe) for DNA quantification.

2.11.2 Extraction method

5 mg particles were resuspended in 500 μ l of TE buffer and 500 μ l of chloroform were added to solubilize the microparticles. The mixture was vortexed briefly and then shaken horizontally on the platform rocker (STR6, Bibby, UK) at ambient temperature for 20 min to facilitate the extraction of pDNA from the organic phase into the aqueous supernatant (Barman *et al.* 2000). After 20 min, the suspension was centrifuged at 10 000 X g for 10 min (IEC micromax, USA) and the aqueous layer was taken off with a microtipped pipette. This extraction method was repeated by adding 500 μ l of fresh TE buffer, followed by vortexing and centrifuging. Then, the aqueous layer was drawn off and put into a fresh centrifuge tube. All collected aqueous layers were used for agarose gel electrophoresis (Bio-Rad wide Mini-sub cell G7

electrophoresis box combined a Bio-Rad Power PAC200 power supply) for structural integrity assays.

2.11.3 PicoGreen® assays

100 µl of TE buffer was added to aqueous supernatant containing pDNA extracted from microparticles. As *per* the manufacturer's instructions (Molecular Probes), stock picogreen reagent was diluted 1:200 in TE buffer and 100 µl was added to each sample containing pDNA. Then, the solution was incubated in the dark at room temperature for 5-10 min. The fluorescence of the pDNA/picogreen complexes was measured using a fluorometer (Wallac Victor² 1420 Multilabel Counter) and the concentration of pDNA was calculated directly from a standard curve generated using the average values of the pDNA standards.

2.12 Agarose gel electrophoresis

Agarose gel electrophoresis was used to assess the binding efficiency of siRNA or pDNA to the nanoparticles. Different types as well as concentrations of gel were used for siRNA and pDNA. For siRNA, Low Melting Point (LMP) agarose at high concentration (4% m/v) was chosen as more suited to the small size of siRNA (21 bp).

2.12.1 siRNA

The binding of siRNA to the nanoparticles was determined by 4% agarose (low melting point, Promega) gel electrophoresis (Bio-Rad wide Mini-sub cell G7 electrophoresis box combined a Bio-Rad Power PAC200 power supply). 20 µl of sample was loaded with 1:6 dilution of loading dye (Blue/orange, Promega) to each well and electrophoresis was carried out at a constant voltage of 55 V for 2 h in TBE buffer (4.45 mM tris-base, 1 mM sodium EDTA, 4.45 mM boric acid, pH 8.3) containing 0.5 µg/ml ethidium bromide (10 mg/ml, BDH). The siRNA bands were then visualised under a UV transilluminator at wavelength of 365 nm.

2.12.2 pDNA

DNA condensation as well as the structural integrity of DNA complexed or adsorbed onto particles was analysed *via* 1% agarose (LE, analytical grade) gel electrophoresis (Bio-Rad wide Mini-sub cell G7 electrophoresis box combined a Bio-

Rad Power PAC200 power supply). 100 ml of Tris-Acetate (TAE) solution (0.04 M Tris-Acetate, 0.002 M EDTA) was added into 1 g of agarose and this was boiled until dissolved. Then, 5 μ l of 10 mg/ml ethidium bromide stock (BDH) solution was added into the cooled agarose solution to a final concentration of 0.5 μ g/ml before pouring into the gel cast. Samples or reference DNA (λ DNA/*Hind III*, Fermentas) containing loading dye (blue/orange, Promega) with a 1:6 dilution were loaded into each well of the gel and the gel was run at 80 V for 1-2 h. After that, the gel was viewed under a UV lamp at 365 nm.

2.13 DNase protection assays for pDNA

Loaded nanoparticles containing 20 μ g/ml of DNA were diluted into 10 mM TE buffer, pH 7.4. To activate DNase activity, 8 μ l of DNase buffer 10 \times (1 M Na-acetate, 50 mM MgCl₂) and 12 μ l of DNase 1 solution (DNase I Boehringer Mannheim, Germany) (50 IU/ml in 50 mM Tris-HCl pH 8, 100 mM KCl) was subsequently added and this was incubated at 37 °C (Gallempkamp Orbital Incubator shaker, Gallempkamp Instrument Inc., USA). Aliquots (100 μ l) were taken at predetermined time points of 0, 30, 60, 90 and 120 min. 12 μ l of stop solution (0.5 M EDTA, pH 8) was added to stop DNase degradation and the samples were immediately put on ice. The DNA was dissociated from the particles by adding 80 μ l of heparin (1000 units/ml) and incubation at 65°C overnight. Then, electrophoresis was carried out as section 2.11.2.

2.14 Serum protection assay for siRNA

Nanoparticles (200 μ l, equivalent to 5 μ g of siRNA) were incubated at 37°C (Gallempkamp Orbital Incubator shaker, Gallempkamp Instrument Inc., USA). with an equal volume of Dulbecco's Modified Eagles Medium (DMEM) supplemented with 5 and 50% final concentration of foetal bovine serum. At each predetermined time interval (0, 30 min, 2, 4, 7, 24, 48 and 72 h), 30 μ l of the mixture was removed and stored at -20°C until gel electrophoresis was performed. To terminate serum activity, samples were incubated in a bath incubator at 80°C for 5 min and 5 μ l heparin (1000 unit/ml) was added for displacing the siRNA from the nanoparticles. The integrity of the siRNA was then analysed by 15% polyacrylamide gel containing 7 M urea and TBE (0.089 M Tris base, 0.089 M boric acid, and 2 mM sodium EDTA, pH 8.3) buffer.

Polyacrylamide-Urea gel (15%) was used due to its high efficiency in separating

small fragments of possibly degraded siRNA. Electrophoresis (Mini-PROTEAN 3 electrophoresis chamber combined a Bio-Rad Power PAC200 power supply) was carried out with a 1X TBE (0.089 M Tris base, 0.089 M boric acid, and 2 mM sodium EDTA, pH 8.3) buffer at a constant voltage of 200 V for 1 h. siRNA bands were visualised under a UV transilluminator after staining for 40 min with a 1:1000 dilution of SYBR-Green II RNA gel stain (Molecular Probes) prepared in DEPC treated water.

2.15 Determination of biological activity of pDNA and siRNA

2.15.1 Transfection studies for pDNA

Transfection studies were performed in HEK 293 cells. The cells were maintained in Dulbecco's Modified Eagles Medium (DMEM, Sigma) supplemented with 2 mM L-glutamine (200 mM, Sigma), 1% of penicillin (10 000 unit/ml) and streptomycin (10 mg/ml) mixture (Sigma) and 10% fetal bovine serum (FBS, Sigma). Cells were incubated at 37 °C in a humidified atmosphere containing 5% CO₂ and used at appropriate degrees of confluence (90% cell confluency). For transfection experiments, HEK 293 cells (2×10^4 per well) were seeded in a 48 well plate 24 h before the transfection. Positive controls were carried out using Superfect (Qiagen) and transfections of pDNA gWiz™ luciferase were performed as *per* manufacturer's instructions. pDNA loaded nanoparticles were diluted in DMEM without serum or antibiotics to a final volume of 100 µl before adding to the wells. Then, cells were incubated another 24 or 48 h to allow luciferase expression.

For luciferase expression analysis, the cells were washed twice with PBS and lysed with reporter lysis buffer (Promega) according to the manufacturer's instructions. Relative Light Units (RLUs) due to luciferase activity after adding 50 µl Luciferase Assay Reagent (Promega, UK) to 20 µl cell lysate were measured with chemiluminometer (Wallac Victor² 1420 Multilabel Counter). RLUs were normalized to protein concentration in the cell extracts. Protein concentration was measured using the BCA (Bicinchoninic acid, Pierce) protein assay method, taking bovine serum albumin (BSA, Sigma) as the standard for comparison.

2.15.2 Gene knockdown studies for siRNA

In-vitro transfection studies were performed in CHO K1 and HEK 293 cells. The cells were seeded in a 96-well plate at a density of 5000 cells per well in Opti-MEM 1 reduced serum medium (Invitrogen) containing 5% of FBS without antibiotics, 24 h prior transfection to give 70% of cell confluency on the day of transfection. On the day of transfection, the cells were co-transfected with pGL3-control and pRL-TK vectors using Lipofectamine 2000™ according to the manufacturer's instructions. After 4 h of transfection, the medium was removed and the cells were washed twice with PBS, followed by replacement of 100 µl fresh medium containing serum although removal of medium is not required according to lipofectamine 2000 transfection protocols. 50 µl of siRNA-nanoparticles in the medium without serum was then added to the cells and incubated at 37°C with a 5% CO₂ atmosphere (CO₂ Incubator, Hertford, UK) for 24 or 48 h. Luciferase activities were determined using the Dual-Glo Luciferase Assay System (Promega, UK).

2.15.3 RNA preparation and reverse-transcriptase PCR (rt-pcr)

Total RNA was prepared using the TRI Reagent® (Sigma, UK). The concentration of RNA was measured by the absorbance at 260 nm using spectrophotometer (Genespec 1, Japan), and RNA integrity was confirmed by formaldehyde-formamide denatured agarose gel electrophoresis (Bio-Rad wide Mini-sub cell G7 electrophoresis box combined a Bio-Rad Power PAC200 power supply). One microgram of RNA isolated from each sample was used for cDNA synthesis. First-strand cDNA synthesis was primed with Anchored oligo (dT)₂₃ and carried out according to the manufacturer's two steps RT-PCR instructions (Enhanced Avian HS RT-PCR Kit, Sigma, UK). The cDNA equivalent to 100 ng of total RNA was subjected to subsequent PCR analysis which was performed in the presence of firefly luciferase primers (forward: CCAGGGATTTTCAGTCGATGT, reverse: AATCTCACGCAGG-CAGTTCT) with an initial denaturation step of 2 min at 94 °C, followed by 50 cycles of 15 s denaturation at 94 °C, 50 s annealing at 55 °C and 1 min elongation time at 68 °C. Finally, final extension step was performed at 68 °C for 5 min. As negative controls, an identical set of reactions was set up without the addition of the cDNA. PCR reactions for the actin control were carried out separately for 25 cycles with β-Actin Primer Pair (Promega, UK). RT-PCR products were then electrophoresed on 4% agarose (LMP)

gel electrophoresis (Bio-Rad wide Mini-sub cell G7 electrophoresis box combined a Bio-Rad Power PAC200 power supply).

2.16 Cytotoxicity studies

The effect of nanoparticles on cytotoxicity was measured by determining cell viability, calculated as a percentage of the cell viability of untreated/non-transfected cells. Cells were seeded in a 96-well plate at a density of 5 000 cells per well in Opti-MEM 1 reduced serum medium containing 5% of FBS and grown overnight. After 24 and 48 h post- incubation of siRNA-nanoparticles at 37°C, 20 µl of MTT (3-(4,5-dimethyl-thiazol-2-yl)-2,5-diphenyl-tetrazolium bromide, Sigma, 5 mg/ml,) in sterile filtered PBS was added to each well and then incubated for 4 h (CO2 Incubator, Hertford, UK) to allow formation of formazan crystals. After 4 h, the unreduced MTT and medium was removed and the cells were washed with PBS. 200 µl of DMSO was then added to each well to dissolve the MTT formazan crystals and the plate was incubated at 37°C for 5 min. The absorbance of formazan products was measured at 540 nm using a microplate reader (Wallac Victor2 1420 Multilabel Counter).

Chapter 3

Studies of physical and biological characteristics of PEI as delivery systems for siRNA

Studies of physical and biological characteristics of PEI as delivery systems for siRNA

Gene therapy based on siRNA has emerged as an exciting novel therapeutic strategy over past few years. However, several biopharmaceutical problems such as insufficient cellular uptake and poor accessibility have limited its usefulness. A number of strategies have been utilised and one of them is biodegradable polymeric delivery systems where PLGA has been extensively studied (Panyam and Labhasetwar 2003; Hughes *et al.* 2001; Jain 2000) due to its relatively low toxicity and biological compatibility. Where adsorption of siRNA on the surface of particles is desired, cationic agents like PEI could be used to produce positively charged particles at physiological pH and PEI's ability to bind polyanions appears to be an important property to achieve this goal. In this study therefore, PEI has been investigated for complexation with siRNA and used as a surface modifier to produce biodegradable nanoparticles with efficient and improved cellular penetration.

PEI (branched, 25 kDa) was complexed to siRNA by simple mixing to produce PEI-siRNA complexes. Meanwhile, to obtain PLGA-PEI nanoparticles, PEI was incorporated into the PLGA particles by a spontaneous modified emulsification diffusion. The influence of certain parameters on nanoparticle characteristics was also investigated where the resultant particles were subject to physical (particle size, surface charge, ability to bind siRNA and stability in serum) and biological (transfection efficiency and cytotoxicity) characterisations.

PEI has been shown to have the ability to complex siRNA by simple mixing. Small and positively charged PEI-siRNA complexes were observed and their particle size found to be between 100 to 200 nm depending on the N/P ratio of PEI to siRNA. On the other hand, incorporation of PEI into PLGA particles (a PLGA to PEI weight ratio 29:1) was found to produce smooth and spherical positively charged nanoparticles. The particle size of PLGA-PEI nanoparticles has also been shown to be affected by several parameters such as type of polymer, type and concentration of surfactant. A smaller particle size around 100 nm was obtained when 5% m/v PVA was used as a surfactant compared to poloxamer-188 or poloxamer-407 at the same concentration which produced particle size about 500 and 700 nm, respectively. In addition, freeze-drying was shown to induce these particles to aggregate and this could be prevented by adding 10% glycerol before the process. Further studies showed that PLGA-PEI nanoparticles (5% m/v PVA) were able to completely bind siRNA at N/P ratio 20:1 and provided protection for siRNA against nuclease degradation for up to 24 h. Experimental data from the cell cultured *in-vitro* studies subsequently revealed that PLGA-PEI nanoparticles with adsorbed siRNA could efficiently transfect cells, better than PEI alone, with no significant loss in cell viability.

PLGA-PEI nanoparticles have been found to be superior to its individual parent compounds; PEI and PLGA particles. These particles therefore, have shown to have a great potential to be a vector to deliver siRNA into cells *in-vitro* and provide more opportunities for further investigation especially for their potential applications *in-vivo*.

3 Studies of physical and biological characteristics of PEI as delivery systems for siRNA

3.1 siRNA-PEI polyplexes

PEI has been known as an efficient gene carrier with a high cationic charge density. In this study, branched PEI of 25 kDa was used because PEI in its branched structure condenses to a greater extent than does linear PEI (Godbey *et al.* 1999). Branched PEI in fact, consists of 25, 50 and 25% of primary, secondary and tertiary amines. The amine family is a family that have at least one sp³ hybridized Nitrogen bonded to as few as one hydrocarbon group and as many as four hydrocarbon groups. If one, two or three hydrocarbon group is bonded to the Nitrogen, it is classified as a primary, secondary and tertiary amine, respectively. In addition, the Nitrogen atom of the primary, secondary, and tertiary amines has a lone pair of electrons that is often in the presence of a more acidic substance capable of donating the lone pair in forming a fourth bonding pair. The use of the lone pair of electrons makes the Nitrogen electron deficient and the Nitrogen atom would then possess a formal charge of +1 and would be classified as a quarternary amine. The first three classes of amines are said to act as weak Lewis Bases (electron donors) due to the presence of a lone pair of electrons that can be donated to an acid.

Therefore, PEI has the ability to be protonated in a wide range of pH and the majority of the amines will exist in a protonated state when the pK_a value exceeds 9. Furthermore, the primary amines of PEI are reported to participate in forming complexes with DNA while secondary and tertiary amines are responsible for substantial endosomal disruption after endocytosis due to their buffering effect at any pH under physiological conditions (Ahn *et al.* 2002, Remy *et al.* 1998, Berh 1997). Therefore to address the ability of PEI to deliver siRNA to the target cells, siRNA-PEI complexes were prepared at different nitrogen to phosphate ratios of PEI to siRNA (N/P ratios). The complexes were further characterised for physical and biological properties.

3.1.1 Effect of nitrogen to phosphate ratio of PEI to siRNA on the physical characteristics of siRNA-PEI complexes

In the presence of sufficient PEI, pDNA will condense (Godbey *et al.* 1999, Dunlop *et al.* 1997) and it has been shown that pDNA-PEI polyplexes with a small particle size could be achieved by adjusting the molar ratio of PEI nitrogen atoms to DNA phosphate (Clamme *et al.* 2003, Finsinger *et al.* 2000, Ogris *et al.* 1998, Boussif *et al.* 1995). In this study therefore, siRNA-PEI polyplexes were prepared at different N/P ratios, from as low as 2:1 to 25:1 in RNase free distilled water. These complexes had a narrow particle size distribution and a measured particle size less than 200 nm depending on N/P ratio except for the ratio of 2:1 as shown in the table below:

N/P ratio of PEI to siRNA	Z-ave diameter, nm	Polydispersity, PI
2:1	*4089 ±186.3	1.00 ±0.01
5:1	139 ±1.5	0.14 ±0.01
10:1	157 ±2.2	0.15 ±0.2
25:1	131 ±0.8	0.15 ±0.01

Table 3.1: Effect of N/P ratio on polyplexes particle size and size distribution (n=3) as determined by Malvern System 4700c Submicron particle analyser (Malvern, U.K). Keynotes: * particle size was inaccurate due to a high polydispersity index.

A great increased in particle size and polydispersity index of these complexes at the ratio of 2:1 was observed and this may have been due to the aggregates formation which arising from its relatively low particle surface charge of only +15.4 ±0.1 mV. It has been shown that particle surface charge is an important factor affecting the stability of colloidal systems as less pronounced positive or negatively charge and neutral particles tend to aggregate as a result of electrical repulsion reduction between individual particles. It was also found that particle surface charge of the siRNA-PEI complexes was increased from +15.4 ±0.1 to +52.5 ±0.1 mV when the N/P ratio of the complex was increased from 2:1 to 5:1. This was predicted as the numbers of free protonated amine groups of PEI was increased with the increment of N/P ratio.

The morphology of the siRNA-PEI complexes are shown on figure 3.1. The complexes were solid small rounded condensates around 150 nm for NP ratio of 5:1

which described a complete binding of siRNA to PEI. It has been reported that complete condensate had rounded forms while unsaturated condensate ranged from bundled, folded loops or loose coils with isolated nodes of condensation (Dunlap *et al.* 1997). This morphology therefore, illustrated sufficient interaction between siRNA and PEI has taken place and these compact particles could provide some protection to the carried siRNA from nuclease degradation. In agreement with particle size measurement using PCS, the siRNA-PEI complexes at N/P ratio of 2:1 was aggregated as seen on the TEM images.

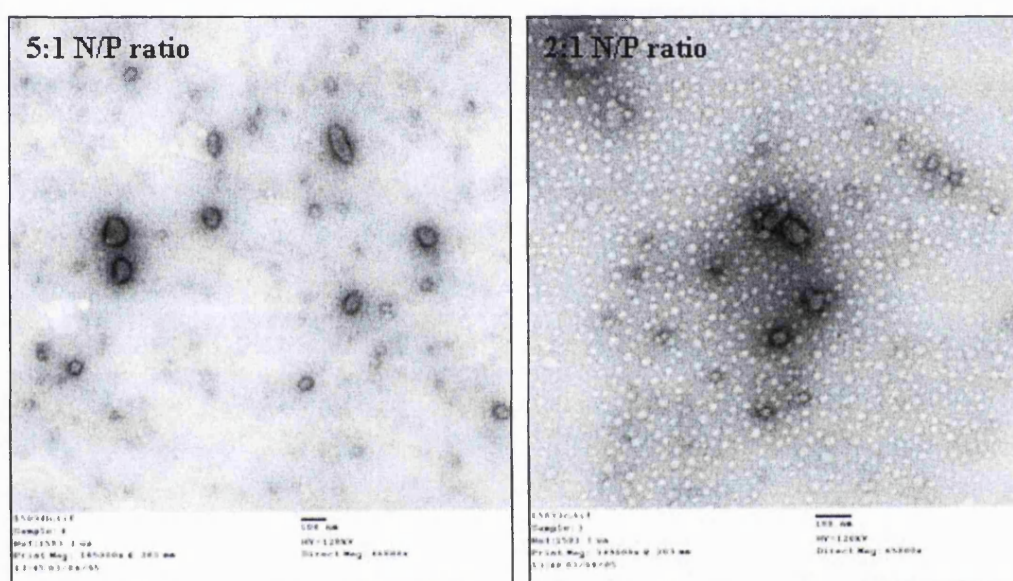


Figure 3.1: Effect of N/P ratio of PEI to siRNA on particle morphology of siRNA-PEI complexes. The complexes with a N/P ratio 5:1 were solid small rounded condensates but aggregation was seen for the complexes at a N/P ratio 2:1 which thought to be due to a relatively less pronounce of its particle surface charge.

On the other hand, gel mobility shift was used to assess siRNA binding to the PEI. A complete binding of siRNA to PEI was achieved at a N/P ratio 5:1 as determined by agarose gel electrophoresis (figure 3.2B). At below this point, siRNA was migrated resulting in a band with a similar position to the control siRNA, indicating the presence of free siRNAs which had been released or not bound to the PEI. On the other hand, siRNA complexed with PEI at the N/P ratio 5:1 (figure 3.2, Lane B2) could not be stained by ethidium bromide which suggesting that siRNA was completely and tightly

complexed with PEI and therefore it was not accessible for the dye to intercalate siRNA.

3.1.2 Comparison of physical characteristics of siRNA- to plasmid DNA-PEI complexes

The results obtained from the characterisation of both siRNA- and pDNA-PEI complexes, showed no significant difference in particle size for the studied N/P ratios except for the N/P ratio of 2:1 where aggregation was observed for siRNA-PEI complexes. No obvious aggregation was observed at this ratio (2:1) for pDNA polyplexes as at this point, the polyplexes had a pronounced positive charge of $+25.2 \pm 0.4$ mV. The strong positive surface charge of pDNA-PEI complexes induced repulsion interactions among the particles and resulted in a more stable colloidal system than siRNA-PEI complexes which consequently prevented aggregation. The size and surface charge of the pDNA polyplexes are shown below:

N/P ratio of PEI to plasmid DNA	Z-ave diameter, nm	Polydispersity, PI	Surface charge, mV \pm (SD)
25:1	139 \pm 5.5	0.18 \pm 0.02	+33.2 \pm 1.2
10:1	126 \pm 3.3	0.11 \pm 0.01	+34.3 \pm 0.4
5:1	178 \pm 10.2	0.28 \pm 0.01	+34.4 \pm 0.4
2:1	335 \pm 32.6	0.25 \pm 0.05	+25.2 \pm 0.3

Table 3.2: Influence of PEI to pDNA N/P ratio on particle size as well as size distribution and surface charge of pDNA-PEI complexes determined by Malvern System 4700c Submicron particle analyser and Malvern ZetaMaster[®], respectively (n=3).

Moreover, pDNA could completely bind to PEI at a lower N/P ratio than siRNA-PEI complexes (1:1) as shown below. These results apparently illustrated that pDNA had better interaction with PEI polymer than siRNA. One reason that could explain this was the ability of pDNA to condense once 70-90% of its phosphate groups were interacted with amine groups of PEI. In contrast, siRNA had no such effect as its linear structure might be responsible for the difficulty of siRNA in binding to the PEI.

Chapter 3

Studies of physical and biological characteristics of PEI as delivery systems for siRNA

Besides, a much larger molecular size of pDNA than siRNA was thought to be attributed to the increase efficiency of pDNA binding to PEI since it has a larger binding surface compared to siRNA. When comparing ratio of PEI to polyanion molecule, one molecule of PEI could interact ~33 times more siRNA molecules compared to pDNA molecule due to a smaller molecule weight of siRNA (21 bp) than pDNA (6732 bp). Therefore, ratio of PEI to siRNA molecule (0.07:1) was lower than to pDNA (23:1) which supporting why PEI-siRNA complexes have a larger particle size than PEI-pDNA complexes.

Decreased fluorescent intensity which was seen for PEI-pDNA complexes with N/P ratio 5:1 (figure 3.2, Lane A9) on the other hand, was thought to be due to the shielding effect of the complexation molecule which restricted the ethidium bromide dye to contact with pDNA. However, it was suggested that binding of the bromophenol blue dye to the complexes could absorb fluorescent light during visualisation which might also attribute to the decreased fluorescent intensity on the gel (Shah *et al.* 2000). In addition, smearing appearance of some bands was also indicated heterogeneity in electrophoretic behaviour (charge/mass) (Medberry *et al.* 2004).

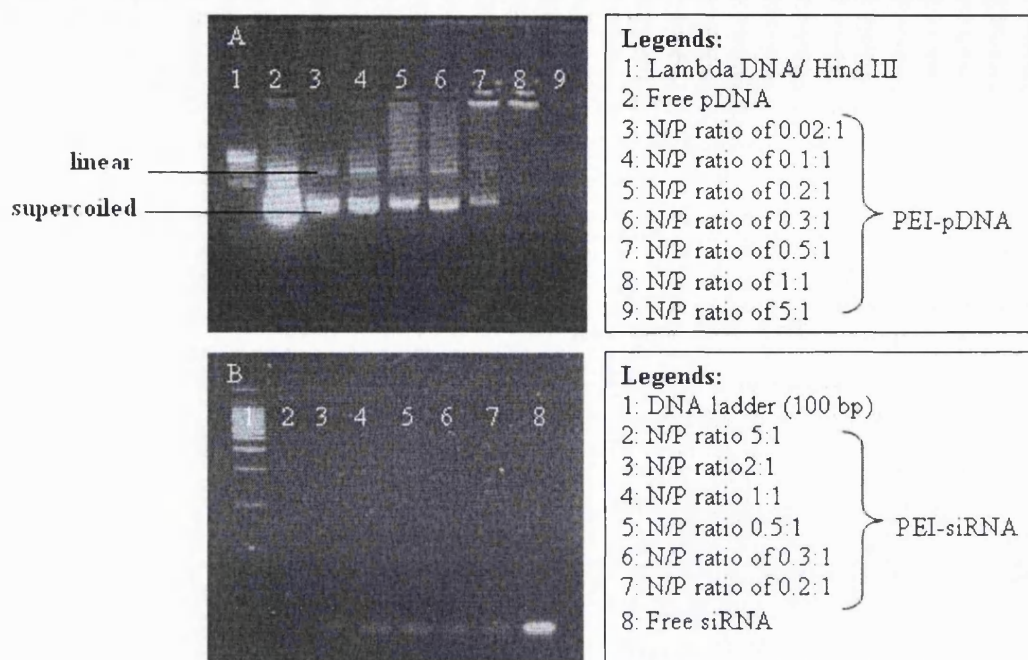


Figure 3.2: Binding efficiency of pDNA (A) and siRNA (B) to the PEI at various N/P ratios. Electrophoresis was carried out using 4 % agarose (LMP) gel in TAE buffer (0.04 M Tris-Acetate, 0.002 M EDTA) and TBE buffer (4.45 mM tris-base, 1 mM sodium EDTA, 4.45 mM boric acid, pH 8.3) containing 0.5 $\mu\text{g/ml}$ ethidium bromide at pH 8 for pDNA and siRNA, respectively. 20 μl of sample was loaded to each well with 1:6 dilution of loading dye (Blue/orange, Promega) and electrophoresis was carried out at a constant voltage of 80 and 55 V for pDNA and siRNA, respectively. Complete binding of pDNA and siRNA to the PEI were at a N/P ratio 1:1 and 5:1, respectively.

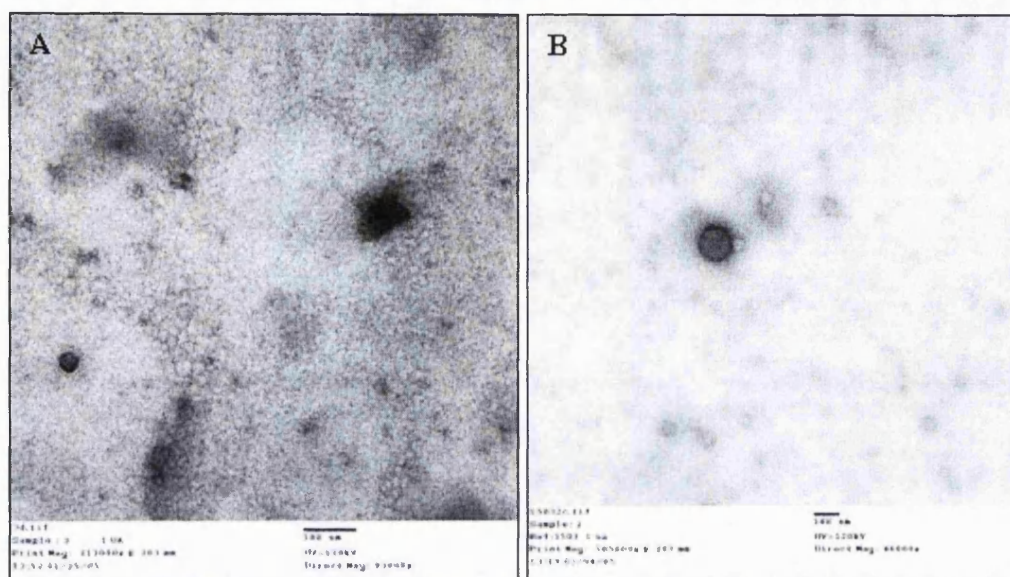


Figure 3.3: Comparison of particle morphology of pDNA-PEI complexes (A) and siRNA-PEI complex (B) at N/P ratio of 10:1.

3.2 PLGA-PEI nanoparticles

It has been mentioned in previous chapter that PEI could be incorporated into the polymeric particles such as PLA or PLGA particles to improve bioavailability, drug loading efficiency and to achieve control release of the encapsulated drugs. In this study, PEI was also incorporated into PLGA particles and these particles were prepared by a spontaneous emulsification diffusion method. Since acetone was used in this method, particle formation was observed immediately after mixing the organic and aqueous phase together because acetone is highly soluble in water which could rapidly diffuse into the aqueous phase. Attempts were made in this study to produce particles of less than 1 μm diameter (preferably less than 500 nm). The advantages of such nanoparticulate systems includes relatively higher intracellular uptake than microparticles. Furthermore, nanoparticles are readily to be taken up by the Peyer's patches in the GALT (gut associated lymphoid tissue) after oral administration and better suited for intravenous delivery due to the fact that the smallest capillaries in the body are 5-6 μm in diameter. Therefore, the size of particles must be less than 5 μm to prevent embolism (Hans and Lowman 2002, Gref *et al.* 1995). From the other physio-chemical aspects, zeta potential (surface charge), loading efficiency and release profiles

are among the most important characteristics of nanoparticles in order to successfully deliver bioactive materials to the target cells.

3.2.1 Effect of formulation parameters on PLGA-PEI nanoparticles

It was reported that the particle size and surface charge of PLGA could be easily adjusted by modifying preparation parameters (Shakweh *et al.* 2005). In this study, the modification of certain parameters was investigated to determine their influence on the physical characteristics of PLGA-PEI nanoparticles such as particle size, surface charge and morphology. Parameters investigated included PLGA to PEI weight ratio, type and concentration of surfactant amongst others which will be discussed further in the following sections.

3.2.1.1 PLGA to PEI weight ratio

The amount of PEI added to the PLGA 50:50 2A was expected to affect not only the cationic density of nanoparticles but also particle size and morphology. Therefore, the amount of PEI added was specified as PLGA to PEI weight ratio, ranging from 59:1 to 5:1 that equivalent to 5-50 mg of PEI in 295-250 mg of PLGA. For this experiment, poloxamer-188 (0.5% m/v) was used as a surfactant. Increasing the amount of PEI in the PLGA, it has been shown resulted in the reduction of particle size by more than 2-fold from 661 to 253 nm.

A reduction in the particle size of PLGA-PEI nanoparticles was observed with the increase amount of PEI added. Lyophilised form of these nanoparticles with a high content of PEI (more than 10 mg of PEI or PLGA-PEI weight ratio 29:1) however, could not be further analysed due to the difficulty to resuspend them in aqueous media. This was corroborated with the SEM studies where these nanoparticles (more than 10 mg PEI) did not exhibit a regular morphology in their freeze-dried form which could be due to the disruption in particle stability during freeze-drying by the high viscosity of PEI. Therefore, only PLGA-PEI weight ratios of 29:1 and 59:1 were used for the following experiments. Particle size shown below was measured before washing by filtration (figure 3.4). A slight increased in particle size after the washing procedure was observed which were 570 ± 30.2 and 705 ± 42.1 nm for PLGA to PEI weight ratio of 29:1 and 59:1, respectively. However, severe aggregation was observed for all the tested particles after freeze drying process where particle size was increased to around 4.1

$\pm 0.35 \mu\text{m}$ for both PLGA-PEI weight ratios 29:1 and 59:1 as measured by Mastersizer[®] (Malvern, U.K).

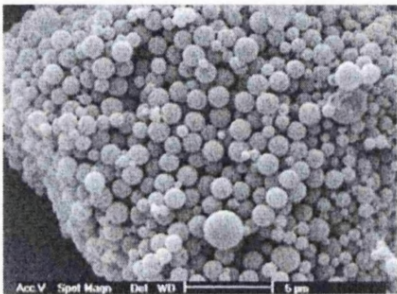
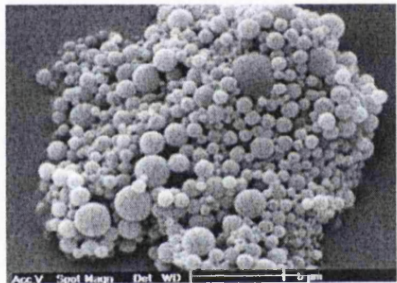
Morphology	Z-average diameter, nm	Polydispersity (PI)
29:1 of PLGA to PEI weight ratio 	562 \pm 28.7	0.24 \pm 0.2
59:1 of PLGA to PEI weight ratio 	661 \pm 36.9	0.3 \pm 0.2

Figure 3.4: Effect of PLGA to PEI weight ratio on particle size (n=3) and morphology of PLGA-PEI nanoparticles by Malvern Zetasizer[®] and SEM, respectively. Particles were prepared using 0.5% m/v poloxamer-188 as stabiliser.

Determination of particle surface charge of PLGA-PEI nanoparticles was a crucial step to evaluate the capability of siRNA adsorption *via* ionic interaction on the particle surface as well as to determine the potential stability of the colloidal system in the aqueous phase. The results indicated that particle surface charge was influenced by the PLGA-PEI weight ratio. Only particles with the incorporation of PEI at lower than a PLGA to PEI weight ratio of 29:1 produced a positive charge. On the other hand, particles with plain PLGA had a negative surface charge around $-24.6 \pm 0.7\text{mV}$. The negative value of the plain PLGA was attributed to the presence of carboxylic groups on its backbone whereas the positive surface charge of the PLGA-PEI nanoparticles was a result of the PEI orientation on the surface of the particles since PEI has a very high

amine density. The surface charge of PLGA-PEI nanoparticles at different PLGA-PEI weight ratios are shown below:

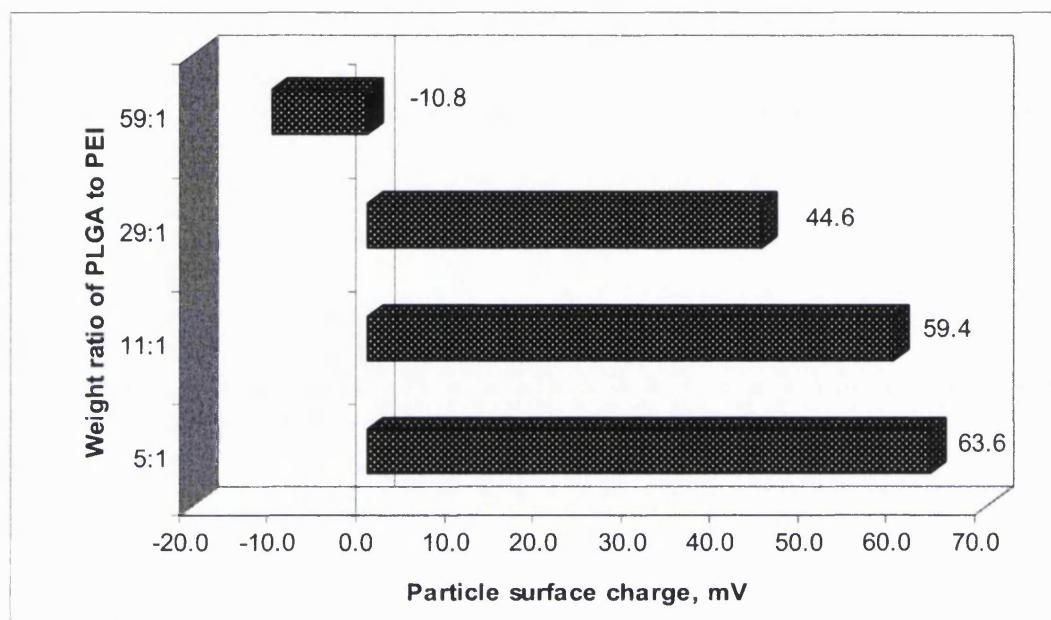


Figure 3.5: Effect of PLGA to PEI weight ratio on the particle surface charge of PLGA-PEI nanoparticles stabilised by poloxamer-188 at 0.5% m/v (n=3). Standard deviation was ± 1.1 , ± 1.3 , ± 0.5 and ± 0.2 for the PLGA to PEI weight ratio of 5:1, 11:1, 29:1 and 59:1, respectively.

3.2.1.2 Type and concentration of surfactant

In the emulsification diffusion method, the stabilisation of droplets by the stabiliser after the diffusion process is important to avoid coalescence and the formation of agglomerates during solvent removal and polymer solidification (Kwon *et al.* 2001, Hsu *et al.* 1999). In this study, poloxamer (Poloxamer-188 and Poloxamer-407) and PVA (13-23 kDa and 30-70 kDa) were studied as stabilisers at different concentrations.

3.2.1.2.1 Poloxamer

Poloxamer is made up of hydrophilic block copolymers of ethylene oxide (EO) and propylene oxide (PO) (figure 3.6). The important difference between these

Chapter 3

Studies of physical and biological characteristics of PEI as delivery systems for siRNA

structures is the additional methyl group of the PO unit, which makes it more hydrophobic, while the EO unit is more hydrophilic. Therefore, the hydrophobic sections of the polymer which contain PO units can be used to adsorb and anchor the molecule to the nanoparticle surface, while the hydrophilic EO can extend into solution and shield the surface of the particle (Owen III and Peppas 2006). These block copolymers are also able to adsorb strongly to microspheres surface as well as sterically stabilize the surface even after extensive washing with water and they have been reported to inhibit neutrophil phagocytosis of microspheres (Jackson *et al.* 2000).

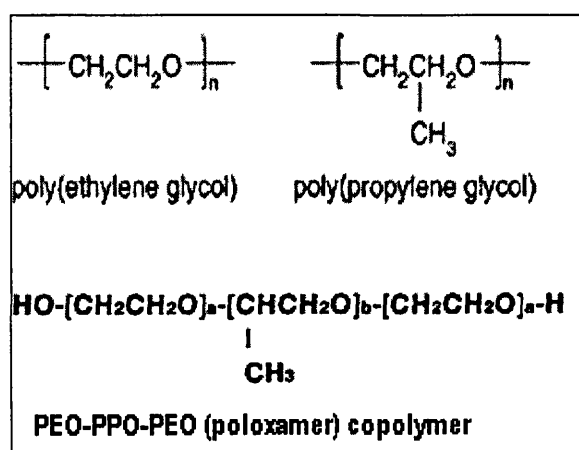


Figure 3.6: Poly(ethylene glycol) and poly(propylene glycol) molecular structures of poloxamer and their copolymer.

These polymeric surfactants proved to be superior to the conventional non-ionic surfactants in maintaining the physical stability of the emulsions (Vasiljevic *et al.* 2006, Tadros *et al.* 1995). Poloxamer-188 and -407 used in this study were different in molecular and percentage of polyethylene-glycol polymers as shown in the table below:

	Molecular weight, gram/mole	percentage of polyethylene-glycol polymers
Poloxamer-188	8436	81.8 ± 1.9
Poloxamer-407	12330	73.2 ± 1.7

Table 3.3: The difference properties of poloxamer-188 and -407 used in the study.

Three different concentrations were used in the preparation of PLGA-PEI nanoparticles which were 0.5, 2 and 5% m/v. Independent of the molecular weight of the poloxamer, the increment of poloxamer concentration apparently had no effect on particle size of PLGA-PEI nanoparticles with a PLGA to PEI weight ratio 29:1, however it reduced the particle size of 59:1 PLGA to PEI weight ratio from 661 to 445 nm for poloxamer-188 and from 1240 to 511 nm for poloxamer-407. The details of their effects on particle size and size distribution of PLGA-PEI nanoparticles are shown in table 3.4.

Poloxamer-188				
PLGA to PEI 29:1			PLGA to PEI 59:1	
concentration, %m/v	Z-ave diameter, nm	Polydispersity (PI)	Z-ave diameter, nm	Polydispersity (PI)
0.5	562 ±50.2	0.24 ±0.03	661 ±25.6	0.30 ±0.01
2.0	567 ±35.6	0.40 ±0.13	413 ±10.2	0.53 ±0.24
5.0	545 ±22.5	0.65 ±0.11	445 ±4.5	0.40 ±0.11
Poloxamer-407				
PLGA to PEI 29:1			PLGA to PEI 59:1	
concentration, %m/v	Z-ave diameter, nm	Polydispersity (PI)	Z-ave diameter, nm	Polydispersity (PI)
0.5	701 ±56.3	0.35 ±0.09	1240 ±112.3	0.37 ±0.02
2.0	739 ±44.3	0.48 ±0.08	683 ± 23.3	0.55 ±0.13
5.0	705 ±33.6	0.73 ±0.1	511 ±11.5	0.48 ±0.05

Table 3.4: Effect of type and concentration of poloxamer on particle size of PLGA-PEI nanoparticles as determined by Malvern Zetasizer® (n=3).

From the table above, the size distribution of the particles was however increased with the increase of poloxamer concentration and this could be obviously

observed from the images of SEM (figure 3.7). Furthermore, these findings described that poloxamer-188 was more effective in stabilising the emulsion during particle preparation than poloxamer -407 as it produced smaller and more homogenous nanoparticles. A larger particle size for the PLGA-PEI nanoparticles stabilised by poloxamer-407 was also thought to be related to a longer chain length of polyethylene oxide segment of the poloxamer -407 (average number of ethylene oxide ≈ 200 units) compared to poloxamer-188 (average number of ethylene oxide ≈ 153 units) (Dunn *et al.* 1997).

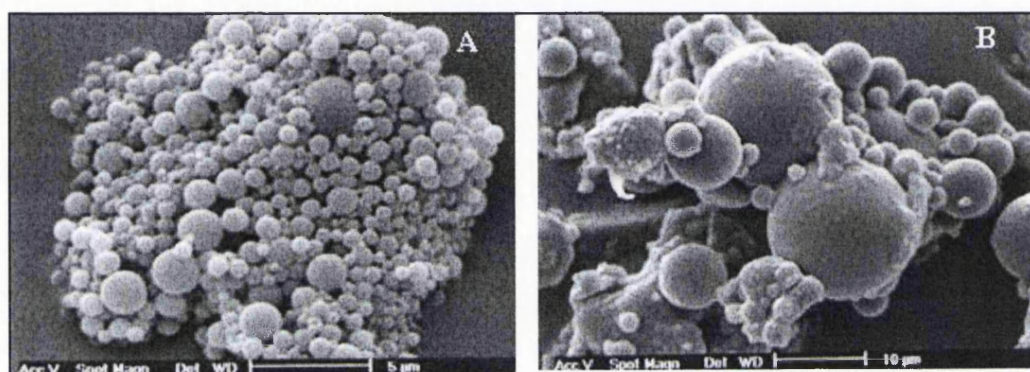


Figure 3.7: Effect of surfactant concentrations on the morphology of PLGA-PEI nanoparticles of 59:1 weight ratio after freeze-drying. A: 0.5% m/v poloxamer-188, B: 2% m/v poloxamer-188.

Particle surface charge of the PLGA-PEI nanoparticles at a weight ratio of 29:1 was positively charge; $+37.6 \pm 0.6$, $+59.7 \pm 0.35$ and $+55.1 \pm 0.8$ mV for 0.5, 2 and 5% m/v of poloxamer-188, respectively while negative values of particle surface charge (-30.5 to -10.8 mV) were observed for PLGA-PEI weight ratio of 59:1 for all the tested poloxamer-188 concentrations. Similar results were obtained for PLGA-PEI nanoparticles made using poloxamer-407 as the particle surface charge was in the range of $+48.0 \pm 1.5$ mV (0.5% m/v) to $+50.7 \pm 1.2$ mV (5% m/v) for a weight ratio of 29:1 and -32.3 ± 1.1 (0.5% m/v) to -19.3 ± 0.87 mV (5% m/v) for a weight ratio of 59:1.

A decrease of particle surface charge of PLGA-PEI nanoparticles at a weight ratio of 59:1 with the increasing concentration of poloxamer was due to the increase of adsorbed poloxamer onto the particle surface which screened the charge arising from

amino and carboxylic groups from PEI and PLGA, respectively. Nevertheless, these results were also indicating that poloxamer as a stabiliser had less effect on particle surface charge where nanoparticles had a PLGA to PEI weight ratio of 29:1. From these results, it can be concluded that the PLGA-PEI weight ratio plays a more important role in determining the particle surface charge of these PLGA-PEI nanoparticles.

3.2.1.2.2 Polyvinyl alcohol

Polyvinyl alcohol (PVA) is a commonly used non-ionic stabiliser for preparing nanoparticles using emulsification techniques. When the emulsion is formed, the hydrophobic backbone of PVA partitions into the organic phase, while the hydrophilic hydroxyl side chains partition into the aqueous phase (Keegan *et al.* 2006). In this study a series of PVA concentrations, ranging from 0.5 to 5% m/v was studied to determine its effects on particle size of PLGA-PEI nanoparticles (PLGA-PEI weight ratio 29:1). Particle size was found to be greatly reduced after increasing PVA concentration from 0.5 to 5% m/v. In addition; PVA with molecular weight of 30-70 kDa was more effective than a molecular weight of 13-23 kDa in reducing particle size. The details of particle size and polydispersity of PLGA-PEI nanoparticles are shown below:

PVA concentration, %m/v	13-23 kDa		30-70 kDa	
	Z-ave diameter, nm	Polydispersity (PI)	Z-ave diameter, nm	Polydispersity (PI)
0.5	605 ±12.1	0.41 ±0.01	437 ±9.8	0.50 ±0.12
2.0	195 ±13.3	0.08 ±0.07	161 ±9.3	0.08 ±0.02
5.0	117 ±1.8	0.10 ±0.02	97 ±4.9	0.08 ±0.02

Table 3.5: Effect of PVA molecular weight and concentration on particle size of PLGA-PEI nanoparticles at a PLGA to PEI weight ratio 29:1 as determined by Malvern Zetasizer[®] before washing (n=3). A smaller particle size and PI were observed with the increase of PVA concentration from 0.5 to 5 % m/v.

The reduction of particle size by increasing PVA concentration was thought to be due to the increasing viscosity of the aqueous phase since the viscosity of the aqueous phase of an emulsion affects the Reynolds number, thus the droplet break-up is

governed by laminar or turbulent flow (Leroux *et al.* 1995). In addition, by increasing stabilizer concentration of PVA, more stabilizer molecules are adsorbed on the interfaces of emulsion droplets, providing increased protection against coalescence and resulting in smaller emulsion droplets.

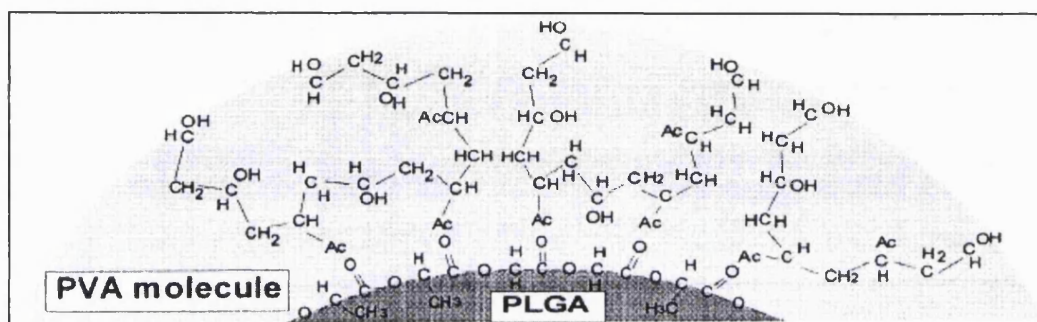


Figure 3.8: Schematic representation of molecular orientation of PVA bound to PLGA molecules at the surface of PLGA nanoparticles. A hydrophobic bonding between the hydroxyl groups of PVA molecules to the acetyl groups of PLGA results in strong adsorption of PVA on the surface of PLGA nanoparticles (courtesy of Murakami *et al.* 1999)

Increasing the concentration of PVA resulted in a reduction of the particle surface charge of PLGA-PEI nanoparticles. The value of PLGA-PEI nanoparticles (PLGA to PEI weight ratio of 29:1) surface charge stabilised by PVA with molecular weight of 13-23 kDa was $+46.1 \pm 1.2$, $+40.1 \pm 1.2$ and $+37.4 \pm 1.0$ mV for 0.5, 2.0 and 5.0% m/v, respectively. The decrease of particle surface charge of these nanoparticles correlated with the increase of PVA adsorbed onto the surface of nanoparticles which shifts the shear plane outwards, resulting in a reduction of zeta potential (figure 3.8) (Dunn *et al.* 1997). A decrease in particle surface charge was also observed for the PLGA-PEI nanoparticles stabilised by PVA with higher molecular weight of 30-70 kDa.

3.2.1.3 PLGA polymer

In the emulsification diffusion method, preparation of conventional oil in water (o/w) emulsion is the most important step that determines the final size of nanoparticles besides rapid diffusion of solvent from the emulsion droplets upon the addition of

Chapter 3

Studies of physical and biological characteristics of PEI as delivery systems for siRNA

water. Therefore, the organic phase consisting of polymer and solvent plays an important key in the preparation of the emulsion. In fact, particle size has been reported could be affected by the polymer structure which differed in polarity or molecular weight (Cegnar *et al.* 2004). Previous researchers have also synthesized PLGA nanoparticles by the emulsification diffusion method and they reported that as the PLGA concentration in the organic phase increases, the mean size of the resultant PLGA nanoparticles increases due to the increase viscosity of the organic phase that increases resistance to shear forces (Kwon *et al.* 2001). On the other hand, Cegnar *et al.* (2004) reported that polymer with free carboxyl end group are more hydrophilic and formed smaller particle size with better polydispersity index than esterified polymer.

In this study, three different types and molecular weight of PLGA 50:50 were studied; 2A (14 kDa), 3A (47 kDa) and 4A (58.8 kDa). Those polymers were “uncapped” or contain different numbers of free carboxylic acid end groups which are represent as ‘A’ and this number increases with the increment of free carboxylic acid groups. To evaluate their effects on particle size as well as surface charge of PLGA-PEI nanoparticles (PLGA-PEI weight ratio 29:1), poloxamer-188 was used as stabiliser at a concentration of 0.5% m/v. In agreement with the previous studies, a reduction of particle size was observed with the increase of PLGA molecular weight (Murakami *et al.* 1997) and degree of “uncapped” end group (Cegnar *et al.* 2004). However, these results were different from the study reported by Kwon *et al.* (2001) which reported otherwise. The particle size and surface charge of the resultant PLGA-PEI nanoparticles using different types of polymer are shown below:

Polymer type	Z-ave diameter, nm	Polydispersity, PI	Particle surface charge, mV SD(±)
2A (14 kDa)	562 ±50.2	0.24 ±0.03	+37.6 ±0.6
3A (47 kDa)	533 ±42.4	0.23 ±0.006	+51.9 ±0.8
4A (58.8 kDa)	473 ±48.7	0.24 ±0.07	+55.7 ±1.0

Table 3.6: Effect of polymer type on particle size and surface charge of PLGA-PEI nanoparticles determined by Malvern Zetasizer® (n=3).

From the above table, independent of type of polymer, particle surface charge of PLGA-PEI nanoparticles was positively charged, ranging from +38 to +56 mV. These findings demonstrated that particle size and surface charge of PLGA-PEI nanoparticles were affected by the types of PLGA which were studied in this experiment. The increment of particle surface charge with the increase of "uncapped" end groups was expected since a higher number of free carboxylic groups within PLGA molecular structure could efficiently interact with PEI's amino groups once they were ionized upon contact with water. On the other hand, images from SEM showed that, independent of polymer type, these particles were round and had a smooth surface morphology as shown below:

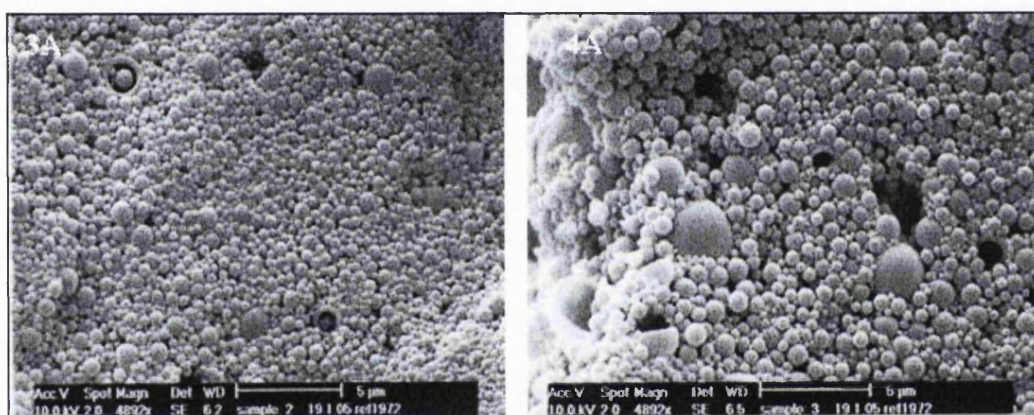


Figure 3.9: SEM images of PLGA-PEI nanoparticles made of PLGA 50:50 3A and 4A.

3.2.1.4 Lyoprotectant agent

The stability of vectors such as nanoparticles can be improved by freeze-drying or lyophilization. This process converts a solution of labile materials into solids of sufficient stability for distribution and storage (Abdelwahed *et al.* 2006, Frank 1998). The advantage of lyophilised products over liquid formulations includes the freeze-dried products are less susceptible to mechanical stresses during shipping and handling because of the removal of air-water interface. Besides, collision between particles in lyophilised form is also greatly reduced which therefore reduces aggregation compared with liquid formulation (Randolph 1997). The induction of particle aggregation

however has been reported as one of the drawbacks of the freeze-drying process. It is thought that this may arise from ice crystallisation during the freeze-drying process which then leads to the phase separation of nanoparticles (Abdelwahed *et al.* 2006). Moreover, this procedure seems to generate a variety of freezing and drying stresses (surface-induced effects, concentration effects and temperature-induced thermodynamic effects) which induce surface modification of the particles leading to the formation of aggregates (Konan *et al.* 2002, Randolph 1997).

A significant increase in particle size of the freeze-dried form of PLGA-PEI nanoparticles was also observed in this study. Independent of the type or concentration of stabiliser used in the particle preparation, the size of the particles was increased 6-fold after the freeze-drying process. For example, the particle size of PLGA-PEI nanoparticles (PLGA to PEI weight ratio of 29:1) stabilised by poloxamer-188 at concentration of 0.5% m/v was greatly increased from 560 nm (before washing/ freeze-drying) to 3400 nm after freeze-drying. The increment of the particle size was thought to be due to the formation of aggregates induced by the freeze-drying process because after two cycles of centrifugation, this process was shown to contribute only slightly to an increase in particle size (774 nm) compared to particle size after freeze-drying.

Excipients used to protect bioproducts during freezing and drying process must form a glassy solid with a glass transition temperature (T_g) that is higher than planned storage conditions when in dried form (Randolph 1997). Numerous studies have shown that lyoprotective agents (LPAs) such as sugars (e.g. mannitol, glucose and trehalose) could protect particles from aggregation during the freeze-drying process (Konan *et al.* 2002). These sugars are favoured as excipients because they are chemically harmless and can be easily vitrified during freezing (Franks 1998). This lyoprotective effect has been attributed to the ability of the sugar to form a glassy amorphous matrix around the particles which subsequently prevents the particles from sticking together during the removal of water (Konan *et al.* 2002, Carpenter *et al.* 1997, Randolph 1997, Ford and Dawson 1993). In this study, various types of LPAs were added to the particle suspensions before freeze-drying to determine their effects on preventing particle aggregation induced by the freeze-drying procedure. The sugars investigated were glucose, mannitol and trehalose at various amounts between 5 to 35% of total polymer used in the particle preparation. These sugars have advantages and disadvantages which

Chapter 3

Studies of physical and biological characteristics of PEI as delivery systems for siRNA

are listed in the table 3.7. Nevertheless, the results obtained were frustrating as none of the above sugars could prevent particle aggregation induced by freeze-drying.

Lyoprotectant agent	Advantages	Disadvantages
Glucose (Carpenter <i>et al.</i> 1997)	~Inhibit protein unfolding during lyophilisation.	~Have the propensity to degrade protein.
Mannitol (Carpenter <i>et al.</i> 1997)	~Tend to crystallize during lyophilisation and form a mechanically strong cake.	~Inadequate stability during processing or storage in the dried solid when used alone
Trehalose (Randolph 1997)	~Higher Tg at any moisture content thus is easier to lyophilise. ~more resistant to acid hydrolysis unless very low pH are employed (around or below pH 4)	~Greater propensity to phase separate from polymer during freezing and drying.

Table 3.7: Advantages and disadvantages of several lyoprotectant agents based on polysaccharides.

In several studies have shown that glycerol could be used as an effective LPA. Therefore, a study to determine the effectiveness of glycerol in protecting PLGA-PEI nanoparticles during freeze-drying was carried out by adding 10% glycerol (m/m glycerol to polymer) to plain PLGA-PEI particles before the process. It was found that glycerol was effective in preventing particle aggregation during the freeze-drying process depending on the type and concentration of stabiliser used in particle preparation.

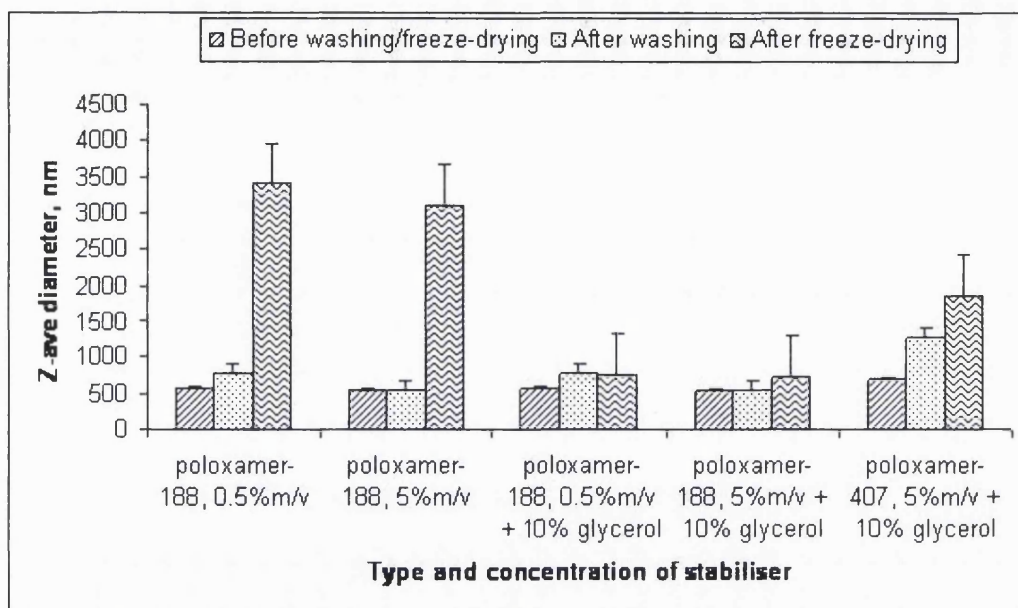


Figure 3.10: Effect of glycerol on particle size of PLGA-PEI nanoparticles (PLGA to PEI weight ratio of 29:1) after freeze-drying (n=3) as determined by Malvern Zetasizer[®]. Particle size of PLGA-PEI nanoparticles which higher than 1 μm was further analysed using Malvern Mastersizer[®] where the size was 4 ± 0.35 , 2.3 ± 0.15 and 1.7 ± 0.3 μm , for lyophilised particles made using poloxamer-188 (0.5% m/v), poloxamer-188 (5% m/v) and poloxamer-407 (5% m/v + 10% glycerol), respectively.

From the graph, it could be seen that by increasing the concentration of poloxamer-188 from 0.5 to 5% m/v, nanoparticles became more stable which could resist the increment of particle size, arising from particle aggregation induced by high speed centrifugation (20 000 rpm). The increment of adsorbed poloxamer-188 on the surface of nanoparticles however could not further protect these particles from the freezing and drying stresses of the freeze-drying process which resulted in the formation of aggregates. The addition of glycerol to the particle suspension was found to prevent particle aggregation as no significant increase in particle size was observed for the freeze-dried samples. Therefore, the addition of glycerol was necessary in order to protect these nanoparticles during the freeze-drying process although nanoparticles had been stabilised during the emulsification step.

In contrast to poloxamer-188, poloxamer-407 appeared to be less effective in protecting particles from the centrifugation process as a significant increase in particle size was observed after centrifugation. The addition of glycerol also had less effect in preventing particle size from increasing after freeze-drying. Furthermore, glycerol as an additive had no effect on particle surface charge of PLGA-PEI nanoparticles as well as their capacity to adsorb pDNA onto the surface of PLGA-PEI nanoparticles. In this study, siRNA was adsorbed after freeze-drying to avoid exposure to any possible stresses related to freezing and drying processes (temperature and concentration changes) which may lead to siRNA denaturation or rapid release of siRNA from the particles. The particle surface charge and pDNA loading efficiency of PLGA-PEI nanoparticles (PLGA to PEI weight ratio of 29:1) are shown below:

Poloxamer-188 concentration, % m/v	Plain particles		10% glycerol	
	Particle surface charge, mV, SD (\pm)	pDNA loading efficiency, %	Particle surface charge, mV, SD (\pm)	pDNA loading efficiency, %
0.5	+37.6 \pm 0.60	43.6 \pm 22.3	+32.7 \pm 0.70	43.8 \pm 8.2
2.0	+59.7 \pm 0.35	98.6 \pm 15.2	+54.3 \pm 0.10	98.1 \pm 2.5
5.0	+55.1 \pm 0.80	99.1 \pm 20.3	+57.1 \pm 0.65	98.3 \pm 5.7

Table 3.8: Effect of glycerol on particle surface charge and pDNA loading efficiency of PLGA-PEI nanoparticles (n=6).

3.2.2 siRNA adsorption onto the surface of PLGA-PEI nanoparticles

In this study, only particles with size of around 100 nm were chosen for siRNA adsorption and therefore only particles made from PLGA-PEI with the weight ratio of 29:1 and stabilised by PVA were used. siRNA adsorption was carried out in RNase free water and the adsorption was done by varying the N/P ratio of PLGA-PEI nanoparticles to siRNA, ranging from 1:1 to 50:1. Adsorption efficiency of siRNA onto the particles was then determined by 4% agarose (LMP) gel electrophoresis. Immobilization of siRNA by the PLGA-PEI nanoparticles only could be seen when the N/P ratio was approaching 20:1 (figure 3:11), indicating siRNA could only be completely adsorbed onto the particles starting at this point and onwards. This ratio was much higher than the

N/P ratio of siRNA-PEI complexes (5:1). This was expected due to the partial exposure of PEI on the surface of PLGA-PEI nanoparticles; a portion of the amino groups of the PEI can be expected to interact with the carboxylic groups of PLGA or be buried inside the particles. Heparin was added to the sample suspensions to show the presence of siRNA adsorbed onto the particles. The migration of siRNA with the addition of heparin therefore confirmed the presence of siRNA on the surface of the particles as shown on figure 3.11. The heparin was used because it is an anion that could competitively displace siRNA from the PLGA-PEI nanoparticles, thus releasing siRNA from the particles.

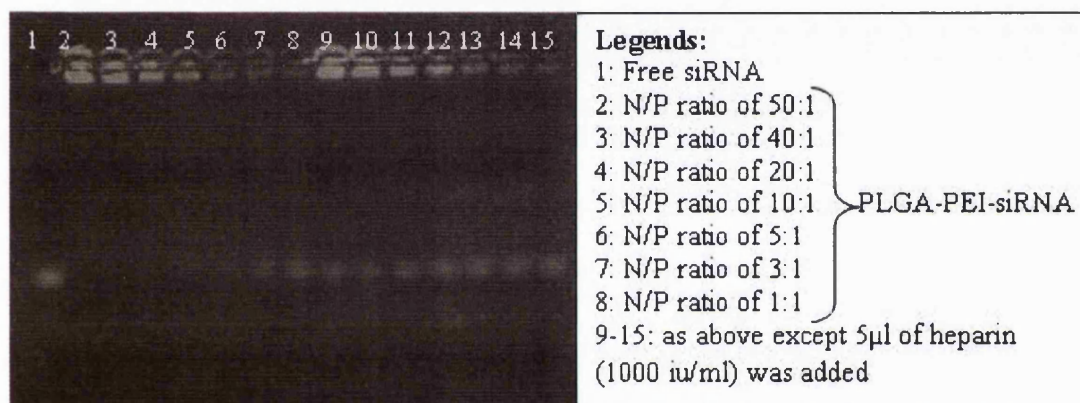


Figure 3.11: Effect of N/P ratio PLGA-PEI to siRNA on efficiency of siRNA adsorption onto the PLGA-PEI nanoparticles made using PVA (MW: 30-70 kDa). Electrophoresis was carried out using 4% agarose (LMP) gel in TBE buffer (4.45 mM tris-base, 1 mM sodium EDTA, 4.45 mM boric acid) containing 0.5 µg/ml ethidium bromide at pH 8. A complete binding of siRNA to the PLGA-PEI nanoparticles was achieved at a N/P ratio 20:1.

On the other hand, immobilisation of pDNA adsorbed onto the surface of PLGA-PEI nanoparticles was observed starting from the N/P ratio of PLGA-PEI nanoparticles to pDNA of 10:1 (figure 3.12). This value was much lower than siRNA adsorbed onto the PLGA-PEI nanoparticles, illustrating that PEI was less efficient in complexing siRNA than pDNA as explained in the previous section.

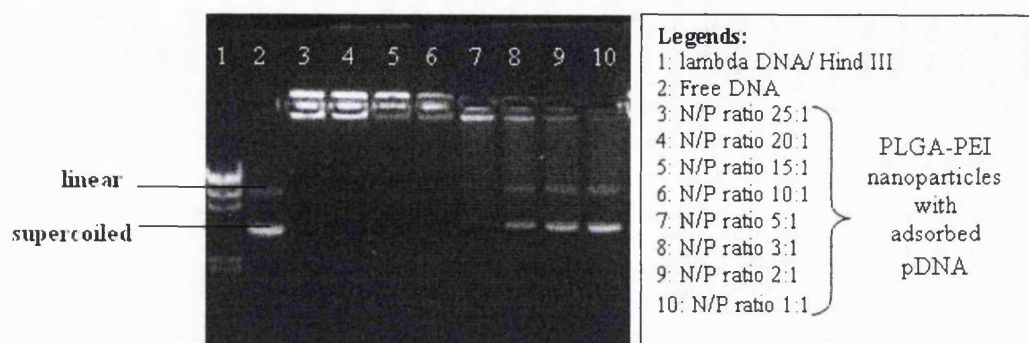


Figure 3.12: Binding efficiency of pDNA adsorbed onto the PLGA-PEI nanoparticles made using PVA (MW: 30-70 kDa) at various N/P ratios. Electrophoresis was carried out using 1% agarose (LE) gel in TAE buffer (0.04 M Tris-Acetate, 0.002 M EDTA) containing 0.5 μ g/ml ethidium bromide at pH 8. A complete binding of pDNA to the PLGA-PEI nanoparticles was achieved at a N/P ratio 10:1.

pDNA loading efficiency of PLGA-PEI nanoparticles was also determined by PicoGreen[®] assays. The results indicated that independent of molecular weight of PVA, pDNA loading efficiency was increased with increasing of PVA concentration as shown in table 3.9. Similar results were obtained for PLGA-PEI nanoparticles stabilised by poloxamer-188 and -407. pDNA loading efficiency of PLGA-PEI nanoparticles (poloxamer-188) was increased from 46% (0.5% m/v) to 78% (5.0% m/v) with increasing stabiliser concentration. Besides this, it was also dependent on the PLGA to PEI weight ratio of PLGA-PEI nanoparticles as lower pDNA loading efficiency was obtained for PLGA to PEI weight ratio of 59:1 than 29:1; 34 and 40% for 0.5 and 5.0% m/v, respectively.

PVA concentration, %m/v	pDNA loading efficiency, %	
	PVA (13-23 kDa)	PVA (30-70 kDa)
2.0	69.4 ±12.8	65.6 ±12.2
5.0	72.4 ±20.1	72.2 ±8.8

Table 3.9: Effect of PVA concentrations on pDNA loading efficiency of PLGA-PEI nanoparticles with adsorbed siRNA at N/P ratio of 3:1 (n=3).

Therefore, analysis of siRNA loading efficiency adsorbed onto the PLGA-PEI nanoparticles was performed using PLGA-PEI nanoparticles prepared from the highest concentration of PVA (5% m/v, MW: 30-70 kDa) and siRNA was adsorbed onto the particles at different N/P ratios. siRNA loading efficiency was then determined by spectrophotometry and the results showed significantly increased siRNA loading efficiency from N/P ratio of 10:1 to 15:1 by 1.84-fold. In agreement with the results obtained from the gel retardation assays, 100% of siRNA loading efficiency was achieved at N/P ratio of 20:1 as at this point, siRNA was completely bound to the PLGA-PEI nanoparticles.

3.2.2.1 Adsorption medium

siRNA adsorption onto the PLGA-PEI nanoparticles was expected to occur *via* electrostatic interaction between negatively charged siRNA and positively charged PLGA-PEI nanoparticles. It was shown that 20% of the amine groups are positively charged at pH 7 and 45% at pH 4.5. In this study, siRNA was adsorbed onto the PLGA-PEI nanoparticles in phosphate buffer 0.2 M at pH 7 and 5.8 (the lowest pH of phosphate buffer that could be prepared in this study) to determine the effects of pH on siRNA adsorption. A N/P ratio of 10:1 was chosen in this study as at this ratio, siRNA was not completely bound to PLGA-PEI nanoparticles in RNase free water as shown in previous experiments. The use of a low N/P ratio was expected to make the evaluation of pH in improving siRNA adsorption easier than at a higher N/P ratio, for example N/P ratio 20:1 as at this point, siRNA was completely adsorbed to the particles even in RNase free water and would be difficult to evaluate any improvement in siRNA loading efficiency.

The results from spectrophotometry revealed that the siRNA loading efficiency adsorbed onto the PLGA-PEI nanoparticles was greatly increased by adsorbing siRNA onto the particles in phosphate buffer 0.2 M regardless the pH of the phosphate buffer (pH 7 or pH 5.8).

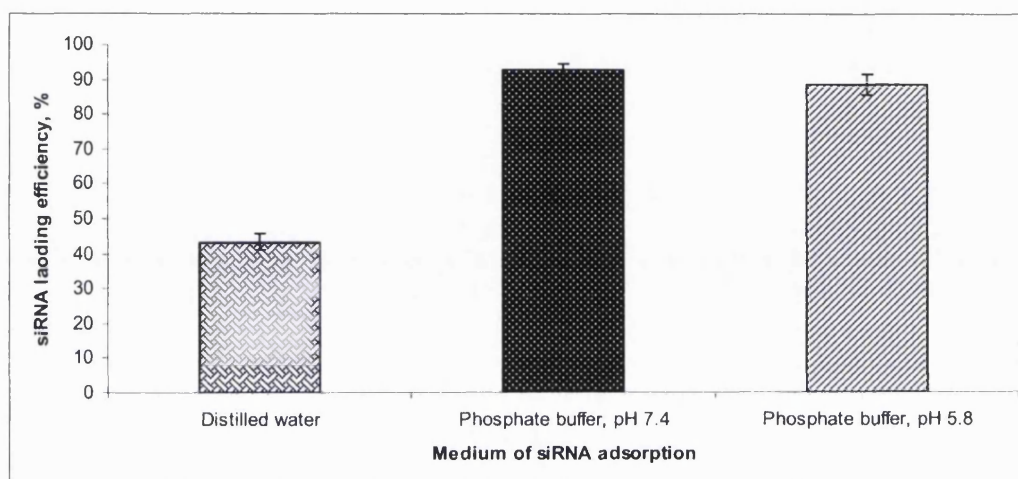


Figure 3.13: Influence of adsorption medium on the siRNA loading efficiency adsorbed onto the PLGA-PEI nanoparticles (n=3). Distilled water used in this study was RNase free.

The significant increment of siRNA loading efficiency was thought to be due to the presence of phosphate salt in the adsorption medium. It was shown by Rehm and Killman that polymer at the particle surface was influenced by salt concentration as in the presence of salt, a loop and tail conformation of the long polymer chain was obtained due to the screening of the colloidal charge. In contrast, in the absence of salt, the conformation of polymer was flat, arising from the charge neutralization (Trimaille *et al.* 2003, Rehm and Killman 1999). Therefore, the loop and tail conformation of PEI at the surface of particles was expected to facilitate the accessibility of siRNA to attract and interact with amino groups of PEI and form complexes. Furthermore, an increased siRNA loading efficiency in the presence of salt was thought to be due to a higher melting temperature (T_m) of siRNA in salt (~ 72.3 °C) than in RNase free water (~ 46.1 °C). T_m is the temperature which half the oligo strands are hybridized to

complementary sequences and another half are free in solution as single strands. Therefore, siRNA is more susceptible to denture into single strands in water, thus it may require twice as many binding sites with PEI compared to in the presence of salt and this could also affect siRNA stability and efficacy in inducing RNAi. The pH of the adsorption medium however, had less effect on siRNA loading efficiency adsorbed onto the PLGA-PEI nanoparticles as shown in the figure 3.13.

The conformation of PEI in the presence of salt was therefore thought to explain the higher siRNA loading efficiency in phosphate buffer than RNase free water because PLGA-PEI nanoparticles had a negative particle surface charge either dispersed in phosphate buffer at pH 7.4 or 5.8. The value of the particle surface charge was -3 mV and -1 mV for pH 7.4 and 5.8, respectively compared to +30 mV in RNase free water. The reduction of particle surface charge of PLGA-PEI nanoparticles in phosphate buffer was due to the screening of the colloidal charge by the salt. This was confirmed by the increment of particle surface charge to +11 and +18 mV for PLGA-PEI-siRNA nanoparticles previously adsorbed in phosphate buffer pH 7.4 and pH 5.8, respectively upon re-suspending nanoparticles pellets in distilled water after centrifugation.

3.2.3 Effect of ionic strength on the colloidal stability of PLGA-PEI nanoparticles

Stabilisation of a colloidal system was shown arising from either electrostatic or steric repulsion which is dependent on added electrolytes and changes in solvency as well as molar mass of the polymer, respectively (Lourenco *et al.* 1996). The stability of PLGA-PEI nanoparticles in the presence of salt was investigated by incubating the particles in the increasing molar concentration of phosphate buffer from 0.0125 to 0.2 M at pH 7.4 and 5.8. Experimental data from this study shown that the increment of particle size induced by salt concentration was only observed at pH 7.4 and no such effect was observed at pH 5.8 (figure 3.14). The increase of the particle size at pH 7.4 was arisen from the particle aggregation in order to compensate for the increase of ionic strength. This could be achieved by forming larger particles to reduce surface area and subsequently, to increase the charge density of the original particles. At pH 5.8 however, amino groups of PEI from PLGA-PEI nanoparticles were highly protonated which attributed to a higher surface charge density and could therefore, resist an alteration in ionic strength by the addition of salt.

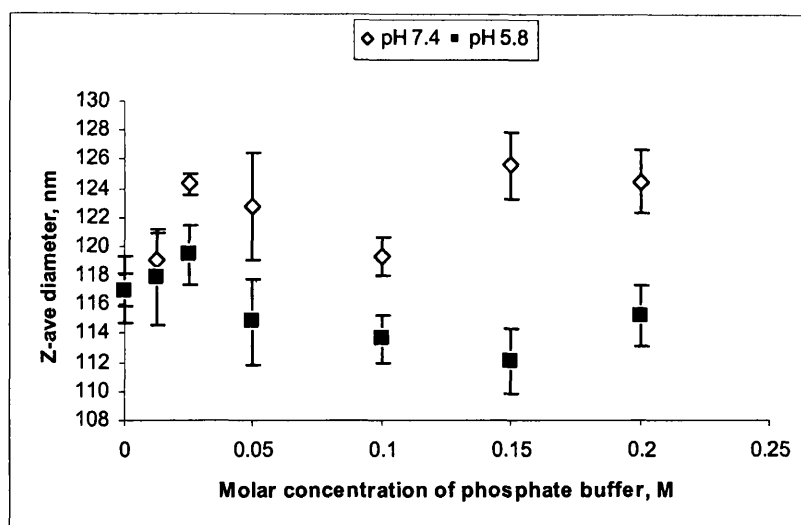


Figure 3.14: Effect of ionic strength on colloidal stability of PLGA-PEI nanoparticles at pH 7.4 and 5.8 (n=3).

Moreover, interaction of siRNA with PLGA-PEI nanoparticles at N/P ratio of 20:1 appeared to be not affected by the increasing molar concentration of sodium chloride (0.0125-0.2 M) as determined by the gel retardation assay. In this experiment, increasing molar concentration of sodium chloride was added to the PLGA-PEI with adsorbed siRNA and this was incubated at room temperature for 2 h. The results showed that no free siRNA was observed to be caused by desorption of siRNA from the particles induced by the increasing salt concentration even at the highest salt concentration (0.2 M) studied in this experiment. This indicated that the interaction between siRNA and PLGA-PEI nanoparticles was not solely through electrostatic interaction but may also involve hydrogen and hydrophobic interactions since PLGA had carbonyl moiety ($-C=O$) as well as hydroxyl group ($-OH$) in its structure which could permit additional stabilisation to the complex (Medberry *et al.* 2004).

3.2.4 Serum protection of PLGA-PEI nanoparticles with adsorbed siRNA

A possible therapeutic application of siRNA requires that siRNA remains intact in physiological environment. In the blood siRNA is exposed to serum RNase known to degrade single stranded RNA as well as dsRNA although the extent of degradation is different between single and double stranded (Haupenthal *et al.* 2006). Assessment of the ability of PLGA-PEI nanoparticles in protecting adsorbed siRNA from nuclease

Chapter 3

Studies of physical and biological characteristics of PEI as delivery systems for siRNA

degradation was performed by incubating these particles in DMEM medium containing 10% of FBS at 37°C for up to 48 h. PLGA-PEI with adsorbed siRNA at N/P ratio of 20:1 was chosen because at this ratio, complete binding of siRNA was achieved as determined earlier. The results obtained elucidated that siRNA was protected against nuclease activity for up to 24 h for PLGA-PEI nanoparticles when PVA with a molecular weight of 13-23 kDa was used as stabiliser whereas naked siRNA was fully degraded after 30 min incubation in serum indicating the vulnerability of siRNA in a serum surrounding. In contrast, PLGA-PEI nanoparticles made of PVA with molecular weight of 30-70 kDa were superior to those made with 13-23 kDa PVA in protecting siRNA as it was protected from nuclease mediated degradation for up to 48 h.

Nevertheless, these results were inconclusive because the bright bands on the top of the gel (in the well) were thought to be due to the presence of siRNA that were interacted with the serum proteins (eg. albumin) during incubation. Therefore, siRNA was unable to migrate through the gel during electrophoresis and the actual degradation kinetics of siRNA might be inaccurate. These were applied to all the serum protection assays performed in this study.

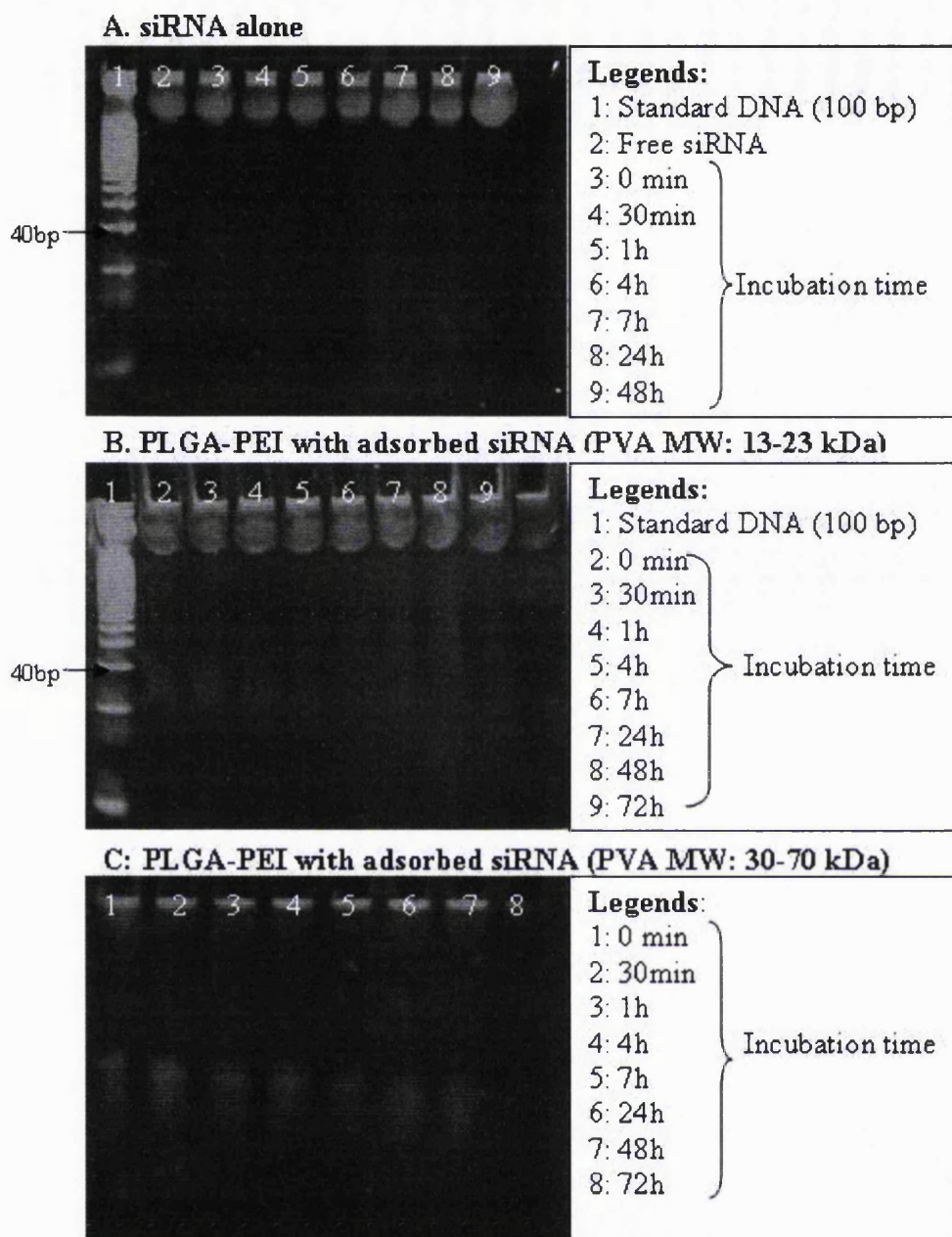


Figure 3.15: Effect of serum (10% FBS in DMEM) on the stability of siRNA adsorbed onto the PLGA-PEI nanoparticles at 37°C. The integrity of siRNA was analysed by 15% polyacrylamide gel containing 7 M urea and TBE (0.089 M Tris base, 0.089 M boric acid, and 2 mM sodium EDTA, pH 8.3) buffer. siRNA bands were visualised under a UV transilluminator after staining for 40 min with a 1:1000 dilution of SYBR-Green II RNA gel stain (Molecular Probes) prepared in DEPC treated water.

3.3 *In-vitro* studies

3.3.1 Biological studies of siRNA-PEI complexes and PLGA-PEI with adsorbed siRNA

Biological studies of siRNA adsorbed onto the surface of PLGA-PEI nanoparticles were assessed in two types of cells, HEK 293 and CHO K1 cell lines. In this study, only particles with a particle size around 100 nm were used and this could be achieved by preparing PLGA-PEI nanoparticles of 29:1 weight ratio using PVA as a stabiliser. In previous studies, PVA with either molecular weight of 13-23 kDa or 30-70 kDa at a concentration of 5% m/v was shown to produce nano-size range particles of around 100 nm. Therefore, these particles were tested for their ability to deliver siRNA by varying their N/P ratio from 25:1 to 50:1 PLGA-PEI nanoparticles to siRNA.

3.3.1.1 Effect of N/P ratio and stabiliser on siRNA silencing

In HEK 293 cells, a very high gene silencing effect of the targeted gene was observed after 24 h post-transfection for all of the cells treated with siRNA adsorbed onto the PLGA-PEI nanoparticles. For the particles prepared using PVA with molecular weight of 13-23 kDa, 99% of gene downregulation of the targeted gene was observed at N/P ratio of 25:1 and the gene downregulation effect was slightly reduced to 96 and 87% for N/P ratio of 35:1 and 50:1, respectively. In contrast, particles prepared using PVA with a molecular weight of 30-70 kDa showed an increase of gene downregulation with the increase of N/P ratio from 25:1 (28.1%) to 50:1 (97.1%) at 24 h post-transfection. Interestingly, PLGA-PEI nanoparticles appeared to be more efficient than PEI as a delivery system for siRNA because only 29% of targeted gene downregulation was observed for siRNA-PEI complexes (N/P ratio of 10:1).

However, no significant reduction in the gene silencing effect was seen after 48 h post-transfection. Less than 30% of the gene silencing effect was measured for the cells treated with siRNA adsorbed with PLGA-PEI nanoparticles and no gene silencing effect was observed for the particles at N/P ratio of 50:1 made using PVA with a molecular weight of 13-23 kDa at this time point. On the other hand, siRNA-PEI complexes showed an increased effect of gene downregulation by 0.58-fold at 48 h post-transfection. Furthermore, PLGA-PEI nanoparticles were comparable to the positive control, Lipofectamine 2000 as a transfection agent for siRNA at 24 h post-

transfection. Dependent on N/P ratio of PLGA-PEI with adsorbed siRNA and molecular weight of PVA used in the particles preparation, these particles have even shown a better gene silencing effect than Lipofectamine 2000 as shown in the figure 3.16 (one way Anova, followed by Post hoc multiple comparison test, $p < 0.05$).

Moreover, the graph showed no significant downregulation of targeted gene for naked siRNA and mismatch siRNA complexed to Lipofectamine 2000. This highlighted that the naked siRNA could not silence the targeted gene inside the cells. This might be because naked siRNA is not resistant to exposure to nuclease mediated degradation and/or may be unable to cross the lipid bilayer of the cell membrane. The findings also show that the gene silencing effect was specific to the target gene as no significant reduction in luciferase protein was observed when the cells was treated with mismatch siRNA complexed to Lipofectamine 2000.

Investigation was further performed by detecting luciferase gene using RT-PCR technique from extracted total RNA of the cells treated with different formulations (at 24 h post-transfection) where the cells transfected with pGL3 and non-treated cells were used as negative controls. On the other hand, Lipofectamine 2000-siRNA complexes were used as a positive control and an overall experiment was controlled by detecting β -actin gene. In this experiment, the absence of the bands for luciferase was observed for both Lipofectamine-2000-siRNA complexes (positive control) and PLGA-PEI nanoparticles with adsorbed siRNA. This therefore, illustrated that the silencing of the targeted gene was occurred at mRNA level of the cells treated with Lipofectamine-2000-siRNA complexes as well as PLGA-PEI nanoparticles with adsorbed siRNA which therefore supported the results obtained in the previous studies using luciferase protein assays.

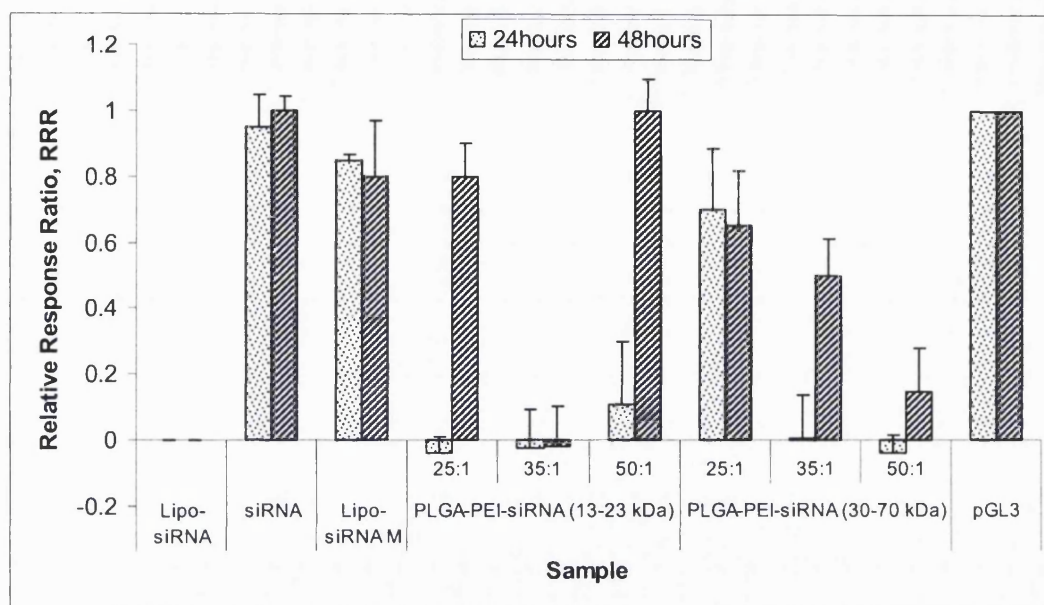


Figure 3.16: Relative Response Ratio of PLGA-PEI nanoparticles with adsorbed siRNA in comparison to siRNA-Lipofectamine 2000 complexes in HEK 294 cells (n=9). Experiments were performed on growing cells at 5×10^3 cell/ well. PLGA-PEI nanoparticles appeared to be more efficient than PEI in transfecting cells with siRNA and showed a comparable effect with Lipofectamine 2000 (Invitrogen). Keynotes: Lipo-siRNA= Lipofectamine 2000-siRNA complexes, Lipo-siRNA M= Lipofectamine 2000-siRNA mismatch complexes and pGL3= control cells without siRNA treatment.

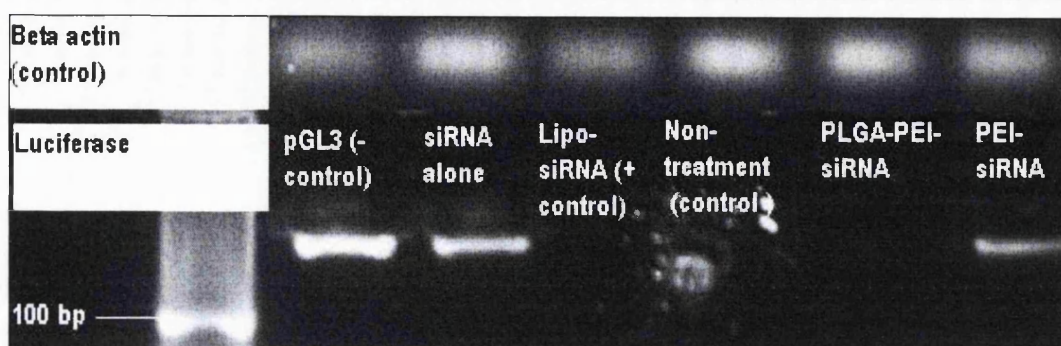


Figure 3.17: RT-PCR of total RNA extracted from HEK 293 cells treated with different formulations at 24 h post-transfection. RT-PCR analysis shows a reduction of mRNA level for firefly luciferase after treatment with the siRNA delivered by PLGA-PEI nanoparticles or Lipofectamine 2000 (Invitrogen) meanwhile PEI-siRNA complexes and siRNA alone show a minimal mRNA reduction. B-actin was used as an internal experimental control. Keynotes: pGL3= cells transfected with pDNA encoded firefly luciferase without siRNA treatment (negative control), non-treatment control = non-treated cells either with pDNA or siRNA (negative control), Lipo-siRNA= Lipofectamine 2000-siRNA complexes (positive control), PLGA-PEI-siRNA= PLGA-PEI nanoparticles (PVA 13-23 kDa was used as stabiliser) with adsorbed siRNA (N/P ratio 35:1) and PEI-siRNA= PEI-siRNA complexes (N/P ratio 10:1).

3.3.1.2 Effect of cell line on siRNA silencing

In a CHO K1 cell line, PLGA-PEI nanoparticles were less effective in delivering siRNA into the cells, as a lower gene silencing effect was observed compared to HEK 293 cells. At 24 h post-transfection, only 54 and 15% of gene downregulation was achieved for a N/P ratio of 35:1 and 50:1 respectively for the PLGA-PEI nanoparticles prepared using PVA with molecular weight of 13-23 kDa whereas 13 and 20% gene silencing was observed for PVA molecular weight of 30-70 kDa for the same N/P ratio as above, respectively. Similar to the results obtained from the HEK 293 cells, the gene silencing effect of siRNA adsorbed onto the PLGA-PEI nanoparticles made using PVA with a molecular weight of 13-23 kDa was reduced for both N/P ratios of 35:1 (32 %) and 50:1 (11 %) at 48 h post-transfection. In contrast, PVA with a molecular weight of 30-70 kDa facilitated slightly increased silencing of the targeted gene at 48 h post-

transfection for both N/P ratios of PLGA-PEI nanoparticles with adsorbed siRNA as shown in the figure below:

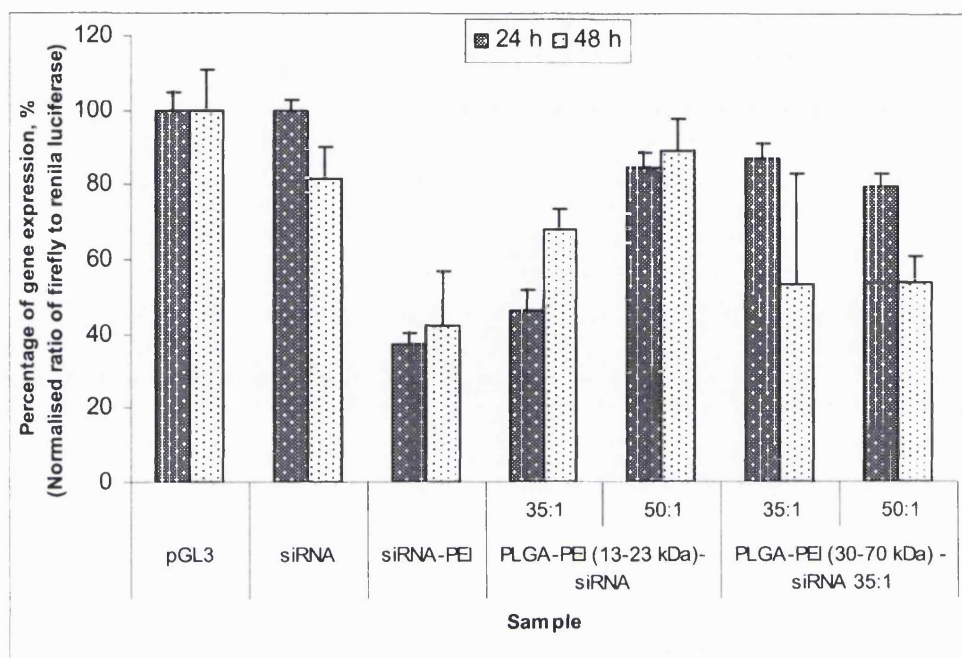


Figure 3.18: Gene silencing effect of PLGA-PEI nanoparticles with adsorbed siRNA and siRNA-PEI complexes in CHO K1 cells (n=9). Experiments were performed on growing cells at 5×10^3 /well. Keynote: pGL3= control cells without siRNA treatment.

In comparison to Lipofectamine 2000, PLGA-PEI nanoparticles with adsorbed siRNA were less efficient in delivering siRNA in the CHO K1 cells. However, these particles showed comparable ability in silencing the targeted gene compared to siRNA-PEI complexes at 24 h post-transfection for PLGA-PEI nanoparticles made using PVA with a molecular weight of 13-23 kDa and at 48 h post-transfection for 30-70 kDa PVA as shown in figure 3.19.

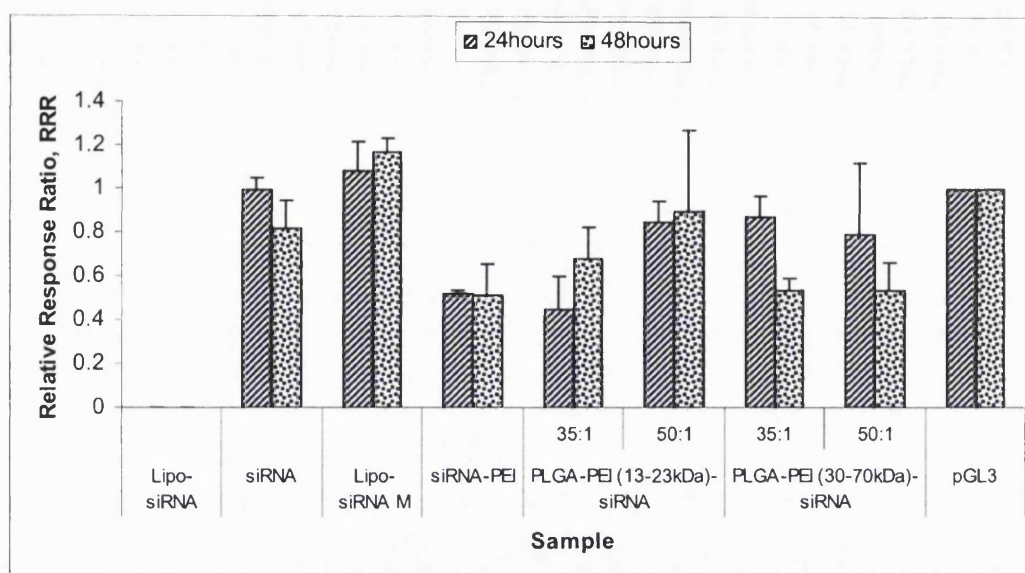


Figure 3.19: Relative Response Ratio of PLGA-PEI nanoparticles with adsorbed siRNA in comparison to siRNA-Lipofectamine 2000 complexes (n=9) in CHO K1 cells. Experiments were performed on growing cells at 5×10^3 / well. Keynotes: Lipo-siRNA= Lipofectamine 2000-siRNA complexes, Lipo-siRNA M= Lipofectamine 2000-siRNA mismatch and pGL3= control cells without siRNA treatment.

3.3.2 Transfection efficiency of PLGA-PEI nanoparticles with adsorbed pDNA

3.3.2.1 Effect of PLGA to PEI weight ratio

In comparison to pDNA, to deliver siRNA to the target site of action is easier in cultured cells because they are small and only need to cross the cell membrane but not the nuclear membrane. Therefore, to transfect the cultured cells with the pDNA were predicted to be more difficult to achieve than siRNA. A previous study that had been done showed that the transfection efficiency of pDNA was dependent on the PLGA to PEI weight ratio of PLGA-PEI nanoparticles. A weight ratio of 29:1 resulted in higher expression of luciferase protein in HEK 293 cells than a 59:1 PLGA to PEI weight ratio. An increase in transfection efficiency of pDNA with the decrease of PLGA to PEI weight ratio was due to the higher amount of free PEI that could interact with the

negatively charged cell surface and facilitate the release of pDNA from Reticulum Endothelium System (RES) through the 'proton sponge' effect.

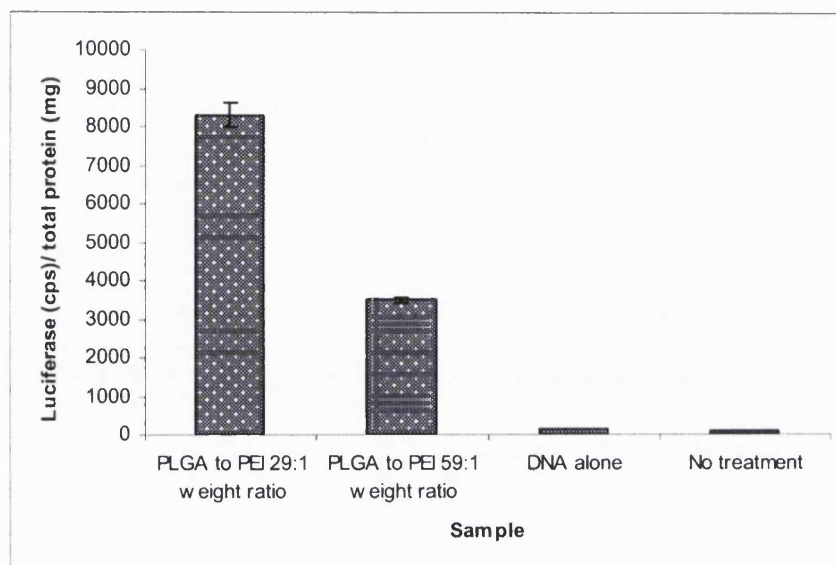


Figure 3.20: Effect of PLGA to PEI weight ratio of PLGA-PEI nanoparticles (poloxamer-188, 5% m/v) on pDNA transfection in HEK 293 cells at 24 h post-transfection (n=3). Experiments were performed on growing cells at 2×10^4 ml/well. Luciferase protein expression was measured using Luciferase assay Reagent (Promega). RLU's were normalised to total protein concentration in the cell extracts. Non-treatment cells were used as a negative control.

3.3.2.2 Effect of stabilisers

It was shown that a certain amount of stabiliser used in the particles preparation could be retained on the surface of the particles. Therefore, different types of PLGA-PEI nanoparticles, particularly those made using different stabilisers used were investigated for their effects on pDNA transfection efficiency. As predicted, poloxamer-188 showed a higher luciferase protein expression than poloxamer-407. This could be due to the smaller particle size and better stability of the particles stabilised by poloxamer-188 than poloxamer-407 which could be more easily to be taken up by the cells. However, the pDNA transfection efficiency of DNA/ superfect complexes was

much greater than these PLGA-PEI nanoparticles with adsorbed pDNA at 24, 48 and 72 h of post-transfection. Furthermore, a reduction of pDNA activity was observed with time for all the samples. The activity of pDNA-superfect complexes was reduced by 0.85-fold at 72 h post-transfection whereas 0.33 and 0.75-fold reductions in pDNA activity were observed for poloxamer-188 and -407, respectively at 72 h post-transfection. The transfection efficiency of pDNA with the different stabilisers used in the particles preparation at 24 h post-transfection is shown below:

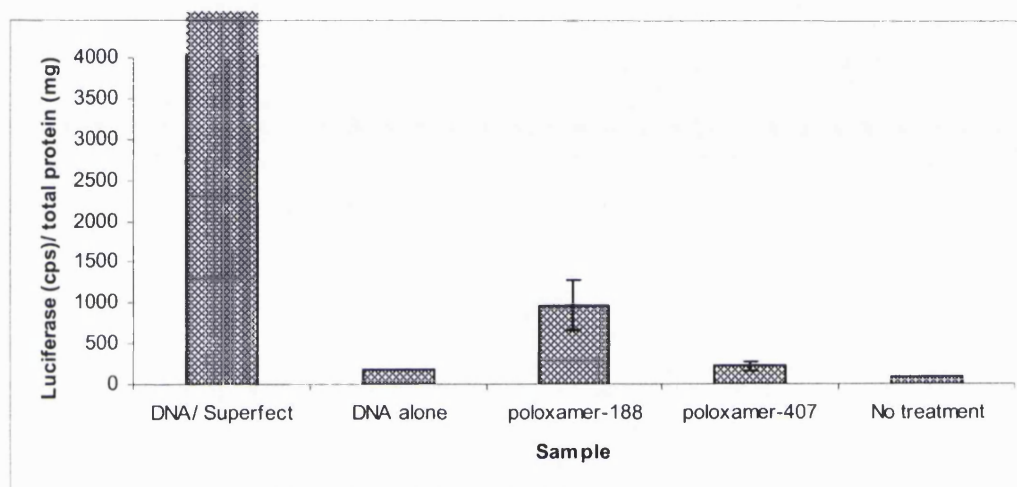


Figure 3.21: Effect of stabiliser types on pDNA transfection of PLGA-PEI nanoparticles with adsorbed pDNA (N/P ratio of 10:1) and stabiliser concentration used was 5.0% m/v (n=3). Experiments were performed on HEK 293 growing cells at 2×10^4 ml/ well. Luciferase protein expression was measured using Luciferase assay Reagent (Promega). RLU were normalised to total protein concentration in the cell extracts. Non-treatment cells were used as a negative control.

Another study was carried out to determine the effect of PLGA-PEI nanoparticles stabilised by PVA of different molecular weight. In this study, low transfection of cells with pDNA was obtained for pDNA adsorbed onto the PLGA-PEI nanoparticles compared to pDNA-PEI complexes at the same N/P ratio. pDNA adsorbed onto the PLGA-PEI nanoparticles stabilised by a lower molecular weight PVA had the highest activity at 48 h post-transfection (except for N/P ratio 15:1) whereas at 24 h post-transfection for a higher molecular weight of PVA. Nevertheless, a reduction

Chapter 3

Studies of physical and biological characteristics of PEI as delivery systems for siRNA

of pDNA activity was observed for all the samples at 72 h post-transfection. These findings therefore confirmed that there were more difficulties in transfecting the cells with pDNA compared to siRNA. Nevertheless, the silencing effects generated by two systems using synthetic siRNA and pDNA encoded siRNA are not comparable. The pDNA encoded siRNA would generate an amplification step in the cells that would result in generation of siRNA or even protein and it may last longer than synthetic siRNA.

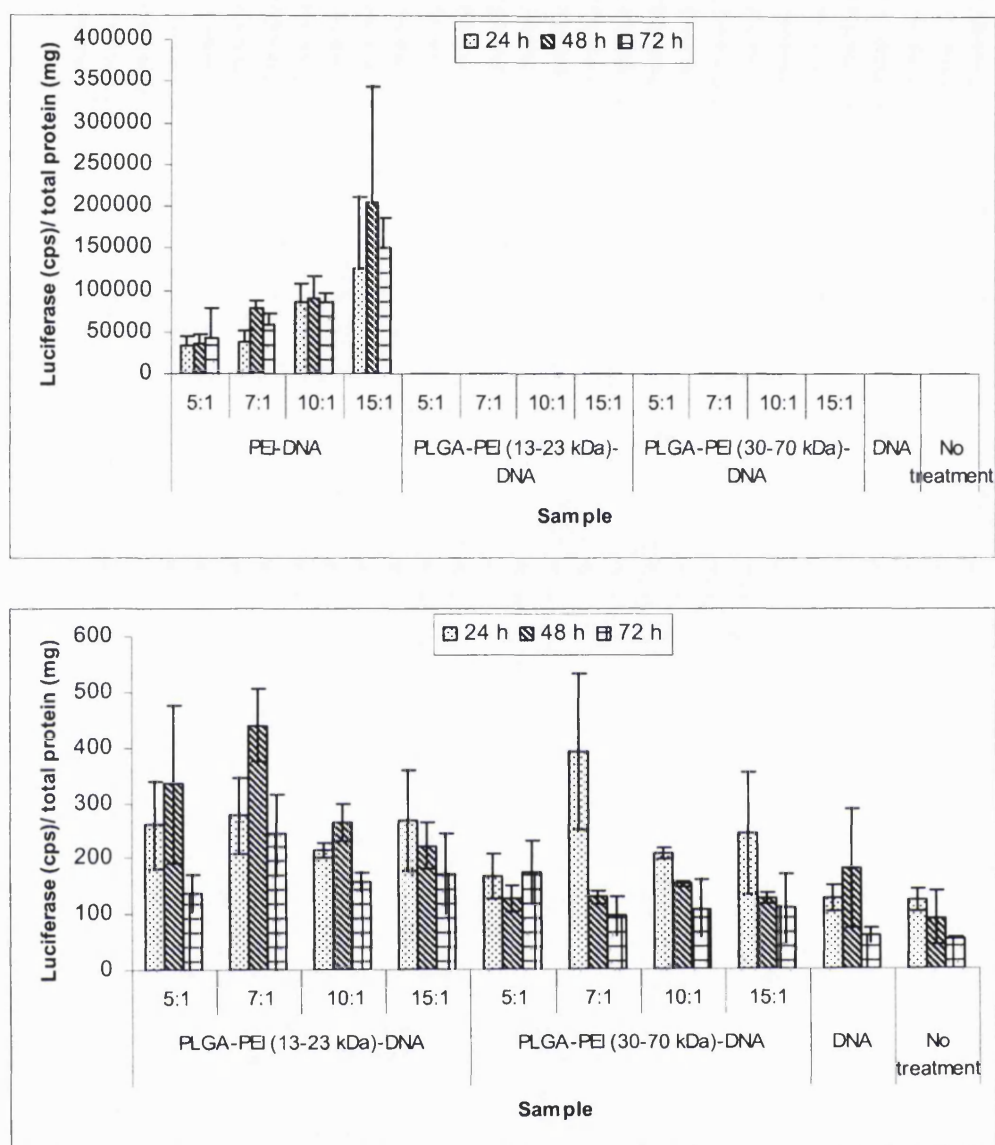


Figure 3.22: pDNA transfection efficiency of PLGA-PEI nanoparticles with adsorbed pDNA at different N/P ratio at 24, 48 and 72 h post-transfection (n=3). Experiments were performed in HEK 293 growing cells at 2×10^4 ml/ well. Luciferase protein expression was measured using Luciferase assay Reagent (Promega). RLU were normalised to total protein concentration in the cell extracts. Non-treatment cells were used as a negative control. Luciferase protein expression was measured using Luciferase assay Reagent (Promega). Non-treatment cells were used as a negative control.

3.4 Cytotoxicity effect

Cytotoxic effects of PLGA-PEI nanoparticles as a delivery system for siRNA to the cells was investigated in cell lines, HEK 293 and CHO K1 using MTT assays. The MTT assay is a simple colorimetric method to measure cytotoxicity, proliferation, or cell viability where metabolically active cells are able to convert this dye into a water-insoluble dark blue formazan by reductive cleavage of the tetrazolium ring. Formazan crystals are then, can be dissolved and quantified by measuring the absorbance of the solution at 570 nm, and the resultant value is related to the number of living cells (Pozzolini *et al.* 2003, Mosmann 1983). The results obtained revealed that the loss of cell viability depended on N/P ratio of PLGA-PEI nanoparticles with adsorbed siRNA and molecular weight of PVA used as stabiliser during the particles preparation. In both cells lines, 15-25% of cell loss was observed at 24 h post-incubation with PLGA-PEI nanoparticles with adsorbed siRNA. In HEK 293 cells, the loss of cell viability was increased with the increasing PLGA-PEI to siRNA ratio. However, the effect was transient as the cell viability was increased at 48 h post-incubation but the cell recovery was apparently slightly slower for the cells treated with PLGA-PEI nanoparticles made using PVA with higher molecular weight compared to the lower molecular weight.

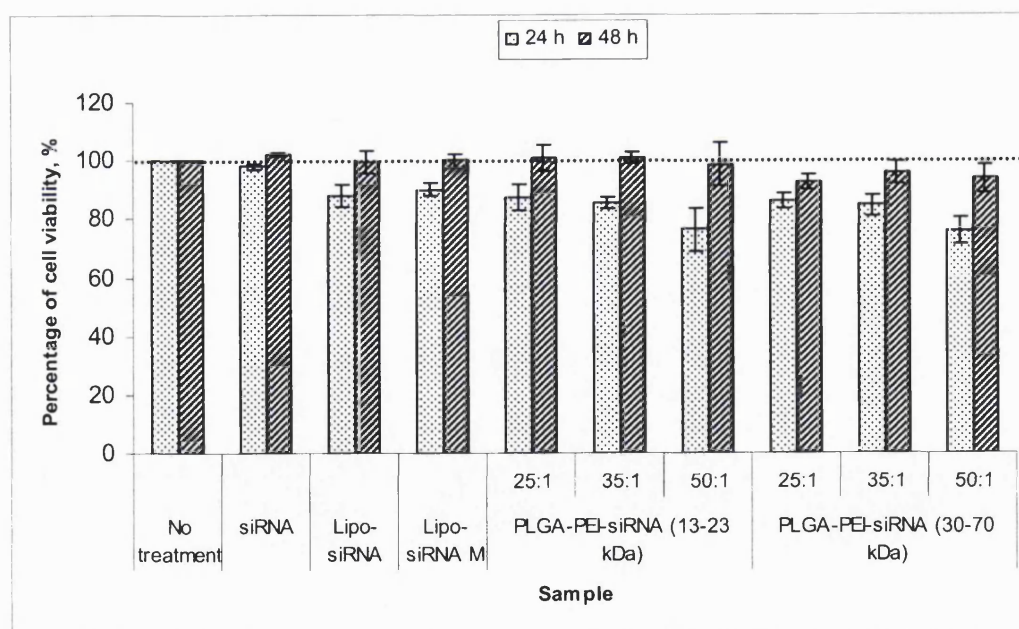


Figure 3.23: Toxicity effect of PLGA-PEI nanoparticles with adsorbed siRNA in HEK 293 cells at 5×10^3 / well, n=3. Keynotes: M siRNA: Mismatch siRNA.

In contrast to HEK 293 cells, loss of cell viability in CHO K1 cells appeared to be insensitive to the molecular weight of PVA but highly dependent on PLGA-PEI nanoparticles to siRNA N/P ratio. Almost 25% loss of cell viability was observed for N/P ratio of 50:1 compared to less than 15% cell loss at 35:1. As predicted from the previous results, the percentage of cell viability was increased at 48 h post-incubation for cells incubated with PLGA-PEI nanoparticles with adsorbed siRNA illustrating the recovery of the cells.

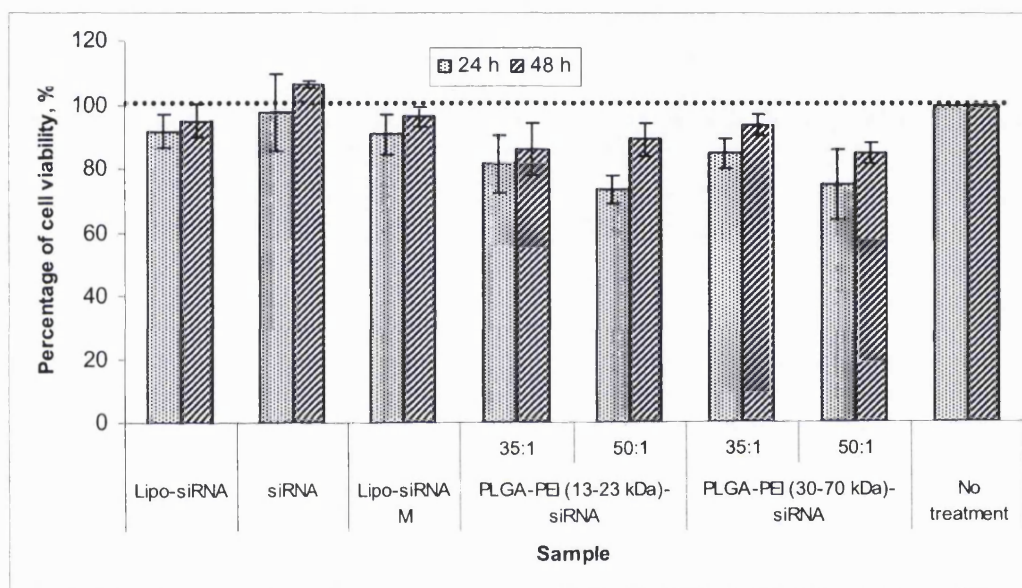


Figure 3.24: Toxicity effect of PLGA-PEI nanoparticles with adsorbed siRNA in CHO K1 cells at 5×10^3 / well (n=3). Keynotes: Lipo-siRNA= Lipofectamine 2000-siRNA complexes and Lipo-siRNA M= Lipofectamine 2000-siRNA mismatch.

3.5 Conclusions

PEI has been shown to have the ability to deliver both pDNA and siRNA into cells. Modification of PLGA nanoparticles by incorporating PEI as well as optimisation of their preparation process (emulsification diffusion method) have led to a formation of a better delivery system for siRNA with a higher transfection efficiency compared to its parent compounds; PEI polymer. The smallest and uniform positively charged particle size of PLGA-PEI nanoparticles prepared using emulsification diffusion method was

Chapter 3

Studies of physical and biological characteristics of PEI as delivery systems for siRNA

obtained when PVA was used as a surfactant at a concentration of 5% m/v with a PLGA to PEI weight ratio 29:1. The adsorption of siRNA onto the surface of PLGA-PEI nanoparticles was highly dependent on the N/P ratio of PLGA-PEI nanoparticles to siRNA and a full or complete binding of siRNA could be achieved at a N/P ratio 20:1 and above. In addition, N/P ratio plays a very important factor in determining the capability of PLGA-PEI nanoparticles to transport siRNA into cells, where a N/P ratio 35:1 was found to be efficiently delivered siRNA into its target sites, thus exerted siRNA effects by knocking-down the targeted gene. PLGA-PEI nanoparticles were also found to have a relatively low cytotoxicity which therefore, it has a great potential to be used therapeutically.

Chapter 4
Manipulation of chitosan as safer carriers for
siRNA

Manipulation of chitosan as safer carriers for siRNA

Polycationic polymers, particularly chitosans have been extensively explored for delivering nucleic acids due to their advantages such as low toxicity, biodegradability and biocompatibility. Chitosans possess a high density of protonated amino groups which allow it to form non-covalent intra-polyelectrolyte complexes with negative charges on polyanions. These complexes provide protection of nucleic acids from nuclease degradation thereby resulting in high delivery efficiency. Therefore, chitosan is a suitable candidate for an effective gene delivery system for siRNA. Several methods have been reported for the preparation of chitosan based nanoparticles. These methods include ionic cross-linking, chemical cross-linking and the use of emulsification, for example, to produce cationic PLGA nanoparticles.

In this study, three different methods have been extensively investigated: simple complexation, ionic gelation using TPP ions and an emulsification diffusion method to produce PLGA-chitosan nanoparticles. For simple complexation and ionic gelation, both methods produced nanosize particles, less than 500 nm depending on type, molecular weight as well as concentration of chitosan used. In the case of ionic gelation, two further factors namely chitosan to TPP weight ratio and pH affected the particle size. *In-vitro* studies in two types of cell lines, CHO K1 and HEK 293 have revealed that the preparation method of siRNA association to the chitosan plays an important role on the silencing effect. Chitosan-TPP nanoparticles with entrapped siRNA are shown to be better vectors as siRNA delivery vehicles compared to chitosan-siRNA complexes possibly due to their high binding capacity and loading efficiency. On the other hand, PLGA-chitosan nanoparticles obtained from the emulsification diffusion method are positively charged with particle size between 0.6 to 1 μm depending on type and molecular weight of chitosan as well as PLGA polymer. Despite their high particle surface charge and stability in serum, this system is unable to successfully deliver siRNA as confirmed by observation of a lower knock-down of the targeted gene (less than 30%) compared to chitosan-TPP nanoparticles with entrapped siRNA (more than 90%).

Different methods of particle preparation have been shown to produce different physical and biological characteristics of chitosan nanoparticles. Chitosan-TPP nanoparticles with entrapped siRNA obtained by ionic gelation have been described to be an ideal delivery system for siRNA into cells and have promising prospects for use as therapeutic agents.

4 Manipulation of chitosan as safer carriers for siRNA

Several methods can be used to prepare chitosan into particles including ionic gelation (Gan *et al.* 2005, Vila *et al.* 2004, Li *et al.* 2003), desolvation (Mao *et al.* 2001), ionic complexation (Huang *et al.* 2005, Kim *et al.* 2005, Ishii *et al.* 2001), covalent cross-linking and self assembly using of chemical modifications. In this study, simple complexation and ionic gelation were chosen to prepare chitosan–siRNA complexes or nanoparticles since both processes are simple and mild (Agnihotri *et al.* 2004, Shu *et al.* 2004, Liu *et al.* 1997, Polk *et al.* 1994). In addition, the use of tripolyphosphate (TPP) as a polyanion to cross-link with the cationic chitosan, particularly through electrostatic interaction could avoid possible toxicity of reagents used in chemical cross-linking (e.g. glutaraldehyde). Modulation of size and surface charge of the particles also could be easily done using both methods (Gan *et al.* 2005, Shu and Zhu. 2000), by adjusting certain process parameters such as chitosan concentration and stirring rate.

4.1 Chitosan-siRNA complexes by simple complexation

Chitosan-siRNA complexes can be formed through electrostatic interaction between positively charged chitosan and negatively charged siRNA. Such complexes are very easy to synthesize, simply by mixing a solution of chitosan with siRNA. These complexes were found to depend on certain parameters such as chitosan to siRNA concentration ratio, type and molecular weight of chitosan but were less affected by pH of solution or medium used to prepare the complexes.

4.1.1 Particle size

Particle size and shape play an important role in transferring genes to cells and they also greatly influence particle distribution in the body (Gref *et al.* 1995). It has been reported that particles in the nanometer size range have a relatively higher intracellular uptake compared to microparticles (Bivas-Benita *et al.* 2004, Panyam *et al.* 2003, Zauner *et al.* 2001). This characteristic is very important in gene transfer as cellular uptake of chitosan-DNA complexes and their subsequent release from the endo-lysosome pathway are two rate limiting steps in the process (Huang *et al.* 2005). Similar to DNA and ODN, siRNA are likely taken up by cells through endocytosis and

if siRNA is not effectively delivered to the cytoplasmic compartment, it will not induce RNAi (Rozema *et al.* 2003).

Normally, low siRNA activity in the cells is thought to be due to the uptake of siRNA by fluid phase endocytosis which does not result in the release of siRNA into cytoplasm. In fact, mammalian cells appear to lack the effective double stranded RNA-uptake machinery that is found in other species such as *Caenorhabditis elegans* (Rozema *et al.* 2003). Therefore, siRNA and its vector should be able to be taken up by the cells and escape the endosomal vesicle to avoid lysosomal degradation, thus, allowing the RNAi to occur. In this study, we tried to obtain nanoparticles of less than 500 nm to facilitate the uptake of the particles by manipulating certain process parameters that are involved in the preparation. Generally, the particle size of chitosan-siRNA complexes or nanoparticles was highly dependent on molecular weight, type and concentration of chitosan used.

4.1.1.1 Effect of chitosan to siRNA concentration ratio

The mean particle size of chitosan-siRNA complexes prepared by simple complexation for higher molecular weight of both chitosan hydrochloride (270 kDa) and glutamate (470 kDa) were increased from 171 to 459 nm and 189 to 291 nm, respectively when the concentration of chitosan was increased from 25-300 $\mu\text{g/ml}$ in RNase free water (figure 4.1). Similar results were obtained for lower molecular weight of chitosan (chitosan hydrochloride: 110 kDa and glutamate: 170 kDa) where the particle size was increased more than 2-fold when the concentration of chitosan was increased from 25-300 $\mu\text{g/ml}$. The increment of particle size with the increasing concentration of chitosan was thought to be due to the overlapping even entanglement of chitosan polymer chains (Cho *et al.* 2006) whereby the amine groups of chitosan were not accessible to interact with the siRNA. In contrast, a lower concentration of chitosan resulted in better solubility in aqueous media and generated its molecular character as a polyelectrolyte material allowing more efficient interaction between negatively charged siRNA and cationic chitosan.

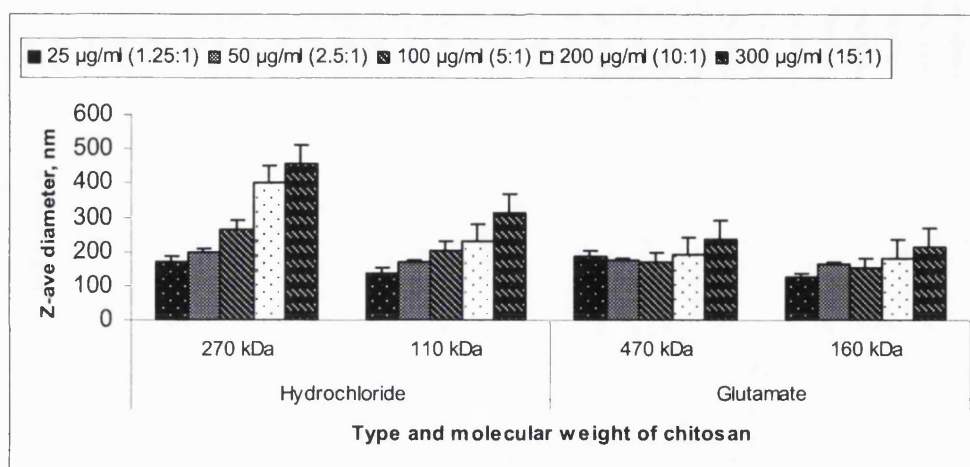


Figure 4.1: The effect of chitosan concentration or chitosan to siRNA weight ratio (in bracket) on mean particle size of siRNA-chitosan complexes using different type and molecular weight of chitosan as determined by Malvern System 4700c Submicron particle analyser (n=3).

4.1.1.2 Effect of type and molecular weight of chitosan

The mean particle size was smaller for all the chitosan concentrations tested when lower molecular weight chitosan was used (figure 4.1). This was also thought to be due to the decreased viscosity of the lower concentration or molecular weight of chitosan which resulted in more efficient interaction between negatively charged of siRNA and cationic chitosan as discussed above. However, although chitosan glutamate 213 (470 kDa, 133 mPa.s) had higher molecular weight than chitosan hydrochloride 213 (270 kDa, 74 mPa.s), it produced smaller complexes with siRNA than chitosan hydrochloride. This is probably due to the chain entanglement effects. As the higher molecular weight chitosan (glutamate 213) has longer polymer chains, it is easier for the polymer chains to entangle siRNA once the initial interaction has occurred. On the other hand, chitosan hydrochloride 213 with the shorter polymer chains was energetically less favourable as they need more energy for the formation of chitosan-siRNA complexes, resulting in larger particle size.

Previous reports had also suggested that the effect of molecular weight in the chitosan-DNA complex could be attributed to the chain entanglement effect and this effect contributed less to the complex formation of low molecular weight of chitosan as

it required more polymer chains to completely interact with negatively charged DNA (Kiang *et al.* 2004). In agreement with this report, lower molecular weight chitosan glutamate 113 (160 kDa) showed only slightly decreased particle size than chitosan hydrochloride 113 (110 kDa) as the chain entanglement effect had less effect on particle formation (figure 4.1). Nevertheless, it is obvious that chitosan glutamate produced smaller particles than chitosan hydrochloride. The difference however, might also due to the different acid salt which could not be excluded as it has been reported that formation of chitosan nanoparticles may vary significantly depending on the purity, acid salt, and molecular weight of chitosan employed (Janes *et al.* 2001).

4.1.1.3 Effect of solution pH

The glucosamine units of chitosan show a high density of amino groups which confers a positive charge to the polymer. These amino groups have a pKa of pH 6.5 and hence undergo protonation in acidic conditions or pH values below 6. To study the effects of lower medium pH on particle size and surface charge of chitosan-siRNA complexes, the complex was prepared in acetate buffer, 0.1 M at pH 4.5 and a series of chitosan concentration were examined. No significant difference was observed on particle size between RNase free water and acetate buffer pH 4.5 used as the reaction medium. This suggested that the pH solution had less effect on the size of chitosan-siRNA complexes.

4.1.2 Particle surface charge

The comparative positive value of surface charge (zeta potential) of the chitosan-siRNA complexes increased with the increasing concentration of chitosan at a constant siRNA concentration (figure 4.2). The increment was due to the increase in the number of positive charges which counteracted with negatively charged siRNA as the amount of siRNA was fixed. The net positive charge of the particles was desirable to prevent particle aggregation and promote electrostatic interaction with the overall negative charge of the cell membrane (Schiffelers *et al.* 2005). In addition, body distribution of nanoparticles after *i.v* injection is highly influenced by their interaction with the biological environment which also dependent on their physicochemical properties like surface charge of nanoparticles (Jeon *et al.* 2000).

From the graph, the positive surface charge was achieved when chitosan concentration was above 50 $\mu\text{g/ml}$ for the lower molecular weight chitosan, whereas this was 100 $\mu\text{g/ml}$ for the higher molecular weight for both types of chitosan. This was thought to be due to the steric hindrance of longer and rigid polymer chains of higher molecular weight chitosan which results in the difficulty of siRNA to interact with the chitosan. Therefore, the presence of free siRNA in the solution was likely to screen the positively charged chitosan.

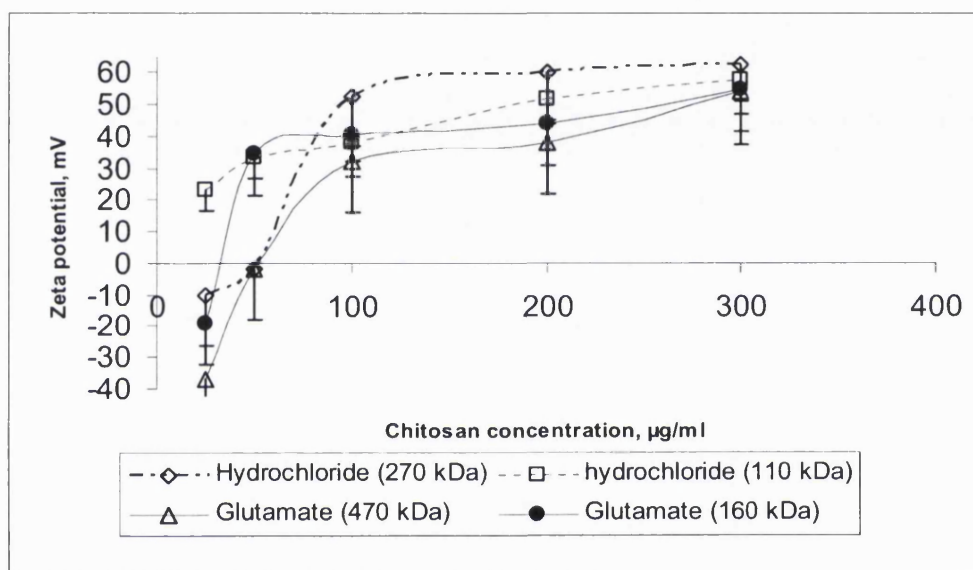


Figure 4.2: Effect of chitosan concentration on particle surface charge of chitosan-siRNA complexes (n=3).

In this case, the degree of deacetylation (DDA) was not assessed for its role in particle surface charge because all of the chitosan used had $\sim 86\%$ of DDA. However, when these complexes were prepared in acetate buffer at pH 4.5, the particle surface charge was decreased. The reduction of particle surface charge could be explained by the presence of salt in the acetate buffer (0.1 M) which might screen particle charges and thus the mobility decreases (Lopez-Leon *et al.* 2005).

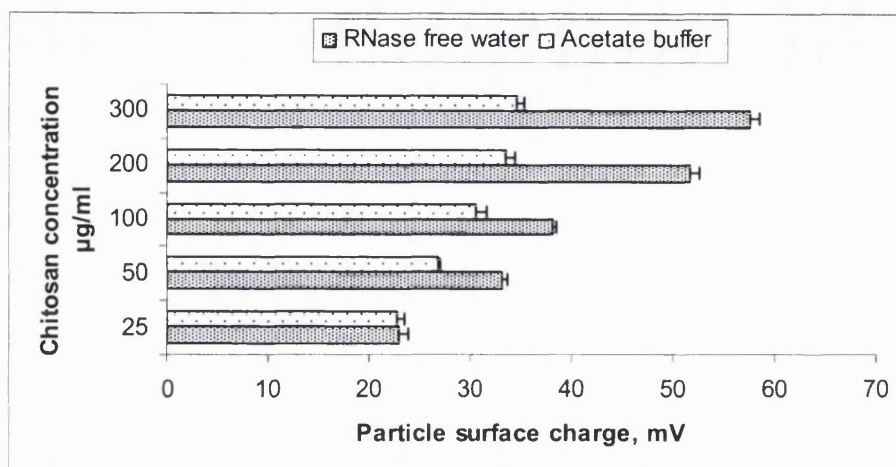


Figure 4.3: Comparison of particle surface charge in RNase free water and acetate buffer (pH 4.5, 0.1 M) for chitosan-siRNA complexes using chitosan hydrochloride, CI113.

4.1.3 Comparing siRNA- to pDNA- chitosan complexes

Polymeric carriers based on chitosan have long been used to deliver pDNA into the target cells. Since the siRNA shares a lot of pDNA properties, it is obvious to adapt formulations that were developed for pDNA to the development of delivery systems for siRNA. However, certain differences in their properties were predicted as siRNA and pDNA differ in their size and form.

4.1.3.1 Particle size

In this study, pDNA was complexed to chitosan at various concentrations in the same manner as siRNA-chitosan complexes. Similar to siRNA-chitosan complexes, the increment of chitosan concentration yielded a larger particle size for chitosan-DNA complexes. However, slightly different to siRNA-chitosan complex, significant increase of particle size could only be seen when the chitosan concentration was above 100 µg/ml as shown in figure 4.4.

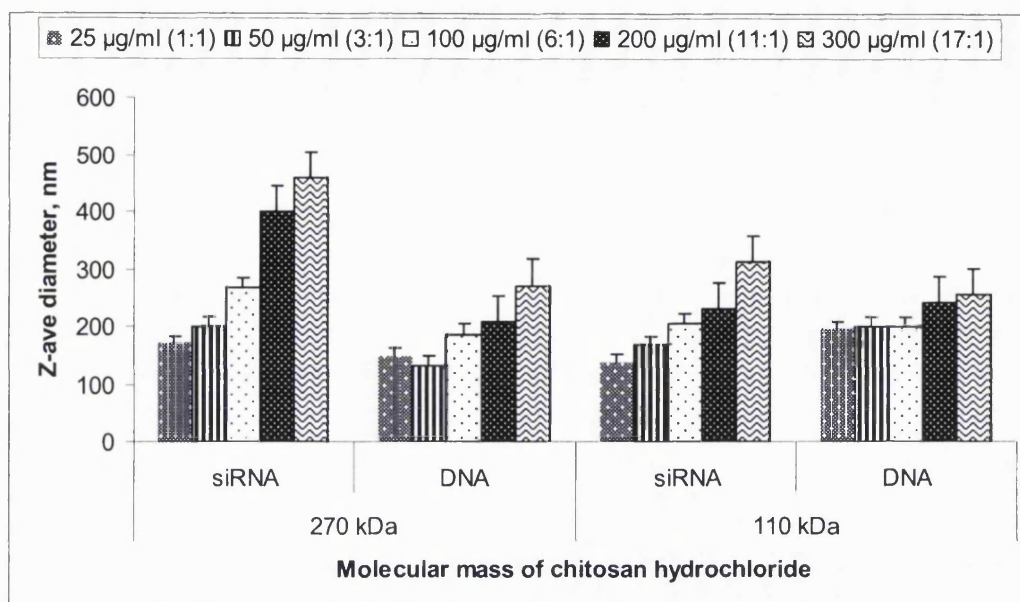


Figure 4.4: Comparison of particle size of chitosan-siRNA and -DNA complexes with increasing concentration of chitosan or chitosan to polyanion weight ratio (in bracket) as determined by Malvern System 4700c Submicron particle analyser, (n=3).

Furthermore, the particle size of pDNA-chitosan complexes was relatively smaller than siRNA-chitosan complex. This was thought to be due to the fact that the volume occupied by a condensed pDNA nanoparticle is about 10 000 times (Keller *et al.* 2005, Tam *et al.* 2000) smaller than its uncondensed counterpart and a minimal length of the DNA of 800 bp is required for a DNA condensation process to occur (Bloomfield 1996, Bloomfield 1991, Bloomfield *et al.* 1991). On the other hand, no such effect was expected occurred to siRNA as it had a shorter length of only 21 bp and it retains its initial volume after complexing with a cationic entity. This was corroborated by the images from the TEM microscopy as pDNA formed a complex with chitosan to a small and condense round particle (figure 4.5A) compared to toroid form of particle for siRNA-chitosan complexes (figure 4.5B). Consequently, these characteristics were expected contributed to the formation of a larger particle size as several copies of siRNA could be complexed with chitosan instead of one molecule *per* cationic entity.

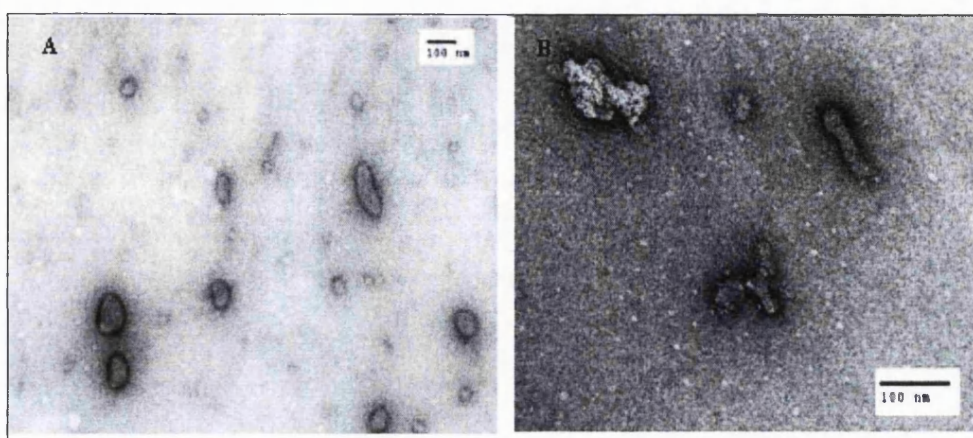


Figure 4.5: Morphology of pDNA-chitosan (A) and siRNA-chitosan (B) complexes at weight ratio of 2.5: 1 of chitosan to pDNA or siRNA.

4.1.3.2 Surface charge

Besides particle size, particle surface charge is one of the most important properties for nanoparticles. The particle surface charge of pDNA-chitosan complexes were increased as the chitosan concentration increased. The increment of positive surface charge was due to the increase of protonated chitosan amino groups that remained uncomplexed. In fact, these values were higher than siRNA-chitosan complexes especially for the chitosan concentrations lower than 50 $\mu\text{g/ml}$ although the same amount of siRNA was complexed to the chitosan. This could be due to the relatively higher numbers of siRNA molecules in the solution compared to pDNA at the same concentration (siRNA is 600 times smaller in size than pDNA) which might not be favourable for the complex to form and they were probably shielded the positive values of chitosan in the case of low chitosan concentration. In fact, the supercoiled structure of pDNA is thought to be less likely to shield the negative charged phosphate groups from interacting with chitosan which in turn require less chitosan to compensate for the available negatively charged phosphate groups and therefore pDNA becomes positively charged more easily than siRNA.

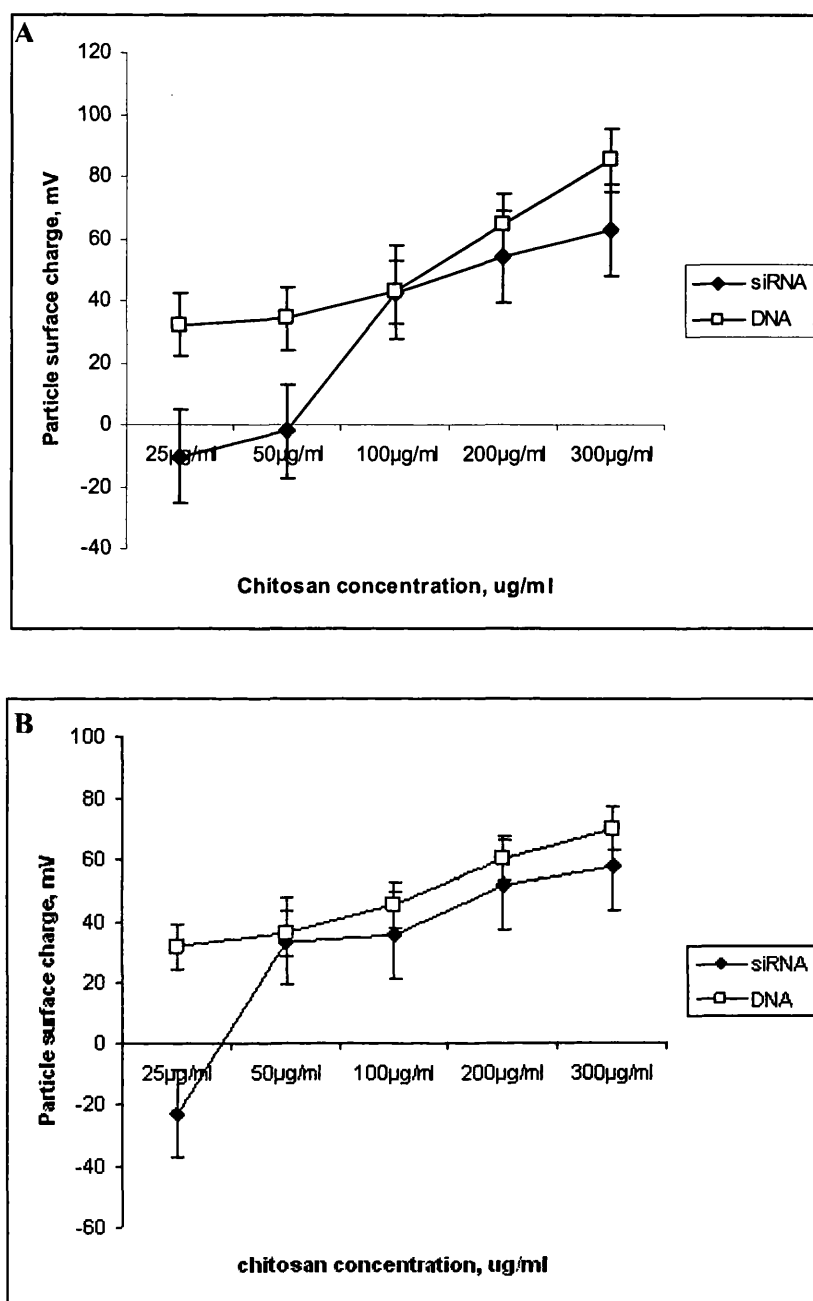


Figure 4.6: Comparison of particle surface charge between siRNA- and pDNA-chitosan complexes. A: CI213, 270 kDa and B: CI113, 110 kDa (n=3).

4.1.3.3 Binding efficiency

Although siRNA is a polyanionic molecule like pDNA, certain characteristics that are really different such as its small size and linearity. These differences may affect the way these molecules interact with polycations such as chitosan. To determine the binding efficiency of siRNA to the chitosan, a series of chitosan concentrations, ranging from 50 to 1000 $\mu\text{g/ml}$ were used to complex a fixed amount of siRNA (10 $\mu\text{g/ml}$) either in RNase free water or sodium acetate buffer, 0.1 M at pH 4.5.

Unfortunately, none of the above chitosan concentrations was able to completely bind siRNA as the migration of free siRNA from the chitosan-siRNA complex was observed even at the highest concentration of chitosan (1 mg/ml, chitosan to siRNA weight ratio 100:1) either in RNase free water or sodium acetate buffer, 0.1 M at pH 4.5. This indicated the weak interactions between chitosan and siRNA by simple complexation and apparently they were easily dissociated from each other. The migration of bands (tailing bands) at higher concentrations of chitosan was not observed from pDNA-chitosan complexes which were prepared in the same conditions as siRNA. In fact, pDNA was completely condensed to the chitosan even at a very low concentration of chitosan, as low as 25 $\mu\text{g/ml}$ (chitosan to DNA ratio of 1.25:1). This suggests that siRNA binds to the chitosan in a different manner from the pDNA because siRNA is a small and linear form of nucleotides compared to pDNA; a larger and supercoiled form of nucleotides. These observations have therefore highlighted the weak interactions between siRNA and chitosan which might be arising from partial interaction of siRNA and chitosan due to several copies of siRNA could complex to one entity of chitosan as discussed in the earlier section.

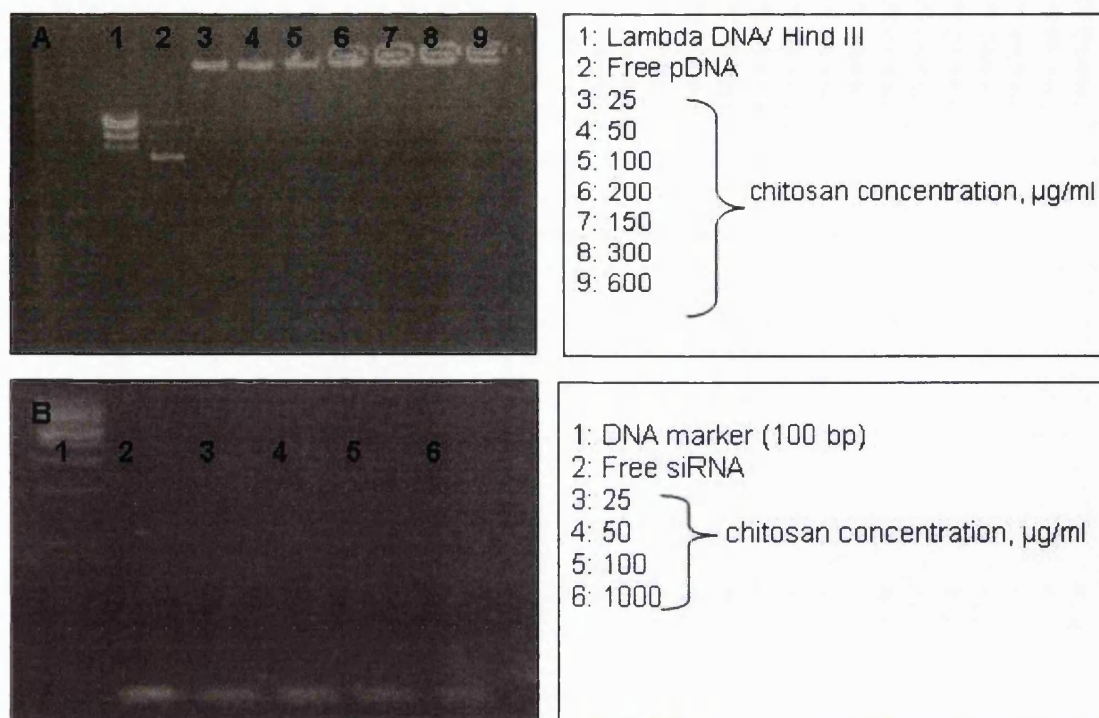


Figure 4.7: Binding efficiency of pDNA-chitosan complexes (A) and siRNA-chitosan complexes (B) at different chitosan concentrations.

4.2 Chitosan-TPP nanoparticles using ionic gelation

Although siRNA-chitosan complexes made by simple complexation are easy to prepare, some authors have reported that such preparation generated wide size distribution and low stability of pDNA-chitosan complexes which may result in lower transfection efficiency (Gan *et al.* 2005, Li *et al.* 2003, MacLaughlin *et al.* 1998). Therefore, to improve stability of these complexes without exposure to harmful chemicals, ionic gelation was used because of the chitosan ability to form a gel spontaneously upon contact with multivalent polyanions such as TPP ions through the formation of inter- and intramolecular cross-linkage mediated by these polyanions (Gan *et al.* 2005).

4.2.1 Optimisation of the gelation process

The formation of chitosan-TPP nanoparticles occurred spontaneously upon the addition of the TPP ions into the chitosan solution as molecular linkages were formed

between TPP phosphates and chitosan amino groups. In agreement with the previous studies, the particle size of chitosan-TPP nanoparticles depends on the speed of stirring during mixing, concentration as well as molecular weight of chitosan. In this study, chitosan-TPP nanoparticles were prepared in RNase free water at room temperature with the chitosan to TPP weight ratio of 6:1 except if specified otherwise.

4.2.1.1 Conditions of mixing

Conditions of mixing such as speed of stirring plays an important role in the process of ionic gelation. Therefore, chitosan-TPP nanoparticles were prepared using two different rates of stirring, low (Ikameg® RET-GS, 1100 rpm) and the high speed (Stuart Scientific magnetic stirrer SM 1, 10 000 rpm, UK). The results obtained showed that the particle size of chitosan-TPP nanoparticles was reduced almost 2-fold when high speed of stirring was applied in the preparation process. Moreover, sonication is a common tool in the preparation of various nanoparticles. It is particularly effective in breaking aggregation as well as reducing the size and polydispersity of nanoparticles (Tang *et al.* 2003, Grieser *et al.* 1999). To assess the effects of sonication on reducing particle size of chitosan-TPP nanoparticles, sonication with 20% of the maximum amplitude in continuous mode (3 mm probe diameter, Sanyo MSE Soniprep 150, with a frequency of 23 kHz) was applied during the mixing of TPP and chitosan solutions instead of magnetic stirring.

Only a slight decrease in particle size was observed when sonication was used for higher molecular weight of chitosan compared to high rate of magnetic stirring. On the other hand, no further reduction of particle size was observed for the lower molecular weight of chitosan neither for chitosan hydrochloride nor glutamate. However, the polydispersity of the particles prepared by sonication was greatly reduced which indicated a narrow size distribution of the particles. The size of chitosan-TPP nanoparticles with different conditions of mixing are shown below:

Sample	Low rate magnetic stirring		
	KCps, SD	Z-ave diameter (nm), SD	Polydispersity (PI), SD
G213 (470 kDa)	36.0 ±0.5	1114 ±55.3	0.63 ±0.02
Cl213 (270 kDa)	42.3 ±1.3	1570 ±128.3	0.92 ±0.01
G113 (160 kDa)	32.0 ±0.8	565 ±23.1	0.93 ±0.01
Cl113 (110 kDa)	42.1 ±0.6	903 ±31.1	0.73 ±0.03
Sample	High rate magnetic stirring		
	KCps, SD	Z-ave diameter (nm), SD	Polydispersity (PI), SD
G213 (470 kDa)	19.7 ±1.1	533 ±16.2	0.49 ±0.05
Cl213 (270 kDa)	21.2 ±2.3	765 ±10.3	0.65 ±0.09
G113 (160 kDa)	25.9 ±0.7	294 ±8.8	0.55 ±0.02
Cl113 (110 kDa)	30.5 ±0.6	423 ±15.2	0.38 ±0.01
Sample	Sonication		
	KCps, SD	Z-ave diameter (nm), SD	Polydispersity (PI), SD
G213 (470 kDa)	67.8 ±0.3	304 ±12.4	0.25 ±0.05
Cl213 (270 kDa)	36.9 ±1.8	633 ±33.5	0.37 ±0.05
G113 (160 kDa)	36.4 ±0.9	328 ±8.7	0.37 ±0.02
Cl113 (110 kDa)	41.9 ±1.2	579 ±25.7	0.65 ±0.04

Table 4.1: Effect of mixing conditions on particle size and size distribution (PI) of chitosan-TPP nanoparticles as determined by Malvern Zetasizer[®]. Chitosan to TPP weight ratio of 6:1 (n=3).

From this study therefore, it could be concluded that the smaller particle size of chitosan nanoparticles generated by ionic gelation could be obtained by magnetic

stirring without the need of harsh condition such as sonication. In most cases, sonication is less preferable to be used in particles preparation where small molecules like siRNA is incorporated into the particles, because this process might expose siRNA to a variety of stresses, such as shear forces, high temperature and pressure as well as generation of reactive species that harmful to siRNA integrity.

4.2.1.2 Molecular weight and concentration of chitosan

Formation of nanoparticles by ionic gelation could only be achieved at some certain specific concentrations of chitosan and TPP. In this study, the formation of nanoparticles or microparticles was observed when the concentration of TPP was fixed at 0.84 mg/ml and the chitosan concentration was ranging from 1.3 to 5 mg/ml which was depend on the molecular weight of chitosan as well as the conditions of mixing. At low rate of magnetic stirring, the particle size of chitosan-TPP was increased with the increased chitosan concentration from 2 mg/ml up to 5 mg/ml. When the chitosan concentration was above 5 mg/ml, separation of two phases was observed. Figure 4.8 shows the effects of chitosan concentration on particle size of chitosan-TPP nanoparticles with two different molecular weights of chitosan hydrochloride and glutamate. From the graph, the size of higher molecular weight of chitosan either hydrochloride or glutamate was more affected by the increased concentration of chitosan whereas this was less so for the lower molecular weight. However, a significant difference between higher and lower molecular weight only could be observed when the concentration of chitosan was 4 mg/ml or above.

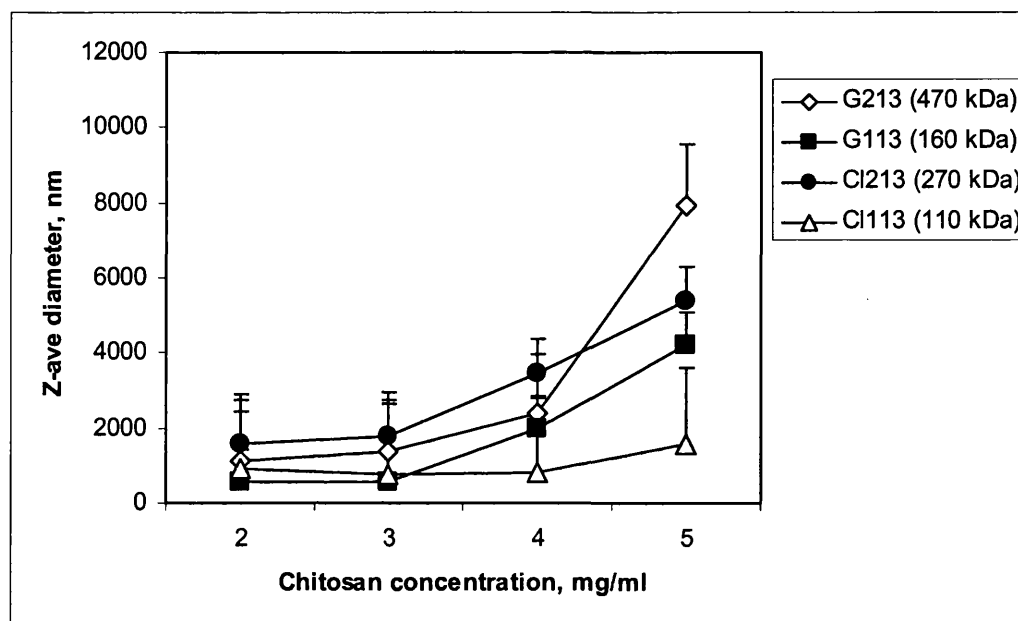


Figure 4.8: Effect of chitosan concentrations on particle size of chitosan-TPP nanoparticles made from four different molecular weights of chitosan as determined by Malvern Zetasizer® (n=3). Chitosan-TPP nanoparticles were prepared by ionic gelation under a low rate of magnetic stirring (1100 rpm). The TPP concentration was fixed at 0.84 mg/ml and the chitosan concentration was ranging from 2 to 5 mg/ml

4.2.1.3 Chitosan to TPP weight ratio

In this study, the concentration of chitosan was fixed at 2 mg/ml (in RNase free water) for all types of chitosan and magnetic stirring was set at the high rate of stirring. The results showed that the appearance of the solution changed when a certain amount of TPP ions was added to the chitosan solution, from a clear to an opalescent solution that indicated a change of the physical states of the chitosan from nanoparticles to microparticles and eventually aggregates (Li *et al.* 2003). For all types of chitosan tested in this study, chitosan and TPP concentration were adjusted to weight ratio of 6:1 to obtain nanoparticles and thus the mean particle size of chitosan-TPP nanoparticles was 510 ± 22.9 , 276 ± 17.9 , 709 ± 50.3 and 415 ± 44.6 nm for G213, G113, Cl213 and Cl113, respectively.

Charge density is an important factor in electrostatic interaction between anions and cationically charged chitosan and it mainly depends on the solution's pH. For TPP ions, the decrease of solution pH to acidic conditions resulted in the reduction of the charge number of TPP accordingly which subsequently leads to the need for more TPP ions to cross-link chitosan by electrostatic interaction (Shu and Zhu 2002a). Therefore, the weight ratio of chitosan to TPP was reduced from 6:1 to 5:1 as the pH of chitosan solution used in the ionic gelation was changed from pH 6 (RNase free water) to pH 4.5 (acetate buffer, 0.1 M). On the other hand, the surface charge of chitosan-TPP nanoparticles was increased from approximately +40 to +60 mV when the weight ratio of the chitosan to TPP was changing from 4:1 to 6:1.

4.2.2 Effect of pH on particle size and surface charge

Chitosan is a weak base polysaccharide that contains an average amino group density of 0.837 per disaccharide unit (Gan *et al.* 2005, Mi *et al.* 2003) and in acidic medium, the amine groups will be protonated resulting in a high positive charge. As the charge number of TPP also decreases in acidic conditions, the formation of chitosan-TPP nanoparticles by ionic gelation is highly pH-dependent which explained the changing of chitosan to TPP weight ratio from 6:1 to 5:1 when the pH of chitosan solution used in ionic gelation was changed from 6 to 4.5. For TPP ions, the decrease of solution pH to acidic conditions resulted in a reduction in the charge number of TPP accordingly which subsequently leads to the need for more TPP ions to cross-link chitosan by electrostatic forces (Shu and Zhu 2000a). Nevertheless, a reduction in particle size was observed when lowering the pH to 4.5 as at this point, the number of protonated amine groups was increased and could efficiently interact with TPP ions to produce smaller and fine particles.

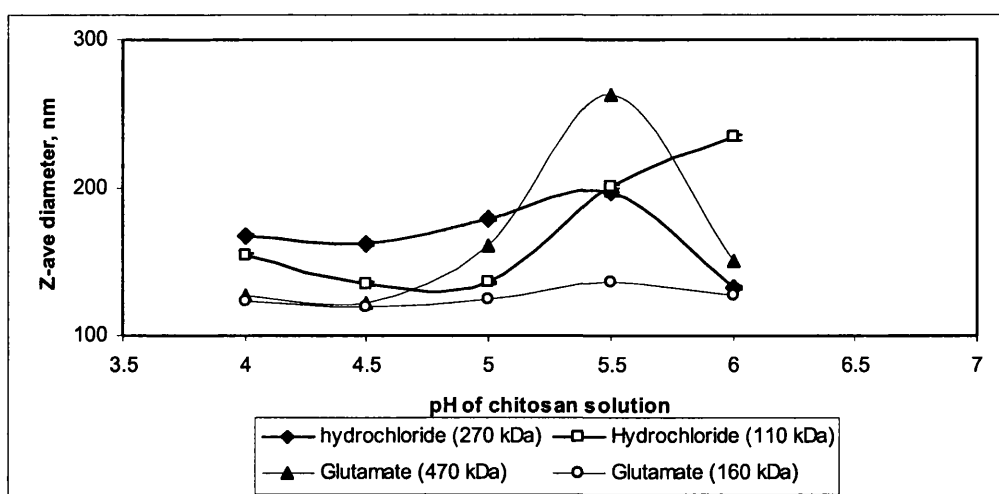


Figure 4.9: Effect of chitosan solution pH on particle size of chitosan-TPP nanoparticles (n=3) as determined by Malvern Zetasizer®.

Additionally, the surface charge of the chitosan-TPP nanoparticles was increased approximately from +20 to +40 mV when the pH changing from 6 to 4 due to the increment of protonated chitosan amine groups in acidic conditions as discussed in earlier section. However, there was no significant difference in particle surface charge from among the different molecular weights of chitosan that had been tested. This was thought to be due to the similar values of degree of deacetylation (DDA) of the investigated chitosans.

4.2.3 Effect of ionic strength

Ionic strength was also one of the important factors that may affect electrostatic interaction between chitosan and anions as salt usually has a shielding effect on ionic cross-linking. The particle size of chitosan nanoparticles usually increased with the increase of ionic strength due to particle swelling. This effect might be different on different chitosan nanoparticles depending on the ionic cross-linking capability of anions with chitosan, as the weakest interaction between chitosan and polyanions were more affected by this compared to the strongest interaction (Shu and Zhu 2002b).

The effects of ionic strength on ionic cross-linking of chitosan and TPP were carried out by adding a sodium chloride (NaCl) solution (0.025-0.2 M) to the chitosan-TPP nanoparticles. Instead of an increment in particle size, the reduction or shrinkage

of chitosan-TPP nanoparticle size was observed from 381 to 267 nm and 685 to 342 nm when the molar ratio of NaCl was increased up to 0.2 M for Cl113 and Cl213, respectively. This unusual phenomenon may have been correlated with the decrease of osmotic pressure with the increase of salt concentration (Shu and Zhu 2002a, Yin and Prudhomme 1992).

Following this, further investigation was carried out to determine the effects of ionic strength on the formation of chitosan-TPP nanoparticles. This was done by examining the size of particles prepared in different molar concentrations of acetate buffer at pH 4.5, 5 and 6, ranging from 0.025 to 0.2 M. A reduction of particle size was observed when molar concentration of acetate buffer was increased at pH 5 and below.

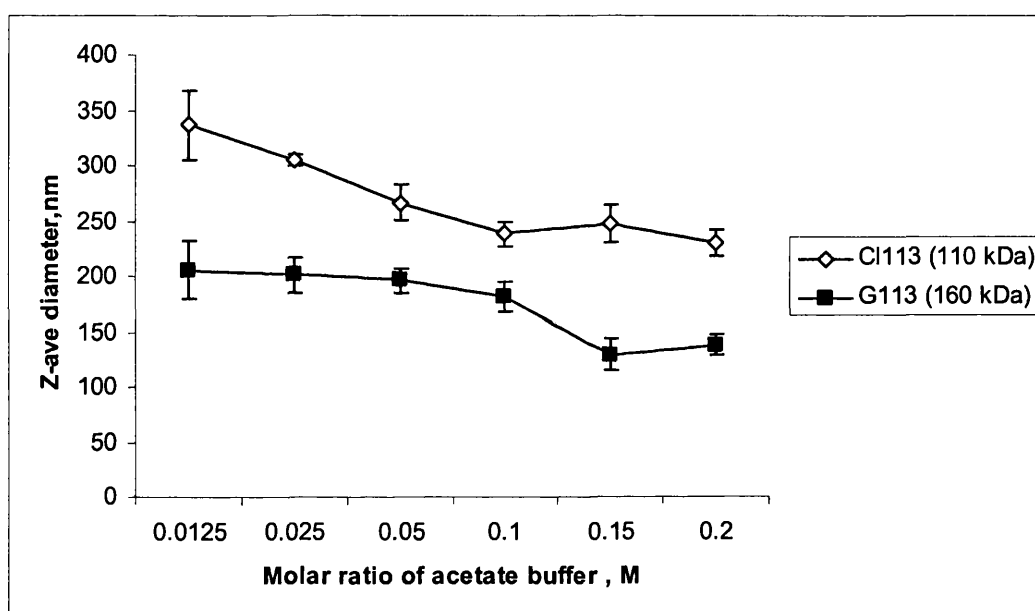


Figure 4.10: Effects of ionic strength on ionic-gelation of chitosan-TPP nanoparticles at pH 5 as determined by Malvern Zetasizer[®] (n=3).

Contrary to that, the particle size of chitosan-TPP nanoparticles was significantly increased at pH 6 from 357 to 643 nm and 162 to 4459 nm for Cl113 and G113, respectively when the molar concentration of acetate buffer was increased from 0.025 to 0.2 M. At higher pH such as at pH 6, the increment of salt concentration resulted in the increment of electrolyte concentration which changes the net charge by altering the number of dissociated groups in the network (López-León *et al.* 2005, Fernández-Nieves *et al.* 2000), leading to particle swelling by electrical repulsion. The

swelling effect was more prominent at higher pH as chitosan was partially ionized whereas at lower pH (e.g. pH 4.5), chitosan was fully ionised. At pH 5 and below, the chitosan-TPP nanoparticles were decreased in size. Further increased in salt concentration more than 0.1 M also resulted in the reduction of the intensity of light scattering (KCps). This may have indicated that the formed particles were unstable and dissociated rapidly with the increase of molar concentration of sodium acetate buffer. The reduction of KCps was thought to be due to the disintegration of particles, arising from the insufficient interaction between chitosan and TPP to withstand the osmotic pressure (López-León *et al.* 2005).

4.2.4 Stability of chitosan-TPP nanoparticles

It has been reported that chitosan nanoparticles prepared by ionic gelation lose their integrity in aqueous media either in the presence or absence of enzymes such as lysozymes (López-León *et al.* 2005). In fact, it has been reported that chitosan-TPP nanoparticles were not stable either stored at 5°C or -10°C. In this study, the stability of chitosan-TPP nanoparticles prepared in three different pH of sodium acetate buffer 0.1 M (pH 4.5, 5 and 6) was determined by storing them at 4 and -20°C and particle size of the nanoparticles was measured at each pre-determined time for 5 weeks. Initial results obtained revealed that the freezing and thawing process of frozen samples (-20°C) induced complete destabilization of the system as severe particle aggregation was observed and the system was discarded.

In the case of samples stored at 4°C, chitosan-TPP nanoparticles prepared at pH 4.5 showed a good stability since the increment of particle size after 5 weeks of storage was only 7.4%. In contrast, chitosan prepared at pH 5 and 6 showed significant increments in particle size after 48 h and 6 h, respectively. Low stability of chitosan-TPP nanoparticles prepared at higher pH could be explained by the lower positive value of particle surface charge, resulting in weaker repulsive electrostatic forces. Therefore, the systems lose their colloidal stability and thus particles start to aggregate. Furthermore, as chitosan-TPP nanoparticles prepared at pH 5 and 6 yielded higher numbers of particles than pH 4.5, their colloidal systems were thermodynamically unstable because of the high surface energy associated with the nanoscale dimensions.

4.2.5 Association of siRNA to chitosan-TPP nanoparticles

Association of siRNA to chitosan-TPP nanoparticles was performed either by adsorbing siRNA onto the preformed nanoparticles or by adding it during the gelation process (entrapment of siRNA into chitosan-TPP nanoparticles).

4.2.5.1 siRNA adsorption onto the chitosan-TPP nanoparticles

Adsorption of the bio-active agent onto the surface of nanoparticles is preferable because this technique could avoid the exposure of the bio-active agent to high shear rates during the nanoparticles preparation process. In this study, the adsorption of siRNA onto the surface of chitosan-TPP nanoparticles was accomplished in RNase free water as well as in sodium acetate buffer, 0.1 M (pH 4-6). To gain better understanding of the adsorption process, certain parameters were investigated which including chitosan-TPP nanoparticles to siRNA weight ratio, pH and ionic strength of the medium used.

4.2.5.1.1 Effect of chitosan-TPP nanoparticles to siRNA weight ratio

A series of concentrations of chitosan-TPP nanoparticles ranging from 0.3 to 1 mg/ml (equivalent to chitosan-TPP nanoparticles to siRNA weight ratio of 30 to 100) was used in order to determine the binding efficiency of siRNA (10 µg/ml) to chitosan-TPP nanoparticles. Agarose gel electrophoresis showed smearing appearance of some bands which may indicate heterogeneity in electrophoretic behaviour (Medberry *et al.* 2004). The complete binding of siRNA to the chitosan-TPP nanoparticles (retained in the well without the presence of a trailing band) however could only be observed when the chitosan-TPP nanoparticles to siRNA weight ratio was approaching 100:1 which indicated the existence of stronger interaction between siRNA and chitosan-TPP nanoparticles compared to siRNA-chitosan complexes (see page 100).

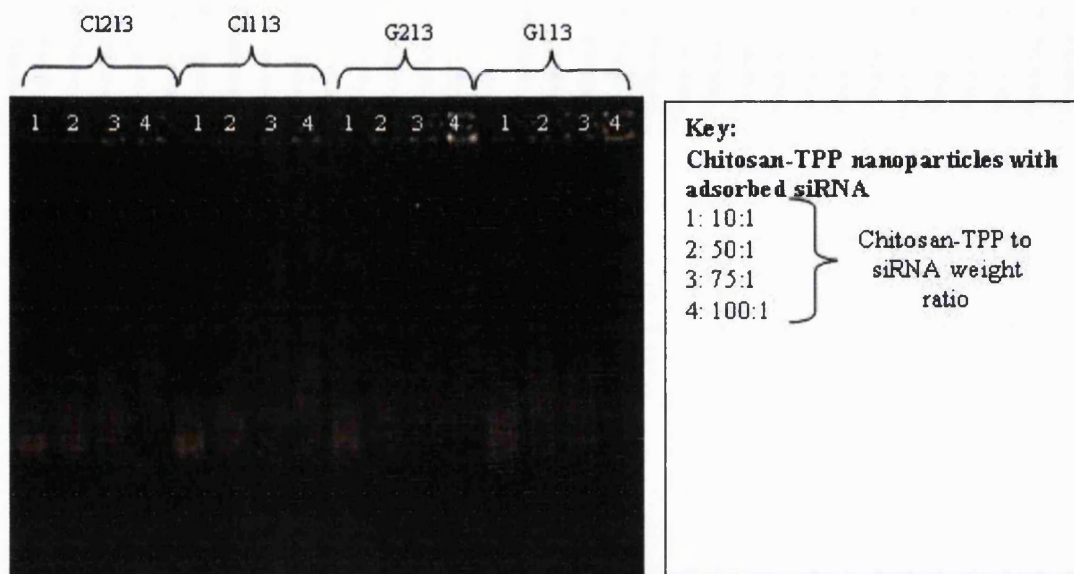


Figure 4.11: Binding capacity of siRNA onto the chitosan-TPP nanoparticles as determined by 4% agarose (LMP) gel electrophoresis in TBE buffer, pH 8 containing 0.5 μ g/ml ethidium bromide.

4.2.5.1.2 Effect of pH and ionic strength of adsorption medium

Adsorption of siRNA to chitosan is thought to be predominantly through electrostatic interaction between opposite charges of chitosan and the siRNA. Therefore, pH and ionic strength are the two factors that are important in influencing siRNA adsorption process onto the surface of chitosan-TPP nanoparticles. In this study, five different pHs (pH 4-6) of sodium acetate buffers (0.1 M) were used as adsorption media and the resultant particles with adsorbed siRNA were subjected to electrophoresis. The results showed that the binding of siRNA to the chitosan-TPP nanoparticles was not affected by the pH, as the profiles of siRNA binding to the chitosan-TPP nanoparticles in sodium acetate buffers for all of the tested pH were similar to the RNase free water. This in fact illustrated that the pH does not further improve their interaction into a stronger or irreversible particle formation.

On the other hand, the loading efficiencies of chitosan-TPP with adsorbed siRNA nanoparticles at a weight ratio of 100:1 were varied and depended on the type of chitosan used as determined by spectrophotometer. Higher siRNA loading efficiency was observed for siRNA adsorbed onto chitosan glutamate (83% \pm 0.9 for G213 and

90% \pm 0.3 for G113) compared to chitosan hydrochloride (72% \pm 1.1 for Cl213 and 59% \pm 0.8 for Cl113). It has been also reported that the addition of salt such as sodium or potassium chloride could enhance the efficiency of pDNA adsorbed onto the surface of cationic nanoparticles. The conformation of the cationic polymer chains was reported to be important in the present of salt and this facilitates the accessibility of pDNA at the interface for interaction with the chitosan. Therefore, siRNA adsorption onto the chitosan-TPP nanoparticles (prepared in RNase free water) was carried out in various molar concentrations of NaCl (0.025-0.2 M). For this experiment, chitosan Cl113 was chosen from among the studied chitosans because it had the lowest siRNA loading efficiency making this the best candidate to be used for investigating the effect of salt in enhancing loading efficiency. The results of siRNA loading efficiency at different salt concentrations are shown below:

Molar concentration of NaCl, M	Loading efficiency, %/ SD (\pm)
0 (double distilled water)	53 \pm 0.8
0.025	57 \pm 1.1
0.05	70 \pm 1.8
0.10	80 \pm 0.89
0.15	50 \pm 0.96
0.20	30 \pm 0.55

Table 4.2: The effects of NaCl molar concentration on siRNA loading efficiency of chitosan-TPP nanoparticles at weight ratio of 100:1 (n=3).

From the table, the loading efficiency of siRNA was increased with the increase of NaCl concentration up to 0.1 M. However, when the salt concentration was increased over 0.1 M, a reduction in siRNA loading efficiency was observed. The decreased in siRNA loading efficiency could be attributed to the reduction of the numbers of chitosan-TPP nanoparticles at higher salt concentration as they were unstable and tended to disintegrate as discussed in section 4.2.3.

4.2.5.2 siRNA entrapment into chitosan-TPP nanoparticles

It has been reported that entrapment of genetic materials within the carriers can offer better protection than adsorbing them onto the surface of polymeric carriers due to the direct exposure of the adsorbed genetic materials toward harsh biological environments. Furthermore, it could offer many other advantages such as controlled release as well as the ability to improve cellular targeting and uptake (Dunne *et al.* 2003). Previous study also reported that the association of ODNs was found to be more efficient when nanoparticles were formed by ionic gelation with TPP in comparison to simple complexation (Jane *et al.* 2001, Calvo *et al.* 1998). Therefore, siRNA was also encapsulated within the chitosan-TPP nanoparticles by adding siRNA (10 µg) together with TPP ions during the ionic gelation process.

4.2.5.2.1 Particle size and surface charge

The chitosan nanoparticles entrapping siRNA showed a slight decrease in particle size compared to the unloaded chitosan-TPP nanoparticles. The size of these particles at chitosan to TPP weight ratio of 6:1 were decreased to 440, 200, 605 and 331 nm for G213, G113, C1213 and C1113, respectively. The reduction of the particle size was expected due to the compaction of long and branch chitosan chains by siRNA through electrostatic interaction of the opposite charge. Furthermore, the addition of siRNA at the chitosan to TPP weight ratio of 6:1 reduced the surface charge of nanoparticles to approximately +20 mV from +60 mV. The differences observed were expected due to the charge neutralization, since phosphate groups of siRNA were interacted to the protonated amino groups of chitosan-TPP nanoparticles, which subsequently reduced the density of positive charge. In addition, a relatively lower positive charge value of chitosan-TPP nanoparticles with entrapped siRNA was expected compared to chitosan-siRNA complexes due to cancellation of chitosan positive charge by TPP ions.

4.2.5.2.2 Effect of pH on chitosan-TPP nanoparticles with entrapped siRNA

The influence of pH on the physical characteristics of the entrapped siRNA inside chitosan-TPP nanoparticles as well as the binding ability of siRNA to the chitosan was investigated by preparing the particles in sodium acetate buffer, 0.1 M at various pH, ranging from pH 4 to pH 6. Briefly, chitosan C1113 was dissolved in

sodium acetate buffer and TPP solution containing 10 μg of siRNA was added to the chitosan solution under magnetic stirring. Figure 4.12 revealed that the smallest particle size was obtained when the pH of sodium acetate buffer was 5. At pH 5, the attractive electrostatic forces involved in the binding process must be stronger than at higher pH and thus more siRNA molecules can be attracted to the chitosan leading to greater packing of siRNA to yield compacted chitosan-TPP-siRNA nanoparticles. Furthermore, the decrease of particle size of chitosan-TPP-siRNA prepared in acetate buffer in comparison to RNase free water might due to the presence of the salt in sodium acetate buffer as it may have induced better conformation of chitosan, arising from the screening of polyelectrolyte and colloid charge to facilitate the accessibility of siRNA for complexation (Trimaille *et al.* 2003, Maruyama *et al.* 1997).

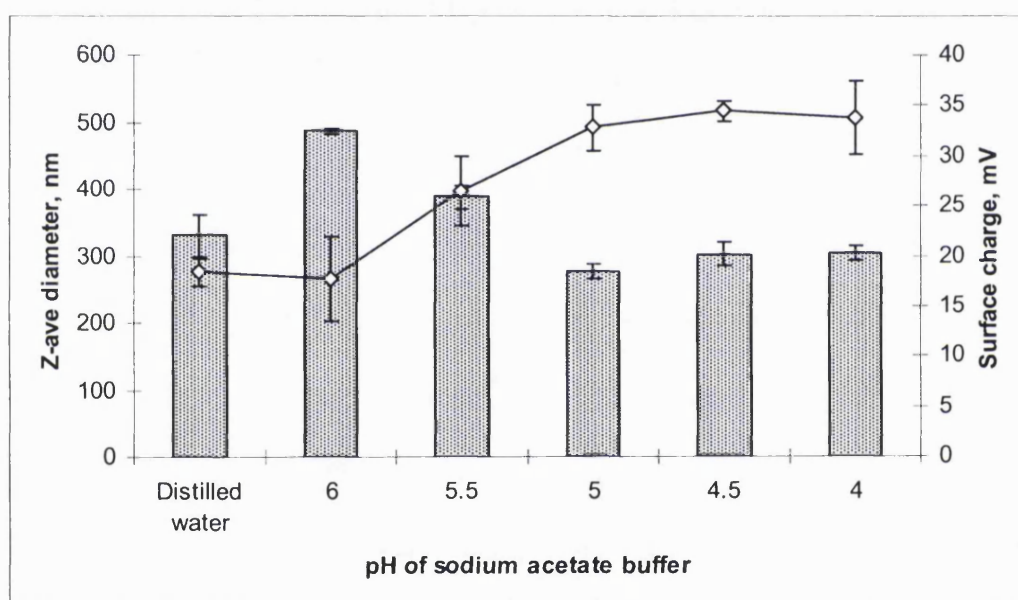


Figure 4.12: Effect of pH on Z-ave diameter and particle surface charge of chitosan-TPP-siRNA as determined by Malvern Zetasizer[®] (n=3). **Keynote:** Bar represents Z-ave diameter (nm) and line represents surface charge (mV)

4.2.6 siRNA binding and loading efficiency

Complete binding of siRNA was observed for all types and molecular weights of chitosan when 10 μg of siRNA was entrapped in chitosan-TPP nanoparticles as determined by gel retardation assay (figure 4.13). Absence of free siRNA detected on

the gel after electrophoresis described that no siRNA was leaked out from the chitosan-TPP nanoparticles, because siRNA was thought to be strongly bound to the chitosan amine groups. The loading efficiency of siRNA was also indirectly measured using spectrophotometry. 100% siRNA loading efficiency was obtained for all the entrapped siRNA within chitosan-TPP nanoparticles.

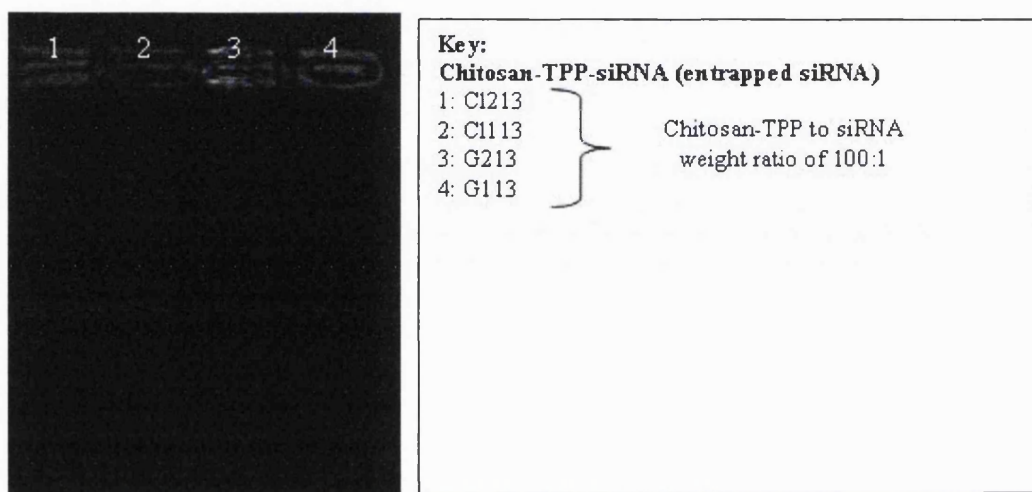


Figure 4.13: Binding efficiency of siRNA entrapped into chitosan-TPP nanoparticles as determined by 4% agarose (LMP) gel electrophoresis in TBE buffer, pH 8 containing 0.5 µg/ml ethidium bromide.

4.2.7 siRNA stability in serum

siRNA must be stable against degradation by nucleases in order to be active (Braasch *et al.* 2003). Therefore, to address the question of chitosan-siRNA nanoparticles stability and protection from nuclease degradation, nanoparticles were incubated in 5% and 50% of fetal bovine serum (FBS) at 37°C. Contrasting results were obtained in a previous report by Braasch *et al.* (2003) who reported that naked siRNA was stable after incubation in 5% serum up to 72 h. However, in this study siRNA was intact only up to 30 min and it was fully degraded after 48 h. Heterogenous results of siRNA in serum was thought to be arising from variable serum stability of the siRNAs depending on their sequence and the presence or absence of overhangs (Hauptenthal *et al.* 2006). In comparison, siRNA recovered from chitosan-TPP

nanoparticles (by displacing siRNA from the particles using heparin sulphate before electrophoresis) started to degrade after 24 h incubation and full degradation was observed after 72 h incubation (figure 4.14A). This experiment was repeated by incubating siRNA as well as chitosan-siRNA nanoparticles in the higher serum concentration of 50% v/v. The chitosan-siRNA nanoparticles significantly protected siRNA from nuclease activity. Complete degradation of siRNA was observed as early as timepoint of 0. In contrast with unformulated siRNA, the siRNA recovered from chitosan-siRNA nanoparticles was intact up to 7 h and fully degraded after 48 h incubation in 50% serum (figure 4.14B).

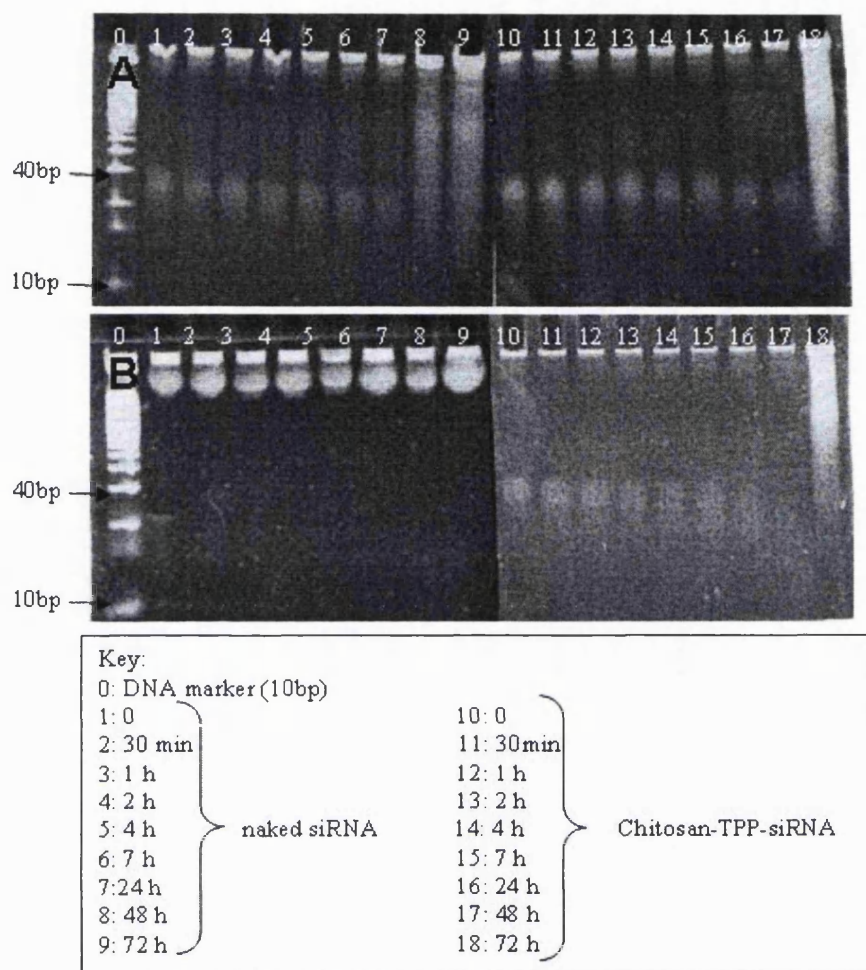


Figure 4.14: Electrophoretic mobility of chitosan-TPP-siRNA nanoparticles following incubation with FBS. The integrity of the siRNA was analysed by 15% polyacrylamide gel containing 7 M urea and TBE (0.089 M Tris base, 0.089 M boric acid, and 2 mM sodium EDTA, pH 8.3) buffer. siRNA bands were visualised under a UV transilluminator after staining for 40 min with a 1:1000 dilution of SYBR-Green II RNA gel stain (Molecular Probes) prepared in DEPC treated water. Image A: 5% FBS and image B: 50% FBS.

4.3 Cationic PLGA-chitosan nanoparticles prepared by the emulsification diffusion method

In this study, attempts were made to produce cationic PLGA nanoparticles using chitosan as a cationic surface modifier in order to allow the adsorption of siRNA to

occur on the PLGA particle surface. The emulsification diffusion method was used to prepare PLGA-chitosan nanoparticles. Briefly, this method uses a partially water soluble solvent like ethyl acetate, benzyl alcohol and propylene carbonate to dissolve the polymer. The polymer solution is then emulsified in the aqueous phase containing surfactant such as PVA to prevent aggregation of emulsion droplets. Finally, the diffusion of solvent from emulsion droplets upon the addition of water leads to the nanoprecipitation of the particles.

4.3.1 Particle size

Various formulation parameters were studied to produce PLGA-chitosan particles that had desirable properties such as nano-size and a positively surface charge as well as good particle morphology (individual particles without aggregation or fusion). In this section, the effects of formulation parameters on particle size of PLGA-chitosan nanoparticles will be first discussed. A preliminary work was carried out to determine appropriate homogenization speed and PVA concentration to produce nanoparticles using the emulsification diffusion method. This work was performed using PLGA without the addition of chitosan as the source of Ultra-pure chitosan was limited and expensive.

4.3.1.1 Homogenization speed

It has been shown that a smaller particle size could be obtained by increasing homogenization speed due to the stronger shear rate which promotes the breakage of droplets during the preparation of emulsion. Therefore, different rates of homogenization (8 000 and 17 500 rpm) were used to study the effects of homogenisation speed on particle size of PLGA nanoparticles. As predicted, the size of PLGA nanoparticles was decreased significantly from 1024 ± 58 to 332 ± 16 nm when the speed of homogenization was increased to 17 500 rpm (PVA concentration was 2% m/v).

4.3.1.2 Effect of PVA concentration

PVA is the most commonly used surfactant to stabilize the emulsion (Zambaux *et al.* 1998, Fong 1981). Several other studies have reported that particle size could be reduced by increasing PVA concentration in the aqueous phase as PVA could improve

the stability of emulsion droplets and prevent the formation of aggregates. A series of PVA concentrations ranging from 0.5 to 2% m/v was tested to evaluate the effect of PVA in reducing the particle size of PLGA nanoparticles. A drop in particle size was observed with the increasing concentration of PVA as shown below:

PVA concentration, %m/v	Before centrifugation		After centrifugation	
	Z-ave diameter, nm/SD (\pm)	Polydispersity, PI/SD (\pm)	Z-ave diameter, nm/SD (\pm)	Polydispersity, PI/SD (\pm)
0.5	334 \pm 22	0.08 \pm 0.04	477 \pm 63	0.4 \pm 0.52
1.0	332 \pm 40	0.05 \pm 0.04	354 \pm 53	0.09 \pm 0.12
2.0	308 \pm 16	0.08 \pm 0.02	320 \pm 20	0.07 \pm 0.02

Table 4.3: Effect of PVA concentration on particle size of PLGA nanoparticles prepared at homogenization speed of 17 500 rpm before and after centrifuging as determined by Malvern Zetasizer[®] (n=3).

Interestingly, utilising higher concentrations of PVA in the aqueous phase could prevent the formation of aggregates induced by centrifugation as shown on the table 4.3. Particle size of PLGA nanoparticles made using PVA at a 0.5% m/v was greatly increased by around 42% and size distribution was also increased indicating the formation of aggregates after centrifugation (table 4.3). In contrast, no significant change in particle size was observed for particles made using PVA at 1 and 2% m/v since the increment of PVA concentration resulted in the increase of PVA molecule adsorbed onto the surface of nanoparticles (Sahoo *et al.* 2002). The adsorption of PVA onto the surface of nanoparticles was reported to occur *via* hydrophobic bonding between hydroxyl groups of PVA and acetyl groups of PLGA, therefore a large number of hydroxyl groups of PVA could hydrate at the surface to stabilize nanoparticles (Abdelwahed *et al.* 2006, Murakami *et al.* 1999). Thus, these nanoparticles were more stable and resistant to aggregation induced by high speed centrifugation. Following these observations in these following experiments, a PVA concentration of 2% m/v was used and the emulsion was prepared at a homogenization speed of 17 500 rpm.

4.3.1.3 Type and molecular weight of chitosan

Four types of Ultra-pure chitosan were used to prepare PLGA incorporated with chitosan nanoparticles. They were chitosan glutamate 213 (470 kDa) and 113 (160 kDa) as well as chitosan hydrochloride 213 (270 kDa) and 113 (110 kDa). In contrast to plain PLGA nanoparticles, these particles were much bigger and their sizes were widely distributed depending on the molecular weight of chitosan used. Particle size of PLGA-chitosan nanoparticles was decreased with the decrease in chitosan molecular weight as shown in figure 4.15. Furthermore, particle size distribution (PI) was also reduced when a lower molecular weight of chitosan was used for both types of chitosan. The size distribution was reduced from 0.96 ± 0.21 to 0.853 ± 0.11 and from 1.00 ± 0.01 to 0.45 ± 0.05 for chitosan glutamate and hydrochloride, respectively. The difference in particle size was thought to arise from the difference in viscosity between these chitosans as a higher molecular weight of chitosan produced a higher viscosity in solution or in this case, organic phase. Therefore, increasing viscosity of the organic phase resulted in the formation of larger emulsion droplets as it is more resistant to the shear forces. This was in agreement with the results obtained from the plain PLGA nanoparticles where a low viscosity organic phase in the absence of chitosan produced smaller particles than in the presence of chitosan.

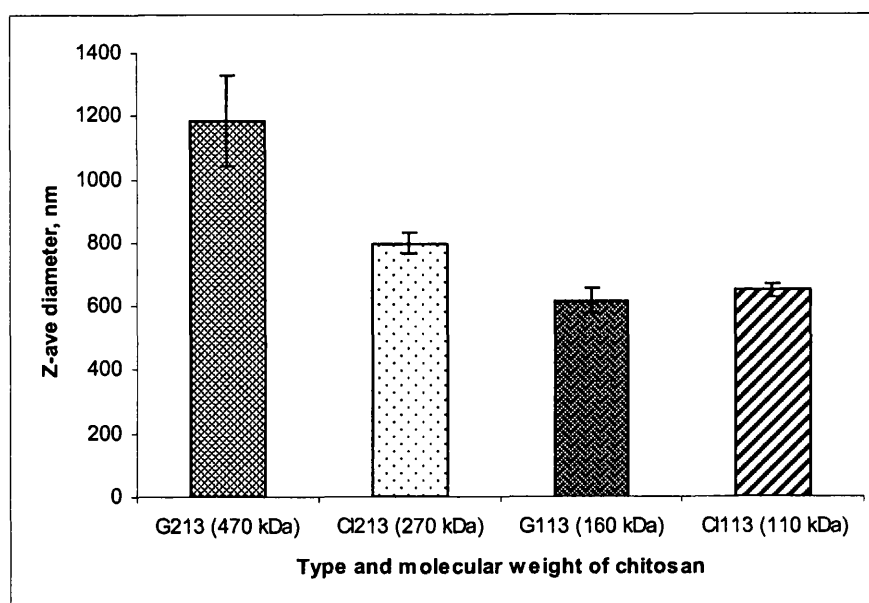


Figure 4.15: Effect of type and molecular weight of chitosan on particle size of PLGA-chitosan nanoparticles as determined by Malvern Zetasizer[®] (n=3).

4.3.2 Surface charge

Salted chitosan is positively charged and soluble when presented in acidic or neutral solution due to the protonation of amino groups on the chitosan backbone. Therefore, incorporation of chitosan into PLGA was expected to result in cationic nanoparticles that were able to interact with pDNA as well as siRNA through electrostatic interaction. However, this would be highly dependent on the amount of chitosan added. Therefore, a series of chitosan (Cl213) concentrations ranging from 0 to 1.2% m/v was added to the aqueous phase to determine the effect of chitosan concentration on particle surface charge. As expected, the particle surface charge of PLGA-chitosan nanoparticles was increased with the increase in chitosan concentration. However, a positive value of the particle surface charge was only achieved when the chitosan concentration was increased to 0.6% m/v and above. This illustrated that starting at this concentration, free protonated amino groups were available since most of them were interacted or bound to the carboxylic groups of PLGA to form cationic nanoparticles. Overall, the particle surface charge was increased from -34.9 ± 2.6 mV at 0% m/v to $+21.3 \pm 0.7$ mV at 1.2% m/v.

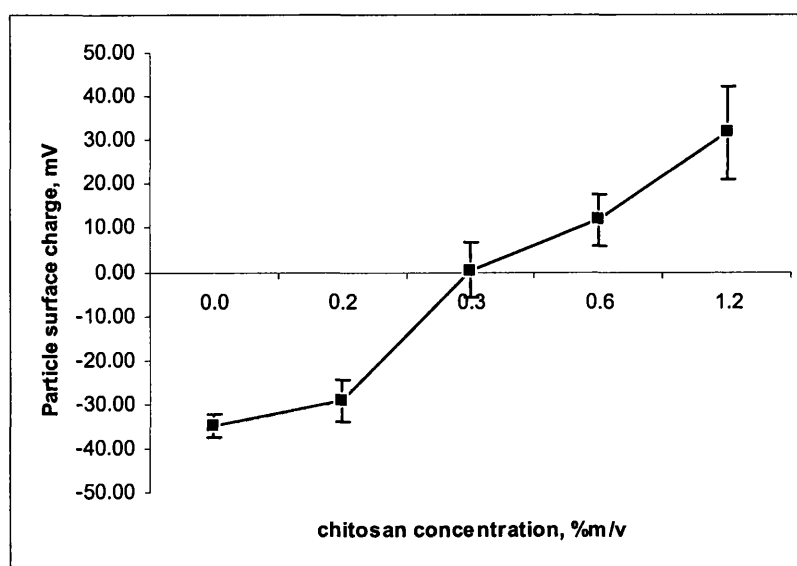


Figure 4.16: Surface charge of PLGA-chitosan nanoparticles at different concentrations of chitosan (n=3).

4.3.3 Effect of centrifugation on particle size

In this study, PLGA-chitosan nanoparticles were normally washed and collected by centrifugation. Centrifugation is one of the most commonly used and convenient techniques to wash and collect particles. However, it was shown that centrifugation could increase particle size due to the compaction of the particles by the high speed of spinning and these particles therefore tend to form aggregates. As mentioned in the earlier section, the size of PLGA nanoparticles was increased after centrifugation except in the presence of PVA at concentration of 1% m/v and above which had been shown could prevent the increment of particle size induced by centrifugation.

However, for the PLGA-chitosan nanoparticles, a surprising drop in particle size was observed after centrifugation as shown on figure 4.17. For example, the size of PLGA-chitosan nanoparticles made of Cl113 dropped almost 2-fold to 360 nm from 650 nm after centrifugation. Moreover, the polydispersity index of these particles was also decreased significantly to 0.6 ± 0.1 , 0.08 ± 0.01 , 0.36 ± 0.05 and 0.18 ± 0.02 for G213, Cl213, G113 and Cl113, respectively.

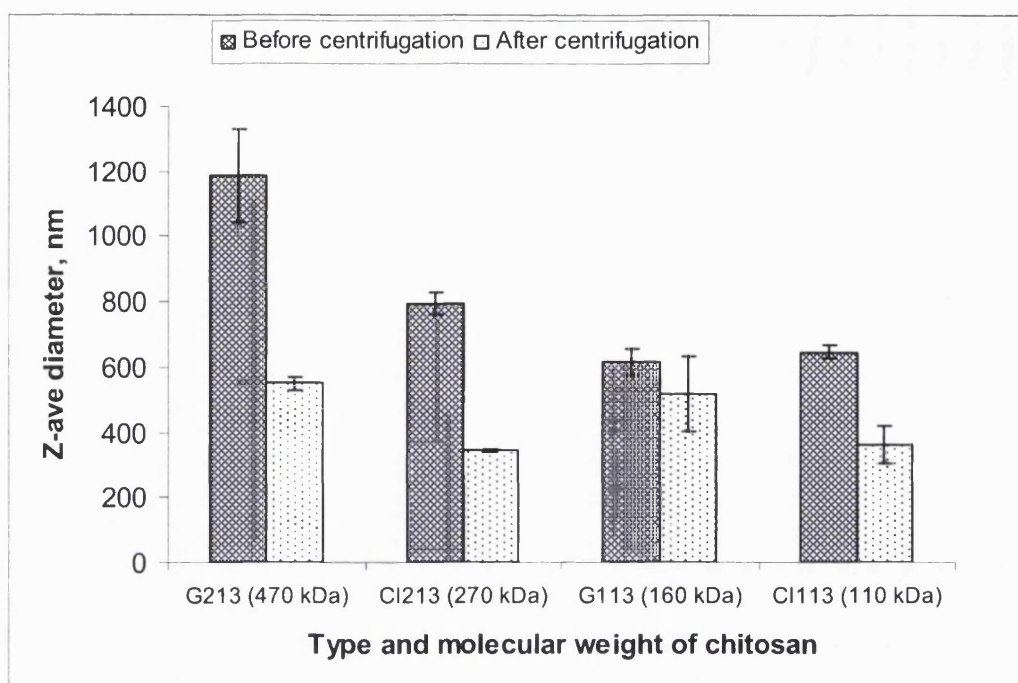


Figure 4.17: Effect of centrifugation on particle size of PLGA-chitosan nanoparticles after two cycles of centrifugation as determined by Malvern Zetasizer®, U.K (n=3). A drop in particle size was observed for the PLGA-chitosan nanoparticles after centrifugation. PLGA-chitosan nanoparticles were prepared by emulsification diffusion method made from different types and molecular weights of chitosan.

This phenomenon was attributed to the addition of chitosan in the aqueous phase. During particle preparation, small emulsion droplets were formed by homogenisation and the solvent diffusion process. In this process, some of the chitosan might be trapped within the particle which interacted with carboxylates from PLGA whereas some of them might be adsorbed and surrounded on the surface of particles *via* partial interaction, leading to the formation of large and widely distributed particles. When the particles were centrifuged, the adsorbed chitosan molecules were therefore washed away from the surface of particles due to the high speed of centrifugation (20 000 rpm), thus explaining the drop in particle size after washing.

This theory was corroborated by the very low particle surface charge when the particles were washed by centrifugation compared to filtration. The particle surface charge of PLGA-chitosan made of CI113 was reduced ($+10.4 \pm 1.9$) when centrifugation

was used to wash the particles compared to filtration ($+63.1 \pm 0.9$ mV). A similar trend occurred with G213 as well as G113 where their surface charges were reduced by 3- and 6-fold to $+19.4 \pm 1.5$ mV and $+13.1 \pm 0.4$ mV, respectively compared to filtered particles. Although filtration yielded a comparatively high positive charge of PLGA-chitosan nanoparticles, potentially more favourable for siRNA adsorption, these particles were 2-fold bigger than before filtration. In fact, the particle size of these nanoparticles was further increased after freeze-drying (figure 4.18). It is thought that this might arise from particle aggregation or fusion induced by the surrounded chitosan on the surface of the particles as the aqueous phase was forced to flow through the membrane by high pressure (0.9 bar). On balance, it is thought that probably the significant reduction of particle size is due to the loss of chitosan molecules from the surface of the particles by centrifugation. Therefore, it is important to adsorb siRNA onto the PLGA-chitosan nanoparticles after this step.

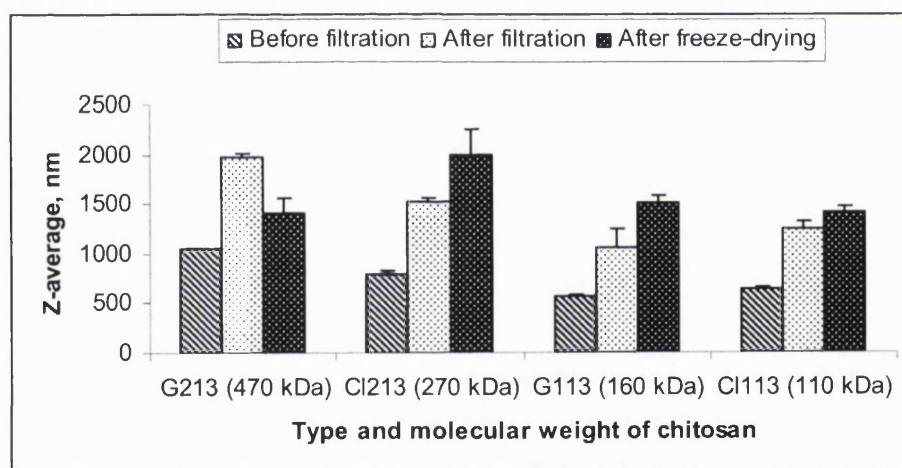


Figure 4.18: Effect of filtration and freeze-drying on particle size of PLGA-chitosan nanoparticles made from different types and molecular weights of chitosan, ($n=3$). Particle size was measured using Malvern Zetasizer[®] (Malvern, UK).

4.3.4 Effect of PLGA polymer

PLGA-chitosan nanoparticles made of PLGA 50:50 2A which was washed and collected by centrifugation suffered from low amount of chitosan actually being

incorporated into PLGA nanoparticles. This was been reflected by relatively low surface charge of those particles after centrifugation compared to before centrifugation. Therefore, attempts have been made to improve this using PLGA with higher degree of "uncapped" end groups. It was hypothesized that a higher degree of "uncapped" end groups of PLGA could provide more carboxylic groups, which would readily interact with protonated amine groups of chitosan through electrostatic interaction, to form positively charged nanoparticles. For this purpose, PLGA 3A was used to prepare PLGA-chitosan nanoparticles instead of PLGA 2A and they were prepared exactly as before.

By using PLGA 3A, the mean particle size of PLGA-chitosan nanoparticles were 464 ± 8.41 and 795 ± 14.33 nm for chitosan hydrochloride C1113 and C1213, respectively. In contrast to earlier nanoparticles (PLGA 2A), centrifugation had no effect on the size of these nanoparticles as only a slight decrease from 464 ± 8.41 nm to 431 ± 15.41 nm after centrifugation was seen for C1113 and C1213 had a corresponding small, insignificant increase in size from 795 ± 14.33 to 806 ± 25.61 nm. Nevertheless, these particles were adversely affected by freeze-drying and lyophilised forms of particles were well beyond nanometer size range (4 and 5 μm for C1113 and C1213, respectively as determined by Malvern Mastersizer[®]). To solve this problem, a lyoprotectant agent, trehalose, was employed at a concentration of from 10 to 20% of trehalose for the total mass of polymer to the particles suspension prior to freeze-drying. It was then found that 20% of trehalose could adequately protect PLGA-chitosan nanoparticles prepared with C1113 but not with C1213. The summary of particle size of PLGA-chitosan nanoparticles before and after freeze-drying is shown below:

Sample	Z-average, nm/ SD (\pm)	Polydispesity index, PI SD (\pm)
CI113 BC	463.8 \pm 8.4	0.28 \pm 0.01
CI113 AC	431.0 \pm 15.4	0.19 \pm 0.08
CI113 AF	*4096.0 \pm 3815.3	1 \pm 0.0
10% trehalose CI113	737.8 \pm 95.6	0.83 \pm 0.29
20% trehalose CI113	538.1 \pm 32.3	0.42 \pm 0.04
CI213 BC	794.8 \pm 14.3	1 \pm 0.0
CI213 AC	806.4 \pm 25.6	0.69 \pm 0.21
CI213 AF	*5390.4 \pm 5111.8	1 \pm 0.0
10% trehalose CI213	*4484.1 \pm 1059.9	1 \pm 0.0
20% trehalose CI213	960.4 \pm 39.2	0.92 \pm 0.10

Table 4.4: Effect of trehalose on particle size and polydispersity index of PLGA-chitosan nanoparticles as determined by Malvern Zetasizer[®] (n=3). Keynotes: BC= before centrifugation and AC= after centrifugation. *Particle size was further measured using Malvern Mastersizer and the particle size was 4 \pm 0.8, 5 \pm 1.1 and 3.5 \pm 0.6 μ m for CI113 AF, CI213 AF and 10% trehalose CI213, respectively.

As stated earlier, incorporation of chitosan and PLGA was to form cationic nanoparticles and elicit nucleic acid complexation. A higher particle surface charge was obtained for PLGA-chitosan nanoparticles prepared from PLGA 3A (+42.5 and +60 mV for CI113 and CI213, respectively) than PLGA 2A (+28 mV for CI213). This was attributed to the increased number of carboxylic groups of PLGA which could interact with chitosan amino groups, leading to the increased incorporation of chitosan with PLGA to form positively charged nanoparticles. The results from spectrophotometer studies using Orange IIC dye consistently showed an incorporation of more than 94% of chitosan into PLGA nanoparticles compared to only 60% for PLGA 2A which explained a high particle surface charge of PLGA 3A for both molecular weight of chitosans.

4.3.5 Morphology

PLGA-chitosan nanoparticles prepared by emulsification diffusion were generally smooth spheres of less than 500 nm as determined by SEM. No difference in

particle morphology was observed when the chitosan concentration was increased from 0.3 to 1.2% m/v except PLGA-chitosan nanoparticles made of 1.2% m/v of chitosan were smaller in size and more homogenous as shown in figure 4.19. However, particles washed and collected by filtration (Amicon Stirred Cell Model 8400, Millipore) were apparently aggregated and fused with each other (figure 4.20B and D). In contrast to filtration, particles washed by centrifugation were less likely to be aggregated as shown in figure 4.20A and C. The observed appearances of freeze-dried products under SEM were thought to be affected by the amount of chitosan remained in the formulation after washing step which also would influence the rehydration properties of these particles. This effect could therefore be seen in the morphology of both filtered and centrifuged formulations where filtered products were looked like sticky fluffy cake and had rehydration problem but not with centrifuged products.

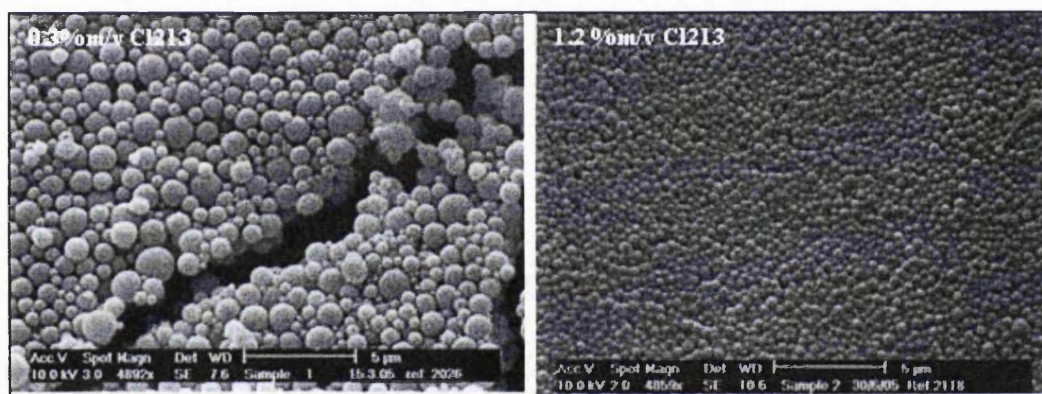


Figure 4.19: Effect of chitosan concentration on particle morphology of PLGA-chitosan nanoparticles (2% m/v PVA).

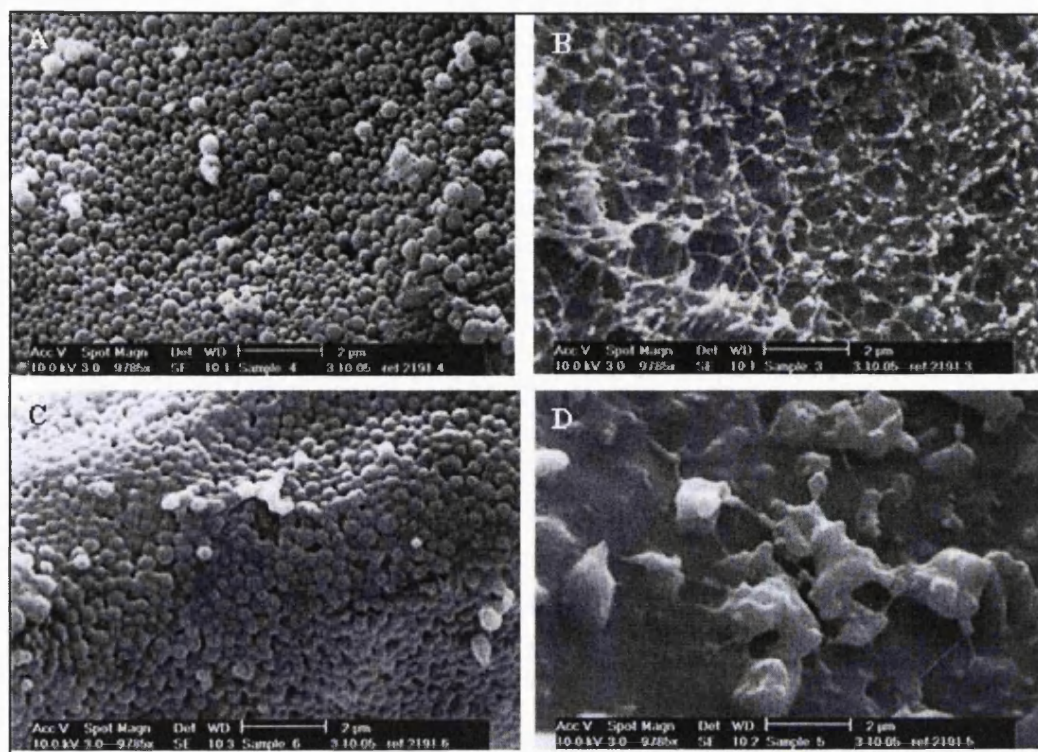


Figure 4.20: Effect of washing technique on particle morphology of PLGA-chitosan nanoparticles (2% m/v PVA). A and C: PLGA-G113 and -G213 washed and collected by centrifugation, B and D: PLGA-G113 and -G213 washed and collected by filtration.

4.3.6 siRNA adsorption onto the surface of PLGA-chitosan nanoparticles

siRNA was adsorbed onto the surface of PLGA-chitosan nanoparticles at different concentrations of nanoparticles from as low as 1 up to 5 mg/ml and siRNA was fixed at 10 μ g/ml. It appeared that siRNA was not completely bound to the PLGA-chitosan nanoparticles collected by centrifugation (as determined by gel retardation assay using 4% agarose (LMP) gel electrophoresis in TBE buffer, pH 8, figure 2.21 and 2.22) even though a very high nanoparticles to siRNA weight ratio was used (500:1). The siRNA binding efficiency was found to be independent on types of chitosan but the higher degree of "uncapped" end groups of PLGA employed apparently had a slight improvement in the adsorption of siRNA as it could incorporate more chitosan into the nanoparticles as determined by spectrophotometry using Orange IIC dye. The results

from quantitative assay (spectrophotometry) for loading efficiency of siRNA adsorbed onto the nanoparticles also revealed that the overall loading efficiency for PLGA 3A samples exceeded 75% with C1213 giving a slightly higher siRNA loading efficiency of more than 80% for its various concentrations (86, 84 and 89% of siRNA loading efficiency for 1, 3 and 5 mg/ml or 100:1, 300:1 and 500:1 nanoparticles to siRNA weight ratio, respectively).

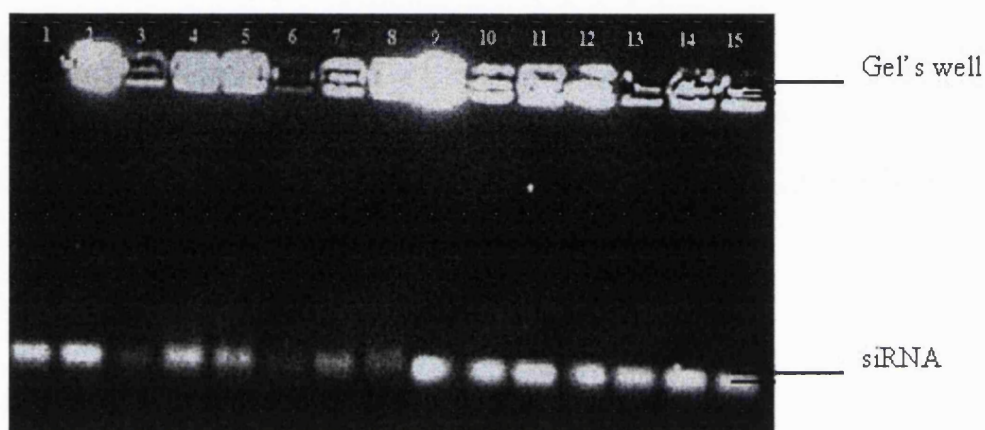


Figure 4.21: siRNA binding efficiency of various PLGA 3A-chitosan nanoparticles. Lane 1: Free siRNA, Lane 2: PLGA nanoparticles (without chitosan), Lane 3-5 respectively are: 1, 3 and 5 mg/ml of PLGA-C1113 nanoparticles, Lane 6-8 respectively are: 1, 3 and 5 mg/ml of PLGA-C1213 nanoparticles, Lane 9-11 respectively are 1, 3 and 5 mg/ml of PLGA-C1113 nanoparticles with heparin, Lane 12-14 respectively are: 1, 3 and 5 mg/ml of PLGA-C1213 nanoparticles with heparin and Lane 15: PLGA nanoparticles with heparin.

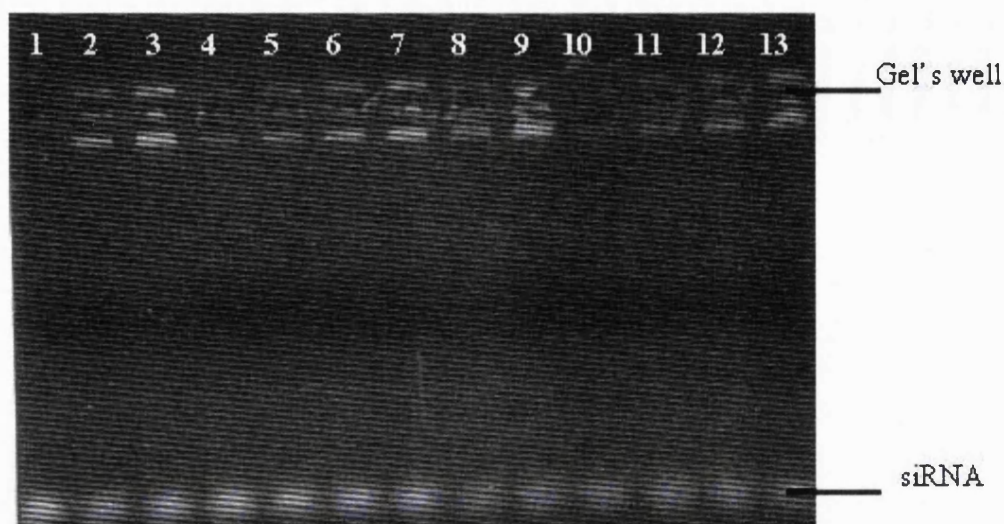


Figure 4.22: siRNA binding efficiency of various PLGA 2A-chitosan nanoparticles. Lane 1: Free siRNA, Lane 2-4 respectively are: 1, 3 and 5 mg/ml of PLGA-CI113 nanoparticles with heparin and Lane 5-7 respectively are 1, 3 and 5 mg/ml of PLGA-CI213 nanoparticles with heparin, Lane 8-10 respectively are: 1, 3 and 5 mg/ml of PLGA-CI113 nanoparticles and Lane 11-13 respectively are: 1, 3 and 5 mg/ml of PLGA-CI213 nanoparticles.

4.3.7 siRNA protection by PLGA-chitosan nanoparticles in serum

Investigation into the influence of serum on the integrity of siRNA is an important factor in assessment of the possible use of siRNA as a therapeutic agent. The ability of PLGA-chitosan nanoparticles to protect siRNA from degradation by nucleases was determined by incubating these nanoparticles with adsorbed siRNA at weight ratio of 400:1 in DMEM containing 50% of FBS for 48 h. The results obtained showed siRNA was protected by PLGA-chitosan nanoparticles for up to 48 h. In contrast, naked siRNA was fully degraded as early as 30 min and this therefore illustrating the ability of PLGA-chitosan nanoparticles to protect siRNA from nuclease degradation.

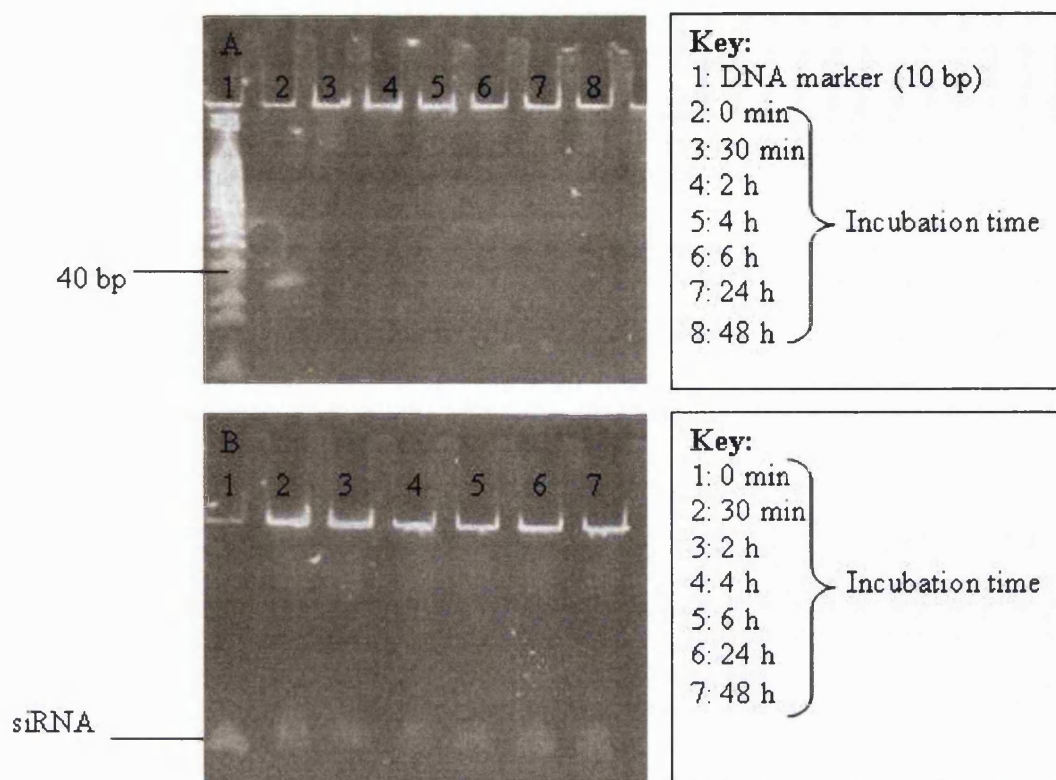


Figure 4.23: Serum protection assay (DMEM containing 50% FBS) of naked siRNA (A) and PLGA-chitosan with adsorbed siRNA (B) at different time points. The integrity of the siRNA was analysed by 15% polyacrylamide gel containing 7 M urea and TBE (0.089 M Tris base, 0.089 M boric acid, and 2 mM sodium EDTA, pH 8.3) buffer. siRNA bands were visualised under a UV transilluminator after staining for 40 min with a 1:1000 dilution of SYBR-Green II RNA gel stain (Molecular Probes) prepared in DEPC treated water.

4.3.8 Comparison of PLGA-chitosan nanoparticles adsorbed with either siRNA or pDNA

Binding capacity of pDNA to PLGA-chitosan nanoparticles was determined by measurement of fluorescence induced by PicoGreen-pDNA interaction. PicoGreen is an asymmetrical cyanine dye that exhibits >1000-fold increase in fluorescence upon binding to double stranded DNA (dsDNA) with relatively little reactivity toward RNA and single stranded DNA (Barman *et al.* 2000, Singer *et al.* 1997). Therefore, this assay only could be applied to quantify pDNA and not siRNA.

Indirect measurement of pDNA in supernatant collected from depletion method revealed that the efficiency of pDNA to adsorb onto the surface of PLGA-chitosan nanoparticles was depended on chitosan concentration. Significant increase of pDNA loading efficiency was observed, from only 55.2% at 0.2% m/v to 99.5% at 1.2% m/v of chitosan. Since the interaction between pDNA and cationic nanoparticles *via* electrostatic interaction, therefore particle surface charge play a crucial role in pDNA adsorption onto the cationic nanoparticles. As PLGA-chitosan nanoparticles made of 1.2% m/v of chitosan exhibited the highest positive value of particle surface charge, high loading efficiency of pDNA was predicted from these particles because pDNA could easily attract to the high density of protonated amino groups of chitosan. In contrast, PLGA-chitosan nanoparticles with lower value of particle surface charge would have lower pDNA loading efficiency due to the insufficient amount of protonated amino groups to interact with pDNA. The relationship of particles surface charge with pDNA loading efficiency is shown below:

Chitosan concentration, %m/v	Particle surface charge, mV SD (\pm)	pDNA loading efficiency, %
0.2	-0.7 \pm 0.3	55 \pm 12.3
0.3	+0.3 \pm 12.6	59 \pm 3.5
0.6	+11.7 \pm 5.8	67 \pm 13.2
1.2	+21.7 \pm 0.7	99 \pm 5.9

Table 4.5: Relationship between particle surface charges with pDNA loading efficiency of PLGA-chitosan nanoparticles with adsorbed pDNA. pDNA adsorption was carried out at nanoparticle to pDNA ratio of 100:1 (n=3).

The binding of the cationic nanoparticles to the polyanionic pDNA was studied using analysis of the electrophoretic mobility of pDNA within agarose gel. Efficient condensation of pDNA by cationic nanoparticles leads to immobilisation of pDNA (Ravi Kumar *et al.* 2004). Complete binding of pDNA adsorbed onto the PLGA-chitosan nanoparticles was observed at nanoparticles to pDNA ratio of 100:1. This interaction was strong and stable as no displacement of pDNA was observed after the particle suspension was treated with heparin sulphate (1000 unit/ml). Glycosaminoglycan such as heparin is an anion that can relax the complex

condensation, resulting in DNA release from the complexes (Kircheis *et al.* 2001, Ruponen *et al.* 1999).

These findings describing that the interaction between pDNA and PLGA-chitosan nanoparticles was strong and stable. Meanwhile, as mentioned in section 4.3.6, the binding of siRNA to PLGA-chitosan nanoparticles was less efficient as siRNA mobilisation still could be seen although at high amount of PLGA-chitosan nanoparticles, 5 mg/ml (500:1 nanoparticles to siRNA weight ratio). The reason behind this phenomenon has been discussed in earlier section.

4.4 Biological activity of siRNA

4.4.1 Chitosan-siRNA complex and chitosan-TPP nanoparticles associated with siRNA

Determination of gene silencing activity of these chitosan nanoparticulate systems was first performed in CHO K1 cells and optimal chitosan to siRNA ratio of 100 and 10 was used for siRNA associated with chitosan-TPP nanoparticles and chitosan-siRNA complex, respectively. The efficiency of gene silencing was measured as a normalised ratio of the silencing pGL3-luciferase expression to pRL-TK expression used as internal standard. In consideration that luciferase expression could be reduced not only by the silencing effect of siRNA but also due to cellular death, a non-targeted gene (renilla luciferase form pRL-TK) was measured to normalise the firefly luciferase expression from pGL3. The observed expression was then also represented as a Relative Response Ratio (RRR) in which Lipofectamine 2000-siRNA complexes were used as a positive control and cells without siRNA silencing treatment (co-transfected with pGL3 and pRL-TK) as a negative control.

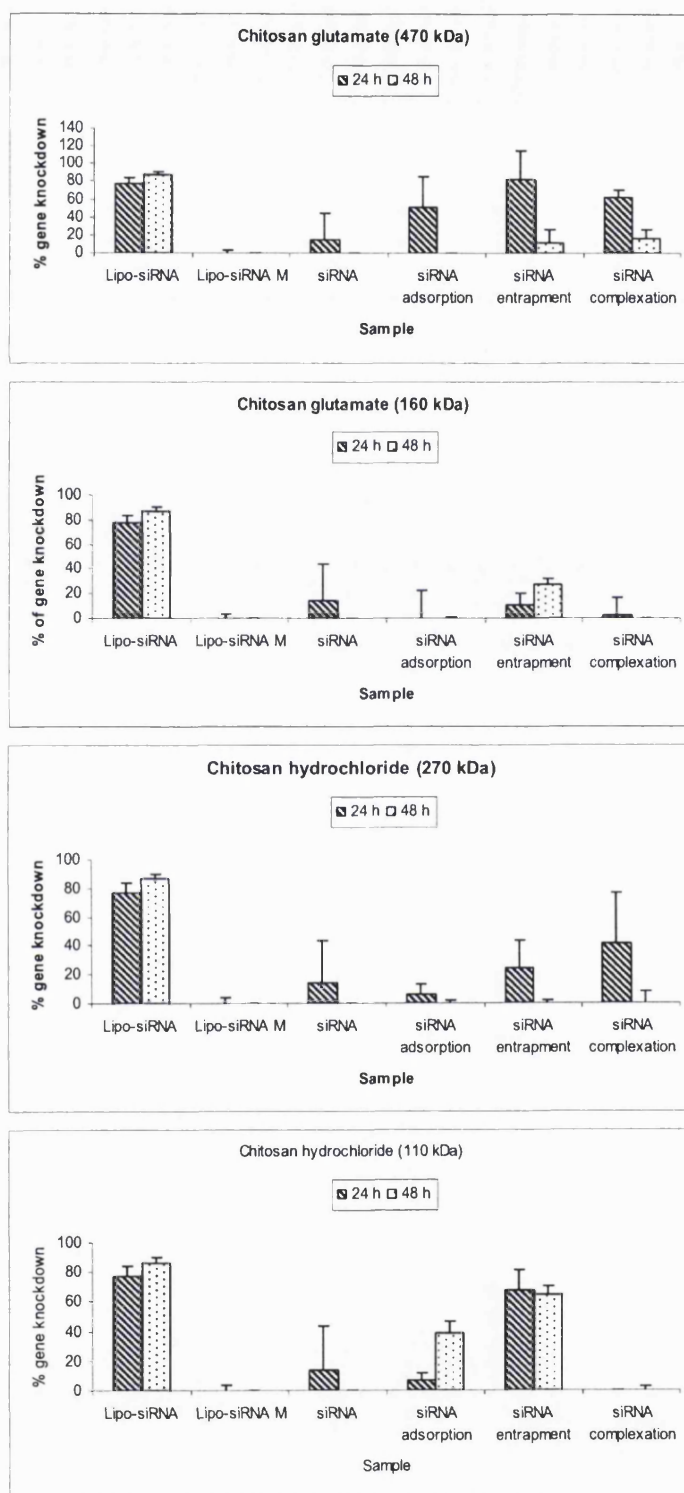


Figure 4.24: Effect of chitosan molecular weight and method of siRNA association to the chitosan nanoparticles on percentage of gene knockdown of pGL3 luciferase in CHO K1 cells (5×10^3 cell/ well) at 24 and 48 h post transfection (n=6). Keynotes: Lipo= Lipofectamine 2000 and siRNA M= siRNA mismatch.

Transfections performed with nanoparticles prepared with different types, molecular weights of chitosan and methods of siRNA association to the chitosan revealed that the silencing effect of certain chitosan-siRNA nanoparticles or complexes had a comparable effect compared to Lipofectamine 2000 (figure 4.24). In contrast, a negligible silencing effect was observed for naked siRNA as well as Lipofectamine 2000-mismatch siRNA (non-silencing) complexes used as a control. The higher ratio of firefly to renilla luciferase expression (low percentage of gene knockdown) for naked siRNA and the cells treated with Lipofectamine 2000-mismatch siRNA complexes indicated that naked siRNA might be degraded before reaching the cytoplasm and the specificity of siRNA silencing effect was important as would be expected.

The ability of these chitosan nanoparticles in delivering siRNA to the cells was apparently independent of the type or molecular weight of chitosan as no obvious correlation could be seen between these parameters with the gene silencing effect. The method of siRNA association to the chitosan, however, apparently had an effect on siRNA silencing. The addition of siRNA together with the TPP ions during the ionic gelation process (siRNA entrapment) showed better gene silencing activities compared to other methods for all types of chitosan. In contrast to that, a low inhibition of gene expression was observed for particles prepared by simple complexation and adsorption of siRNA onto the preformed chitosan-TPP nanoparticles. This finding might be attributed to lack of protection against degradation due to the weak binding between the chitosan and siRNA complex (determined by gel retardation assay) or exposure of adsorbed siRNA to the nuclease activity. In addition, chitosan glutamate, G213 (470 kDa) showed the highest gene silencing effect at 24 h post-transfection when prepared either by simple complexation (51% of gene knockdown) or ionic gelation (82% and 63% of gene knockdown for siRNA entrapment and siRNA adsorption, respectively) compared to its lower molecular weight or chitosan hydrochloride. siRNA entrapped in chitosan-TPP nanoparticles prepared from chitosan glutamate, G213 even showed a comparable transfection efficiency to Lipofectamine 2000 (figure 4.24). Nevertheless, when comparing these gene silencing activities at 24 and 48 h post-transfection, a higher activity was obtained at 24 than 48 h post-transfection for the cells treated with siRNA associated with chitosan nanoparticles or complexes, suggesting the release of siRNA might occur within the first 24 h for most of the tested chitosans. Contrary to

that, chitosan C1113 for siRNA entrapment had shown a sustain effect of gene silencing as a higher knockdown activity was detected at 48 h post-transfection.

On the other hand, transfection studies performed in HEK 293 human kidney cells showed lower gene silencing activities for these chitosan nanoparticles either at 24 or 48 h post-transfection compared to CHO K1 cells. Chitosan G213 for example was 22, 14 and 64% less efficient than Lipofectamine 2000 for chitosan-TPP with adsorbed siRNA, chitosan-TPP with entrapped siRNA and chitosan-siRNA complexes, respectively (figure 4.25). Further study also showed that no significant increase in the gene silencing effect was detected for the higher weight ratio of chitosan-siRNA complexes (100:1) which indicates that the lower gene silencing effect of chitosan-siRNA complexes was not due to the 10-fold lower amount of chitosan compared to siRNA associated with chitosan-TPP nanoparticles. Moreover, stability studies revealed that these chitosan nanoparticles were stable in medium containing up to 10% serum for chitosan-siRNA complexes and chitosan-TPP-siRNA nanoparticles (10-fold increased in particle size was observed at serum concentration of 10% v/v), which indicates that poor results or gene silencing effect for those particles were unlikely to be due to aggregation as only 5% serum was used during the transfection.

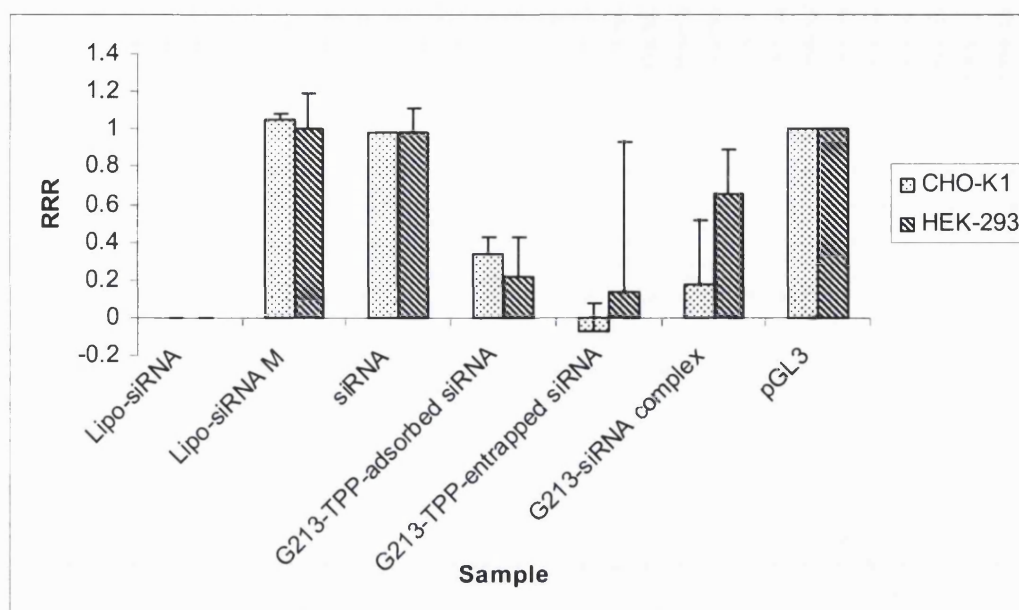


Figure 4.25: Relative Response Ratio (RRR) of chitosan nanoparticles prepared from chitosan glutamate, G213 in CHO K1 and HEK 293 cells (5×10^3 cell/ well) at 24 h post-transfection. Keynotes: Lipo-siRNA M= Lipofectamine 2000-siRNA mismatch complexes, pGL3= pDNA encoded luciferase gene delivered by lipofectamine 2000.

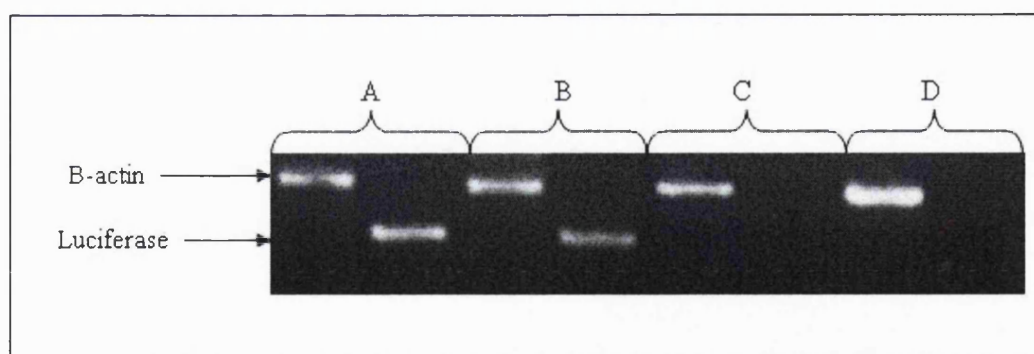


Figure 4.26: RT-PCR analysis of firefly luciferase downregulation by chitosan-TPP nanoparticles with entrapped siRNA in CHO K1 cells which transiently integrated with pGL3 luciferase control (at 24 h post-transfection). Lane A: untreated cells, Lane B: Lipofectamine 2000-mismatch siRNA, Lane C: chitosan-TPP nanoparticles with entrapped siRNA and Lane D: Lipofectamine 2000-siRNA. B-actin was used as a control.

Investigation of gene silencing by chitosan-TPP nanoparticles with entrapped siRNA at cellular mRNA level was carried out by semi quantitative reverse transcriptase PCR (rt-PCR). As shown on figure 4.26, samples from the cells treated with Lipofectamine 2000-siRNA mismatch complexes resulted in intense band comparable to that of untreated cells which describing the specificity of siRNA activity. In contrast, no obvious bands were detected for the samples treated with either chitosan-TPP nanoparticles with entrapped siRNA or Lipofectamine 2000-siRNA complexes. The suppression of firefly luciferase expression by those nanoparticles was indeed caused by degradation of firefly luciferase mRNA that was directly related to RNAi activity. These findings therefore further confirming the ability of chitosan-TPP nanoparticles to deliver siRNA into the cells and facilitating siRNA activity in sequence specific manner.

4.4.2 PLGA-chitosan nanoparticles with adsorbed siRNA

Transfection study of siRNA by PLGA-chitosan nanoparticles (PLGA 3A incorporated either with C1113 or C1213) was carried out in HEK 293 cells by varying nanoparticles to siRNA weight ratios. Increasing percentage of gene silencing was detected in this study with the increasing nanoparticles to siRNA weight ratio from 100:1 to 500:1 as would be expected except for nanoparticles to siRNA weight ratio 500:1 of C1213 as shown on figure 4.27. The low gene silencing effect of C1213 with nanoparticles to siRNA weight ratio 500:1 could be expected due to the aggregation since this batch showed difficulty in redispersion in the cell medium. From the graph, it could be seen that chitosan hydrochloride C1213 with higher molecular weight had a higher gene silencing effect than C1113. Rt-PCR analysis further demonstrated that downregulation of luciferase mRNA by PLGA-chitosan nanoparticles with adsorbed siRNA only occurred to some extent (figure 4.27).

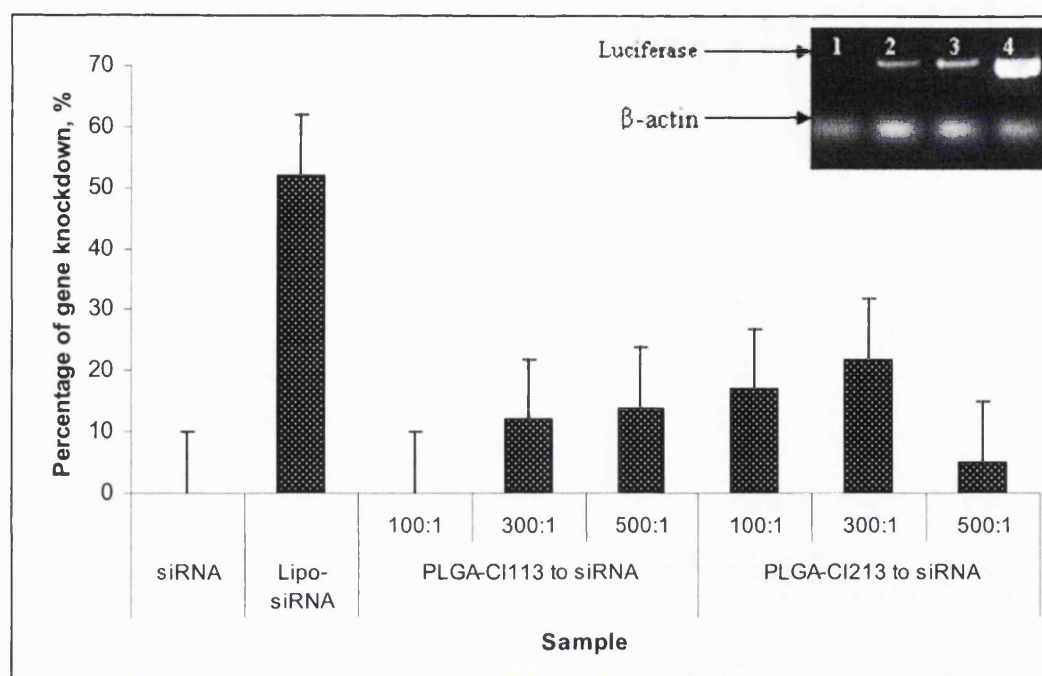


Figure 4.27: Effect of nanoparticles to siRNA weight ratio on percentage of gene knockdown by PLGA-chitosan nanoparticles with adsorbed siRNA targeting against firefly luciferase at 24 h post-transfection in HEK 293 cells (n=3). Gel image shows downregulation of firefly luciferase mRNA by PLGA-chitosan nanoparticles with adsorbed siRNA in HEK 293 cells transiently integrated pGL3 luciferase gene at 24 h post-transfection. Lane 1: Lipofectamine 2000, Lane 2: PLGA-chitosan (CI113) nanoparticles, PLGA-chitosan (CI213) nanoparticles and Lane 4: untreated cells.

4.5 Cytotoxicity assay

4.5.1 Chitosan-siRNA complex and chitosan-TPP nanoparticles associated with siRNA

To investigate the potential cytotoxicity effects of chitosan-siRNA nanoparticulate systems, the cell viability was determined by MTT assays as described in chapter 2. Over 90% average cell viability was observed for chitosan-siRNA complexes and naked siRNA in comparison to untreated cells. However, 18-40% loss of cell viability was observed for siRNA associated with chitosan-TPP nanoparticles

although individual TPP and chitosan solutions did not show any loss of cell viability. The cell viabilities observed with siRNA associated with chitosan-TPP nanoparticles were however, not significantly different between the different chitosan derivatives. Nevertheless, the cell viability for certain siRNA associated with chitosan-TPP formulations was increased at 48 h post-incubation which indicates a new cell growth was observed within this period (Independent Sample *t*-test, $p < 0.05$). From the studied formulations, chitosan G113 showed significant recovery of cells either by adsorbing or incorporating siRNA with chitosan-TPP nanoparticles during the preparation process (chitosan-TPP-siRNA). However, for C1213, significant recovery was observed when adsorbing siRNA onto the chitosan-TPP nanoparticles. In contrast, C1113 showed high recovery of the cells when siRNA was added to the chitosan during the ionic gelation process (figure 4.28). Although only a small improvement of cell viability was observed for other chitosan-TPP formulations, this finding still gave an indication of a transient cytotoxicity effect induces by these formulations.

Although chitosan-TPP nanoparticles associated with siRNA showed higher loss of cell viability than lipofectamine 2000 and chitosan-siRNA complexes, this effect may be due to the 26.5- and 10-fold higher concentration of chitosan added to the cells (5.3 μg) compared to only 0.2 μg of Lipofectamine 2000 and 0.53 μg of chitosan-siRNA complexes, respectively. Moreover, the gene silencing effect of siRNA delivered by chitosan nanoparticles is not thought to be facilitated by damaged cells or compromise the cellular membrane, as no reduction in cell viability was observed after transfecting the cells with pGL3 and pRL-TK vectors by Lipofectamine 2000 (before transfecting cells with siRNA) as determined by MTT assay after 4 h of post-incubation.

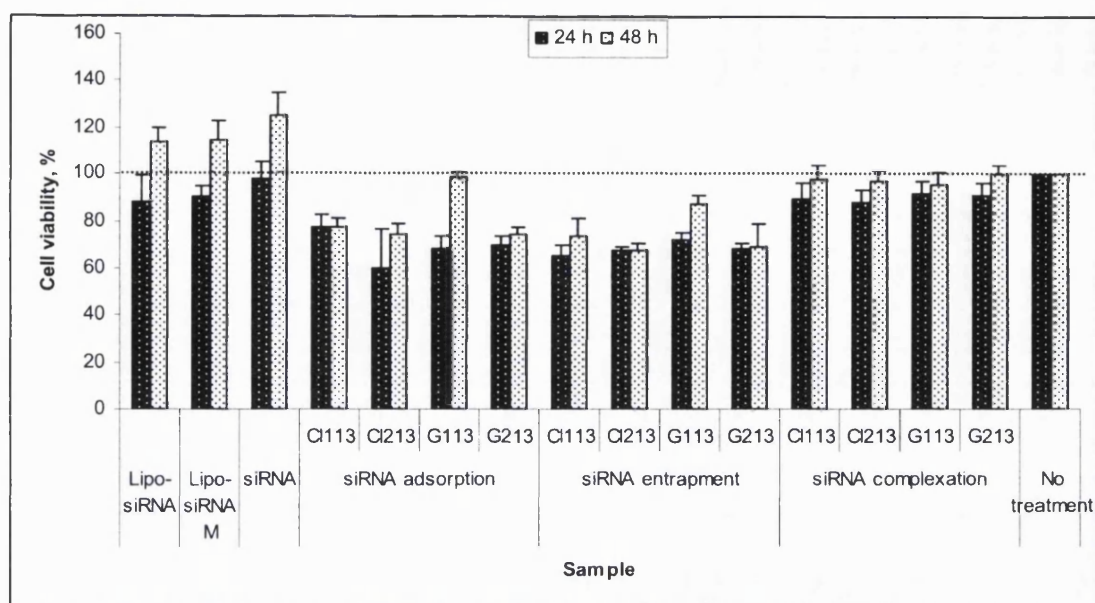


Figure 4.28: Effect of chitosan molecular weight and method of preparation on percentage of cells viability of CHO K1 with cells density of 5×10^3 cell/ well ($n=3$). **Keynotes:** non-treatment cells were used as control, lipo-siRNA= lipofectamine 2000-siRNA complexes and Lipo-siRNA M= Lipofectamine 2000-siRNA mismatch complexes.

4.5.2 PLGA-chitosan nanoparticles with adsorbed siRNA

MTT assay showed that all the formulations of PLGA-chitosan nanoparticles were non toxic to the cells giving percentage cell viability more than 95% for the tested nanoparticles to siRNA weight ratio (100:1 to 500:1) as shown in figure 4.29. They were also relatively less toxic in comparison to Lipofectamine 2000 (85% cell viability). Further analyses were also discovered that no significant difference in cell viability was observed with different molecular weight of chitosan (CI113 or CI213). Although, this system was relatively non-toxic, but its ability to deliver siRNA was frustrating and need further optimisation before it can be used therapeutically.

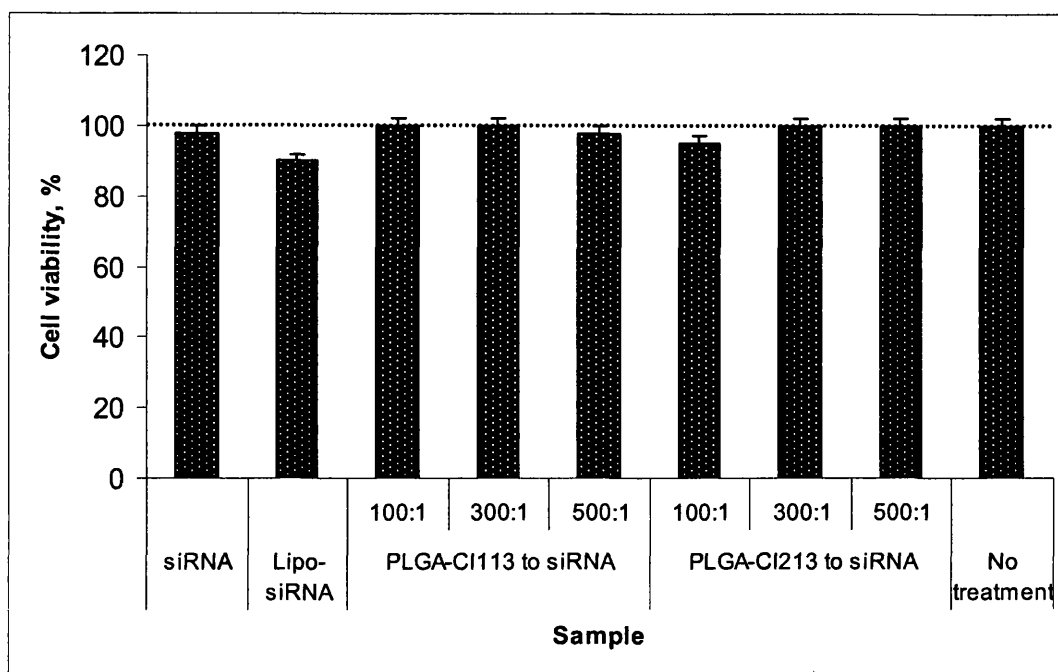


Figure 4.29: Effect of PLGA-chitosan nanoparticles with adsorbed siRNA on percentage of HEK 293 (5×10^3 cell/ well) cell viability ($n=3$). Keynotes: 100:1, 300:1, 500:1 PLGA-CI113 and PLGA-CI213 respectively represent the varying weight ratio of PLGA-chitosan nanoparticles of CI113 and CI213 to siRNA. Lipo-siRNA= Lipofectamine 2000-siRNA complexes.

4.6 Conclusions

Different physical and biological properties of chitosan nanoparticles were obtained with a different method of particle preparation used; simple mixing, ionic gelation and emulsification diffusion method. Optimised ionic gelation method has shown to be the most ideal method to prepare chitosan-based nanoparticles for siRNA delivery which could protect siRNA from nuclease degradation and successfully delivered siRNA into cells with an acceptable cell viability profiles. The particle size of chitosan-TPP nanoparticles less than 500 nm could be obtained by adjusting certain preparation parameters such as stirring rate, chitosan to TPP weight ratio and pH of chitosan solution. In addition, *in-vitro* cell cultured studies revealed that from among the investigated chitosan-based nanoparticles, chitosan-TPP nanoparticles with entrapped siRNA showed the highest efficiency in delivering siRNA (~90% knockdown

of the targeted gene) compared to other systems. Although, PLGA-chitosan nanoparticles were relatively non-toxic to cells, but further optimization is needed to improve its ability to deliver siRNA into cells *in-vitro*, as only ~30% of the targeted gene was knocked-down..

Chapter 5

The use of TAT-peptide to deliver siRNA

The use of TAT-peptide to deliver siRNA

Cell penetrating peptides (CPP), particularly HIV-TAT-derived peptide have been widely used to improve cellular delivery of proteins, peptides and nucleic acids (Brooks *et al.* 2005). Thus, it has emerged as an attractive gene delivery tool. TAT-peptides have been recently employed to deliver pDNA and siRNA into cells through chemical conjugation either to genetic material itself or cationic delivery vehicles such as polycationic polymers (Kleeman *et al.* 2005) as well as liposomes (Torhillin *et al.* 2003). In this study, attempts have been made to develop delivery systems of siRNA based on TAT-peptides by simple complexation or mixing without any involvement of chemical conjugation. TAT-peptide has also been reported to have the ability to translocate materials across the plasma membrane into the cytoplasm and thus bypassing endocytosis and acting as a direct cytosolic delivery vector (Fretz *et al.* 2004). However, recent reports have demonstrated that the uptake of TAT-peptide also involves the endosomal pathway (Shiraishi *et al.* 2004). Therefore, calcium was added to the siRNA-TAT-peptide suspension to enhance transfection efficiency as calcium has been shown to facilitate endosomal release of polycations (Shiraishi *et al.* 2004).

siRNA-TAT peptide was prepared by simple mixing and complexation facilitated through electrostatic interactions between the opposite charges of siRNA and TAT-peptide. The potential of this method has been investigated in terms of physical properties of the complexes (e.g. particle size and surface charge), the ability of TAT-peptide to bind siRNA and subsequently, to transfect cells with siRNA.

The siRNA-TAT peptide complexes had particle sizes between 170 to 193 nm, depending on the concentration of TAT-peptide. The particle surface charge (zeta potential) was also dependent on the concentration of TAT-peptides, ranging from -47 to +34 mV when the concentration was increased from 40 to 200 µg/ml. Complete binding of siRNA and TAT-peptides was achieved with a TAT-peptide to siRNA weight ratio approaching 15:1, as determined by gel retardation assay. *In-vitro* cell culture studies showed that these complexes were able to delivered siRNA into cells with relatively low cytotoxicity. The addition of 6 mM calcium was also found to significantly enhance gene knockdown activities of siRNA-TAT-peptide complexes, almost 2-fold, and was as effective as the commercially available transfection agent, Lipofectamine 2000®. These findings therefore, illustrate that the delivery of siRNA-TAT-peptide complexes might also involve endocytosis as calcium has been reported to facilitate the release of cationic polymer from endosomes (Shiraishi *et al.* 2005).

TAT peptide has been shown to have promising prospects to deliver siRNA by simply mixing siRNA with the TAT-peptide in solution without the need of conjugation. Finally, *in-vitro* cellular delivery of TAT-peptide could be enhanced by the addition of calcium to the complex suspension.

5 The use of TAT-peptide to deliver siRNA

The most important aspect in gene therapy is to specifically deliver genetic materials to the targeted cells. Unfortunately, the unfavourable physicochemical properties of these macromolecules such as large molecular weight, hydrophilicity and the charged nature of these moieties, contributes to the inefficient for those molecules in crossing the cellular membrane and reaching their intracellular target sites (Frezts *et al.* 2004, Lebleu 1996). Attempts to improve cellular delivery of these molecules are being made. Recently, cell penetrating peptides (CPP), particularly TAT-peptide have attracted such enormous attentions due to their ability to translocate genetic materials across the plasma membrane into cytoplasm (Frezts *et al.* 2004, Lindgren *et al.* 2000, Prochiantz 2000). Therefore, TAT-peptides have been employed to deliver DNA and recently siRNA into cells by chemical conjugation either to genetic material itself or nanoparticles (Kleeman *et al.* 2005). In this study, attempts have been made to develop delivery systems for siRNA based on TAT-peptides by simple complexation or mixing without any involvement of chemical conjugation because it needs more complicated methods to get rid of unwanted chemical reactants or even to asses the final products.

5.1 siRNA-TAT-peptide complexes

SiRNA-TAT-peptide complexes were prepared by simply mixing a siRNA solution to the TAT-peptide solution. The complex was formed through electrostatic interaction between negatively charged phosphate groups of siRNA and positively charged amino acid residues of the TAT-peptide. In this experiment, these complexes were analysed as a function of TAT-peptide to siRNA weight ratio.

5.1.1 Particle size

The particle size of siRNA-TAT-peptides was found to be in the nanosize scale with narrow particle size distribution ($PI < 0.5$) dependent on the concentration of TAT-peptide. The size of these complexes was increased from 170 ± 1.2 to 205 ± 0.9 nm as the TAT-peptide to siRNA ratio was increased from 2:1 to 20:1. The results obtained are shown below:

TAT-peptide to siRNA ratio	Z-ave diameter, nm	Polydispersity Index, PI
2:1	170 ±1.2	0.01 ±0.01
4:1	*2645 ±75.5	1.00 ±0.04
5:1	198 ±1.3	0.13 ±0.01
7.5:1	197 ±2.9	0.13 ±0.01
10:1	193 ±1.3	0.11 ±0.00
20:1	205 ±0.9	0.09 ±0.02

Table 5.1: Effect of TAT-peptide to siRNA weight ratio on the particle size of siRNA-TAT-peptide complexes as determined by Malvern System 4700c Submicron particle analyser (n=3). *The particle size was inaccurate due to high polydispersity index.

From the table above, the increase in particle size at the TAT-peptide to siRNA weight ratio of 4:1 to micro-size particles was thought to be due to the formation of aggregates as their particle surface charge was almost neutral (-6.3 ± 0.3 mv) that consequently reduced the electrical repulsions between the particles and therefore these particles may have had more tendency to form aggregates.

5.1.2 Particle surface charge

Besides particle size, particle surface charge of nanoparticles has been reported to be a critical factor in facilitating gene transfer as nanoparticles with a net positive surface charge could easily interact with the negatively charged cell membrane components, principally the phosphate groups of the phospholipids heads, leading to membrane adsorption and subsequently, cellular uptake of the particle into the cells. The particle surface charge of siRNA-TAT-peptide complexes was highly dependent on the TAT-peptide to siRNA ratio and the surface charge could be increased by increasing the concentration of TAT-peptide. The presence of arginine and lysine residues within the 13-mer TAT-peptide has been reported to contribute to the highly cationic charge of the TAT-peptide and they are also responsible in facilitating cellular binding and subsequently, cellular uptake by the cells.

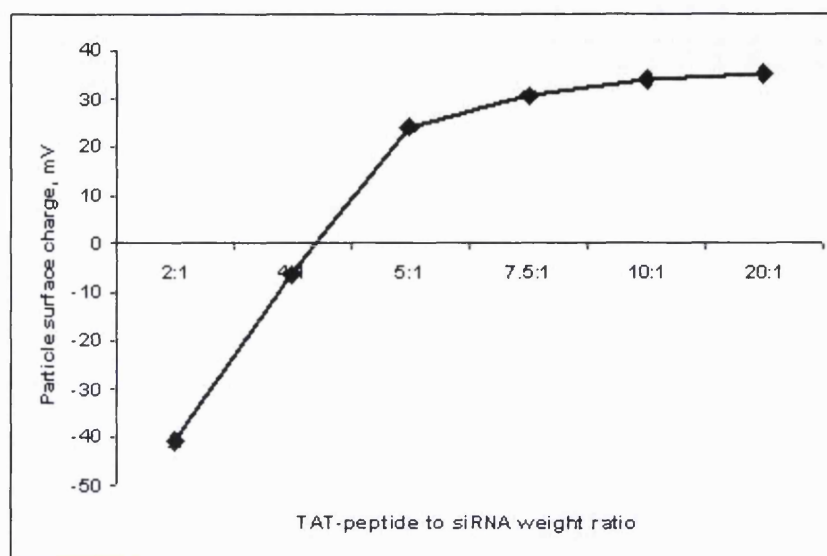


Figure 5.1: Particle surface charge of siRNA-TAT-peptide complexes at different TAT-peptide to siRNA weight ratio (n=3).

5.1.3 siRNA binding efficiency

It has been reported that the cationic nature of the TAT-peptide alone promotes the cellular delivery of very different entities in terms of molecular size, structure and overall physicochemical properties (Brooks *et al.* 2005). As mentioned in the earlier section, the TAT-peptide has been applied to deliver such cargo through chemical conjugation and the most convenient bond formation for this purpose is that of a disulfide bridge between the TAT-peptide and the cargo. In fact, some authors reported a simple mixing of the peptide with an oligonucleotide (Brooks *et al.* 2005, Moulton and Moulton 2003) was unsuccessful due to the lack of cargo internalisation into the cells but sufficient to increase transfection rate of DNA when complexing with pDNA by simple mixing (Brooks *et al.* 2005, Tung *et al.* 2002). This therefore illustrates that covalent linkage may be necessary to facilitate gene transfer in TAT-peptide based cellular delivery systems.

However, full analysis of complexation would be required in order to address properly the potential of this method for delivery of siRNA. In this study, attempts to apply simple complexation as a preparation method for siRNA-TAT-peptide complex was made by determining their binding efficiency at different weight ratios of TAT-

peptide to siRNA (TAT-peptide concentrations were varied from 40 to 200 $\mu\text{g/ml}$ and siRNA concentration was fixed at 20 $\mu\text{g/ml}$) in order to assess its ability in protecting siRNA. In this study, complete binding of siRNA to TAT-peptide was only achieved when the TAT-peptide to siRNA weight ratio was approaching 7.5:1 (TAT-peptide and siRNA concentration of 150 $\mu\text{g/ml}$ and 20 $\mu\text{g/ml}$, respectively) as very little migration of siRNA was observed at this ratio (figure 5.2). Furthermore, heparin was added to the sample at TAT-peptide to siRNA ratio of 20:1 in order to confirm the presence of siRNA in the sample. The heparin was used because it is an anion that could competitively displace siRNA from the TAT-peptide.

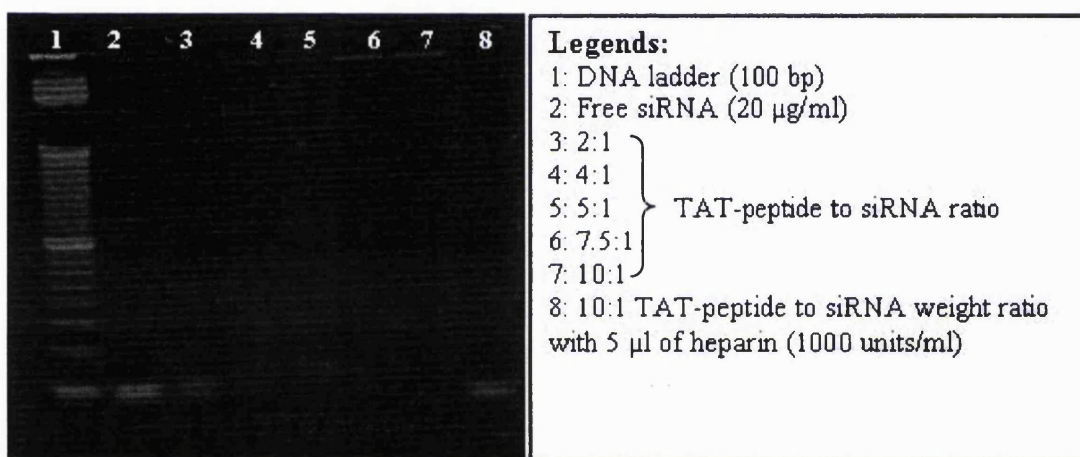


Figure 5.2: Binding efficiency of siRNA to TAT-peptide at different TAT-peptide to siRNA weight ratio as determined by 4% agarose (LMP) gel electrophoresis in TBE buffer, pH 8 containing 0.5 $\mu\text{g/ml}$ ethidium bromide.

5.1.4 siRNA protection by TAT-peptide in the serum

The ability of TAT-peptide complexes to protect siRNA was evaluated by incubating them in DMEM containing 10% FBS for 48 h. A TAT-peptide to siRNA weight ratio of 7.5:1 was chosen as at this ratio, siRNA was completely bound to the TAT-peptide as determined by gel retardation assay. From this study, siRNA was only protected by TAT-peptide from nuclease digestion up to 24 h. Therefore, TAT-peptide has shown to protect siRNA from fully degraded by nuclease activity since naked siRNA was totally degraded even after 10 min incubation in serum.

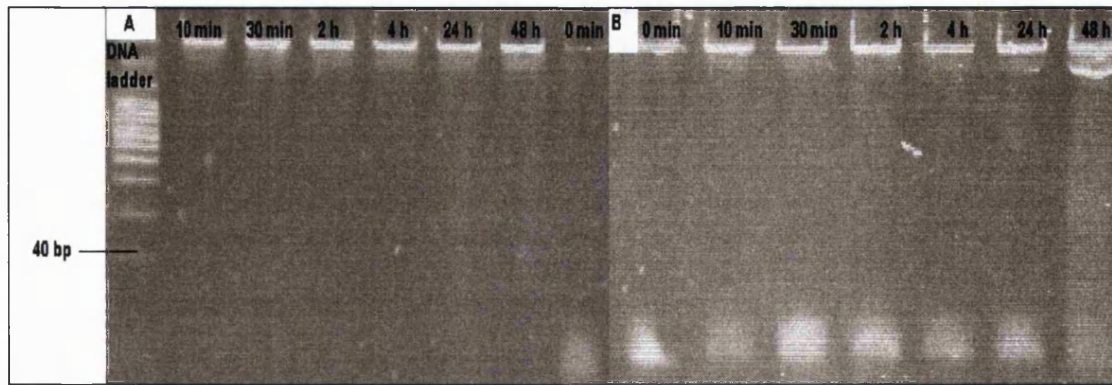


Figure 5.3: Effect of serum (10% FBS) on stability of siRNA alone (A) and siRNA-TAT-peptide complexes (B) with time. The integrity of the siRNA was analysed by 15% polyacrylamide gel containing 7 M urea and TBE (0.089 M Tris base, 0.089 M boric acid, and 2 mM sodium EDTA, pH 8.3) buffer. siRNA bands were visualised under a UV transilluminator after staining for 40 min with a 1:1000 dilution of SYBR-Green II RNA gel stain (Molecular Probes) prepared in DEPC treated water.

5.1.5 Biological activities of siRNA-TAT-peptide complexes

In-vitro study of siRNA-TAT-peptide complexes was first studied in CHO K1 cells with the TAT-peptide to siRNA weight ratio ranging from 5:1 to 25:1. To study biological activities of siRNA-TAT peptide complexes, the cells were first transfected with reporter vectors, pGL3 control and pRL-TK (Promega) and after 4 h of incubation, siRNA targeted to the luciferase pGL3 gene was introduced to the cells either complexed with TAT-peptide or naked in order to evaluate silencing of the expression of the targeted gene. Analysis of the degree of downregulation of expression of the targeted gene expression was carried out by measuring the Relative Light Units (RLU) of luciferase expression using a Dual-Glo assay system kit (Promega) which allows for the measurement of two types of luciferase protein, firefly and renilla luciferase to be measured. This is crucial because by normalising the expression of an experimental (firefly luciferase) to the expression of a control reporter (renilla luciferase) can help to differentiate between specific and non-specific cellular responses such as cell death, inhibition of cell growth and variable initial cell numbers (Technical Manual, Promega).

Additionally, expressing the results as a relative response ratio (RRR) permits the comparison of multiple treatments from the different experiments. However it requires the inclusion of two sets of controls on each plate, a positive control that provides maximal luminescence and a negative control that provides minimal luminescence. Therefore, the RRR can be used to assist in determination of the effect of a new experimental treatment on reporter gene expression within the context of positive and negative control (Technical Manual, Promega).

5.1.5.1 Effect of TAT-peptide to siRNA ratio

TAT-peptide to siRNA weight ratio plays an important role in physical properties of siRNA-TAT-peptide complexes as particle size, surface charge and binding efficiency of siRNA to TAT-peptide were affected by this ratio. The results obtained from this study revealed that 47% downregulation of gene expression were observed when the cells were treated with the complex at the TAT-peptide to siRNA ratio of 20:1. Ratios less than 20:1 seemingly had no great impact on gene expression as only $4.39\% \pm 5.22$ and $12.67\% \pm 11.1$ of gene downregulation were observed for the cells treated with 5:1 and 15:1 TAT-peptide to siRNA weight ratios, respectively. The minimal effect of TAT-peptide to siRNA of 5:1 weight ratio was expected because of the suboptimal binding of siRNA to the TAT-peptide as shown in figure 5.2, leading to the degradation of siRNA due to the exposure of the siRNA towards nuclease.

On the other hand, minimal effects of gene silencing for TAT-peptide to siRNA weight ratio of 15:1 were also observed although at this ratio, complete binding of siRNA to the TAT-peptide was achieved. In this case, the suboptimal effects might be due to the minimal exposure of arginine residues of the TAT-peptide. The guanidium group of the arginine side chain was shown to be more potent in mediating cellular uptake than other cationic groups such as those on lysine, histidine or ornithines (Brooks *et al.* 2005, Mitchell *et al.* 2000) and deletion of a single arginine residue severely reduced internalisation (Silhol *et al.* 2002, Werder *et al.* 2000, Vivès *et al.* 1997). At this ratio (15:1), it was thought that the exposure level of arginine residues at the molecular surface of the complex was limited since they were bound with the siRNA to form a complex. Therefore, they were unable to deliver siRNA efficiently. In addition, no significant downregulation of gene expression was observed after 24 h of incubation when the ratio was increased to 25:1 as only 9% of gene downregulation was

obtained. Furthermore, incubating the treated cells for a longer period (48 h) apparently did not increase the silencing effect of those siRNA-TAT-peptide complexes.

5.1.5.2 Effect of cell lines

The ability of the TAT-peptide to successfully deliver siRNA in various cells has been reported previously in various literatures such as human lung epithelial cell line, A549 (Kleeman *et al.* 2005), human ovarian carcinoma cell line, OVCAR-3 (Fretz *et al.* 2004) and HeLa cells (Silhol *et al.* 2002). Therefore, in this study, another type of cell line was used to determine the effects of cells line on biological activities of siRNA complexed to TAT-peptide. The same transfection protocols were carried out in HEK 293 cells and the results showed that only 18% downregulation of gene expression was obtained when the cells were treated with siRNA-TAT-peptide complex of 20:1 weight ratio (TAT-peptide to siRNA). Indeed, there was no significant difference on gene silencing activities of siRNA-TAT-peptide complexes when the TAT-peptide to siRNA weight ratio was increased from 5:1 to 20:1. These results demonstrated that the ability of TAT-peptide to deliver siRNA was dependent on the cell lines (partially cell specific) as different cell lines have different characteristics and cellular surface components. The mechanism of the internalization of the TAT-peptides however, is not completely understood but the peptides show a strong ionic interaction with sulphated glycosaminoclycans and with the phospholipid head groups at the membrane surface and subsequently, internalisation into the cells.

5.1.5.3 Effect of calcium

TAT-peptide has been reported to show the ability to translocate material across the plasma membrane into the cytoplasm and thus it could bypass endocytosis and acts as a direct cytosolic delivery vector. However, recent reports have demonstrated that the uptake of TAT-peptide also involves the endosomal pathway. It has been reported that calcium could enhance transfection efficiency of cell penetrating peptides and several other polycation/DNA complexes (e.g. protein Histone H1) presumably by facilitating endosomal release (Shiraishi *et al.* 2005, Haberland *et al.* 1999, Bottger *et al.* 1998). The effects of calcium on biological activities of siRNA-TAT-peptide complexes were therefore investigated in the HEK 293 cells by adding various concentrations of calcium

chloride, ranging from 3 to 6 mM to the complex suspension (20:1 TAT-peptide to siRNA ratio) before adding to the cells. The results obtained are shown below:

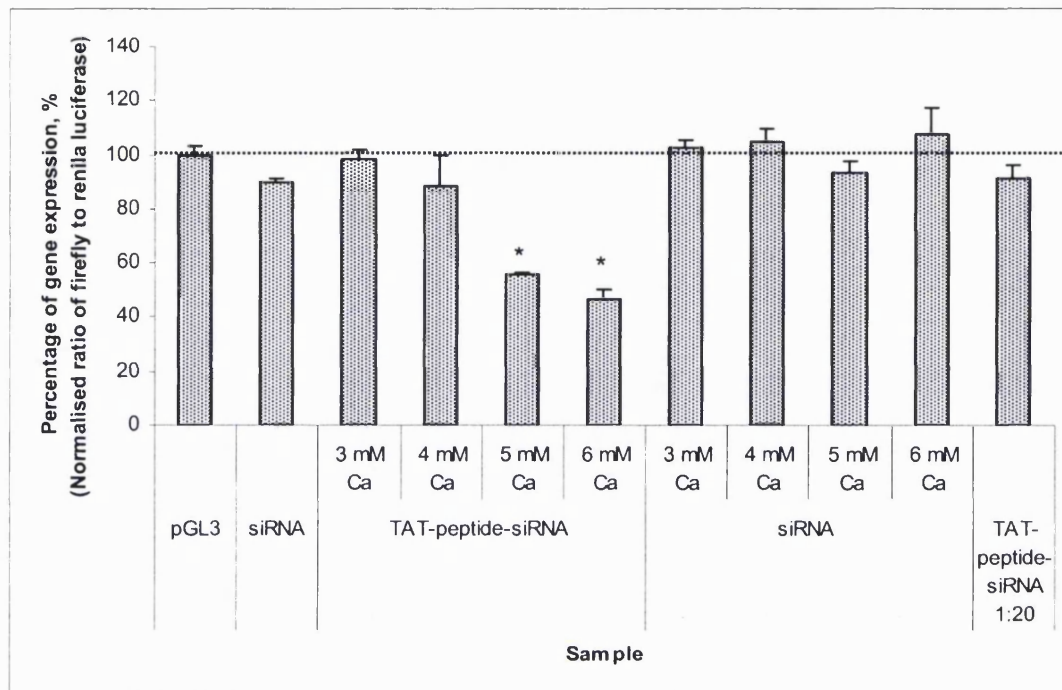


Figure 5.4: Effect of calcium on biological activities of siRNA-TAT-peptide complexes in HEK 293 cell with cells density of 5×10^3 cell/ well at 24 h post-transfection (n=3). Keynotes: pGL3 alone= without siRNA treatment (negative control). * The difference between the addition of calcium at 5 or 6 mM to the suspension of TAT-peptide-siRNA complexes and TAT-peptide-siRNA complexes (without calcium) was significant ($p < 0.05$).

From the graph, the addition of calcium above 4 mM could enhance downregulation of luciferase gene expression and the effect was increased with the increase of calcium molar concentration. 16.5 ± 2.7 , 42.1 ± 8.8 and 53.0 ± 18.2 % of targeted gene knockdown was gained when the cells were treated with siRNA-TAT-peptide complexes containing 4, 5 and 6 mM of calcium chloride, respectively. Furthermore, the gene silencing activity of the siRNA-TAT-peptide was 1.7-, 4.5- and 5.7-fold increased in the presence of 4, 5 and 6 mM calcium chloride respectively compared to siRNA alone or 1.4-, 3.7- and 4.7-fold increased in comparison to TAT-peptide-siRNA complexes without the addition of calcium. In contrast, addition of

calcium into the siRNA solution did not significantly induce gene downregulation and a higher calcium molar concentration than 6 mM did not further increase the gene silencing effect of the siRNA-TAT-peptide complexes as at this point, cell viability started to decrease significantly. These results demonstrate that calcium as low as 5 and 6 mM (one way ANOVA, followed by Post hoc comparable test, $p < 0.05$) could significantly enhance the effect of siRNA complexed to TAT-peptide presumably by facilitating endosomal escape of these complexes after cell entry. However, formation of co-precipitates between calcium ions and TAT-peptide complexes by reacting with phosphate ions in the medium which subsequently leading to their uptake into the cells (Haberland *et al.* 1999) could not be absolutely excluded and need further investigations.

Additionally, further analysis showed that the addition of 6 mM calcium to the siRNA-TAT-peptide complexes was as effective as siRNA complexed to the commercially transfection agent, siRNA-Lipofectamine 2000 complexes in silencing the expression of the luciferase gene. The effect of siRNA-TAT-peptide complexes was also specific to the targeted gene as no significant reduction of expression was observed for mismatch siRNA complexed to Lipofectamine 2000 as shown below:

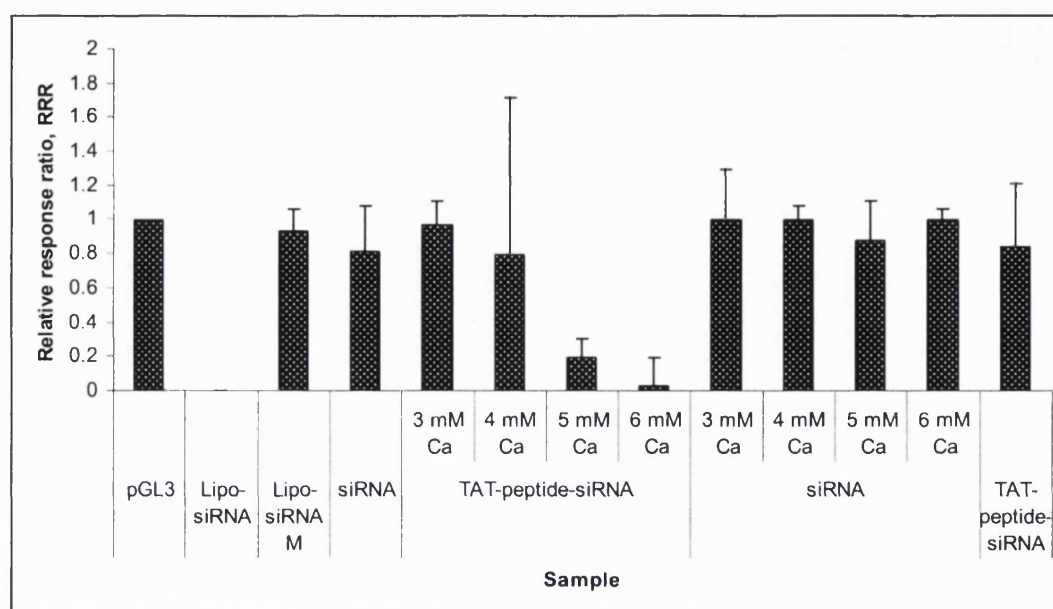


Figure 5.5: Comparison of gene silencing efficiency of siRNA-TAT-peptide complexes with increasing molar ratios of calcium compared to the negative control of siRNA-Lipofectamine 2000 complexes (Lipo-siRNA) and positive control of without siRNA treatment (pGL3) (n=3). Keynote: Lipo-siRNA M= Lipofectamine 2000-siRNA mismatch complexes, TAT-peptide-siRNA=siRNA-TAT-peptide-complexes at a TAT-peptide to siRNA ratio 20:1.

These findings therefore illustrating that the delivery of siRNA-TAT-peptide complexes might also involve endocytosis pathway as calcium has been reported to facilitate the release of cationic polymer from endosomes (Shiraishi *et al.* 2005).

5.1.6 Cytotoxicity assays of siRNA-TAT-peptide complexesA-TAT-peptide complexes

No significant loss of cells or inhibition of cell growth were observed for the cells treated with siRNA-TAT-peptide complexes in both types of cells except TAT-peptide to siRNA weight ratio of 15:1 (this was confirmed by statistical analysis, one way ANOVA ($p < 0.05$), followed by Post hoc multiple comparison test), illustrating these complexes were relatively non-toxic to the cells and these findings were independent on TAT-peptide to siRNA weight ratio (figure 5.6). Additionally, no sign of cell death was observed when the treated cells were incubated for 48 h (one way

ANOVA, $F(7)=2.101$, $p=0.73$). Perhaps, the observed increase cell viability is likely due to cell growth although it is only statistically significant for Lipofectamine-2000-siRNA complexes (Independent Sample T-test, $p<0.05$).

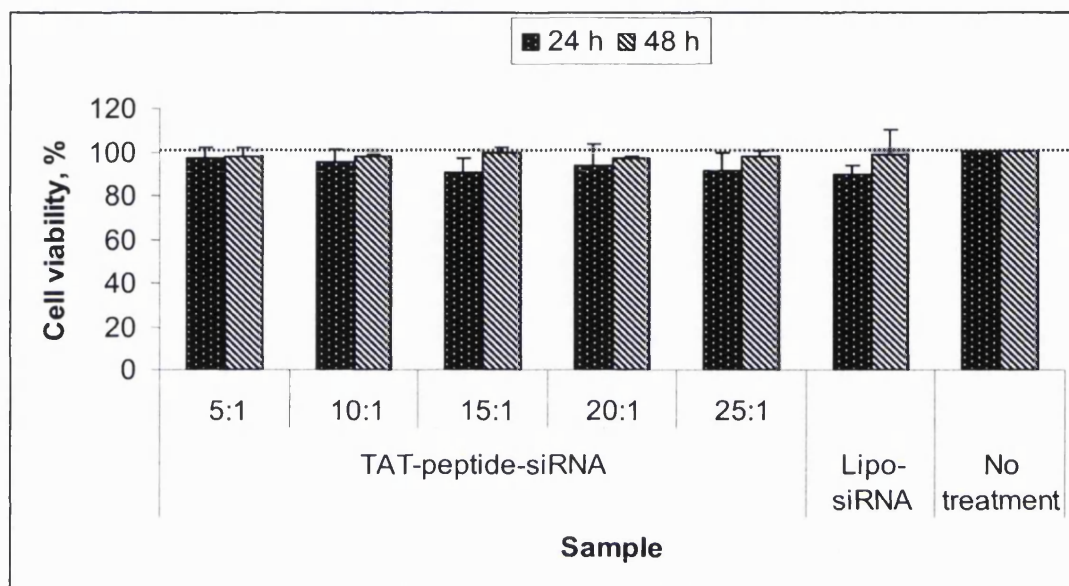


Figure 5.6: Effect of siRNA-TAT-peptide complexes at different TAT-peptide to siRNA ratio on percentage of CHO K1 cells viability 5×10^3 cell/ well after 24 and 48 h of post-incubation (n=6). Keynote: Lipo-siRNA= Lipofectamine 2000 siRNA complexes.

Furthermore, calcium as a cellular delivery enhancer for the siRNA-TAT-peptide was also assessed for its effects on the cells. To investigate this effect, calcium (3 to 6 mM) was added to siRNA-TAT-peptide complexes and naked siRNA before treating the cells. It was found that the addition of calcium up to 6 mM showed no significant loss of cells or inhibition of cell growth (one way Anova and $F(15)=0.997$, $p=0.481$).

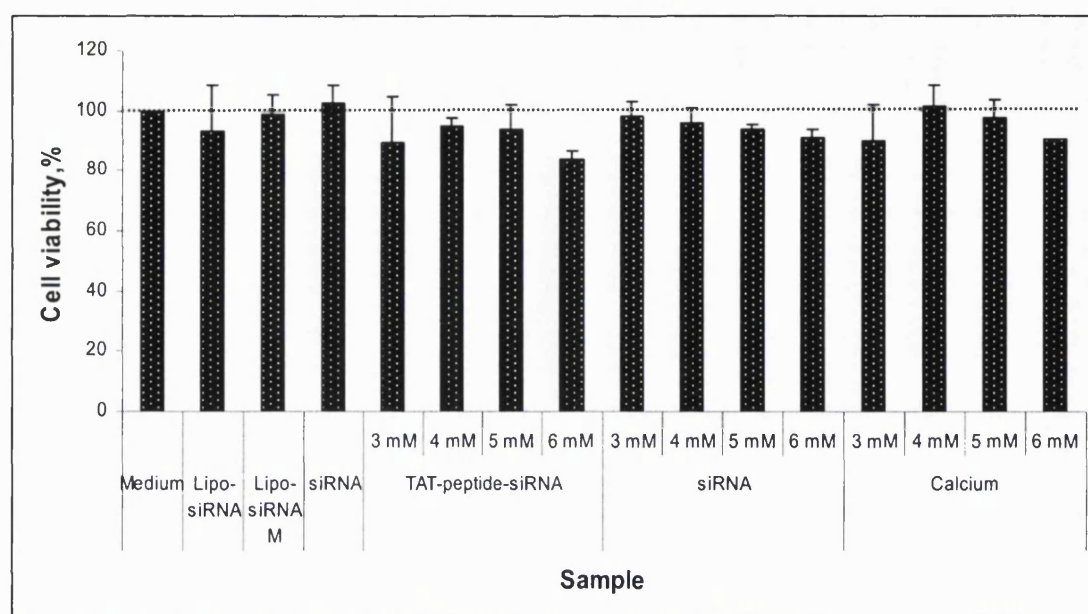


Figure 5.7: Effect of calcium at various molar concentrations on percentage of HEK 293 cell viability (5×10^3 cell/ well) ($n=3$). Keynotes: Lipo-siRNA= Lipofectamine 2000 siRNA complexes, Lipo-siRNA M= Lipofectamine 2000-siRNA mismatch complexes, medium=untreated cells (control).

However, an earlier study that was carried out in order to determine the optimal concentration of calcium as a possible cellular delivery enhancer agent discovered that the maximum desirable molar concentration of calcium was 6 mM as at molar concentrations higher than this point, significant reduction of cell viability was observed. The loss of cells was thought to be due to the osmotic effect induced by salt that led to the cellular death.

5.2 Conclusions

Simple complexation method, through mixing, enables the TAT-peptide to deliver siRNA without the use of chemical conjugation. TAT-peptide to siRNA weight ratio was found to affect both physical (particle size, surface charge and siRNA binding capacity) and biological properties (delivering siRNA into cells) of resultant TAT-peptide-siRNA complexes. Additionally, calcium could be used as an effective enhancer for *in-vitro* delivery of siRNA-TAT-peptide complexes and the system has been shown

to be a relatively non- toxic to the cells. Therefore, this system has a promising future to be used as a delivery system for a therapeutic siRNA.

Chapter 6
***In-vitro* investigation of chitosan-TPP
nanoparticles with entrapped siRNA by targeting
p38-MAPK gene**

***In-vitro* investigation of chitosan-TPP nanoparticles with entrapped siRNA by targeting p38-MAPK gene**

Since discovery of siRNA a decade ago, siRNA has been subjected to intensive investigation and further development for the treatment of several diseases. Many lung diseases like asthma and chronic obstructive pulmonary disease (COPD) have been reported to be related to inflammatory responses to injury or certain stimuli. The mitogenic-activated protein kinase (MAPK); p38 has been linked to inflammatory cytokine production and cell death following cellular stress and it may be involved in pathogenesis of lung diseases. Inhibition of p38 α MAPK and its signalling have therefore been investigated as a strategy in the treatment of these diseases. One approach to this inhibition is to use siRNA to silence the targeted gene.

In this study, siRNA MAPK14 was used to target the p38 α gene. To facilitate siRNA transfer to cells, chitosan-TPP nanoparticles were investigated as a vector. These particles were prepared by ionic gelation using TPP ions and siRNA was entrapped into the particles by adding siRNA together with the ions during the gelation process. These particles were then subjected to serum protection assays as well as further transfection and toxicity studies in J774A.1 macrophage cells by using real-time RT-PCR and the MTT assay, respectively.

The results obtained showed that chitosan-TPP nanoparticles were able to protect siRNA from nuclease activity up to 48 h after incubation in 50% v/v mouse serum. Transfection studies also revealed that chitosan-TPP nanoparticles could deliver siRNA to cells and allow siRNA to exert its effect for up to 72 h. Chitosan-TPP nanoparticles with entrapped siRNA (10 nM) was observed to knockdown 40% \pm 1.3 of the targeted gene expression at 24 h post-transfection and this was further increased to 80% \pm 17.7 at 72 h post-transfection. The system was also found to be less toxic than Lipofectmaine 2000[®] as determined by the MTT assay in J774A.1 and L929 cells.

Chitosan-TPP nanoparticles have been illustrated to be a better delivery system than a commercially available transfection agent, Lipofectamine 2000[®] in transfecting cells with siRNA and this system also has a relatively lower cytotoxicity. Chitosan-TPP nanoparticles therefore, have a great potential as therapeutic delivery systems for siRNA.

6 *In-vitro* investigation targeting p38 MAPK

Further *in-vitro* investigation has been carried out by targeting p38 mitogenic activated protein kinases or MAPKs. MAPKs are a group of cytoplasmic serine threonine kinases which are involved in cell recognition and responses to extracellular stimuli (Tai *et al.* 2004). They have also been reported to play a vital role in the regulation of cell activities; from gene expression, mitosis, metabolism, cell survival and apoptosis as well as cell differentiation (Roux and Blenis 2004). There are five distinct groups of MAPKs that have been characterized in mammals: extracellular signal-regulated kinases (ERKs) 1 and 2 (ERK1/2), c-Jun amino-terminal kinases (JNKs) 1, 2, and 3, p38 isoforms α , β , γ , and δ , ERKs 3 and 4, and ERK5. From among these groups only ERKs, JNKs and p38 have been extensively studied to date (Chen and Khalil 2006).

Activation of ERK 1 or 2 has been associated with cell survival and proliferation whereas JNK and p38 MAPK are linked to cell apoptosis (Luppi *et al.* 2005, Moreno-Manzano *et al.* 1999) whereby cell fate is regulated by a balance between these three MAPK kinase pathways (Luppi *et al.* 2005, Makin and Dive 2001). Although the activation of these pathways could be induced by the same stimuli, the ERKs are mainly activated by growth factors. Meanwhile, JNKs and p38 are preferentially induced by stress-inducing agents (osmotic shock and ionizing radiation) and proinflammatory cytokines (Roux and Blenis 2004, Victoria Sanz-Moreno *et al.* 2003, Pearson *et al.* 2001, Whitmarsh and Davis 1996).

The p38 MAPK pathway has been targeted in this work because of its vital role in orchestrating inflammation in diseases like arthritis, cystic fibrosis (CF) (Raia *et al.* 2005), chronic obstructive pulmonary disease (COPD) (Luppi *et al.* 2005) and hypertension (Ono *et al.* 2006). Various stimuli (cellular stresses) that act on the cell may cause activation of p38 MAPK by dual phosphorylation of tyrosine and threonine. This phosphorylation is catalyzed by MAPK kinases (MKKs) *via* activation of MAPK kinase kinases (MAP3K) which in turn phosphorylate and activate the MKKs (Newton and Holden 2006) as shown in figure 6.1. Once activated, p38 is translocated to the nucleus where it phosphorylates and activates different transcription factors and transactivates target genes including a key regulator of proinflammatory cytokines' transcriptional machinery, transcription factor AP-1 (Dong *et al.* 2006).

There are four members of the p38 MAPK family. p38 α however is the most studied and relevant kinase involved in inflammatory responses (Nath *et al.* 2006, Kumar *et al.* 2003). It has been described that p38 α is activated in macrophages, epithelia or endothelia cells which are involved in cell signalling and mediating inflammatory responses by phosphorylating several cellular targets, including cytosolic phospholipase A2, the microtubule-associated protein Tau, and the transcription factors ATF1 and -2, MEF2A, Sap-1, Elk-1, NF- κ B, Ets-1, and p53 (Roux and Blenis 2004). From among those cellular targets, MEF2C, AFT-2 and Elk-1 have been reported to be involved in initiating c-Fos and c-Jun; constituent proteins of AP-1 which therefore, suggests that the p38 MAPK pathway might be involved in the activation of AP-1 and subsequently inflammation.

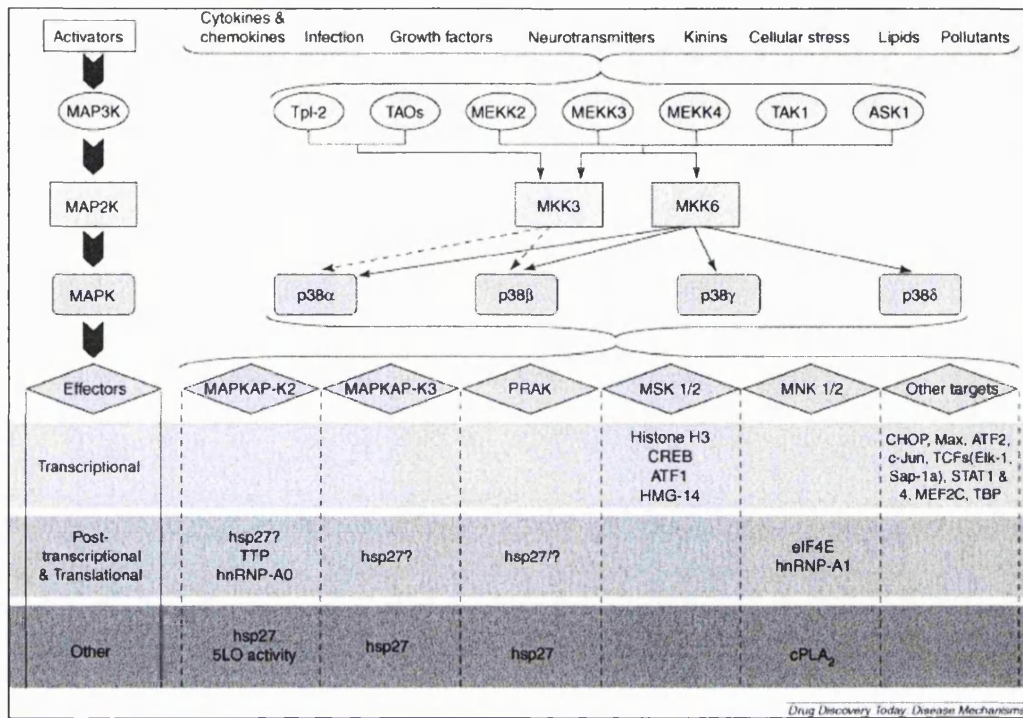


Figure 6.1: The p38 mitogen activated protein (MAP) kinase (MAPK) activation cascade. This schematic diagram shows activation pathways which leads to the activation of p38 MAPK isoforms. Various stimuli or stresses that act on cells may cause activation of p38 MAPK isoforms through the sequential activation of the MAP kinase kinases (MAP3K), which phosphorylate and activate the MAP kinase kinases (MAP2K). These in turn phosphorylate the p38 MAPKs, which on activation, are able to phosphorylate several targets including downstream kinases as well as other effectors (courtesy of Newton and Holden 2006). Keynotes: ARE, AU response element; ASK1, apoptosis signal-regulating kinase 1; ATF, activating transcription factor; CHOP, CCAAT/enhancer-binding protein (C/EBP) homologous protein; cPLA₂, cytosolic phospholipase A₂; CREB, cyclic AMP response element binding protein; eIF4E, eukaryotic initiation factor 4E; HMG-14, high mobility group 14; hsp27, heat shock protein 27; MAPK, mitogen-activated protein kinase; MAP2K, mitogen-activated protein kinase kinase; MAP3K, mitogen-activated protein kinase kinase kinase; MAPKAP-K (or MK), MAPK-activated protein kinase; MEF2C, myocyte-specific enhancer binding factor 2C; MEKK, mitogen-activated protein kinase/extracellular protein kinase kinase kinase; MKK, MAP kinase kinase; MNK, MAPK-interacting kinase; MSK, mitogen- and stress-activated protein kinase; PRAK, p38-related/activated protein kinase; STAT, signal transducer and activator of transcription; TAK, TGFβ activated kinase; TAOs, thousand and one kinases; TBP, TATA-binding protein; TTP, Tristetraprolin, TCF, ternary complex factor; 5LO, 5-lipoxygenase; hnRNP, heterogenous nuclear ribonuclear protein.

The role of p38 MAPK in several disease models has been investigated by inhibiting the p38 MAPK pathway. A second generation p38 MAPK inhibitor, SB 203580 has been widely used to investigate this. This inhibitor for example has been used to show the involvement of p38 MAPK in mediating the release of TNF- α and IL-1 β and it has been reported to reduce the pulmonary inflammatory response after cardiopulmonary bypass (Dong *et al.* 2006). In different study, Nash and Heuertz (2005) reported that the inhibition of p38 MAPK by SD203580 could offer protection in the lungs from both neutrophil influx as well as protein leakage associated with acute lung injury. Other types of p38 MAPK inhibitor are an orally active p38 MAPK inhibitor, SD282 that has been used in a chronic model of allergen exposure (Nath *et al.* 2006) and ODN in single allergen exposure model (Duan *et al.* 2005). These findings support fact notion that p38 MAPK is involved in the pathogenesis of asthma. In addition, the inhibition of p38 MAPK has also been shown to be efficacious in several other disease models including CF, arthritis, septic shock and myocardial infarction.

Due to increasing development in RNAi based technology, siRNA has also been investigated for utilisation in the inhibition of p38 MAP kinase. The siRNA that has been used in this study is MAPK14 siRNA which targets p38 MAP kinase in order to treat various lung diseases related to inflammation, for example acute lung injury and acute respiratory distress syndrome. The sequence of siRNA MAPK14 (RNA-TEC, Belgium) that has been used is 5-GGGAGGUGCCCGAACGAUAUIdT-3 and 3-idTUCCCUCCACGGGCUUGCUAU-5 for sense and antisense strands, respectively.

A previous study that has been done by Moschos (2006) in male BALB/c mice reported that p38 α MAPK gene expression was detected in most of the body parts including small intestine, liver, heart, eyes, lung and kidneys. On the other hand, up to 45% of gene knockdown was observed when MAPK14 siRNA was administered to mice and the activity was found to be dose-dependent. In addition, no immunological response to MAPK14 siRNA constructs was detected *in-vivo* as no effect upon relevant protein level (e.g. IFN α , TNF α) were observed at 6, 12 and 24 h. Further study using TAT-peptide (YGRKKRRQRRK) to deliver siRNA MAPK14 revealed that no significant improvement in both knockdown efficiency and duration of action up to 24 h between naked and conjugate siRNA MAPK14 (Moschos 2006). These observations emphasise that the need for better vectors is paramount to enable siRNA MAPK14 to be used therapeutically.

6.1 Chitosan-TPP nanoparticles as a vector

In this study, chitosan was chosen to deliver siRNA MAPK14 due to its advantages over PEI such as its excellent biodegradability and biocompatibility properties. Earlier *in-vitro* studies have shown that only chitosan with entrapped siRNA made from chitosan G213 and C1113 had the capability to delivered siRNA into mammalian cells with a high knockdown of luciferase gene expression. Therefore, only these chitosans were used for further study using MAPK14 siRNA.

6.1.1 Particle size and surface charge

The same method as in the previous studies has been used to prepare MAPK14 siRNA whereby siRNA is entrapped into chitosan-TPP nanoparticles. The method used was ionic gelation with a chitosan to TPP ions weight ratio 5:1 and chitosan was dissolved in acetate buffer (0.1 M) at pH 4.5. The yielded nanoparticles had a particle size less than 150 nm dependent on the type of chitosan used (either chitosan G213 or C1113). These particles were positively charged and siRNA was completely bound to the chitosan nanoparticles as determined by Zetamaster[®] measurement and gel retardation assay. The size and surface charge of these nanoparticles are shown below:

Chitosan	Z-average, nm SD (\pm)	Polydispersity index, PI SD (\pm)	Surface charge, mV SD (\pm)
G213	108.7 \pm 0.9	0.250 \pm 0.002	+19.9 \pm 1.4
C1113	148.7 \pm 0.7	0.249 \pm 0.010	+27.6 \pm 2.7

Table 6.1: Particle size and surface charge of chitosan-TPP nanoparticles with entrapped siRNA, n=9.

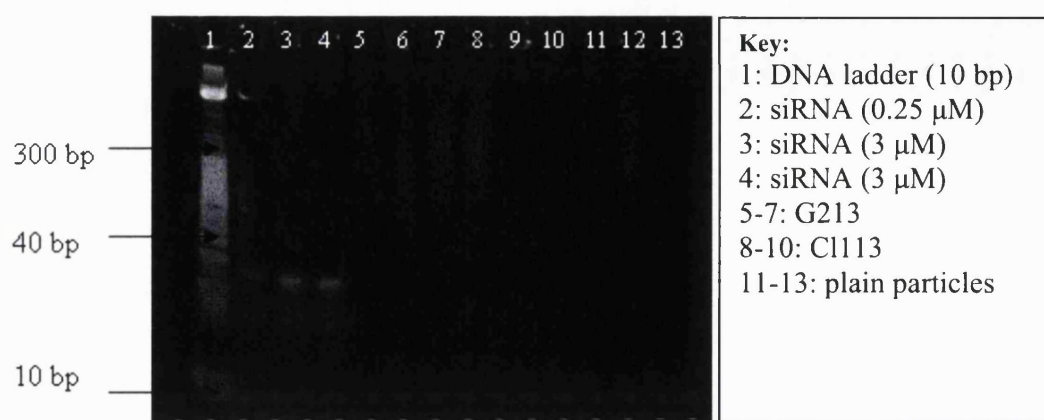


Figure 6.2: siRNA binding efficiency to the chitosan-TPP nanoparticles by gel retardation assay using 20% polyacrylamide gel in TBE buffer (pH 8), followed by 40 min staining with Sybr Gold (Invitrogen).

6.1.2 Serum stability

Before any *in-vitro* studies were carried out with siRNA MAPK14, a series of stability testing in serum was performed to determine the ability of these vector systems to protect siRNA from nuclease activity. For this analysis, siRNA entrapped in chitosan-TPP nanoparticles was incubated in 50% v/v final concentration mouse serum for 72 h at 37 °C. At each pre-determined time, 20 μl of the mixture was taken and transferred to a new centrifuge tube, followed by centrifugation thrice at 22 000 X g for 30 min. Each sample from the chitosan-TPP nanoparticles with entrapped siRNA was also treated with 2 μl chitosanase (chitosanase from *Streptomyces* sp.15 unit/ mg protein, Sigma) to degrade and in turn to release siRNA from the particles before electrophoresis at 150 mV for 1 h using polyacrylamide-TBE gel (20%, Invitrogen, UK). After electrophoresis, the gel was stained with Sybr Gold (Invitrogen, UK) and viewed under UV light at 365 nm.

The results obtained from this study showed that siRNA entrapped in chitosan-TPP nanoparticles was protected from nuclease activity for up to 48 h compared to naked siRNA which had been degraded after 10 min incubation in mouse serum. In fact, more than 50% of intact siRNA could still be recovered from the chitosan-TPP nanoparticles made from chitosan Cl113 and less than 10% recovered from chitosan G213 after 24 h incubation in mouse serum as shown below (figure 6.3):

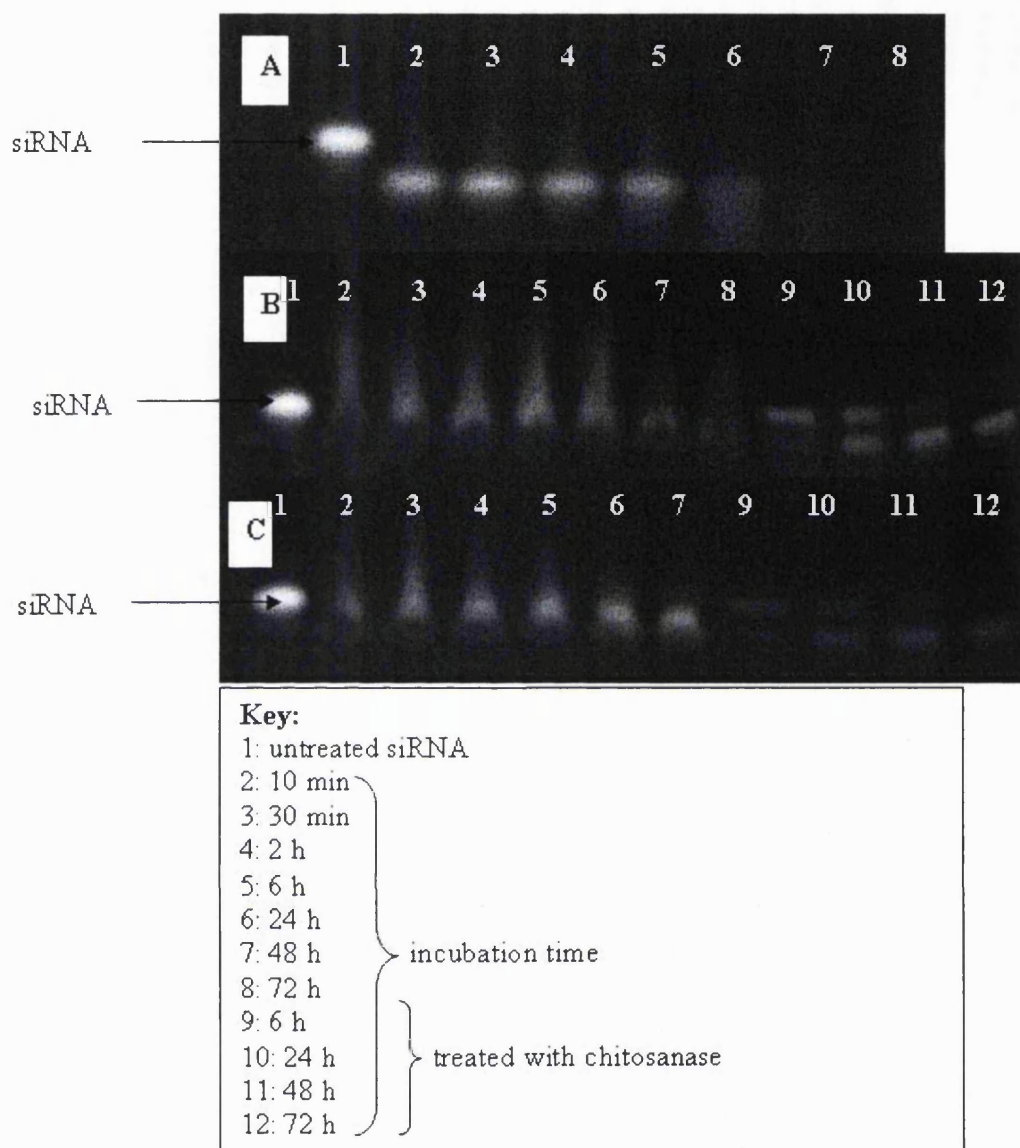


Figure 6.3: siRNA stability in 50% v/v mouse serum. A: naked siRNA, B: siRNA entrapped in chitosan-TPP nanoparticles (Cl113) and C: siRNA entrapped in chitosan-TPP nanoparticles (G213).

This experiment therefore, illustrated that chitosan Cl113 was able to protect siRNA more efficiently than chitosan G213 from nuclease degradation. These findings were also corresponded with a previous *in-vitro* cell cultured study that was done using an encoded siRNA firefly luciferase gene where gene silencing activity of siRNA delivered by chitosan-TPP nanoparticles prepared from Cl113 showed a sustained effect of gene knockdown up to 48 h compared to a more transient effect mediated by chitosan

G213. A high gene silencing using chitosan G213 was only detected up to 24 h post transfection which was thought to be due to the observation that more than 90% of siRNA was degraded by nuclease activity at 48 h.

6.1.3 *In-vitro* study

The ability of the chitosan-TPP nanoparticles to mediate RNA interference in primary cells was evaluated in J774.A.1 cells line. This cell line is a macrophage cell type from female adult BALB/cN mice which shows antibody dependent phagocytosis (American type cell collection) and plays an important role in inflammatory as well as viral diseases, and a suitable target for RNAi therapies (Howard *et al.* 2006). Only chitosan-TPP nanoparticles prepared from chitosan C1113 were used in this *in-vitro* study because it has been shown to be superior over chitosan G213 in protecting siRNA from nuclease activity. Two doses were investigated in this experiment (1 and 10 nM) and expression of the targeted gene was monitored for up to 72 h using RT-real-time PCR.

For this work, cells were seeded and grown 24 h before transfection in 96-well plate format with a cell number of 1×10^4 in OptiMEM reduced serum (Invitrogen) containing 5% of FCS. On the day of transfection, 100 μ l of naked siRNA solution or chitosan-TPP nanoparticles with entrapped siRNA suspension was added to the cells in triplicate and incubated at 37°C with 5% CO₂ in a humid environment for 12 h before the medium was replaced with fresh growth medium. At each pre-determined time-point, total RNA was extracted using RNeasy mini column kits (Qiagen, UK) according to the manufacturer's instructions. Lipofectamine 2000 (Invitrogen, UK)-siRNA complexes and cell media were used as positive and negative controls, respectively for each experiment. Each formulation was tested in three separate experiments.

Gene knockdown efficiency of siRNA either alone or transfected with chitosan-TPP nanoparticles/ Lipofectamine-2000 was analysed by quantitative real time RT-PCR (Applied Biosystems AB 7500 thermal cyclers) using primers and taqman probes. In addition, 18S rRNA was used as an internal standard. In this experiment, cDNA was generated from RNA extract (0.5 μ g in RNase free water up to 19.25 μ l) using random hexamers as primers by mixing it with the following components (all reagents from Applied Biosystems) to give a final volume of 50 μ l: 5 μ l 10X RT buffer, 11 μ l MgCl₂

(10 mM), 10 μ l dNTP (10 mM), 2.5 μ l random hexamers (50 mM), 1 μ l RNase inhibitors (40 units/ μ l) and 1.25 μ l MultiScribeTM (50 units/ μ l). The RT reaction was performed at 25°C for 10 min, followed by 48°C for 30 min and 95°C for 2 min. On the other hand, quantitative real time PCR was performed using an Assay on Demand (AOD, Taqman Gene Expression Assay for mouse MAPK14, Applied Biosystems) in addition to the ubiquitously expressed control (Eukaryotic 18S rRNA endogenous control (VIC/ TAMRA probe, Applied Biosystem). Briefly, the sample was prepared by mixing 3 μ l of cDNA (2.5 ng/ μ l) with 12.5 μ l Universal Master Mix (2x), 1.25 μ l AOD (20x), 1.25 μ l 18 S (20x) and 7 μ l nuclease-free water (Promega).

The results obtained showed that a significant gene knockdown was observed for the cells treated with siRNA delivered by chitosan-TPP nanoparticles at 1 nM 24 h post-transfection where only 60% \pm 1.3 of the targeted gene was expressed compared to 90% \pm 33.6 and 85% \pm 6.14 for naked siRNA and Lipofectamine-siRNA complexes, respectively (oneway ANOVA, followed by Post hoc multiple comparison test, $p < 0.05$). In contrast, no significant difference in gene expression was detected between all the formulations with the dose of 10 nM although the cells treated with chitosan-TPP-siRNA nanoparticles showed a slightly lower gene expression compared to naked siRNA or Lipofectamine 2000-siRNA complexes. Nevertheless, a significant reduction in gene expression with chitosan-TPP-siRNA nanoparticles at 10 nM could be observed after 72 h post-transfection, in which almost 80% \pm 17.7 of the targeted gene expression was knocked down compared to only 65% \pm 26.8 for Lipofectamine-2000-siRNA complexes. A higher gene knockdown for siRNA vectorised by chitosan-TPP nanoparticles was thought to be linked to the chitosan's ability in activating and entering macrophages *via* manose-type lectin receptors as well as the ability of macrophages to phagocytose nanoparticles (Howard *et al.* 2006, Mori *et al.* 2005, Fung *et al.* 2004). On the other hand, no further significant reduction in the targeted gene expression was detected for formulations at 1 nM either at 48 or 72 h post-transfection as shown in figure 6.4. An increase in expression of the targeted gene for the cells treated with Lipofectamine 2000-siRNA complexes (1 nM) at 72 h post-transfection however is not yet understood.

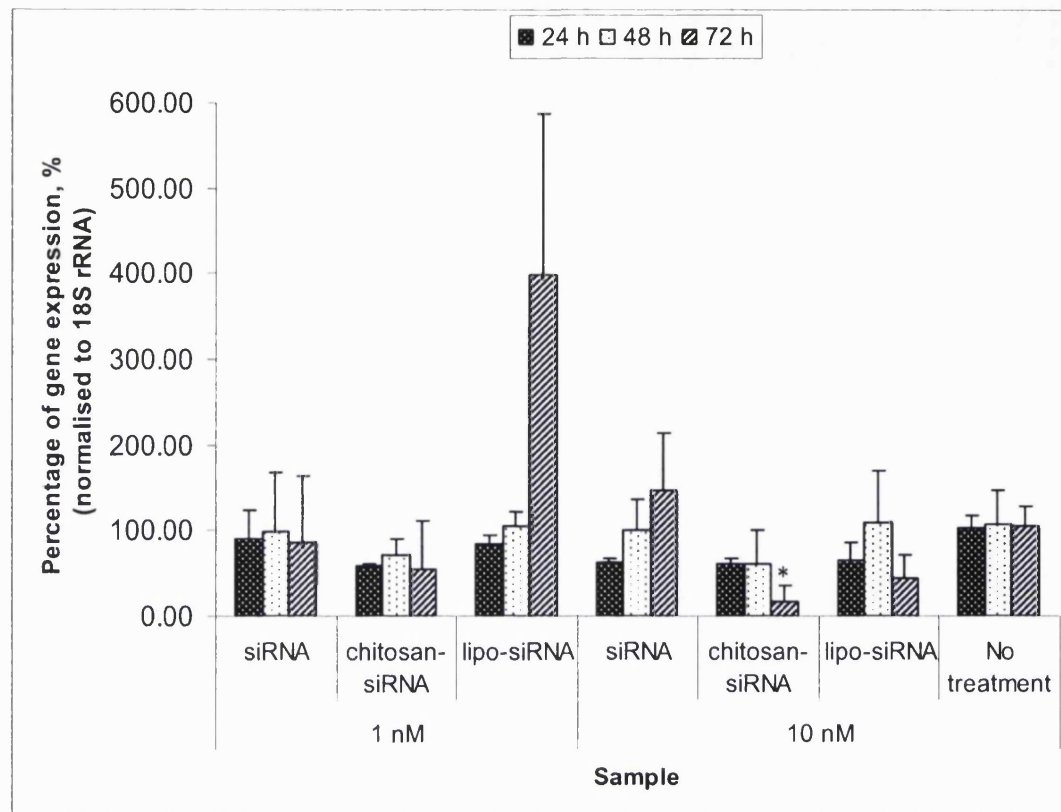


Figure 6.4: Percentage of gene expression for naked siRNA, chitosan-TPP-siRNA (chi-siRNA) nanoparticles and Lipofectamine-2000-siRNA complexes (lipo-siRNA) in J774A.1 cells at different time-points post-transfection, (n=9). Gene expression of the total RNA from the lysis cells was analysed by quantitative real-time PCR using primers and taqman probe. In addition, 18S rRNA was used as an internal standard (housekeeping gene). Transfections were performed in J774A.1 cells at density of 1×10^4 cells/ well. * The difference between chitosan-TPP-siRNA nanoparticles and Lipofectamine 2000-siRNA complexes was significant ($p < 0.05$).

MTT assays were also performed to investigate the presence of any toxic effect to the treated cells from the formulations in terms of inhibition of cell growth or cell death. The results obtained showed that the percentage of cell viability was dependent on the dose of formulation used to transfect the cells as well as the duration of incubation with the formulation (figure 6.5). A slight loss in cell viability was detected which ranged from 20 to 30 % of cell loss for all the formulation at the dose of 10 nM at 72 h post-incubation. Contrary to that, no significant reduction in cell viability could be seen in the cells treated with the dose of 1 nM even after up to 72 h post-incubation.

The inhibition of cell growth or cell death was thought to arise from the components of the transfection agents either chitosan-TPP nanoparticles or Lipofectamine 2000 as approximately 15% cell loss was observed when the cells were treated with the agent alone and this effect could be observed with a higher concentration which in turn might lead to cell death and reduce the activity of mitochondrial dehydrogenase. The cytotoxicity effect of these transfecting agents was also closely related to the increase in density of their positive charge as no charge neutralisation by siRNA occurs in the case of transfecting agent alone. A higher charge density contributing to the cytotoxic effect has been reported as possibly due to strong electrostatic interaction with cellular anionic macromolecules such as proteins, various types of RNA and genomic DNA which would impair the normal cellular functions of these polyanions, resulting in toxicity (Thomas *et al.* 2005). This corresponds with the findings that a significant decrease in cell viability was observed for the cells treated with chitosan-TPP nanoparticles (10 nM or 280 µg/ml) or Lipofectamine 2000 (10 nM or 1 µg/ml) alone in comparison to entrapped or complexed with siRNA at the same molar concentration (one way ANOVA, followed by Post hoc multiple comparison test, $p < 0.05$). Although, the experimental data obtained from this study described that chitosan-TPP nanoparticles could also cause a loss in cell viability (at 10 nM), but the concentration of nanoparticles used was in fact, almost 300 times higher than Lipofectamine 2000 as dose was determined by altering only siRNA molar concentration and not the mass ratio between siRNA and nanoparticles or Lipofectamine 2000. Therefore, direct comparison of toxic effects between chitosan-TPP nanoparticles and Lipofectamine 2000 could not be done. However, it is important to investigate the effect of formulations on the cells as they are during transfection studies to ensure the reliability of the data in terms of direct relevance for a comparable dose of the active agent.

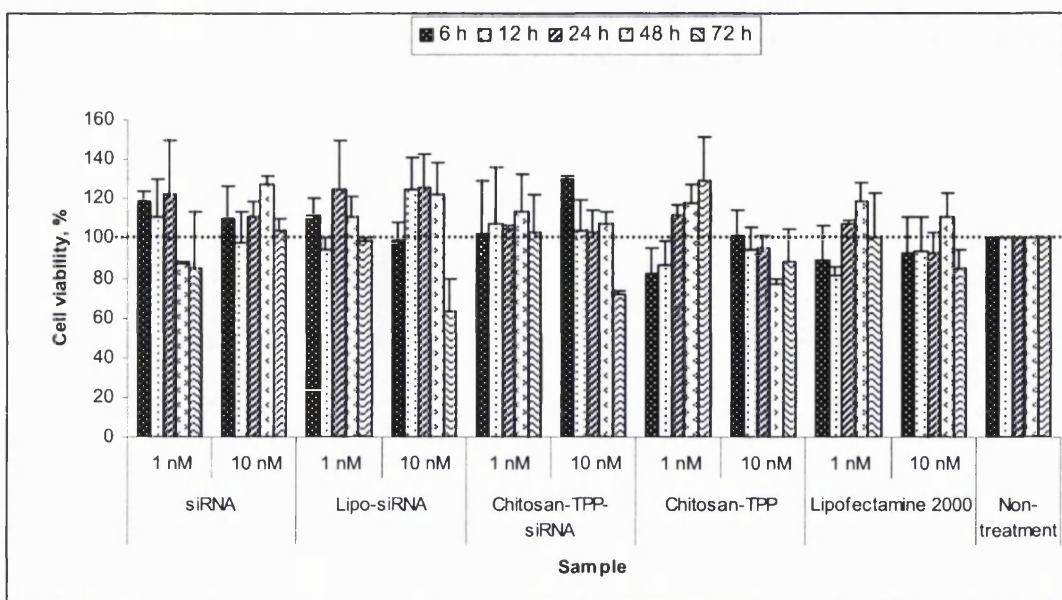


Figure 6.5: Effect of dose and duration of incubation with naked siRNA, trasfecting agents or combination of both on percentage of J774A.1 cell viability, n=9.

Toxicity studies were also performed in L929s cells, a mouse fibroblast cell line, L929s cells (A gift from Dr. Simon Jones, Astra Zeneca). In this study, siRNA mismatch (GCGAGCUGCGCGAAGGAUAdTdT, Astra Zeneca) was used to evaluate the tendency of siRNA MAPK14 to induce cytotoxicity on its own. From the graph below (figure 6.4), no toxicity was observed when the cells were treated with the naked siRNA either siRNA MAPK14 or mismatch even at a concentration as high as 100 nM. These results therefore, clearly confirmed that the silencing activity of siRNA MAPK14 could be enhanced by using a non-toxic and serum resistant delivery system.

On the other hand, Lipofectamine 2000 was shown to be toxic to the cells and significant cell death was observed at 100 nM for Lipofectmaine 2000-siRNA complexes where $70\% \pm 0.95$ and $80\% \pm 0.6$ cell loss was detected when complexing with siRNA MAPK14 and mismatch, respectively (ANOVA followed by Post hoc comparable test, $p < 0.05$). In contrast to Lipofectmaine 2000, chitosan-TPP nanoparticles were found to be a relatively less toxic even at 100 nM either entrapped with siRNA or chitosan nanoparticles alone.

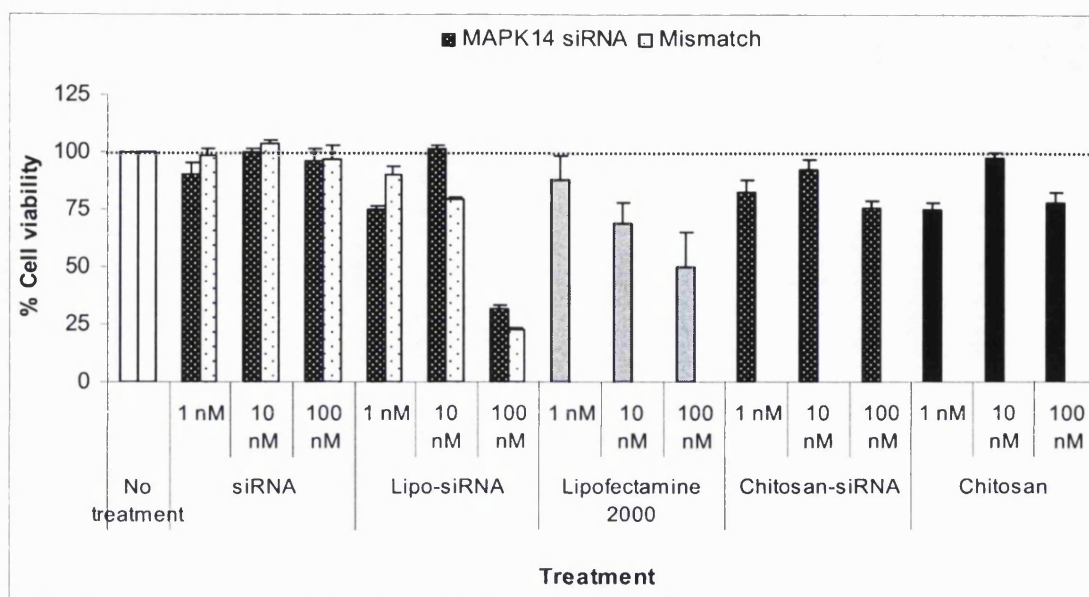


Figure 6.6: Cell viability of formulations in L929s cells at 24 h post-incubation, n=9. Keynotes: Lipo-siRNA = Lipofectamine 2000-siRNA and chitosan=chitosan-TPP nanoparticles.

Further investigation also showed that chitosan nanoparticles were much less toxic than Lipofectamine 2000 even at 72 h post-incubation. Less than 10% \pm 1.2 of the cells treated with Lipofectamine 2000-siRNA complexes were viable at 100 nM at 72 h post-incubation whereas viability of the cells treated with chitosan nanoparticles was more than 50% \pm 5.1 even at 100 nM (figure 6.7). These findings therefore, suggest that chitosan nanoparticles have a relatively low cytotoxicity and have a great potential to be used as a vector for siRNA.

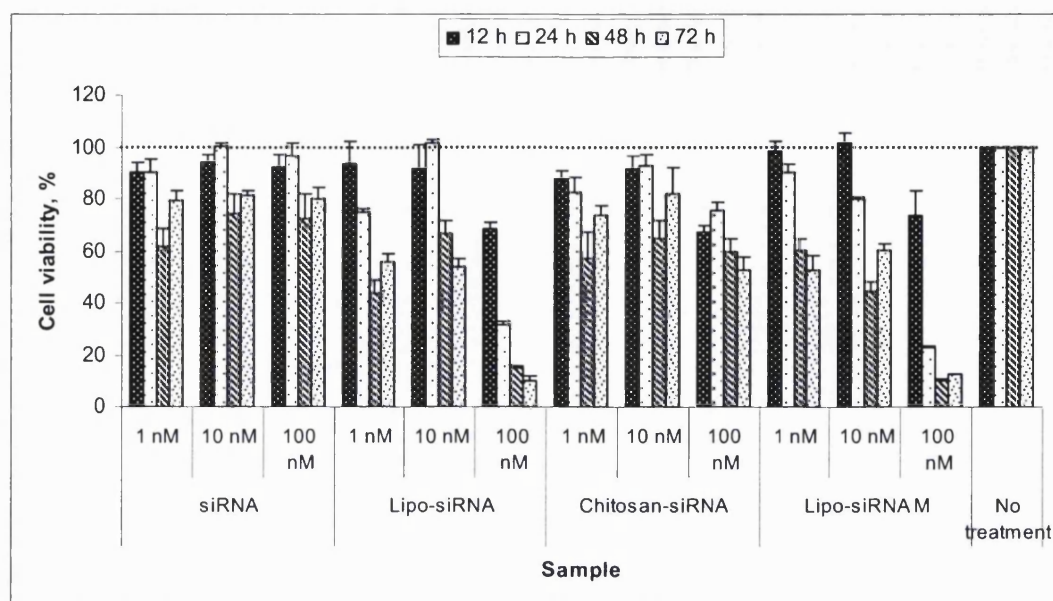


Figure 6.7: Cell viability of formulations in L929s cells at different time-points, n=9. Keynotes: Lipo-siRNA=Lipofectamine 2000-siRNA MAPK14 complexes and Lipo-siRNA M= Lipofectamine 2000-siRNA mismatch.

6.2 Conclusion

Chitosan-TPP nanoparticles with entrapped siRNA have been discovered to be a nuclease-resistant delivery system which has the ability to protect and deliver siRNA into cells. This system has also been shown to allow the vectorised siRNA to silence an endogenous gene; P38 α MAPK with sustained activity and low cytotoxicity up to 72 h at a siRNA concentration of 10 nM.

Chapter 7
General Discussion and Future Works

7 General discussion and future works

The use of cationic polymeric nanoparticulate systems to deliver genetic materials such as pDNA has been explored for more than a decade. Only recently, these carrier systems have been studied for a new and potent gene regulator, short interfering RNA or siRNA. From among these cationic polymers, only three types of cationic polymers have been used in this study. All these cationic polymers enable a high efficiency of macromolecules delivery but each of them has different structural properties. These polymers are PEI, chitosan and TAT-peptide which possess a high density of positive charge particularly from cationic-NH-groups which allow them to form a non-covalent intra-polyelectrolyte complex with anionic phosphodiester backbone on the polyanions like pDNA or siRNA. These complexes provide protection of nucleic acids from nuclease degradation thereby resulting in high transfection efficiency. Therefore, they are among the most suitable candidates for effective delivery systems for nucleic acids.

In this study, siRNA-chitosan complexes have been found to be relatively larger in particle size than pDNA-chitosan complexes in which their particle size is highly dependent on the molecular weight as well as concentration of chitosan used. However, none of the different molecular mass or concentrations of chitosan tested here has shown the capability to completely complex with siRNA although pDNA has found to be completely bound to the chitosan as low as 25 $\mu\text{g/ml}$ (equivalent to 2.5:1 chitosan to pDNA weight ratio). In contrast to chitosan, no significant difference in particle size in the range of studied N/P ratios (except for N/P ratio of 2:1 as aggregation was observed for the siRNA-PEI complexes) has been observed for both siRNA- and pDNA-PEI complexes. Nevertheless, a higher N/P ratio is needed for PEI to completely complex with siRNA compared to pDNA. These findings therefore, illustrate that pDNA apparently has a better interaction with the polycation polymers than siRNA and this is thought to possibly arise from the differences in their physical properties.

Although pDNA and siRNA are both polyanions, they are different in certain aspects including size and molecular structure. siRNA (21 bp) is a linear molecule that is hundreds of times smaller than pDNA (pDNA size varies from 1-250 kbp) whereby its binding profile to polycations is thought to be different from pDNA. One reason for this could be that the ability of pDNA to condense into small and condense complexes

once 70-90% of its phosphate groups interact with amine groups of both PEI and chitosan (Keller 2005). On the other hand, siRNA has no ability for such condensation because the size of siRNA is thought to be maintained after its interaction with cationic entities and this may also contribute to the difficulty of siRNA to attract with the long and branched polycationic polymer chains. In addition, due to its much smaller size, more than one siRNA molecule can probably interact with one entity of polycation which results in a larger particle size than pDNA.

Experimental data has also shown that chitosan appears to be less efficient in forming complexes with siRNA compared to PEI. This is thought to be due to a higher ratio of amine groups to molecular mass with PEI than chitosan. This characteristic has therefore probably attributed to the formation of stable siRNA-PEI complexes with a small particle size. Besides this, steric hindrance induced by a relative stiffness of the chitosan polymer chain might also contribute to the difficulty of siRNA to be attracted to the chitosan (Munier *et al.* 2005). Therefore, this has clearly suggested that different condensing agents will in fact, produce different sizes of complexes and require different concentrations to form a stable complex. As predicted, siRNA-PEI complexes have been found to be more potent than siRNA-chitosan complexes in silencing *luciferase* gene expression. Only 15% of *luciferase* gene expression has been knocked-down by siRNA-chitosan complexes compared to 48% with siRNA-PEI complexes. This may arise from suboptimal siRNA binding to the chitosan which leads to siRNA being released before arriving in the targeted site and being more exposed to nuclease degradation. A full or complete binding of siRNA is essential in maintaining its double stranded form, which the principle role of the sense strand was to protect antisense strand from the nuclease degradation after being release into cytoplasm (Hutvagner *et al.* 2001) and its identity was checked by the gateway kinase before allowing siRNA incorporation into the RISC complex in RNAi pathway (Nykanen *et al.* 2001). A higher transfection efficiency of siRNA-PEI complexes compared to siRNA-chitosan complexes is also thought to be due to a high charge density of PEI where its protonable secondary and tertiary amines on the PEI's chain consequently contribute to a high buffering capacity. Chitosan on the other hand, has only one primary amine group and less able to protonate in the acidic environment of endosomes (Li 2005, Illum 1998). Therefore, enzymatic degradation of chitosan has also been reported to be a likely mechanism of endosomal escape of chitosan-based nanoparticles where degradation

products (e.g. oligo and monosaccharides) are thought to be responsible for inducing water influx by increasing endosome osmolarity, subsequently lead to endosomal swelling and eventually rupture to release its bioactive materials (Li 2005, Kopping-Hoggard 2003, Erbacher *et al.* 1998).

To improve chitosan as a carrier for siRNA, another method known as ionic gelation has also been studied because chitosan has been known to have the ability to gel with multivalent polyanions such as TPP ions. TPP ions are derived from ionization of penta sodium tripolyphosphate which has the ability to condense as well as solidify chitosan-polyanion complexes. In addition, this method has been shown to be a more practical technique than simple mixing in controlling particle size and even surface charge of the yielded chitosan nanoparticles. Controlling several preparation parameters such as stirring rate, chitosan to TPP weight ratio and pH of the interaction medium, a smaller particle size of chitosan nanoparticles could be obtained using this technique.

Similar to siRNA-chitosan complexes, particle size and surface charge of the chitosan-TPP nanoparticles are a function of the molecular weight, concentration as well as type of chitosan salt (glutamate or hydrochloride). Chitosan glutamate has also been shown to produce smaller particles than chitosan hydrochloride using both methods (simple mixing and ionic gelation). A lower molecular weight of chitosan glutamate produces a smaller particle than a higher molecular weight. Although in simple mixing techniques, pH apparently has no effect either on particle size or siRNA binding efficiency, but pH has been shown to play an important factor in influencing particle size of chitosan-TPP nanoparticles prepared by ionic gelation since a smaller particle size is observed when lowering the pH of the chitosan solution from pH 6 to 4.

This is thought to be due to the increased density of protonated amine groups of chitosan which could efficiently interact with TPP ions together with siRNA to form nanoparticles. In addition, the pH of the chitosan solution has a significant effect in this method because the TPP ion has been reported to have a higher charge/ mass ratio than pDNA or even siRNA (Li 2005). The charge/ mass ratios are 1/44 and 1/326 for TPP ion and siRNA, respectively and therefore the addition of TPP ions is thought to be beneficial in entrapping siRNA in the chitosan nanoparticles.

Ionic gelation is not only beneficial in controlling particle size or surface charge of the chitosan nanoparticles but also in providing more options in the techniques of

siRNA association to the particles. siRNA could be either entrapped inside the chitosan-TPP nanoparticles (by adding siRNA during preparation process) or adsorbed onto the surface of preformed nanoparticles. It has been found that these systems show different profiles in siRNA binding efficiency whereby entrapping siRNA inside the chitosan-TPP nanoparticles has a higher capacity or efficiency to bind siRNA compared to the other systems (adsorbing or complexing siRNA). The presence of TPP ions is believed to facilitate the entrapment of siRNA to the chitosan nanoparticles and therefore, to form stable chitosan-TPP-siRNA nanoparticles. By entrapping siRNA to the chitosan-TPP nanoparticles, a higher knockdown of the targeted gene could also be achieved *in-vitro*. A higher gene knockdown of the targeted gene has been detected for chitosan-TPP nanoparticles made from G213 and Cl113 but no obvious correlation has been observed between transfection efficiency with the type or molecular weight of chitosan employed although based on experimental data, molecular weight of chitosan has been shown to significantly affect the size of chitosan-siRNA nanoparticles. It has been reported that particle size could influence cellular uptake or entry of particulate systems and subsequently cellular transfection in which a smaller particle size (less than 500 nm) is favourable as it could overcome the extracellular barrier of cellular entry. However, the mechanism of cellular transfection by this nanoparticulate system is apparently more complicated than that because based on this work, no clear correlation between particle size and transfection efficiency was observed. Therefore, it could be concluded that cellular transfection of this nanoparticulate system is affected by multiple factors which include cell type, cell viability, particle size as well as surface charge.

Since cationic polymers can be incorporated into the polymers that have negatively charge, they have been widely used to prepare positively charged nanoparticles of biodegradable polymers like PLGA and PLA. In this study, an emulsification diffusion method has been utilised to prepare these nanoparticles due to its advantages over the solvent evaporation method.

In the case of PLGA-PEI nanoparticles, a spontaneous emulsification diffusion method has been used. The mixture of acetone and dichloromethane has been utilised as an organic phase. In this preparation, the amount of PEI that has been added to the PLGA is a crucial factor in determining particle formation as a lower mass ratio than 29:1 of PLGA to PEI could lead to aggregated particles. Besides this, other factors such

as type and concentrations of stabiliser have been observed to highly influence the size of PLGA-PEI nanoparticles. A higher concentration of stabiliser has been shown to produce a smaller particle size as more stable particles are formed due to the increased amount of stabiliser adsorbed onto the particles that could prevent the particles from coalescence or aggregation during solvent diffusion to the aqueous phase.

Although these particles are stable, they have been discovered to be less protected against the harsh environment during freeze-drying. Therefore, glycerol has been added to the particle suspensions before freeze-drying to prevent aggregate formation. However, the effectiveness of glycerol to prevent aggregation was also dependent on the stability of particles which may directly correlate to the type and concentration of stabiliser used during particle preparation. On the other hand, between poloxamer and PVA, only PVA (either a higher or lower molecular weight) with a higher concentration (5% m/v) has been found to produce a smaller particle size of around 100 nm which therefore has been used for these experiments.

Besides PEI, chitosan has also been incorporated into PLGA particles by an emulsification diffusion method. This preparation however utilises a different solvent from a spontaneous emulsification diffusion method, and ethyl acetate and PVA have been used as a solvent and surfactant, respectively. Experimental data has revealed that physical properties of PLGA-chitosan nanoparticles particularly particle size and surface charge are also affected by certain preparation parameters. Particle size of these nanoparticles for example is dependent on the PVA concentration as well as homogeniser speed during emulsification because a reduction in particle size has been observed with the increase of both parameters. Different types and molecular weights of chitosan have also been observed to affect particle size of the yielded nanoparticles in which a lower molecular weight or chitosan glutamate produces a smaller particle than a higher molecular weight or chitosan hydrochloride. An increase in particle size with a higher molecular weight of chitosan could be explained by the increased viscosity of the organic phase that would be expected to be more resistant to shear forces during emulsification, which in turn produces a larger emulsion droplet and subsequently a larger particle.

Unlike PLGA-PEI nanoparticles, centrifugation has been observed to cause a drop in particle size as well as particle size distribution. This drop has been hypothesized to be due to the loss of some of the chitosan molecules which partially

interacted with the PLGA and they could easily wash away during centrifugation. This hypothesis has also been supported by a lower particle surface charge of these nanoparticles after centrifugation compared to those particles washed by filtration. These nanoparticles have also been shown to suffer from a poor siRNA loading capacity or binding efficiency due to the chitosan loss during washing and harvesting steps using centrifugation. Further study therefore, has been performed to improve chitosan loading to the PLGA particles by using a higher degree of 'uncapped' end groups of PLGA polymers due to the fact that this could provide a stronger interaction between chitosan and PLGA as more carboxylate groups of PLGA could interact with amino groups of the chitosan. By increasing the degree of 'uncapped' end groups of PLGA polymers, centrifugation has shown to have no effect on particle size but could improve particle surface charge as well as siRNA loading capacity which means that an increased amount of chitosan can be incorporated onto the PLGA particles. This has also been confirmed by chitosan loading analysis using Orange III dye and spectrophotometry.

For these cationic PLGA nanoparticles, siRNA has been adsorbed onto their surface in order to protect siRNA from the harsh environment of particle preparation and it has been thought that siRNA is prone to undergo degradation due to its smaller size in comparison to pDNA. Since adsorption of siRNA onto the cationic particles of PLGA-PEI and PLGA-chitosan nanoparticles is largely *via* electrostatic interaction between amino groups of PEI or chitosan and phosphate groups of siRNA, nitrogen to phosphate ratio (N/P ratio) plays an important factor in determining complete adsorption of siRNA. Both delivery systems required a higher N/P ratio to completely adsorb siRNA onto their surface compared to their parent compound, siRNA-PEI or siRNA-chitosan complexes. The need of a higher N/P ratio is thought to be due to parts of amino groups of these cationic polymers interacting with carboxylates of PLGA or even being buried inside the particles which therefore require more cationic entities to interact with siRNA. A lower amount of free amine groups of chitosan may also explain why PLGA-chitosan nanoparticles were not as efficient as chitosan-TPP nanoparticles in delivering siRNA into cells where most of its amine groups were interacted with siRNA and PLGA or buried inside the particles. In gene delivery, an efficient delivery system should facilitate cellular uptake of nucleic acid into the target cells by providing excess positive surface charge, so that the system can be taken up by the cells via endocytosis, after initial interaction with negatively charged cell

membrane components (glycoprotein, glycolipids and proteoglycans). In addition, protonated amine groups of chitosan-based nanoparticles was also an important factor to induce endosomal escape for siRNA to exert its effects by triggering endosomal swelling and eventually endosomal rupture.

As shown in this study, PEI has been observed to have a better binding profile with siRNA and transfection efficiency than chitosan. Similar findings have also been obtained when incorporating PEI or chitosan to PLGA nanoparticles. PLGA-chitosan nanoparticles have been shown to be unable to completely adsorb siRNA even at a very high N/P ratio as determined by gel retardation assay. This is thought to be due to the partial interaction between cationic entities and siRNA induced by the stiffness of the chitosan chain which leads to difficulty of siRNA to attract to the amino groups on the chitosan polymer chains. This characteristic therefore, results in a lower gene silencing of the targeted gene compared to PLGA-PEI nanoparticles as siRNA is being exposed to nuclease degradation. In all cases, a higher transfection efficiency has been observed for siRNA compared to pDNA in *in-vitro* cultured cells. It has been predicted that pDNA delivery into the cultured cells is more difficult than siRNA because pDNA needs to cross nuclear membrane in order to exert its effect. Meanwhile, siRNA does not require cross through nuclear membrane, because siRNA exerts its effect directly in the cytoplasm.

As mentioned in the earlier section, TAT-peptide has also been reported to have the ability to deliver siRNA in a wide range of cell lines due to its ability to translocate genetic materials across the plasma membrane into the cytoplasm (Frezts *et al.* 2004, Lindgren *et al.* 2000, Prochiantz 2000). Most of these studies have utilised a covalent or chemical conjugation to attach siRNA to the TAT-peptide which needs more complicated methods to get rid of unwanted chemical reactants or even to assess the final products. Therefore in this study, siRNA has been complexed with TAT-peptide to address the lack of information regarding the suitability of TAT-peptide to complex with siRNA by a simpler method, simple mixing or complexation.

In this study, a small particle size of siRNA-TAT-peptide complexes have been obtained in which TAT-peptide concentrations or TAT-peptide to siRNA weight ratios have been observed to influence particle size and surface charge of the complexes. The increment of particle surface charge by increasing the ratio of TAT-peptide to siRNA is thought to arise from the increased amount of cationic entities in TAT-peptide

structures, such as arginine and lysine residues. Analysis of siRNA binding to the TAT-peptide has also revealed that TAT-peptide has the ability to bind siRNA by simple complexation/ mixing and this could be achieved effectively at certain TAT-peptide to siRNA ratios (7.5: 1 and above). A series of *in-vitro* studies in cultured cells has further suggested that siRNA-TAT-peptide complexes have the ability to deliver siRNA into cells but the degree of transfection efficiency is dependent on the TAT-peptide to siRNA weight ratios and types of cell line. In the case of TAT-peptide to siRNA weight ratio, a higher ratio (20:1) is needed because a number of cationic groups of TAT-peptide have been used to bind siRNA and since a guanidium group of the arginine side chain has been shown to be more potent in mediating cellular uptake, it is logical that a higher amount of TAT-peptide is required to efficiently deliver siRNA into cells. Recent studies have also reported that TAT-peptide internalisation is predominantly through endocytosis following the interaction of TAT-peptide with the negatively charged cell surface components. On the other hand, due to the difference in characteristics and cell surface components of different cell types, variability in gene silencing of siRNA by TAT-peptide is expected and this therefore, could explain a higher gene silencing effect of siRNA-TAT-peptide complexes in CHO K1 cells compared to in HEK 293 cells. Furthermore, calcium has been found to enhance the delivery of siRNA-TAT-peptide complexes presumably by facilitating endosomal release of these complexes without affecting the viability of the transfected cells.

Finally, siRNA inhibition experiments with an endogenous target, MAPK p38 α have been performed in J774A.1 cells. Further *in-vitro* investigations with one of the formulations developed in this study (chitosan-TPP nanoparticles with entrapped siRNA) has demonstrated that the system had a high stability and can protect the entrapped siRNA from nuclease degradation even after 48 h incubation in 50% v/v mouse serum. This system also has been found to allow very high transfection efficiency (90% gene knockdown) in the tested cells. In addition, the system has been shown to have a relatively low cytotoxicity (~80% cell viability) which means that this system has a great potential to be used as a vector for siRNA. This data therefore, suggested that chitosan-TPP nanoparticles could efficiently deliver siRNA into cells and have a great potential to be used therapeutically. For example, this system is suitable to be delivered as an aerosol into the lung, due to muco/ bioadhesive properties of chitosan.

7.1 Future works

The *in-vitro* studies that have been performed in this project have clearly revealed that chitosan-TPP nanoparticles entrapping siRNA has a great potential to be used as a vector for siRNA. However, it is currently unclear to what extent it can be used *in-vivo*. Therefore, further *in-vivo* studies in a suitable animal model (e.g. rat) need to be pursued using this formulation to investigate its potential therapeutically. These studies may not only evaluate the effectiveness of the formulation to deliver siRNA into cells, but it would also be of interest to examine its distribution in the body as well as to thoroughly investigate any unwanted side effects related to the system.

The data obtained from the project have also showed that some other formulations investigated have a potential to be used as a delivery system for siRNA *in-vitro* such as PLGA-PEI nanoparticles with adsorbed siRNA and TAT-peptide-siRNA complexes which could not be further investigated in this study due to time constraints. Therefore, it would be of interest to examine their effects in further *in-vitro* studies using RT-real time PCR either targeting MAPK p38a genes and later proceed with *in-vivo* animal studies if successful. Other technology used to induce siRNA such as pDNA encoded siRNA/ shRNA or PCR cassette could also be investigated and optimised using above vectors to offer versatility in their pharmaceutical usage as a delivery system. Nevertheless, the complexity of the process by which siRNA is delivered and RNAi is induced offers a wide opportunity for the improvement of existing carrier systems and further development of a new one.

References

Abdelwahed, W., Degobert, G., & Fessi, H. 2006, "A pilot study of freeze drying of poly(epsilon-caprolactone) nanocapsules stabilized by poly(vinyl alcohol): Formulation and process optimization", *International Journal Of Pharmaceutics*, vol. 309, no. 1-2, pp. 178-188.

Agnihotri, S. A., Mallikarjuna, N. N., & Aminabhavi, T. M. 2004, "Recent advances on chitosan-based micro- and nanoparticles in drug delivery", *Journal of Controlled Release*, vol. 100, no. 1, pp. 5-28.

Agrawal, N., Dasaradhi, P. V. N., Mohammed, A., Malhotra, P., Bhatnagar, R. K., & Mukherjee, S. K. 2003, "RNA interference: Biology, Mechanism, and applications", *Microbiology and Molecular Biology Reviews*, vol. 67, no. 657, pp. 685.

Agrawal, S. & Akhtar, S. 1995, "Advances in antisense efficacy and delivery", *Trends in Biotechnology*, vol. 13, no. 6, pp. 197-199.

Ahn, C. H., Chae, S. Y., Bae, Y. H., & Kim, S. W. 2002, "Biodegradable poly(ethylenimine) for plasmid DNA delivery", *Journal of Controlled Release*, vol. 80, no. 1-3, pp. 273-282.

Aigner, A. 2006, "Gene silencing through RNA interference (RNAi) in vivo: Strategies based on the direct application of siRNAs", *Journal of Biotechnology*, vol. 124, no. 1, pp. 12-25.

Akbuga, J., Ozbas-Turan, S., & Erdogan, N. 2004, "Plasmid-DNA loaded chitosan microspheres for in vitro IL-2 expression", *European Journal of Pharmaceutics and Biopharmaceutics*, vol. 58, no. 3, pp. 501-507.

Akhtar, S. 1998, "Antisense technology: Selection and delivery of optimally acting antisense oligonucleotides", *Journal of Drug Targeting*, vol. 5, no. 4, pp. 225-234.

Akhtar, S., Hughes, M. D., Khan, A., Bibby, M., Hussain, M., Nawaz, Q., Double, J., & Sayyed, P. 2000, "The delivery of antisense therapeutics", *Advanced Drug Delivery Reviews*, vol. 44, no. 1, pp. 3-21.

References

Allemann, E., Gurny, R., & Doelker, E. 1993, "Drug loaded nanoparticles-Preparation methods and drug targeting issues", *European Journal of Pharmaceutics and Biopharmaceutics*, vol. 39, no. 1, pp. 173-191.

Anderson, K. P., Fox, M. C., Brown-Driver, V., Martin, M. J., & Azad, R. F. 1996, "Inhibition of human cytomegalovirus immediate-early gene expression by an antisense oligonucleotide complementary to immediate-early RNA", *Antimicrobial Agents And Chemotherapy*, vol. 40, no. 9, pp. 2004-2011.

Artursson, P., Lindmark, T., Davis, S. S., & Illum, L. 1994, "Effect of chitosan on the permeability of monolayers of intestinal epithelial cells (Caco-2)", *Pharmaceutical Research*, vol. 11, no. 9, pp. 1358-1361.

Astriab-Fisher, A., Sergueev, D. S., Fisher, M., Ramsay Shaw, B., & Juliano, R. L. 2000, "Antisense inhibition of P-glycoprotein expression using peptide-oligonucleotide conjugates", *Biochemical Pharmacology*, vol. 60, no. 1, pp. 83-90.

Barman, S. P., Lunsford, L., Chambers, P., & Hedley, M. L. 2000, "Two methods for quantifying DNA extracted from poly(lactide-co-glycolide) microspheres", *Journal of Controlled Release*, vol. 69, no. 3, pp. 337-344.

Bartel, D. P. 2004, "MicroRNAs: Genomics, Biogenesis, Mechanism, and Function", *Cell*, vol. 116, no. 2, pp. 281-297.

Beal, J. 2005, "Silence is golden: can RNA interference therapeutics deliver?", *Drug Discovery Today*, vol. 10, no. 3, pp. 169-172.

Beale, G., Hollins, A. J., Benboubetra, M., Sohail, M., Fox, S. P., Benter, I., & Akhtar, S. 2003, "Gene silencing nucleic acids designed by scanning arrays: anti-EGFR activity of siRNA, ribozyme and DNA enzymes targeting a single hybridization-accessible region using the same delivery system", *Journal of Drug Target*, vol. 11, no. 7, pp. 449-456.

Behlke, M. A. 2006, "Progress towards in Vivo Use of siRNAs", *Molecular Therapy*, vol. 13, no. 4, pp. 644-670.

Behr, J. P. 1997, "The proton sponge: a trick to enter cells the viruses did not exploit". *Chimica*, vol. 51, pp. 34-36.

References

Bernstein, E., Caudy, A. A., Hammond, S. M., & Hannon, G. J. 2001, "Role for a bidentate ribonuclease in the initiation step of RNA interference", *Nature*, vol. 409, no. 6818, pp. 363-366.

Berton, M., Allemann, E., Stein, C. A., & Gurny, R. 1999, "Highly loaded nanoparticulate carrier using an hydrophobic antisense oligonucleotide complex", *European Journal of Pharmaceutical Sciences*, vol. 9, no. 2, pp. 163-170.

Berton, M., Benimetskaya, L., Allemann, E., Stein, C. A., & Gurny, R. 1999, "Uptake of oligonucleotide-loaded nanoparticles in prostatic cancer cells and their intracellular localization", *European Journal of Pharmaceutics and Biopharmaceutics*, vol. 47, no. 2, pp. 119-123.

Bertrand, J. R., Pottier, M., Vekris, A., Opolon, P., Maksimenko, A., & Malvy, C. 2002, "Comparison of antisense oligonucleotides and siRNAs in cell culture and in vivo", *Biochemical and Biophysical Research Communications*, vol. 296, no. 4, pp. 1000-1004.

Bivas-Benita, M., Ottenhoff, T. H. M., Junginger, H. E., & Borchard, G. 2005, "Pulmonary DNA vaccination: Concepts, possibilities and perspectives", *Journal of Controlled Release*, vol. 107, no. 1, pp. 1-29.

Bivas-Benita, M., Romeijn, S., Junginger, H. E., & Borchard, G. 2004, "PLGA-PEI nanoparticles for gene delivery to pulmonary epithelium", *European Journal of Pharmaceutics and Biopharmaceutics*, vol. 58, no. 1, pp. 1-6.

Bloomfield, V. A. 1991, "Condensation of DNA by multivalent cations: considerations on mechanism", *Biopolymers*, vol. 31, no. 13, pp. 1471-1481.

Bloomfield, V. A. 1996, "DNA condensation", *Current Opinion in Structural Biology*, vol. 6, no. 3, pp. 334-341.

Bloomfield, V. A., He, S., Li, A. Z., & Arscott, P. B. 1991, "Light scattering studies on DNA condensation", *Biochemical Society Transactions*, vol. 19, no. 2, p. 496.

Boden, D., Pusch, O., Lee, F., Tucker, L., & Ramratnam, B. 2003, "Human immunodeficiency virus type 1 escape from RNA interference", *Journal of Virology*, vol. 77, no. 21, pp. 11531-11535.

References

Borchard, G. 2001, "Chitosans for gene delivery", *Advanced Drug Delivery Reviews*, vol. 52, no. 2, pp. 145-150.

Borchard, G., en, H. L., de Boer, A. G., Verhoef, J. C., Lehr, C. M., & Junginger, H. E. 1996, "The potential of mucoadhesive polymers in enhancing intestinal peptide drug absorption. III: Effects of chitosan-glutamate and carbomer on epithelial tight junctions in vitro", *Journal of Controlled Release*, vol. 39, no. 2-3, pp. 131-138.

Bottger, M., Zaitsev, S. V., Otto, A., Haberland, A., & Vorob'ev, V. I. 1998, "Acid nuclear extracts as mediators of gene transfer and expression", *Biochimica et Biophysica Acta (BBA) - Gene Structure and Expression*, vol. 1395, no. 1, pp. 78-87.

Boussif, O. L. F., Zanta, M. A., Mergny, M. D., Scherman, D., Demeneix, B., & Berh, J. P. 1995, "A versatile vector for gene and oligonucleotide transfer into cells in culture and in vivo: polyethylenimine". *Proceedings of the National Academy of Sciences of the United States of America*, vol. 92, pp. 7297-7301.

Braasch, D. A., Jensen, S., Liu, Y., Kaur, K., Arar, K., White, M. A., & Corey, D. R. 2003, "RNA interference in mammalian cells by chemically-modified RNA", *Biochemistry*, vol. 42, no. 26, pp. 7967-7975.

Braasch, D. A., Paroo, Z., Constantinescu, A., Ren, G., Oz, O. K., Mason, R. P., & Corey, D. R. 2004, "Biodistribution of phosphodiester and phosphorothioate siRNA", *Bioorganic & Medicinal Chemistry Letters*, vol. 14, no. 5, pp. 1139-1143.

Brigger, I., Dubernet, C., & Couvreur, P. 2002, "Nanoparticles in cancer therapy and diagnosis", *Advanced Drug Delivery Reviews*, vol. 54, no. 5, pp. 631-651.

Brooks, H., Lebleu, B., & Vives, E. 2005, "Tat peptide-mediated cellular delivery: back to basics", *Advanced Drug Delivery Reviews*, vol. 57, no. 4, pp. 559-577.

Brownlie, A., Uchegbu, I. F., & Schatzlein, A. G. 2004, "PEI-based vesicle-polymer hybrid gene delivery system with improved biocompatibility", *International Journal Of Pharmaceutics*, vol. 274, no. 1-2, pp. 41-52.

Brummelkamp, T. R., Bernards, R., & Agami, R. 2002, "A system for stable expression of short interfering RNAs in mammalian cells", *Science*, vol. 296, no. 5567, pp. 550-553.

References

Calvo, P., Bougaba, A., Appel, M., Fattal, E., Alonso, M. J., & Couvreur, P. 1998 "Oligonucleotide-chitosan nanoparticles as new gene therapy vector", *Proceeding of World Meeting, APGI/APV 2*, pp. 1111-1112.

Carpenter, J. F., Pikal, M. J., Chang, B. S., & Randolph, T. W. 1997, "Rational design of stable lyophilized protein formulations: some practical advice", *Pharmaceutical Research*, vol. 14, no. 8, pp. 969-975.

Cavalier, M., Benoit, J. P., & Thies, C. 1986, "The formation and characterization of hydrocortisone-loaded poly((+/-)-lactide) microspheres", *The Journal Of Pharmacy And Pharmacology*, vol. 38, no. 4, pp. 249-253.

Chalfie, M., Horvitz, H. R., & Sulston, J. E. 1981, "Mutations that lead to reiterations in the cell lineages of *C. elegans*", *Cell*, vol. 24, no. 1, pp. 59-69.

Chang, H. C., Samaniego, F., Nair, B. C., Buonaguro, L., & Ensoli, B. 1997, "HIV-1 Tat protein exits from cells via a leaderless secretory pathway and binds to extracellular matrix-associated heparan sulfate proteoglycans through its basic region", *AIDS (London, England)*, vol. 11, no. 12, pp. 1421-1431.

Cegnar, M., Kos, J., & Kristl, J. 2004, "Cystatin incorporated in poly(lactide-co-glycolide) nanoparticles: development and fundamental studies on preservation of its activity", *European Journal of Pharmaceutical Sciences*, vol. 22, no. 5, pp. 357-364.

Chen, G. & Khalil, N. 2006, "TGF-beta1 increases proliferation of airway smooth muscle cells by phosphorylation of map kinases", *Respiratory Research*, vol. 7, pp. 2.

Chirila, T. V., Rakoczy, P. E., Garrett, K. L., Lou, X., & Constable, I. J. 2002, "The use of synthetic polymers for delivery of therapeutic antisense oligodeoxynucleotides", *Biomaterials*, vol. 23, no. 2, pp. 321-342.

Chiu, Y. L., Ali, A., Chu, C. y., Cao, H., & Rana, T. M. 2004, "Visualizing a Correlation between siRNA Localization, Cellular Uptake, and RNAi in Living Cells", *Chemistry & Biology*, vol. 11, no. 8, pp. 1165-1175.

Cho, J., Heuzey, M. C., Begin, A., & Carreau, P. J. 2006, "Viscoelastic properties of chitosan solutions: Effect of concentration and ionic strength", *Journal of Food Engineering*, vol. 74, no. 4, pp. 500-515.

References

Choi, S. W., Kwon, H. Y., Kim, W. S., & Kim, J. H. 2002, "Thermodynamic parameters on poly(-lactide-co-glycolide) particle size in emulsification-diffusion process", *Colloids and Surfaces A: Physicochemical and Engineering Aspects*, vol. 201, no. 1-3, pp. 283-289.

Cioca, D. P., Aoki, Y., & Kiyosawa, K. 2003, "RNA interference is a functional pathway with therapeutic potential in human myeloid leukemia cell lines", *Cancer Gene Therapy*, vol. 10, no. 2, pp. 125-133.

Clamme, J. P., Azoulay, J., & Mely, Y. 2003, "Monitoring of the formation and dissociation of polyethylenimine/DNA complexes by two photon fluorescence correlation spectroscopy", *Biophysical Journal*, vol. 84, no. 3, pp. 1960-1968.

Cleland, J. L. 1998, "Solvent evaporation processes for the production of controlled release biodegradable microsphere formulations for therapeutics and vaccines", *Biotechnology Progress*, vol. 14, no. 1, pp. 102-107.

Cocks, B. G. & Theriault, T. P. 2004, "Developments in effective application of small inhibitory RNA (siRNA) technology in mammalian cells", *Drug Discovery Today: TARGETS*, vol. 3, no. 4, pp. 165-171.

Cogoni, C. & Macino, G. 2000, "Post-transcriptional gene silencing across kingdoms", *Current Opinion in Genetics & Development*, vol. 10, no. 6, pp. 638-643.

Cohen, S., Alonso, M. J., & Langer, R. 1994, "Novel approaches to controlled-release antigen delivery", *International Journal Of Technology Assessment In Health Care*, vol. 10, no. 1, pp. 121-130.

Dahl, T. G. & Burke, G. 1990, "Feasibility of manufacturing a solid dosage form using a liquid nonvolatile drug carrier: a physico-chemical characterisation". *Drug Development and Industrial Pharmacy*, vol. 16, pp. 1881-1891.

Dailey, L. A., Kleemann, E., Merdan, T., Petersen, H., Schmehl, T., Gessler, T., Hanze, J., Seeger, W., & Kissel, T. 2004, "Modified polyethylenimines as non viral gene delivery systems for aerosol therapy: effects of nebulization on cellular uptake and transfection efficiency", *Journal of Controlled Release*, vol. 100, no. 3, pp. 425-436.

Das, A. T., Brummelkamp, T. R., Westerhout, E. M., Vink, M., Madiredjo, M., Bernards, R., & Berkhout, B. 2004, "Human immunodeficiency virus type 1 escapes

References

from RNA interference-mediated inhibition", *Journal of Virology*, vol. 78, no. 5, pp. 2601-2605.

Davis, M. E. 2002, "Non-viral gene delivery systems", *Current Opinion in Biotechnology*, vol. 13, no. 2, pp. 128-131.

De Rosa, G., Bochot, A., Quaglia, F., Besnard, M., & Fattal, E. 2003, "A new delivery system for antisense therapy: PLGA microspheres encapsulating oligonucleotide/polyethyleneimine solid complexes", *International Journal of Pharmaceutics*, vol. 254, no. 1, pp. 89-93.

Dean, N. M. 2001, "Functional genomics and target validation approaches using antisense oligonucleotide technology", *Current Opinion in Biotechnology*, vol. 12, no. 6, pp. 622-625.

Delie, F., Berton, M., Allemann, E., & Gurny, R. 2001, "Comparison of two methods of encapsulation of an oligonucleotide into poly(D,L-lactic acid) particles", *International Journal of Pharmaceutics*, vol. 214, no. 1-2, pp. 25-30.

Diebold, S. S., Kursa, M., Wagner, E., Cotten, M., & Zenke, M. 1999, "Mannose polyethylenimine conjugates for targeted DNA delivery into dendritic cells", *The Journal of Biological Chemistry*, vol. 274, no. 27, pp. 19087-19094.

Dong, X., Liu, Y., Du, M., Wang, Q., Yu, C. T., & Fan, X. 2006, "P38 mitogen-activated protein kinase inhibition attenuates pulmonary inflammatory response in a rat cardiopulmonary bypass model", *European Journal of Cardio-Thoracic Surgery*, vol. 30, no. 1, pp. 77-84.

Dunlap, D. D., Maggi, A., Soria, M. R., & Monaco, L. 1997, "Nanosopic structure of DNA condensed for gene delivery", *Nucleic Acids Research*, vol. 25, no. 15, pp. 3095-3101.

Dunn, R. L. & Ottenbrite, R. M. 1991, "Polymeric drugs and drug delivery systems", *American Chemical Society*.

Dunn, S. E., Coombes, A. G. A., Garnett, M. C., Davis, S. S., Davies, M. C., & Illum, L. 1997, "In vitro cell interaction and in vivo biodistribution of poly(lactide-co-glycolide) nanospheres surface modified by poloxamer and poloxamine copolymers", *Journal of Controlled Release*, vol. 44, no. 1, pp. 65-76.

References

Dunne, M., Bibby, D. C., Jones, J. C., & Cudmore, S. 2003, "Encapsulation of protamine sulphate compacted DNA in polylactide and polylactide-co-glycolide microparticles", *Journal of Controlled Release*, vol. 92, no. 1-2, pp. 209-219.

Elbashir, S. M., Lendeckel, W., & Tuschl, T. 2001, "RNA interference is mediated by 21- and 22-nucleotide RNAs", *Genes and Development*, vol. 15, no. 2, pp. 188-200.

Elmen, J., Thonberg, H., Ljungberg, K., Frieden, M., Westergaard, M., Xu, Y., Wahren, B., Liang, Z., Orum, H., Koch, T., & Wahlestedt, C. 2005, "Locked nucleic acid (LNA) mediated improvements in siRNA stability and functionality", *Nucleic Acids Research*, vol. 33, no. 1, pp. 439-447.

Erbacher, P., Zou, S., Bettinger, T., Steffan, A. M., & Remy, J. S. 1998, "Chitosan-based vector/DNA complexes for gene delivery: biophysical characteristics and transfection ability", *Pharmaceutical Research*, vol. 15, no. 9, pp. 1332-1339.

Feng, J., Zhao, L., & Yu, Q. 2004, "Receptor-mediated stimulatory effect of oligochitosan in macrophages", *Biochemical and Biophysical Research Communications*, vol. 317, no. 2, pp. 414-420.

Fernandez-Carneado, J., Van Gool, M., Martos, V., Castel, S., Prados, P., de Mendoza, J., & Giralt, E. 2005, "Highly efficient, nonpeptidic oligoguanidinium vectors that selectively internalize into mitochondria", *Journal Of The American Chemical Society*, vol. 127, no. 3, pp. 869-874.

Fernández-Nieves, A., Fernández-Barbero, A., de las Nieves, F. J., & Vincent, B. 2000, *Journal of Physics. Condensed Matter*, pp. 3605.

Finsinger, D., Remy, J. S., Erbacher, P., Koch, C., & Plank, C. 2000, "Protective copolymers for nonviral gene vectors: synthesis, vector characterization and application in gene delivery", *Gene Therapy*, vol. 7, no. 14, pp. 1183-1192.

Fire, A., Xu, S., Montgomery, M. K., Kostas, S. A., Driver, S. E., & Mello, C. C. 1998, "Potent and specific genetic interference by double-stranded RNA in *Caenorhabditis elegans*", *Nature*, vol. 391, no. 6669, pp. 806-811.

Fong, J. W. 1981, FRA 81 11694 (patent).

References

Ford, A. W. & Dawson, P. J. 1993, "The effect of carbohydrate additives in the freeze-drying of alkaline phosphatase", *The Journal of Pharmacy and Pharmacology*, vol. 45, no. 2, pp. 86-93.

Franks, F. 1998, "Freeze-drying of bioproducts: putting principles into practice", *European Journal of Pharmaceutics and Biopharmaceutics*, vol. 45, no. 3, pp. 221-229.

Fretz, M. M., Koning, G. A., Mastrobattista, E., Jiskoot, W., & Storm, G. 2004, "OVCAR-3 cells internalize TAT-peptide modified liposomes by endocytosis", *Biochimica et Biophysica Acta (BBA) - Biomembranes*, vol. 1665, no. 1-2, pp. 48-56.

Futami, T., Miyagishi, M., Seki, M., & Taira, K. 2002, "Induction of apoptosis in HeLa cells with siRNA expression vector targeted against bcl-2", *Nucleic Acids Research Supplement*, no. 2, pp. 251-252.

Gan, Q., Wang, T., Cochrane, C., & McCarron, P. 2005, "Modulation of surface charge, particle size and morphological properties of chitosan-TPP nanoparticles intended for gene delivery", *Colloids and Surfaces B: Biointerfaces*, vol. 44, no. 2-3, pp. 65-73.

Garcia del Barrio, G., Novo, F. J., & Irache, J. M. 2003, "Loading of plasmid DNA into PLGA microparticles using TROMS (Total Recirculation One-Machine System): evaluation of its integrity and controlled release properties", *Journal of Controlled Release*, vol. 86, no. 1, pp. 123-130.

Gilmore, I. R., Fox, S. P., Hollins, A. J., Sohail, M., & Akhtar, S. 2004, "The design and exogenous delivery of siRNA for post-transcriptional gene silencing", *Journal of Drug Target*, vol. 12, no. 6, pp. 315-340.

Gitlin, L., Karelsky, S., & Andino, R. 2002, "Short interfering RNA confers intracellular antiviral immunity in human cells", *Nature*, vol. 418, no. 6896, pp. 430-434.

Gitlin, L., Stone, J. K., & Andino, R. 2005, "Poliovirus escape from RNA interference: short interfering RNA-target recognition and implications for therapeutic approaches", *Journal of Virology*, vol. 79, no. 2, pp. 1027-1035.

Godbey, W. T. & Mikos, A. G. 2001, "Recent progress in gene delivery using non-viral transfer complexes", *Journal of Controlled Release*, vol. 72, no. 1-3, pp. 115-125.

References

Godbey, W. T., Wu, K. K., & Mikos, A. G. 1999, "Poly(ethylenimine) and its role in gene delivery", *Journal of Controlled Release*, vol. 60, no. 2-3, pp. 149-160.

Gref, R., Domb, A., Quellec, P., Blunk, T., Muller, R. H., Verbavatz, J. M., & Langer, R. 1995, "The controlled intravenous delivery of drugs using PEG-coated sterically stabilized nanospheres", *Advanced Drug Delivery Reviews*, vol. 16, no. 2-3, pp. 215-233.

Grieser, F., Ashokkumar, M., & Sostaric, J. Z. 1996, *Sonochemistry and sonoluminescence in colloidal systems*. Kluwer Academic Publishers.

Grishok, A. & Mello, C. C. 2002, "11 RNAi (nematodes: *Caenorhabditis elegans*)," in *Advances in Genetics*, Volume 46 edn, Academic Press, pp. 339-360.

Gun'ko, V. M., Klyueva, A. V., Levchuk, Y. N., & Leboda, R. 2003, "Photon correlation spectroscopy investigations of proteins", *Advances in Colloid and Interface Science*, vol. 105, no. 1-3, pp. 201-328.

Gupta, K. C. & Jabrail, F. H. 2006, "Glutaraldehyde and glyoxal cross-linked chitosan microspheres for controlled delivery of centchroman", *Carbohydrate Research*, vol. 341, no. 6, pp. 744-756.

Gurunathan, S., Klinman, D. M., & Seder, R. A. 2000, "DNA vaccines: immunology, application, and optimization", *Annual Review of Immunology*, vol. 18, pp. 927-974.

Haack, T., Peczuh, M. W., Salvatella, X., Sanchez-Quesada, J., De Mendoza, J., Hamilton, A. D., & Giralt, E. 1999, "Surface recognition and helix stabilization of a tetraaspartate peptide by shape and electrostatic complementarity of an artificial receptor", *Journal Of The American Chemical Society*, vol. 121, no. 50, pp. 11813-11820.

Haberland, A., Knaus, T., Zaitsev, S. V., Stahn, R., Mistry, A. R., Coutelle, C., Haller, H., & Bottger, M. 1999, "Calcium ions as efficient cofactor of polycation-mediated gene transfer", *Biochimica et Biophysica Acta (BBA) - Gene Structure and Expression*, vol. 1445, no. 1, pp. 21-30.

Hans, M. L. & Lowman, A. M. 2002, "Biodegradable nanoparticles for drug delivery and targeting", *Current Opinion in Solid State and Materials Science*, vol. 6, no. 4, pp. 319-327.

References

Hao, T., McKeever, U., & Hedley, M. L. 2000, "Biological potency of microsphere encapsulated plasmid DNA", *Journal of Controlled Release*, vol. 69, no. 2, pp. 249-259.

Hauptenthal, J., Baehr, C., Kiermayer, S., Zeuzem, S., & Piiper, A. 2006, "Inhibition of RNase A family enzymes prevents degradation and loss of silencing activity of siRNAs in serum", *Biochemical Pharmacology*, vol. 71, no. 5, pp. 702-710.

Hassani, Z., Lemkine, G. F., Erbacher, P., Palmier, K., Alfama, G., Giovannangeli, C., Behr, J. P., & Demeneix, B. A. 2005, "Lipid-mediated siRNA delivery down-regulates exogenous gene expression in the mouse brain at picomolar levels", *The Journal of Gene Medicine*, vol. 7, no. 2, pp. 198-207.

Hollins, A. J., Benboubetra, M., Omidi, Y., Zinselmeyer, B. H., Schatzlein, A. G., Uchegbu, I. F., & Akhtar, S. 2004, "Evaluation of generation 2 and 3 poly(propylenimine) dendrimers for the potential cellular delivery of antisense oligonucleotides targeting the epidermal growth factor receptor", *Pharmaceutical Research*, vol. 21, no. 3, pp. 458-466.

Howard, K. A., Rahbek, U. L., Liu, X., Damgaard, C. K., Glud, S. Z., Andersen, M. O., Hovgaard, M. B., Schmitz, A., Nyengaard, J. R., Besenbacher, F., & Kjems, J. "RNA Interference in Vitro and in Vivo Using a Novel Chitosan/siRNA Nanoparticle System", *Molecular Therapy*, vol. 14, no. 4, pp. 476-484.

Hsu, Y. Y., Hao, T., & Hedley, M. L. 1999, "Comparison of process parameters for microencapsulation of plasmid DNA in poly(D,L-lactic-co-glycolic) acid microspheres", *Journal of Drug Target*, vol. 7, no. 4, pp. 313-323.

Huang, M., Fong, C. W., Khor, E., & Lim, L. Y. 2005, "Transfection efficiency of chitosan vectors: Effect of polymer molecular weight and degree of deacetylation", *Journal of Controlled Release*, vol. 106, no. 3, pp. 391-406.

Hudson, A. J., Lee, W., Porter, J., Akhtar, J., Duncan, R., & Akhtar, S. 1996, "Stability of antisense oligonucleotides during incubation with a mixture of isolated lysosomal enzymes", *International Journal Of Pharmaceutics*, vol. 133, no. 1-2, pp. 257-263.

References

Hughes, M. D., Hussain, M., Nawaz, Q., Sayyed, P., & Akhtar, S. 2001, "The cellular delivery of antisense oligonucleotides and ribozymes", *Drug Discovery Today*, vol. 6, no. 6, pp. 303-315.

Hutvagner, G. & Zamore, P. D. 2002, "RNAi: nature abhors a double-strand", *Current Opinion in Genetics & Development*, vol. 12, no. 2, pp. 225-232.

Illum, L. 1998, "Chitosan and its use as a pharmaceutical excipient", *Pharmaceutical Research*, vol. 15, no. 9, pp. 1326-1331.

Ishii, T., Okahata, Y., & Sato, T. 2001, "Mechanism of cell transfection with plasmid/chitosan complexes", *Biochimica et Biophysica Acta (BBA) - Biomembranes*, vol. 1514, no. 1, pp. 51-64.

Islam, A., Handley, S. L., Thompson, K. S., & Akhtar, S. 2000, "Studies on uptake, sub-cellular trafficking and efflux of antisense oligodeoxynucleotides in glioma cells using self-assembling cationic lipoplexes as delivery systems", *Journal of Drug Target*, vol. 7, no. 5, pp. 373-382.

Jackson, A. L., Bartz, S. R., Schelter, J., Kobayashi, S. V., Burchard, J., Mao, M., Li, B., Cavet, G., & Linsley, P. S. 2003, "Expression profiling reveals off-target gene regulation by RNAi", *Nature Biotechnology*, vol. 21, no. 6, pp. 635-637.

Jain, R. A. 2000, "The manufacturing techniques of various drug loaded biodegradable poly(lactide-co-glycolide) (PLGA) devices", *Biomaterials*, vol. 21, no. 23, pp. 2475-2490.

Jalil, R. & Nixon, J. R. "Biodegradable poly(lactic acid) and poly(lactide-co-glycolide) microcapsules: problems associated with preparative techniques and release properties", *Journal of Microencapsulation*, vol. 7, no. 3, pp. 297-325.

Janes, K. A., Calvo, P., & Alonso, M. J. 2001, "Polysaccharide colloidal particles as delivery systems for macromolecules", *Advanced Drug Delivery Reviews*, vol. 47, no. 1, pp. 83-97.

Jarver, P. & Langel, U. 2004, "The use of cell-penetrating peptides as a tool for gene regulation", *Drug Discovery Today*, vol. 9, no. 9, pp. 395-402.

Jeffery, H., Davis, S. S., & O'Hagan, D. T. 1993, "The preparation and characterization of poly(lactide-co-glycolide) microparticles. II. The entrapment of a

References

model protein using a (water-in-oil)-in-water emulsion solvent evaporation technique", *Pharmaceutical Research*, vol. 10, no. 3, pp. 362-368.

Jelcic, Z. "Solvent molecular descriptors on poly(, -lactide-co-glycolide) particle size in emulsification-diffusion process", *Colloids and Surfaces A: Physicochemical and Engineering Aspects*, vol. In Press, Corrected Proof.

Jeon, H. J., Jeong, Y. I., Jang, M. K., Park, Y. H., & Nah, J. W. 2000, "Effect of solvent on the preparation of surfactant-free poly(-lactide-co-glycolide) nanoparticles and norfloxacin release characteristics", *International Journal of Pharmaceutics*, vol. 207, no. 1-2, pp. 99-108.

Jeong, J. H., Kim, S. W., & Park, T. G. 2003, "A new antisense oligonucleotide delivery system based on self-assembled ODN-PEG hybrid conjugate micelles", *Journal of Controlled Release*, vol. 93, no. 2, pp. 183-191.

Kakizawa, Y., Furukawa, S., Ishii, A., & Kataoka, K. 2006, "Organic-inorganic hybrid-nanocarrier of siRNA constructing through the self-assembly of calcium phosphate and PEG-based block anionomer", *Journal of Controlled Release*, vol. 111, no. 3, pp. 368-370.

Kakui, T., Miyauchi, T., & Kamiya, H. 2005, "Analysis of the action mechanism of polymer dispersant on dense ethanol alumina suspension using colloidal probe AFM", *Journal of the European Ceramic Society*, vol. 25, no. 5, pp. 655-661.

Kang, F. & Singh, J. 2003, "Conformational stability of a model protein (bovine serum albumin) during primary emulsification process of PLGA microspheres synthesis", *International Journal of Pharmaceutics.*, vol. 260, no. 1, pp. 149-156.

Kasturi, S. P., Sachaphibulkij, K., & Roy, K. 2005, "Covalent conjugation of polyethyleneimine on biodegradable microparticles for delivery of plasmid DNA vaccines", *Biomaterials*, vol. 26, no. 32, pp. 6375-6385.

Keegan, M. E., Royce, S. M., Fahmy, T., & Saltzman, W. M. 2006, "In vitro evaluation of biodegradable microspheres with surface-bound ligands", *Journal of Controlled Release*, vol. 110, no. 3, pp. 574-580.

Keller, M. 2005, "Lipidic carriers of RNA/DNA oligonucleotides and polynucleotides: What a difference a formulation makes!", *Journal of Controlled Release*, vol. 103, no. 3, pp. 537-540.

References

Kiang, T., Wen, J., Lim, H. W., & Leong, K. W. K. 2004, "The effect of the degree of chitosan deacetylation on the efficiency of gene transfection", *Biomaterials*, vol. 25, no. 22, pp. 5293-5301.

Kim, T. H., Kim, S. I., Akaike, T., & Cho, C. S. 2005, "Synergistic effect of poly(ethylenimine) on the transfection efficiency of galactosylated chitosan/DNA complexes", *Journal of Controlled Release*, vol. 105, no. 3, pp. 354-366.

Kircheis, R. & Wagner, E. 2000, "Polycation/DNA complexes for in vivo gene delivery". *Gene Therapy and Regulation*, vol. 1, no. 1, pp. 95-114.

Kircheis, R., Schuller, S., Brunner, S., Ogris, M., Heider, K. H., Zauner, W., & Wagner, E. 1999, "Polycation-based DNA complexes for tumor-targeted gene delivery in vivo", *The Journal of Gene Medicine*, vol. 1, no. 2, pp. 111-120.

Kircheis, R., Wightman, L., & Wagner, E. 2001, "Design and gene delivery activity of modified polyethylenimines", *Advanced Drug Delivery Reviews*, vol. 53, no. 3, pp. 341-358.

Kircheis, R., Wightman, L., Schreiber, A., Robitza, B., Rossler, V., Kurs, M., & Wagner, E. 2001, "Polyethylenimine/DNA complexes shielded by transferrin target gene expression to tumors after systemic application", *Gene Therapy*, vol. 8, no. 1, pp. 28-40.

Kitchell, J. P. & Wise, D. L. 1985, "Poly(lactic/glycolic acid) biodegradable drug-polymer matrix systems", *Methods in Enzymology*, vol. 112, pp. 436-448.

Kleemann, E., Neu, M., Jekel, N., Fink, L., Schmehl, T., Gessler, T., Seeger, W., & Kissel, T. 2005, "Nano-carriers for DNA delivery to the lung based upon a TAT-derived peptide covalently coupled to PEG-PEI", *Journal of Controlled Release*, vol. 109, no. 1-3, pp. 299-316.

Konan, Y. N., Cerny, R., Favet, J., Berton, M., Gurny, R., & Allemann, E. 2003, "Preparation and characterization of sterile sub-200 nm meso-tetra(4-hydroxyphenyl)porphyrin-loaded nanoparticles for photodynamic therapy", *European Journal of Pharmaceutics and Biopharmaceutics*, vol. 55, no. 1, pp. 115-124.

Koping-Hoggard, M., Mel'nikova, Y. S., Varum, K. M., Lindman, B., & Artursson, P. 2003, "Relationship between the physical shape and the efficiency of

References

oligomeric chitosan as a gene delivery system in vitro and in vivo", *The Journal of Gene Medicine*, vol. 5, no. 2, pp. 130-141.

Kost, J. & Goldbart, R. 1997, "Natural and modified polysaccharides," in *Handbook of biodegradable and polymers*, vol. 7 A. J. Domd, D. M. Wiseman, & J. Kost, eds., Hardwood Academic Publishers, Amsterdam, pp. 275-289.

Krishnamurthy, R., Lumpkin, J. A., & Sridhar, R. 2000, "Inactivation of lysozyme by sonication under conditions relevant to microencapsulation", *International Journal of Pharmaceutics.*, vol. 205, no. 1-2, pp. 23-34.

Kumar, S., Boehm, J., & Lee, J. C. 2003, "p38 MAP kinases: key signalling molecules as therapeutic targets for inflammatory diseases", *Nature Reviews Drug Discovery*, vol. 2, no. 9, pp. 717, 726

Kunath, K., von Harpe, A., Fischer, D., Petersen, H., Bickel, U., Voigt, K., & Kissel, T. 2003, "Low-molecular-weight polyethylenimine as a non-viral vector for DNA delivery: comparison of physicochemical properties, transfection efficiency and in vivo distribution with high-molecular-weight polyethylenimine", *Journal of Controlled Release*, vol. 89, no. 1, pp. 113-125.

Kwon, H. Y., Lee, J. Y., Choi, S. W., Jang, Y., & Kim, J. H. 2001, "Preparation of PLGA nanoparticles containing estrogen by emulsification-diffusion method", *Colloids and Surfaces A: Physicochemical and Engineering Aspects*, vol. 182, no. 1-3, pp. 123-130.

Lambert, G., Fattal, E., & Couvreur, P. 2001, "Nanoparticulate systems for the delivery of antisense oligonucleotides", *Advanced Drug Delivery Reviews*, vol. 47, no. 1, pp. 99-112.

Langer, R. 1990, "New methods of drug delivery", *Science*, vol. 249, no. 4976, pp. 1527-1533.

Lappalainen, K., Jaaskelainen, I., Syrjanen, K., Urtti, A., & Syrjanen, S. 1994, "Comparison of cell proliferation and toxicity assays using two cationic liposomes", *Pharmaceutical Research*, vol. 11, no. 8, pp. 1127-1131.

Lasic, D. D. 1998, "Novel applications of liposomes", *Trends in Biotechnology*, vol. 16, no. 7, pp. 307-321.

Lasic, D. D. 1993, *Liposomes: From physics to application*, Elseviers.

References

Lebedeva, I., Benimetskaya, L., Stein, C. A., & Vilenchik, M. 2000, "Cellular delivery of antisense oligonucleotides", *European Journal of Pharmaceutics and Biopharmaceutics*, vol. 50, no. 1, pp. 101-119.

Lebleu, B. 1996, "Delivering information-rich drugs -prospects and challenges", *Trends in Biotechnology*, vol. 14, no. 4, pp. 109-110.

Lee, L. K. & Roth, C. M. 2003, "Antisense technology in molecular and cellular bioengineering", *Current Opinion in Biotechnology*, vol. 14, no. 5, pp. 505-511.

Lee, M. K., Chun, S. K., Choi, W. J., Kim, J. K., Choi, S. H., Kim, A., Oungbho, K., Park, J. S., Ahn, W. S., & Kim, C. K. 2005, "The use of chitosan as a condensing agent to enhance emulsion-mediated gene transfer", *Biomaterials*, vol. 26, no. 14, pp. 2147-2156.

Lee, N. S., Dohjima, T., Bauer, G., Li, H., Li, M. J., Ehsani, A., Salvaterra, P., & Rossi, J. 2002, "Expression of small interfering RNAs targeted against HIV-1 rev transcripts in human cells", *Nature Biotechnology*, vol. 20, no. 5, pp. 500-505.

Lee, S. H. & Sinko, P. J. 2006, "siRNA--Getting the message out", *European Journal of Pharmaceutical Sciences*, vol. 27, no. 5, pp. 401-410.

Leonetti, J. P., Mechti, N., Degols, G., Gagnor, C., & Lebleu, B. 1991, "Intracellular distribution of microinjected antisense oligonucleotides", *Proceedings Of The National Academy Of Sciences Of The United States Of America*, vol. 88, no. 7, pp. 2702-2706.

Leroux, J. C., Cozens, R., Roesel, J. L., Galli, B., Kubel, F., Doelker, E., & Gurny, R. 1995, "Pharmacokinetics of a novel HIV-1 protease inhibitor incorporated into biodegradable or enteric nanoparticles following intravenous and oral administration to mice", *Journal of Pharmaceutical Sciences.*, vol. 84, no. 12, pp. 1387-1391.

Leroux, L.-C., Allemann, E., Doelker, E., & Gurny, R. 1995. "New approach for the preparation of nanoparticles by an emulsification-diffusion method". *European Journal of Biopharmaceutics*, vol. 41, pp.14-18.

Leung, R. K. M. & Whittaker, P. A. 2005, "RNA interference: From gene silencing to gene-specific therapeutics", *Pharmacology & Therapeutics*, vol. 107, no. 2, pp. 222-239.

References

Lewis, D. H. 1990, "Controlled release of bioactive agents from lactide/glycolide polymers," in *Biodegradable polymers as drug delivery systems*, M. Chasin & R. Langer, eds., Marcel Dekker, New York, pp. 1-41.

Lewis, D. L. & Wolff, J. A. 2005, "Delivery of siRNA and siRNA Expression Constructs to Adult Mammals by Hydrodynamic Intravascular Injection," in *Methods in Enzymology RNA Interference*, vol. 392 edn, R. E. David, ed., Academic Press, pp. 336-350.

Lewis P. F. & Emerman, M. 1994, "Passage through mitosis is required for oncoretroviruses but no for the human immunodeficiency virus", *Journal of Virology*, vol. 68, pp. 510-516.

Li, Q., Kay, M. A., Finrgold, M., Stratford-Perricaudet, L. D., & Woo, S. L. 1993, "Assessment of recombinant adenoviral vectors for hepatic gene therapy", *Gene Therapy*, vol. 4, pp. 403-409.

Li, X. W. 2005, Development of novel DNA vaccines utilising polymeric gene delivery sytem.

Li, X. W., Lee, D. K. L., Chan, A. S. C., & Alpar, H. O. 2003, "Sustained expression in mammalian cells with DNA complexed with chitosan nanoparticles", *Biochimica et Biophysica Acta (BBA) - Gene Structure and Expression*, vol. 1630, no. 1, pp. 7-18.

Lieberman, J., Song, E., Lee, S. K., & Shankar, P. 2003, "Interfering with disease: opportunities and roadblocks to harnessing RNA interference", *Trends in Molecular Medicine*, vol. 9, no. 9, pp. 397-403.

Lindgren, M., Hallbrink, M., Prochiantz, A., & Langel, U. 2000, "Cell-penetrating peptides", *Trends in Pharmacological Sciences*, vol. 21, no. 3, pp. 99-103.

Litzinger, D. C. 1997, "Limitations of cationic liposomes for antisense oligonucleotide delivery in vivo", *Journal of Liposome Research*, vol. 7, no. 1, pp. 51-61.

Liu, L. S., Liu, S. Q., Ng, S. Y., Froix, M., Ohno, T., & Heller, J. 1997, "Controlled release of interleukin-2 for tumour immunotherapy using alginate/chitosan porous microspheres", *Journal of Controlled Release*, vol. 43, no. 1, pp. 65-74.

References

Liu, W., Sun, S., Cao, Z., Zhang, X., Yao, K., Lu, W. W., & Luk, K. D. K. 2005, "An investigation on the physicochemical properties of chitosan/DNA polyelectrolyte complexes", *Biomaterials*, vol. 26, no. 15, pp. 2705-2711.

Lopez-Leon, T., Carvalho, E. L. S., Seijo, B., Ortega-Vinuesa, J. L., & Bastos-Gonzalez, D. 2005, "Physicochemical characterization of chitosan nanoparticles: electrokinetic and stability behavior", *Journal of Colloid and Interface Science*, vol. 283, no. 2, pp. 344-351.

Lorenz, C., Hadwiger, P., John, M., Vornlocher, H. P., & Unverzagt, C. 2004, "Steroid and lipid conjugates of siRNAs to enhance cellular uptake and gene silencing in liver cells", *Bioorganic & Medicinal Chemistry Letters*, vol. 14, no. 19, pp. 4975-4977.

Lourenco, C., Teixeira, M., Simoes, S., & Gaspar, R. 1996, "Steric stabilization of nanoparticles: Size and surface properties", *International Journal of Pharmaceutics*, vol. 138, no. 1, pp. 1-12.

Lund, E., Guttinger, S., Calado, A., Dahlberg, J. E., & Kutay, U. 2004, "Nuclear export of microRNA precursors", *Science*, vol. 303, no. 5654, pp. 95-98.

Luppi, F., Aarbiou, J., van Wetering, S., Rahman, I., de Boer, W. I., Rabe, K. F., & Hiemstra, P. S. 2005, "Effects of cigarette smoke condensate on proliferation and wound closure of bronchial epithelial cells in vitro: role of glutathione", *Respiratory Research*, vol. 6, p. 140.

MacLaughlin, F. C., Mumper, R. J., Wang, J., Tagliaferri, J. M., Gill, I., Hinchcliffe, M., & Rolland, A. P. 1998, "Chitosan and depolymerized chitosan oligomers as condensing carriers for in vivo plasmid delivery", *Journal of Controlled Release*, vol. 56, no. 1-3, pp. 259-272.

Makin, G. & Dive, C. 2001, "Apoptosis and cancer chemotherapy", *Trends in Cell Biology*, vol. 11, no. 11, p. S22-S26.

Manuel, S. W., Zheng, J., & Hornby, P. J. 2001, "Transfection by polyethyleneimine-coated microspheres", *Journal of Drug Targeting*, vol. 9, no. 1, pp. 15-22.

Mao, H. Q., Roy, K., Troung-Le, V. L., Janes, K. A., Lin, K. Y., Wang, Y., August, J. T., & Leong, K. W. 2001, "Chitosan-DNA nanoparticles as gene carriers:

References

synthesis, characterization and transfection efficiency", *Journal of Controlled Release*, vol. 70, no. 3, pp. 399-421.

Maruyama, A., Ishihara, T., Kim, J. S., Kim, S. W., & Akaike, T. "Nanoparticle DNA carrier with poly(L-lysine) grafted polysaccharide copolymer and poly(D,L-lactic acid)", *Bioconjugate Chemistry*, vol. 8, no. 5, pp. 735-742.

Matzke, M., Aufsatz, W., Kanno, T., Daxinger, L., Papp, I., Mette, M. F., & Matzke, A. J. M. 2004, "Genetic analysis of RNA-mediated transcriptional gene silencing", *Biochimica et Biophysica Acta (BBA) - Gene Structure and Expression*, vol. In Press, Corrected Proof.

Maurer, N., Mori, A., Palmer, L., Monck, M. A., Mok, K. W., Mui, B., Akhong, Q. F., & Cullis, P. R. 1999, "Lipid-based systems for the intracellular delivery of genetic drugs", *Molecular Membrane Biology*, vol. 16, no. 1, pp.129-140.

McCaffrey, A. P., Meuse, L., Pham, T. T., Conklin, D. S., Hannon, G. J., & Kay, M. A. 2002, "RNA interference in adult mice", *Nature*, vol. 418, no. 6893, pp. 38-39.

McManus, M. T., Haines, B. B., Dillon, C. P., Whitehurst, C. E., van Parijs, L., Chen, J., & Sharp, P. A. 2002, "Small interfering RNA-mediated gene silencing in T lymphocytes", *Journal of Immunology*, vol. 169, no. 10, pp. 5754-5760.

Medberry, P., Dennis, S., Van Hecke, T., & DeLong, R. K. 2004, "pDNA bioparticles: comparative heterogeneity, surface, binding, and activity analyses", *Biochemical and Biophysical Research Communications*, vol. 319, no. 2, pp. 426-432.

Mellman, I. 1996, "Endocytosis and molecular sorting", *Annual Review of Cell and Developmental Biology*, vol. 12, pp. 575-625.

Merdan, T., Kopecek, J., & Kissel, T. 2002, "Prospects for cationic polymers in gene and oligonucleotide therapy against cancer", *Advanced Drug Delivery Reviews*, vol. 54, no. 5, pp. 715-758.

Meredith, E. & Tobias, C. W. 1961, "Conductivities in emulsions". *Journal of Electrochemical Society*, vol. 108, pp. 286-290.

Messai, I. & Delair, T. 2006, "Cationic biodegradable particles: Comparison of one or two step processes", *Colloids and Surfaces A: Physicochemical and Engineering Aspects*, vol. 278, no. 1-3, pp. 188-196.

References

Messai, I., Lamalle, D., Munier, S., Verrier, B., Ataman-Onal, Y., & Delair, T. 2005, "Poly(D,L-lactic acid) and chitosan complexes: interactions with plasmid DNA", *Colloids and Surfaces A: Physicochemical and Engineering Aspects*, vol. vol. 255, no. 1-3, pp. 65-72.

Messai, I., Munier, S., Ataman-Onal, Y., Verrier, B., & Delair, T. 2003, "Elaboration of poly(ethyleneimine) coated poly(-lactic acid) particles. Effect of ionic strength on the surface properties and DNA binding capabilities", *Colloids and Surfaces B: Biointerfaces*, vol 32, no. 4, pp. 293-305.

Mi, F. L., Sung, H. W., Shyu, S. S., Su, C. C., & Peng, C. K. 2003, "Synthesis and characterization of biodegradable TPP/genipin co-crosslinked chitosan gel beads", *Polymer*, vol. 44, no. 21, pp. 6521-6530.

Miller, D. G., Adam, M. A., Miller, A.D. 1994, "Gene transfer by retrovirus occurs only in cells that are actively replicating at the time of infection", *Molecular and Cellular Biology*, vol. 10, pp. 4239-4242.

Mitchell, D. J., Kim, D. T., Steinman, L., Fathman, C. G., & Rothbard, J. B. 2000, "Polyarginine enters cells more efficiently than other polycationic homopolymers", *The Journal Of Peptide Research: Official Journal Of The American Peptide Society*, vol. 56, no. 5, pp. 318-325.

Miyagishi, M. & Taira, K. 2002, "U6 promoter-driven siRNAs with four uridine 3' overhangs efficiently suppress targeted gene expression in mammalian cells", *Nature Biotechnology*, vol. 20, no. 5, pp. 497-500.

Moreno-Manzano, V., Ishikawa, Y., Lucio-Cazana, J., & Kitamura, M. 1999, "Suppression of apoptosis by all-trans-retinoic acid. Dual intervention in the c-Jun n-terminal kinase-AP-1 pathway", *The Journal of Biological Chemistry*, vol. 274, no. 29, pp. 20251-20258.

Mori, T., Murakami, M., Okumura, M., Kadosawa, T., Uede, T., & Fujinaga, T. 2005, "Mechanism of macrophage activation by chitin derivatives", *The Journal Of Veterinary Medical Science / The Japanese Society Of Veterinary Science*, vol. 67, no. 1, pp. 51-56.

References

Moschos, S. 2006 "RNA interference in the lung", Seminar of Targeting the lung using siRNA and therapeutic proteins, *Joint BALR, BIRA and BPS Spring Meeting*, Girton College, Cambridge.

Mosmann, T. 1983, "Rapid colorimetric assay for cellular growth and survival: Application to proliferation and cytotoxicity assays", *Journal of Immunological Methods*, vol. 65, no. 1-2, pp. 55-63.

Moulton, H. M. & Moulton, J. D. 2003, "Peptide-assisted delivery of steric-blocking antisense oligomers", *Current Opinion in Molecular Therapeutics*, vol. 5, no. 2, pp. 123-132.

Müller, H. R. 1991, *Colloidal carriers for controlled drug delivery and targeting : Modification, characterization and in vivo distribution*, CRS Press.

Munier, S., Messai, I., Delair, T., Verrier, B., & Ataman-Onal, Y. 2005, "Cationic PLA nanoparticles for DNA delivery: Comparison of three surface polycations for DNA binding, protection and transfection properties", *Colloids and Surfaces B: Biointerfaces*, vol. 43, no. 3-4, pp. 163-173.

Murakami, H., Kawashima, Y., Niwa, T., Hino, T., Takeuchi, H., & Kobayashi, M. 1997, "Influence of the degrees of hydrolyzation and polymerization of poly(vinylalcohol) on the preparation and properties of poly(-lactide-co-glycolide) nanoparticle", *International Journal of Pharmaceutics*, vol. 149, no. 1, pp. 43-49.

Murakami, H., Kobayashi, M., Takeuchi, H., & Kawashima, Y. 1999, "Preparation of poly(-lactide-co-glycolide) nanoparticles by modified spontaneous emulsification solvent diffusion method", *International Journal of Pharmaceutics*, vol. 187, no. 2, pp. 143-152.

Muratovska, A. & Eccles, M. R. 2004, "Conjugate for efficient delivery of short interfering RNA (siRNA) into mammalian cells", *FEBS Letters*, vol. 558, no. 1-3, pp. 63-68.

Murthy, N., Campbell, J., Fausto, N., Hoffman, A. S., & Stayton, P. S. 2003, "Design and synthesis of pH-responsive polymeric carriers that target uptake and enhance the intracellular delivery of oligonucleotides", *Journal of Controlled Release*, vol. 89, no. 3, pp. 365-374.

References

Nakase, I., Niwa, M., Takeuchi, T., Sonomura, K., Kawabata, N., Koike, Y., Takehashi, M., Tanaka, S., Ueda, K., Simpson, J. C., Jones, A. T., Sugiura, Y., & Futaki, S. 2004, "Cellular Uptake of Arginine-Rich Peptides: Roles for Macropinocytosis and Actin Rearrangement", *Molecular Therapy*, vol. 10, no. 6, pp. 1011-1022.

Napoli, C., Lemieux, C., & Jorgensen, R. 1990, "Introduction of a Chimeric Chalcone Synthase Gene into Petunia Results in Reversible Co-Suppression of Homologous Genes in trans", *Plant Cell*, vol. 2, no. 4, pp. 279-289.

Nash, S. P., & Heuertz, R. M. 2005, "Blockade of p38 map kinase inhibits complement-induced acute lung injury in a murine model", *International Immunopharmacology*, vol. 5, no. 13-14, pp. 1870-1880.

Nath, P., Leung, S-Y., Williams, A., Noble, A., Chakravarty, S. D. S., Luedtke, G. R., Medicherla, S., Higgins, L. S., Protter, A. & Chung, K. F. 2006, "Importance of p38 mitogen-activated protein kinase pathway in allergic airway remodelling and bronchial hyperresponsiveness", *European Journal of Pharmacology*, vol. 544, no. 1-3, pp. 160-167.

Newton, R., & Holden, N. S. 2006, "New aspects of p38 mitogen activated protein kinase (MAPK) biology in lung inflammation", *Drug Discovery Today: Disease Mechanisms*, vol. 3, no. 1, pp. 53-61.

Nicol, S. 1991, Life after death for empty shells. *New Science*, vol. 129, pp. 46-48.

Niidome, T. & Huang, L. 2002, "Gene therapy progress and prospects: nonviral vectors", *Gene Therapy*, vol. 9, no. 24, pp. 1647-1652.

Noguchi, S., Hirashima, N., Furuno, T., & Nakanishi, M. 2003, "Remarkable induction of apoptosis in cancer cells by a novel cationic liposome complexed with a bcl-2 antisense oligonucleotide", *Journal of Controlled Release*, vol. 88, no. 2, pp. 313-320.

Nori, A., Jensen, K. D., Tijerina, M., Kopeckova, P., & Kopecek, J. 2003, "Subcellular trafficking of HPMA copolymer-Tat conjugates in human ovarian carcinoma cells", *Journal of Controlled Release*, vol. 91, no. 1-2, pp. 53-59.

References

Nykanen, A., Haley, B., & Zamore, P. D. 2001, "ATP requirements and small interfering RNA structure in the RNA interference pathway", *Cell*, vol. 107, no. 3, pp. 309-321.

Ogris, M., Brunner, S., Schuller, S., Kircheis, R., & Wagner, E. 1999, "PEGylated DNA/transferrin-PEI complexes: reduced interaction with blood components, extended circulation in blood and potential for systemic gene delivery", *Gene Therapy*, vol. 6, no. 4, pp. 595-605.

Ogris, M., Steinlein, P., Kursa, M., Mechtler, K., Kircheis, R., & Wagner, E. 1998, "The size of DNA/transferrin-PEI complexes is an important factor for gene expression in cultured cells", *Gene Therapy*, vol. 5, no. 10, pp. 1425-1433.

Ohki, E. C., Tilkins, M. L., Ciccarone, V. C., & Price, P. J. 2001, "Improving the transfection efficiency of post-mitotic neurons", *Journal of Neuroscience Methods*, vol. 112, no. 2, pp. 95-99.

Okuda, T., Sugiyama, A., Niidome, T., & Aoyagi, H. 2004, "Characters of dendritic poly(-lysine) analogues with the terminal lysines replaced with arginines and histidines as gene carriers in vitro", *Biomaterials*, vol. 25, no. 3, pp. 537-544.

Ong, J. T. H. & Manoukian, E. 1988, "Release of lonapalene from two-phase emulsion-type ointment systems", *Pharmaceutical Research*, pp. 11-20.

Ono, H., Ichiki, T., Ohtsubo, H., Fukuyama, K., Imayama, I., Iino, N., Masuda, S., Hashiguchi, Y., Takeshita, A., & Sunagawa, K. 2006, "cAMP-response element-binding protein mediates tumor necrosis factor- α -induced vascular cell adhesion molecule-1 expression in endothelial cells", *Hypertension Research*, vol. 29, no. 1, pp. 39-47.

Owens III, D. E. & Peppas, N. A. 2006, "Opsonization, biodistribution, and pharmacokinetics of polymeric nanoparticles", *International Journal of Pharmaceutics*, vol. 307, no. 1, pp. 93-102.

Paddison, P. J., Caudy, A. A., Bernstein, E., Hannon, G. J., & Conklin, D. S. 2002, "Short hairpin RNAs (shRNAs) induce sequence-specific silencing in mammalian cells", *Genes & Development*, vol. 16, no. 8, pp. 948-958.

Pang, S. W., Park, H. Y., Jang, Y. S., Kim, W. S., & Kim, J. H. 2002, "Effects of charge density and particle size of poly(styrene/(dimethylamino)ethyl methacrylate)

References

nanoparticle for gene delivery in 293 cells", *Colloids and Surfaces B: Biointerfaces*, vol. 26, no. 3, pp. 213-222.

Panyam, J. & Labhasetwar, V. 2003, "Biodegradable nanoparticles for drug and gene delivery to cells and tissue", *Advanced Drug Delivery Reviews*, vol. 55, no. 3, pp. 329-347.

Patel, J., Galey, D., Jones, J., Ray, P., Woodward, J. G., Nath, A., & Mumper, R. J. 2006, "HIV-1 Tat-coated nanoparticles result in enhanced humoral immune responses and neutralizing antibodies compared to alum adjuvant", *Vaccine*, vol. 24, no. 17, pp. 3564-3573.

Pearson, L. L., Castle, B. E., & Kehry, M. R. 2001, "CD40-mediated signaling in monocytic cells: up-regulation of tumor necrosis factor receptor-associated factor mRNAs and activation of mitogen-activated protein kinase signaling pathways", *International Immunology*, vol. 13, no. 3, pp. 273-283.

Pekarik, V. 2005, "Design of shRNAs for RNAi--A lesson from pre-miRNA processing: Possible clinical applications", *Brain Research Bulletin*, vol. 68, no. 1-2, pp. 115-120.

Perrin, D. E. & English, J. P. 1997, "Polyglycolide and polylactide," in *Handbook of biodegradable polymers*, vol. 7 J. Kost & R. Goldbart, eds., Harwood Academic Publishers, Amsterdam, pp. 3-21.

Polk, A., Amsden, B., De Yao, K., Peng, T., & Goosen, M. F. 1994, "Controlled release of albumin from chitosan-alginate microcapsules", *Journal of Pharmaceutical Sciences*, vol. 83, no. 2, pp. 178-185.

Potocky, T. B., Menon, A. K., & Gellman, S. H. 2003, "Cytoplasmic and nuclear delivery of a TAT-derived peptide and a beta-peptide after endocytic uptake into HeLa cells", *The Journal of Biological Chemistry*, vol. 278, no. 50, pp. 50188-50194.

Pozzolini, M., Scarfi, S., Benatti, U., & Giovine, M. 2003, "Interference in MTT cell viability assay in activated macrophage cell line", *Analytical Biochemistry*, vol. 313, no. 2, pp. 338-341.

Prochiantz, A. 2000, "Messenger proteins: homeoproteins, TAT and others", *Current Opinion in Cell Biology*, vol. 12, no. 4, pp. 400-406.

References

Pujals, S., Fernandez-Carneado, J., Lopez-Iglesias, C., Kogan, M. J., & Giralt, E. 2006, "Mechanistic aspects of CPP-mediated intracellular drug delivery: Relevance of CPP self-assembly", *Biochimica et Biophysica Acta (BBA) - Biomembranes*, vol. 1758, no. 3, pp. 264-279.

Quantine, B, Perricaudet, L. D., Tajbakhsh, S., Mandell, J. L., 1992, "Adenovirus as an expression vector in muscle cells in vivo", *Proceeding of the National Academy of Sciences of the United States of America*, vol. 89, pp. 2581-2584.

Quintanar-Guerrero, D., Allemann, E., Doelker, E., & Fessi, H. 1998, "Preparation and characterization of nanocapsules from preformed polymers by a new process based on emulsification-diffusion technique", *Pharmaceutical Research*, vol. 15, no. 7, pp. 1056-1062.

Quintanar-Guerrero, D., Fessi, H., Allemann, E., & Doelker, E. 1996, "Influence of stabilizing agents and preparative variables on the formation of poly(-lactic acid) nanoparticles by an emulsification-diffusion technique", *International Journal of Pharmaceutics*, vol. 143, no. 2, pp. 133-141.

Raia, V., Maiuri, L., Ciacci, C., Ricciardelli, I., Vacca, L., Auricchio, S., Cimmino, M., Cavaliere, M., Nardone, M., Cesaro, A., Malcolm, J., Quarantino, S., & Londei, M. 2005, "Inhibition of p38 mitogen activated protein kinase controls airway inflammation in cystic fibrosis", *Thorax*, vol. 60, no. 9, pp. 773-780.

Randolph, T. W. 1997, "Phase separation of excipients during lyophilization: Effects on protein stability", *Journal of Pharmaceutical Sciences*, vol. 86, pp. 1198-1202.

Ravi Kumar, M. N. V., Bakowsky, U., & Lehr, C. M. 2004, "Preparation and characterization of cationic PLGA nanospheres as DNA carriers", *Biomaterials*, vol. 25, no. 10, pp. 1771-1777.

Rehmet, R. & Killmann, E. 1999, "Adsorption of cationic poly(diallyl-dimethyl-ammoniumchloride), poly(diallyl-dimethyl-ammoniumchloride-co-N-methyl-N-vinylactamide) and poly(N-methyl-N-vinyl-acetamide) on polystyrene latex", *Colloids and Surfaces A: Physicochemical and Engineering Aspects*, vol. 149, no. 1-3, pp. 323-328.

References

Remy, J. S., Abdallah, B., Zanta, M. A., Boussif, O., Behr, J. P., & Demeneix, B. 1998, "Gene transfer with lipospermines and polyethylenimines", *Advanced Drug Delivery Reviews*, vol. 30, no. 1-3, pp. 85-95.

Ren, X., Luo, G., Xie, Z., Zhou, L., Kong, X., & Xu, A. 2006, "Inhibition of multiple gene expression and virus replication of HBV by stable RNA interference in 2.2.15 cells", *Journal of Hepatology*, vol. 44, no. 4, pp. 663-670.

Richard, J. P., Melikov, K., Vives, E., Ramos, C., Verbeure, B., Gait, M. J., Chernomordik, L. V., & Lebleu, B. 2003, "Cell-penetrating peptides. A reevaluation of the mechanism of cellular uptake", *The Journal of Biological Chemistry*, vol. 278, no. 1, pp. 585-590.

Richardson, S. C. W., Kolbe, H. V. J., & Duncan, R. 1999, "Potential of low molecular mass chitosan as a DNA delivery system: biocompatibility, body distribution and ability to complex and protect DNA", *International Journal Of Pharmaceutics*, vol. 178, no. 2, pp. 231-243.

Roux, P. P. & Blenis, J. 2004, "ERK and p38 MAPK-activated protein kinases: a family of protein kinases with diverse biological functions", *Microbiology and Molecular Biology Reviews*, vol. 68, no. 2, pp. 320-344.

Rozema, D. B. & Lewis, D. L. 2003, "siRNA delivery technologies for mammalian systems", *TARGETS*, vol. 2, no. 6, pp. 253-260.

Rudolph, C., Schillinger, U., Plank, C., Gessner, A., Nicklaus, P., Muller, R. H., & Rosenecker, J. 2002, "Nonviral gene delivery to the lung with copolymer-protected and transferrin-modified polyethylenimine", *Biochimica et Biophysica Acta (BBA) - General Subjects*, vol. 1573, no. 1, pp. 75-83.

Ruponen, M., Yla-Herttuala, S., & Urtili, A. 1999, "Interactions of polymeric and liposomal gene delivery systems with extracellular glycosaminoglycans: physicochemical and transfection studies", *Biochimica et Biophysica Acta (BBA) - Biomembranes*, vol. 1415, no. 2, pp. 331-341.

Sah, H., Smith, M. S., & Chern, R. T. 1996, "A novel method of preparing PLGA microcapsules utilizing methylethyl ketone", *Pharmaceutical Research*, vol. 13, no. 3, pp. 360-367.

References

Sahoo, S. K., Panyam, J., Prabha, S., & Labhasetwar, V. 2002, "Residual polyvinyl alcohol associated with poly (D,L-lactide-co-glycolide) nanoparticles affects their physical properties and cellular uptake", *Journal Of Controlled Release: Official Journal of The Controlled Release Society*, vol. 82, no. 1, pp. 105-114.

Salvatella, X., Martinell, M., Gairi, M., Mateu, G., Feliz, M., Hamilton, A. D., De Mendoza, J., & Giralt, E. 2003, *A tetraguanidinium ligand binds to the surface of the tetramerization domain of protein P53*, 43 edn, Angew. Chem. Int.

Sanchez-Quesada, J., Seel, C., Prados, P., De Mendoza, J., Dalcol, I., & Giralt, E. 1996, "Anion helicates: double strand helical self-assembly of chiral bicyclic guanidinium dimers and tetramers around sulfate templates". *Journal of American Chemical Society*, vol. 118, pp. 277-278.

Sanz-Moreno, V., Casar, B., & Crespo, P. 2003, "p38alpha isoform Mxi2 binds to extracellular signal-regulated kinase 1 and 2 mitogen-activated protein kinase and regulates its nuclear activity by sustaining its phosphorylation levels", *Molecular Cell Biology*, vol. 23, no. 9, pp. 3079-3090.

Schiffelers, R. M., Mixson, A. J., Ansari, A. M., Fens, M. H. A. M., Tang, Q., Zhou, Q., Xu, J., Molema, G., Lu, P. Y., & Scaria, P. V. 2005, "Transporting silence: Design of carriers for siRNA to angiogenic endothelium", *Journal of Controlled Release*, vol. 109, no. 1-3, pp. 5-14.

Schiffelers, R. M., Woodle, M. C., & Scaria, P. 2004, "Pharmaceutical prospects for RNA interference", *Pharmaceutical Research*, vol. 21, no. 1, pp. 1-7.

Schipper, N. G. M., Varum, K. M., Stenberg, P., Ocklind, G., Lennernas, H., & Artursson, P. 1999, "Chitosans as absorption enhancers of poorly absorbable drugs: 3: Influence of mucus on absorption enhancement", *European Journal of Pharmaceutical Sciences*, vol. 8, no. 4, pp. 335-343.

Schipper, N. G., Olsson, S., Hoogstraate, J. A., deBoer, A. G., Varum, K. M., & Artursson, P. 1997, "Chitosans as absorption enhancers for poorly absorbable drugs 2: mechanism of absorption enhancement", *Pharmaceutical Research*, vol. 14, no. 7, pp. 923-929.

Schipper, N. G., Varum, K. M., & Artursson, P. 1996, "Chitosans as absorption enhancers for poorly absorbable drugs. 1: Influence of molecular weight and degree of

References

acetylation on drug transport across human intestinal epithelial (Caco-2) cells", *Pharmaceutical Research*, vol. 13, no. 11, pp. 1686-1692.

Sen, G. C. 2001, "Viruses and interferons", *Annual Review of Microbiology*, vol. 55, pp. 255-281.

Sessa, G. & Weissmann, G. 1968, "Phospholipid spherules (liposomes) as a model for biological membranes", *Journal Of Lipid Research*, vol. 9, no. 3, pp. 310-318.

Shah, D. S., Sakthivel, T., Toth, I., Florence, A. T., & Wilderspin, A. F. 2000, "DNA transfection and transfected cell viability using amphipathic asymmetric dendrimers", *International Journal Of Pharmaceutics*, vol. 208, no. 1-2, pp. 41-48.

Shakweh, M., Besnard, M., Nicolas, V., & Fattal, E. 2005, "Poly (lactide-co-glycolide) particles of different physicochemical properties and their uptake by peyer's patches in mice", *European Journal of Pharmaceutics and Biopharmaceutics*, vol. 61, no. 1-2, pp. 1-13.

Shi, Y. 2003, "Mammalian RNAi for the masses", *Trends in Genetics*, vol. 19, no. 1, pp. 9-12.

Shiraishi, T., Pankratova, S., & Nielsen, P. E. 2005, "Calcium Ions Effectively Enhance the Effect of Antisense Peptide Nucleic Acids Conjugated to Cationic Tat and Oligoarginine Peptides", *Chemistry & Biology*, vol. 12, no. 8, pp. 923-929.

Shu, X. Z. & Zhu, K. J. 2000, "A novel approach to prepare tripolyphosphate/chitosan complex beads for controlled release drug delivery", *International Journal of Pharmaceutics*, vol. 201, no. 1, pp. 51-58.

Shu, X. Z. & Zhu (a), K. J. 2002, "The influence of multivalent phosphate structure on the properties of ionically cross-linked chitosan films for controlled drug release", *European Journal of Pharmaceutics and Biopharmaceutics*, vol. 54, no. 2, pp. 235-243.

Shu, X. Z. & Zhu (b), K. J. 2002, "Controlled drug release properties of ionically cross-linked chitosan beads: the influence of anion structure", *International Journal of Pharmaceutics*, vol. 233, no. 1-2, pp. 217-225.

Shuey, D. J., McCallus, D. E., & Giordano, T. 2002, "RNAi: gene-silencing in therapeutic intervention", *Drug Discovery Today*, vol. 7, no. 20, pp. 1040-1046.

References

Silhol, M., Tyagi, M., Giacca, M., Lebleu, B., & Vives, E. 2002, "Different mechanisms for cellular internalization of the HIV-1 Tat-derived cell penetrating peptide and recombinant proteins fused to Tat", *European Journal of Biochemical*, vol. 269, no. 2, pp. 494-501.

Singer, V. L., Jones, L. J., Yue, S. T., & Haugland, R. P. 1997, "Characterization of PicoGreen Reagent and Development of a Fluorescence-Based Solution Assay for Double-Stranded DNA Quantitation", *Analytical Biochemistry*, vol. 249, no. 2, pp. 228-238.

Sioud, M. & Sorensen, D. R. 2003, "Cationic liposome-mediated delivery of siRNAs in adult mice", *Biochemical and Biophysical Research Communications*, vol. 312, no. 4, pp. 1220-1225.

Sioud, M. 2004, "Therapeutic siRNAs", *Trends in Pharmacological Sciences*, vol. 25, no. 1, pp. 22-28.

Song, K. C., Lee, H. S., Choung, I. Y., Cho, K. I., Ahn, Y., & Choi, E. J. 2006, "The effect of type of organic phase solvents on the particle size of poly(d,l-lactide-co-glycolide) nanoparticles", *Colloids and Surfaces A: Physicochemical and Engineering Aspects*, vol. 276, no. 1-3, pp. 162-167.

Soppimath, K. S., Aminabhavi, T. M., Kulkarni, A. R., & Rudzinski, W. E. 2001, "Biodegradable polymeric nanoparticles as drug delivery devices", *Journal of Controlled Release*, vol. 70, no. 1-2, pp. 1-20.

Soutschek, J., Akinc, A., Bramlage, B., Charisse, K., Constien, R., Donoghue, M., Elbashir, S., Geick, A., Hadwiger, P., & Harborth et, a. 2004, "Therapeutic silencing of an endogenous gene by systemic administration of modified siRNAs", *Nature*, vol. 432, no. 7014, pp. 173-178.

Spagnou, S., Miller, A. D., & Keller, M. 2004, "Lipidic carriers of siRNA: differences in the formulation, cellular uptake, and delivery with plasmid DNA", *Biochemistry*, vol. 43, no. 42, pp. 13348-13356.

Stephens, B. G. & Felkel, H. L. 1975, "Extraction of copper (II) from aqueous thiocyanate solutions into propylene carbonate and subsequent atomic spectrophotometric determination", *Analytical Chemistry*, vol. 47, pp. 1676-1679.

References

Stephens, B. G. & Suddeth, H. A. 1967, "Extraction of the 1, 10, -phenantroline, 4,7-diphenyl-1,10-phenantroline and 2,4,6-tripyridyl-sym-triazine complexes of iron(II) into propylene carbonate", *Analytical Chemistry*, vol. 39, no. 1478, pp. 1480.

Schwarz, D. S., Hutvagner, G., Du, T., Xu, Z., Aronin, N., & Zamore, P. D. 2003, "Asymmetry in the assembly of the RNAi enzyme complex", *Cell*, vol. 115, no. 2, pp. 199-208.

Tabara, H., Grishok, A., & Mello, C. C. 1998, "RNAi in *C. elegans*: soaking in the genome sequence", *Science*, vol. 282, no. 5388, pp. 430-431.

Tadros, T. F., Py, C., Rouviere, J., Taelman, M. C., & Loll, P. 1995, "Fundamental investigation of the stability of w/o/w multiple emulsions for cosmetic applications", *Conference Proceedings of Cosmetic Exhibition*, Augsburg.

Tai, C. J., Chang, S. J., Leung, P. C., & Tzeng, C. R. 2004, "Adenosine 5'-triphosphate activates nuclear translocation of mitogen-activated protein kinases leading to the induction of early growth response 1 and raf expression in human granulosa-luteal cells", *The Journal of Clinical Endocrinology and Metabolism*, vol. 89, no. 10, pp. 5189-5195.

Tam, P., Monck, M., Lee, D., Ludkovski, O., Leng, E. C., Clow, K., Stark, H., Scherrer, P., Graham, R. W., & Cullis et, a. 2000, "Stabilized plasmid-lipid particles for systemic gene therapy", *Gene Therapy*, vol. 7, no. 21, pp. 1867-1874.

Tang, E. S. K., Huang, M., & Lim, L. Y. 2003, "Ultrasonication of chitosan and chitosan nanoparticles", *International Journal of Pharmaceutics*, vol. 265, no. 1-2, pp. 103-114.

Technical Manual of Dual-Glo™ Luciferase Assay System, Instructions for use of product E2920, E2940 and E2980. Last revised 2006, Promega, USA.

Thioune, O., Fessi, H., Devissaguet, J. P., & Puisieux, F. 1997, "Preparation of pseudolatex by nanoprecipitation: Influence of the solvent nature on intrinsic viscosity and interaction constant", *International Journal of Pharmaceutics*, vol. 146, no. 2, pp. 233-238.

Thomas, M., Lu, J. J., Ge, Q., Zhang, C., Chen, J., & Klibanov, A. M. 2005, "Full deacetylation of polyethylenimine dramatically boots its gene delivery efficiency

References

and specificity to mouse lung", *Proceeding of the National Academy of Sciences of the United States of America*, vol. 102, no. 16, pp. 5679-5684.

Thoren, P. E. G., Persson, D., Isakson, P., Goksor, M., Onfelt, A., & Norden, B. 2003, "Uptake of analogs of penetratin, Tat(48-60) and oligoarginine in live cells", *Biochemical and Biophysical Research Communications*, vol. 307, no. 1, pp. 100-107.

Tice, T. R. & Cowsar, D. R. 1984, "Biodegradable controlled-release parenteral systems", *Pharmaceutical Technology*, vol. 11, no. 1, pp. 26-35.

Tijsterman, M., Ketting, R. F., & Plasterk, R. H. A. 2002, "The genetics of RNA silencing", *Annual Review of Genetics*, vol. 36, pp. 489-519.

Tomalia, D. A. and Killat, G.R. In: J.I. Kroschwitz Editor, (second ed. ed.), *Encyclopedia of Polymer Science and Engineering* 1 Wiley, New York (1985), pp. 680-739.

Tomanin, R. & Scarpa, M. 2004, "Why do we need new gene therapy viral vectors? Characteristics, limitations and future perspectives of viral vector transduction", *Current Gene Therapy*, vol. 4, no. 4, pp. 357-372.

Timmons, L., Court DL, & Fire, A. 2001, "Ingestion of bacterially expressed dsRNAs can produce specific and potent genetic interference in *Caenorhabditis elegans*", *Gene*, vol. 263, no. 1-2, pp. 103-112.

Tracy, M. A., Ward, K. L., Firouzabadian, L., Wang, Y., Dong, N., Qian, R., & Zhang, Y. 1999, "Factors affecting the degradation rate of poly(lactide-co-glycolide) microspheres in vivo and in vitro", *Biomaterials*, vol. 20, no. 11, pp. 1057-1062.

Trimaille, T., Pichot, C., & Delair, T. 2003, "Surface functionalization of poly(-lactic acid) nanoparticles with poly(ethylenimine) and plasmid DNA by the layer-by-layer approach", *Colloids and Surfaces A: Physicochemical and Engineering Aspects*, vol. 221, no. 1-3, pp. 39-48.

Tsuruo, T., Naito, M., Tomida, A., Fujita, N., Mashima, T., Sakamoto, H., & Haga, N. 2003, "Molecular targeting therapy of cancer: drug resistance, apoptosis and survival signal", *Cancer Science*, vol. 94, no. 1, pp. 15-21.

Tung, C. H., Mueller, S., & Weissleder, R. 2002, "Novel Branching Membrane Translocational Peptide as Gene Delivery Vector", *Bioorganic & Medicinal Chemistry*, vol. 10, no. 11, pp. 3609-3614.

References

Turner, J. J., Arzumanov, A. A., & Gait, M. J. 2005, "Synthesis, cellular uptake and HIV-1 Tat-dependent trans-activation inhibition activity of oligonucleotide analogues disulphide-conjugated to cell-penetrating peptides", *Nucleic Acids Research*, vol. 33, no. 1, pp. 27-42.

Uprichard, S. L. 2005, "The therapeutic potential of RNA interference", *FEBS Letters*, vol. 579, no. 26, pp. 5996-6007.

Van Rij, R. P. & Andino, R. 2005, "RNAi as an antiviral mechanism and therapeutic approach," in *Molecular Pathogenesis of Virus Infections*, P.Digard et al., ed., Cambridge University Press, pp. 179-201.

Van Rij, R. P. & Andino, R. 2006, "The silent treatment: RNAi as a defense against virus infection in mammals", *Trends in Biotechnology*, vol. 24, no. 4, pp. 186-193.

Vasiljevic, D., Parojcic, J., Primorac, M., & Vuleta, G. 2006, "An investigation into the characteristics and drug release properties of multiple W/O/W emulsion systems containing low concentration of lipophilic polymeric emulsifier", *International Journal of Pharmaceutics*, vol. 309, no. 1-2, pp. 171-177.

Vickers, T. A., Koo, S., Bennett, C. F., Crooke, S. T., Dean, N. M., & Baker, B. F. 2003, "Efficient reduction of target RNAs by small interfering RNA and RNase H-dependent antisense agents. A comparative analysis", *The Journal of Biological Chemistry*, vol. 278, no. 9, pp. 7108-7118.

Vila, A., Sanchez, A., Janes, K., Behrens, I., Kissel, T., Jato, J. L. V., & Alonso, M. J. 2004, "Low molecular weight chitosan nanoparticles as new carriers for nasal vaccine delivery in mice", *European Journal of Pharmaceutics and Biopharmaceutics*, vol. 57, no. 1, pp. 123-131.

Vives, E. 2005, "Present and future of cell-penetrating peptide mediated delivery systems: "Is the Trojan horse too wild to go only to Troy?""", *Journal of Controlled Release*, vol. 109, no. 1-3, pp. 77-85.

Vivès, E., Granier, C., Prevor, P., & Lebleu, B. 1997, "Structure activity relationship study of the plasma membrane translocating potential of a short peptide from HIV-1 Tat protein", *Structure Lettres Peptide Sciences*, vol. 4, pp. 429-436.

Wada, R., Hyon, S.-H., Ike, O., Watanabe, S., Shimizu, Y., & Ikida, Y. 1998,

References

"Preparation of lactic acid oligomer microspheres containing anti-cancer drug by o/o type solvent evaporation process", *Polymer Material Science Engineering*, vol. 59, pp. 803-806.

Wadia, J. S. & Dowdy, S. F. 2005, "Transmembrane delivery of protein and peptide drugs by TAT-mediated transduction in the treatment of cancer", *Advanced Drug Delivery Reviews*, vol. 57, no. 4, pp. 579-596.

Wang, J. & Barr, M. M. 2005, RNA Interference in *Caenorhabditis elegans*. David, R. Engelke. *Methods in Enzymology RNA Interference. Methods in Enzymology*, Vol. 392, pp. 36-55. Academic Press.

Wender, P. A., Mitchell, D. J., Pattabiraman, K., Pelkey, E. T., Steinman, L., & Rothbard, J. B. 2000, "The design, synthesis, and evaluation of molecules that enable or enhance cellular uptake: Peptoid molecular transporters", *Proceedings of the National Academy of Sciences*, vol. 97, no. 24, pp. 13003-13008.

Whitmarsh, A. J. & Davis, R. J. 1996, "Transcription factor AP-1 regulation by mitogen-activated protein kinase signal transduction pathways", *Journal of Molecular Medicine*, vol. 74, no. 10, pp. 589-607.

Wilson, J. A. & Richardson, C. D. 2005, "Hepatitis C virus replicons escape RNA interference induced by a short interfering RNA directed against the NS5b coding region", *Journal of Virology*, vol. 79, no. 11, pp. 7050-7058.

Wooddell, C. I., Van Hout, C. V., Reppen, T., Lewis, D. L., & Herweijer, H. 2005, "Long-term RNA interference from optimized siRNA expression constructs in adult mice", *Biochemical and Biophysical Research Communications*, vol. 334, no. 1, pp. 117-127.

Woodle, M. C., Scaria, P., Ganesh, S., Subramanian, K., Titmas, R., Cheng, C., Yang, J., Pan, Y., Weng, K., Gu, C., & Torkelson, S. 2001, "Sterically stabilized polyplex: ligand-mediated activity", *Journal of Controlled Release*, vol. 74, no. 1-3, pp. 309-311.

Wu, X. S. 1995, "Synthesis and properties of biodegradable lactic/glycolic acid polymers," in *Wise Encyclopedic Handbook of Biomaterials and Bioengineering*, Marcel Dekker, New York, pp. 1015-1054.

References

Xie, S. Y., Zhang, J. Z., Huang, S. Z., Sun, D., Ren, Z. R., & Zeng, Y. T. 2005, "Suppression of eGFP expression in erythroid-specific transgenic mice by siRNA", *Blood Cells, Molecules, and Diseases*, vol. 34, no. 3, pp. 220-225.

Yamauchi, M., Kusano, H., Saito, E., Iwata, T., Nakakura, M., Kato, Y., & Aoki, N. 2006, "Development of wrapped liposomes: Novel liposomes comprised of polyanion drug and cationic lipid complexes wrapped with neutral lipids", *Biochimica et Biophysica Acta (BBA) - Biomembranes*, vol. 1758, no. 1, pp. 90-97.

Yi, R., Qin, Y., Macara, I. G., & Cullen, B. R. 2003, "Exportin-5 mediates the nuclear export of pre-microRNAs and short hairpin RNAs", *Genes & Development*, vol. 17, no. 24, pp. 3011-3016.

Yin, Y.-L. & Prudhomme, R. K. 1992, "Donnan equilibrium of mobile ions in polyelectrolyte gels", *Polym.Prepr.* vol. 32, pp. 507-508.

Zambaux, M. F., Bonneaux, F., Gref, R., Maincent, P., Dellacherie, E., Alonso, M. J., Labrude, P., & Vigneron, C. 1998, "Influence of experimental parameters on the characteristics of poly(lactic acid) nanoparticles prepared by a double emulsion method", *Journal Of Controlled Release: Official Journal Of The Controlled Release Society*, vol. 50, no. 1-3, pp. 31-40.

Zangemeister-Wittke, U. 2003, "Antisense to apoptosis inhibitors facilitates chemotherapy and TRAIL-induced death signaling", *Annals of the New York Academy of Sciences*, vol. 1002, pp. 90-94.

Zanta, M. A., Boussif, O., Adib, A., & Behr, J. P. "In vitro gene delivery to hepatocytes with galactosylated polyethylenimine", *Bioconjugate Chemistry*, vol. 8, no. 6, pp. 839-844.

Zauner, W., Farrow, N. A., & Haines, A. M. R. 2001, "In vitro uptake of polystyrene microspheres: effect of particle size, cell line and cell density", *Journal of Controlled Release*, vol. 71, no. 1, pp. 39-51.

Zhang, C., Tang, N., Liu, X., Liang, W., Xu, W., & Torchilin, V. P. 2006, "siRNA-containing liposomes modified with polyarginine effectively silence the targeted gene", *Journal of Controlled Release*, vol. 112, no. 2, pp. 229-239.

Zhang, C., Yadava, P., & Hughes, J. 2004, "Polyethylenimine strategies for plasmid delivery to brain-derived cells", *Methods*, vol. 33, no. 2, pp. 144-150.

References

Zimmer, A., Atmaca-Abdel Aziz, S., Gilbert, M., Werner, D., & Noe, C. R. 1999, "Synthesis of cholesterol modified cationic lipids for liposomal drug delivery of antisense oligonucleotides", *European Journal of Pharmaceutics and Biopharmaceutics*, vol. 47, no. 2, pp. 175-178.

Zou, S. M., Erbacher, P., Remy, J. S., & Behr, J. P. "Systemic linear polyethylenimine (L-PEI)-mediated gene delivery in the mouse", *The Journal Of Gene Medicine*, vol. 2, no. 2, pp. 128-134.

Appendix 1: Abbreviations

A represents a number of uncapped end groups or free carboxylates of PLGA polymer

AIDS Acquired Immune Deficiency Syndrome

APC Antigen Presenting Cell

Arg Arginine

ATF Activated transcription factor

ATP Adenosine 5'-triphosphate, a nucleotide that performs many essential roles in the cells

Bar unit of pressure

1 bar = 100 000 pascals (Pa)

1 mbar = 0.001 bar = 100 Pa

(A pascal is one newton per square meter)

bp base pair

kbp kilo base pair, 10^3

BCA Bicinchoninic acid

BSA Bovine serum albumin

BZA Benzyl alcohol

C Carbon

CCR5 a chemokine receptor that predominantly expressed on T cells, macrophages, dendritic cells and microglia it is likely plays a role in inflammatory responses to infection

CD4 surface protein CD4

C *elegans* *Caenorhabditis elegans*

CF Cystic fibrosis

CHO K1 cells epithelial cell from Chinese hamster ovary

CI113 Chitosan hydrochloride with molecular weight of 110 kDa

CI213 Chitosan hydrochloride with molecular weight of 270 kDa

COPD chronic obstructive pulmonary disease

CPPs Cell penetrating peptides

CXCR4 an alpha-chemokine receptor and also called fusin that specific for stromal-derived-factor-1 (SDF-1 also called CXCL12), a molecule endowed with potent chemotactic activity for lymphocytes.

DCM Dichloromethane

Appendix 1: Abbreviations

DDA	Degree of deacetylation of chitosan
DEPC	Diethylpyrocarbonate
DMEM	Dulbecco's modified Eagle's Medium, a cell culture medium
DNA	Deoxyribonucleic acid
DNAzymes	DNA enzymes
DOPE	Dioleoyl phosphatidylethanolamine
DOTAP	1,2-dioleoyl-3-trimethylammonium propane
dsRNA	Double stranded Ribonucleic acid
EC	Ethyl acetate
EDTA	Ethylenediaminetetraacetic acid
Elk	eukaryotic initiation factor
EO	Ethylene oxide
ER	Endoplasmic recticulum
ERK	extracellular signal-regulated kinases
ERK ½	extracellular signal-regulated kinases 1 and 2
Ets-1	E twenty-six-1
FBS	Foetal Bovine Serum
g	gram, unit of mass
mg	mili gram, 10^{-3}
µg	micro gram, 10^{-6}
ng	nano gram, 10^{-9}
GALT	Gut associated lymphoid tissue
G113	Chitosan glutamate with molecular weight of 470 kDa
G213	Chitosan glutamate with molecular weight of 160 kDa
g/ml	gram per ml, unit of concentration
mg/ml	mili gram per mili litre, 10^1
µg/ml	micro gram per mili litre, 10^{-3}
ng/ml	nano gram per milli litre, 10^{-6}
G3PDH	Glyceraldehyde-3-phosphate dehydrogenase
h	hour, unit of time
HBV	Hepatitis B virus
HEK 293 cells	a epithelial cell line from human embryo kidney transformed with adenovirus 5 DNA
HIV	Human immunodeficiency virus

Appendix 1: Abbreviations

HK polymer	Histidine –lysine polymers
HPMA	N-(2-hydroxypropyl)methacrylamide
HSPGs	Heparan sulphate proteoglycans
IL	Interleukin
<i>In-vitro</i>	outside of living body and artificial environment
<i>In-vivo</i>	in the living body of animal or plant
IU	International unit
<i>I.v</i>	Intravenous injection
JNK	c-Jun amino-terminal kinases
KCps	intensity of light
kDa	kilo dalton, unit of molecular weight
L	Litre, unit of volume
ml	mili litre, 10^{-3}
μl	micro litre, 10^{-6}
LMP	Low melting point
LNA	Locked Nucleic Acids
LPA	Lyoprotectant agent
LPAs	Lyoprotectant agents
M	Molar, unit of concentration
mM	mili molar, 10^{-3}
m	meter, unit of length
μm	micro meter, 10^{-6}
nm	nano meter, 10^{-9}
mA	mili ampere, unit of electric
MAPK	mitogenic activated protein kinase
MAP3K	MAPK kinase kinases MAP3K
MEF	Myocyte-specific enhancer binding factor
MEK	Methyl ethyl ketone
MgCl₂	Magnesium chloride
min	minute, unit of time
miRNA	MicroRNA
MKKs	MAPK kinases
mRNA	messenger RNA

Appendix 1: Abbreviations

mPa.s mili pascal second, unit of dynamic viscosity. If a fluid with a viscosity of one Pa.s is placed between two plates, and one plate is pushed sideways with a shear stress of one pascal, it moves a distance equal to the thickness of the layer between the plates in one second.

MTT 3-(4, 5-dimethyl-thiazol-2-yl)-2, 5-diphenyl-tetrazolium bromide

m/v mass per volume

MW molecular weight

n number of sample

Na Sodium

NaCl Sodium chloride

NF- κ B Nuclear Factor kappa B

N/P ratio Nitrogen to phosphate ratio

O Oxigen

ODN oligonucleotide

ODNs Oligonucleotides

OVCAR-3 cells Human ovarian carcinoma cells

o/w Oil in water composite emulsion

PBS Phosphate buffered saline

PC Propylene carbonate

PCR Polymerase chain reaction

PCS Photon correlation spectroscopy

pDNA plasmid DNA

PEG Polyethylene glycol

PEGylation chemical process by which chemical materials are coupled with PEG to improve the hydrophilicity and stability

PEI Polyetylenimine

PGs proteoglycans

pGL3-control a pDNA vector coding luciferase with control of simian virus 40 promoter and enhancer for monitoring and normalising expression in eukaryotic cells. The family has been redesign from the backbone of the pGL2 Luciferase Reporter Vectors and contains a modified coding region for firefly (*Photinus pyralis*) luciferase. The modified reporter vector has resulted in higher level of luciferase expression than pGL2 luciferase reporter while maintaining relatively low background luciferase expression.

Appendix 1: Abbreviations

pGWIZ a pDNA vector contains a proprietary modified promoter followed by intron A from the human cytomegalovirus (CMV) immediate early gene and a high-efficiency artificial transcription terminator. This plasmid is suitable for *in-vitro* and *in-vivo* gene expression studies and applications.

pH a measurement of the acidity of a solution, in terms of activity of hydrogen ions (H^+).

PI Polydispersity index, size distribution of particles

PKR Protein kinase response

PLA Poly(lactic acid)

PLGA Poly (lactic-co-glycolic) acid

PO Propylene oxide

Pol II Polymerase II

Pol III Polymerase III

pRL-TK a pDNA vector contains the herpes simplex virus thymidine kinase (HSV-TK) promoter to provide low to moderate levels of *Renilla* luciferase expression in co-transfected mammalian cells. The pRL-TK Vector is intended for use as an internal control reporter and may be used in combination with any experimental reporter vector to cotransfect mammalian cells. All of the pRL Reporter Vectors contain a cDNA (*Rluc*) encoding *Renilla* luciferase, which was originally cloned from the marine organism *Renilla reniformis*

PVA polyvinyl alcohol

p53 tumour protein 53

R Exchange ratio [$R=D_{sw}/D_{ws}$; diffusion coefficients= $D_{\text{solvent water}}, D_{\text{water solvent}}$]

RES Reticuloendothelial system

RGD Arginine-glycine-aspartic acid

RISC RNA-induced silencing complex

RLU Relative light unit

RNA Ribonucleic acid

RNAi RNA interfering

rpm Revolution per minute

rcf Relative centrifugal force, a measurement unit of the force applied to a sample within a centrifuge. This can be calculated from the speed and rotational radius using following formulation:

Appendix 1: Abbreviations

RCF= $0.000011118 \times r \times N^2$

R=rotational radius (cm)

N= rotaring speed (rpm)

RRR Relative response ratio

Rt-PCR Reverse transcriptase polymerase chain reaction

s second, unit of time

Sap Stomach cancer-associated protein tyrosine phosphatase

SD Standard deviation

SEM Scanning electron microscope

shRNA short hairpin RNA

siRNA Small interfering RNA

TAE Tris-acetate-EDTA

TBE Tris-borate-EDTA

TE Tris(Tris(hydroxymethyl)-aminomethane)-EDTA

TEM Transmission electron microscope

TPP Tripolyphosphate

UV Ultra violet

V Volt, unit of voltage

mV milli Volt, unit of electric

w/o/w Water in oil in water composite emulsion

X Interaction parameter

Z-ave Mean of particle size diameter measured by photon correlation spectroscopy

°C Celcius, unit of temperature

Conversion formula:

Celsius to Fahrenheit: $^{\circ}\text{F} = ^{\circ}\text{C} \times 1.8 + 32$

Fahrenheit to Celsius: $^{\circ}\text{C} = (^{\circ}\text{F} - 32) / 1.8$

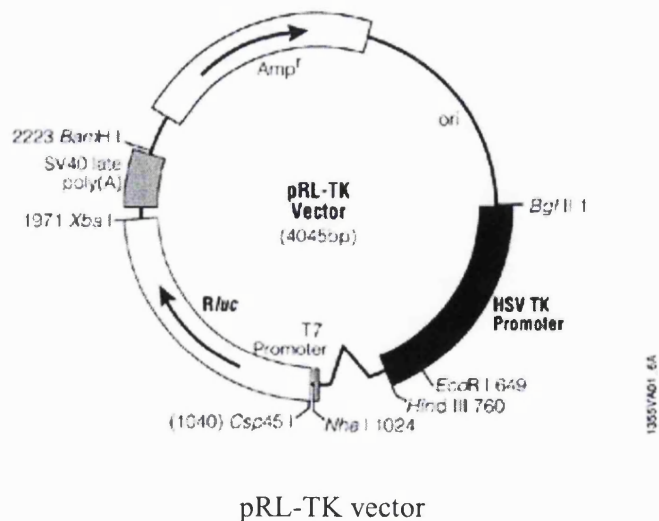
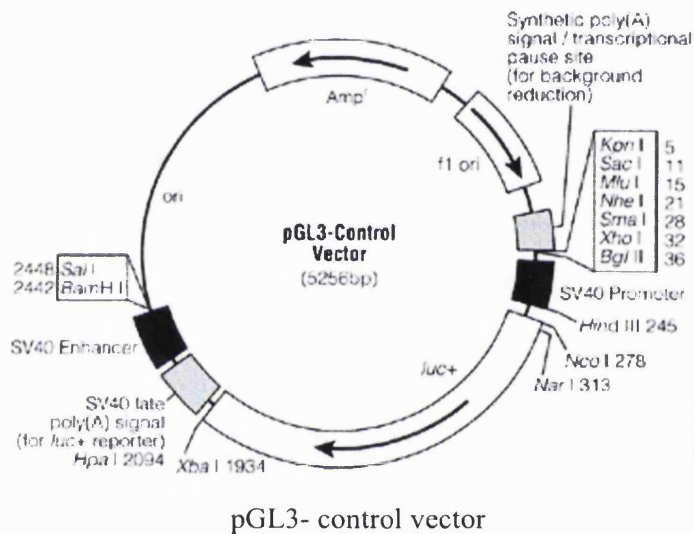
Celsius to Kelvin: $\text{K} = ^{\circ}\text{C} + 273.15$

Kelvin to Celsius: $^{\circ}\text{C} = \text{K} - 273.15$

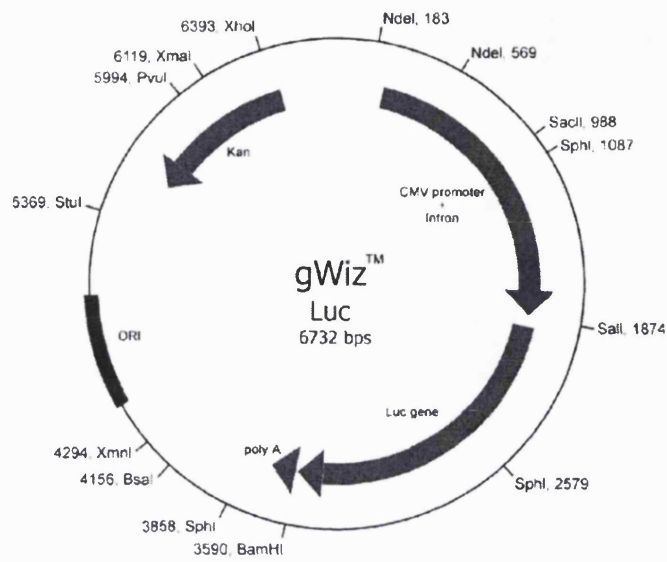
Appendix 2: Maps of pDNA used in this work

Artificially constructed pDNA contains (Gurunathan *et al.* 2000):

- A eukaryotic promoter to allow protein expression in mammalian cells (e.g. promoters derived from virus such as cytomegalovirus (CMV) or simian virus 40 (SV40))
- a cloning site for insertion of heterologous genes
- inclusion of polyadenylation A (polyA) to provide stabilisation of mRNA transcripts (e.g. bovine growth hormone (BGH) or SV40 polyadenylation sequence)



Appendix 2: Maps of pDNA



gWIZ™-luciferase reporter

Appendix 3: The compositions of the basic classic solutions

Appendix 3: The compositions of the basic classic solutions used in the work

(a) 1 M Tris (tris(hydroxymethyl)aminomethane)

Tris base; FW=121.14

Dissolve 121.1 g Tris Base (TRIZMA) in 700 ml dH₂O

Add concentrated HCl to desired pH:

- pH 7.4: 70 ml

- pH 8.0: 42 ml

- pH 9.0: ~8 ml

Bring volume to 1 L with dH₂O.

Filter and autoclave.

Store at room temperature.

(b) 0.5 M EDTA, pH 8.0

Ethylenediaminetetraacetic acid disodium salt or disodium ethylenediaminetetraacetic acid; FW= 372.24

- 186.1 g Na₂EDTA-2H₂O)

- 700 ml dH₂O

- ~50 ml 10N NaOH to pH 8.0

Stir until dissolved; bring volume to 1 L with dH₂O.

Filter and autoclave.

Store at room temperature.

(c) Tris-EDTA (TE, 10 mM Tris, 1 mM EDTA) buffer

- 0.5 ml 1 M Tris-Cl, pH 7.4 (sterile)
- 0.1 ml 0.5 M EDTA, pH 8.0 (sterile)
- 49.4 ml ddH₂O (sterile) to 50 mL.

Store at room temperature.

(d) Tris-Borate-EDTA (TBE) buffer

For 1 liter of 10× stock :

Add:

- 108 g Tris base (890 mM)
- 55 g boric acid (890 mM)
- 40 mL 0.5 M EDTA, pH 8.0

Adjust pH to 8.3 with boric acid. Adjust volume to 1L with H₂O.

(e) Tris-acetate-EDTA (TAE) buffer

For 50 X Stock Add:

- 242 g Tris base
- 57.1 ml glacial acetic acid
- 37.2 g Na₂EDTA·2H₂O

Adjust volume with H₂O to 1 liter

(f) Phosphate buffered saline (PBS)

To 800 ml distilled water adds:

- 8 g NaCl
- 0.2 g KCl
- 1.44 g Na₂HPO₄
- 0.24 g KH₂PO₄

(g) Phosphate buffer

Prepare a 0.2 M monobasic stock by dissolving 27.6 g of monobasic sodium phosphate, monohydrate, in water and q.s to 1 liter.

Prepare a dibasic 0.2 M stock solution by dissolving 28.4 g dibasic sodium phosphate in water and q.s. to 1 liter.

Mix appropriate volumes of monobasic and dibasic sodium phosphate stocks and add up to 200 ml to obtain a 0.1 M phosphate buffer with the desired pH.

(h) Acetate buffer (3 M)

Combine

- 123 g sodium acetate

Adjust pH with glacial acetic acid.

Adjust volume with H₂O to 500 ml.

Sterilize by autoclaving.

Appendix 4: The calculation of molecular weight of a unit with primary amine if chitosan

Appendix 4: The calculation of molecular weight of a unit with primary amine of chitosan

Chitosan consists of acetyl glucosamine (X) and deacetyl glucosamine (Y). The components of part X are $C_8H_{13}O_5N$. The MW of a unit of part X is $8 \times 12 + 13 \times 1 + 5 \times 16 + 14 = 203$.

The components of a unit of part Y are $C_6H_{10}O_4N$. The MW of a unit of part Y is $6 \times 12 + 10 \times 1 + 4 \times 16 + 14 = 160$.

If glucosamine units are glutamated, the MW of glutamated Y part is $160 + 128 = 288$ (MW of glutamate acid is 128).

If glucosamine units are hydrochloride, the MW of hydrochloride Y part is $160 + 36 = 196$.

In a chitosan molecule, if the deacetylation is 86%, therefore, $X/Y = 0.14/0.86 = 0.16$.

The average MW of a unit is $203 \times 0.14 + 160 \times 0.86 = 166$.

1. in the case of chitosan glutamate

If the MW of chitosan is 470 000 Da, the average MW of a unit containing a primary amine is calculated as the following:

$$203 \times X + 288 \times Y = 470\,000$$

$$X = 0.16 Y, \text{ therefore } 203 \times 0.16Y + 288Y = 470\,000$$

Here, Y is the amount of deacetylated glucosamine unit, $Y = 470\,000/320 = 1469$.

Therefore, the average MW of a unit containing a primary amine is

$$470\,000/1469 = 320.$$

2. In the case of chitosan hydrochloride

If the MW is 270 000 Da, the average MW of a unit containing a primary amine is calculated as the following:

$$203 \times X + 196 \times Y = 270\,000$$

$$X = 0.16 Y, \text{ therefore } 203 \times 0.16Y + 196Y = 270\,000$$

Here, Y is the amount of deacetylated glucosamine unit, $Y = 270\,000/228 = 1184$.

Appendix 4: The calculation of molecular weight of a unit with primary amine if chitosan

Therefore, the average MW of a unit containing a primary amine is

$$470\ 000 / 1184 = 400.$$

Appendix 5: Conversion of weight ratio to N/P ratio of chitosan to siRNA

$$\text{Mol} = \text{mass} / \text{MW}$$

The average MW of a unit siRNA containing a primary amine is 326.

Therefore, the average mol of a unit siRNA containing primary amine is

$$\text{Mol}_{\text{siRNA}} = 10 \mu\text{g} / 326 = 0.03 \mu\text{mol}$$

If the weight of chitosan glutamate is 1000 μg , the average mol of a unit siRNA containing primary amine is:

$$\text{Mol}_{\text{chitosan}} = 1000 \mu\text{g} / 320 = 3$$

Therefore, N/P ratio for chitosan to siRNA weight ratio of 100:1 is calculated as the following:

$$\text{N/P ratio} = 3 / 0.03 = 100:1$$

If the weight of chitosan hydrochloride is 1000 μg , the average mol of a unit siRNA containing primary amine is:

$$\text{Mol}_{\text{chitosan}} = 1000 \mu\text{g} / 400 = 2.5$$

Therefore, N/P ratio for chitosan to siRNA weight ratio of 100:1 is calculated as the following:

$$\text{N/P ratio} = 2.5 / 0.03 = 83:1$$